UNIVERSITY OF
BIRMINGHAM

Networked Control of Distributed Energy Systems

By

ASHRAF F. KHALIL

A Thesis Submitted To
The University Of Birmingham
For The Degree Of
DOCTOR OF PHILOSOPHY

School Of Electronic, Electrical
& Computer Engineering
College Of Engineering & Physical Science
The University Of Birmingham, UK
February 2012

DECLARATION

I confirm that the work in this which is thesis entitled “Networked Control of Distributed Energy Systems”, is my own work.

Ashraf Khalil

ABSTRACT

Networked control systems have attracted a great attention in the last decade, and their applications in distributed energy systems have been addressed by many researchers. Replacing the complex wiring system with a shared network can improve the system performance, reliability and stability. When a shared network is adopted in the control loops, the control signals will suffer time delays or data dropouts which may destabilize the system. So it is necessary to find the maximum time delay that the system can withstand. The methods available in the literature either are an extension from those designed for time delay systems or are too complex to be used in practice.

This thesis reports a new method for stability analysis and maximum time delay estimation in networked control systems with applications to distributed energy systems. The proposed new method is based on using finite difference approximation for the delay term and then the Lyapunov system stability theorem is applied to derive the time delay boundary allowed to the system. The proposed method has been applied to networked control systems with state feedback controllers, with dynamic controllers, and to multi-units interconnected networked control systems. The proposed method is then extended to a class of networked control system with bounded nonlinearity and uncertainties. Compared with most of the methods reported in the published literature, the new method is simple to use while the results are comparable.

The characteristics of time delays are analyzed in this thesis, and the results show that time delays can be constant, periodic, random and bounded, random governed by Markov Chain and in some cases the time delay may be unbounded. The proposed method

is suitable for systems with bounded time delays which is required in networked control systems. The method is applied to analyze the stability of a system with parallel connections of DC/DC buck converters where the control signals are exchanged through the shared network. With the proposed method, the parameters that affect the maximum allowable delay boundary are investigated.

When the time delay can be modelled using Markov Chain the Markovian jump system approach is used to study the stability of the networked control system. With this approach, the stability of the networked control system is formulated as finding the solutions for a Bilinear Matrix Inequality. In this thesis, an improved V-K iteration algorithm is used to solve the Bilinear Matrix Inequality in order to derive a controller to stabilize the systems. This approach is used to study the stability of the parallel DC/DC converters with stochastic time delays.

The proposed method is extended for a class of nonlinear networked control systems and uncertain networked control systems. This extension has resulted in two theorems to determine the stability of such a networked control system. The method supported by the theorem for the nonlinear networked control system involves less computation compared with the methods published in the literature, and the designed controller has established the relationship between the maximum allowable delay bound and the maximum nonlinearity. It is found that increasing the nonlinearity in the system will result in decreasing the maximum allowable time delay. The proposed method in this thesis is simple in structure and applications with comparable performance to most of the published methods in the literature. With the increase reliance on shared networks in industry and distributed energy systems in control engineering practice the method can be used as a fast and simple design tool.

ACKNOWLEDGEMENT

I am grateful to Allah the Almighty who gives me all what I need, who guides and helps me during my journey in this life.

I would like to express my gratitude to my supervisor Prof. Jihong Wang, who guided me during my research, and I appreciate her patience and advice. Her encouragement and support were really great motivation for me. I really have benefited from each minute of discussion with Prof. Jihong Wang. The suggestions, criticisms and the guidance I received from her were valuable, which made this thesis possible.

To Dr. Mourad Oussalah and Dr. Stuart Hillmansen thank you for your suggestions and criticisms. The comments which I received from Dr. Mourad were very important for improving this work.

I am really grateful for the scholarship I received from the ministry of the higher education in Libya.

Thanks to my parents, brothers, sisters and friends for their encouragement and support. I am really grateful to my wife for her patience during my research. I would like to thank her for the endless love and support. And finally to her and my kids Mouhanad, Khalid, Sondes and Malik I dedicate my thesis.

Table of Contents

List of Figures

List of Abbreviations

AC	Alternating Current
ACE	Area Control Error
AGC	Automatic Gain Control
AWSS	Asymptotic Wide Sense Stationary Stability
BMI	Bilinear Matrix Inequality
CAN	Controlled Area Network
CCL	Cone Complementary Linearization
CSMA/AMP	Carrier-Sense Multiple Access Protocol with Arbitration on Message Priority
CSMA/CD	Carrier-Sense Multiple Access with Collision Detection
DC	Direct Current
DES	Distributed Energy System
DTMJLS	Discrete-Time Markovian Jump Linear System
EVP	Eigenvalue Problem
FIB	Field Bus
FP	Feasibility Problem
GCE	Generator Control Error
GEVP	Generalized Eigenvalue Problem
ICCI	Integrated Communication and Control Systems
JLS	Jump Linear System
LAN	Local Area Network
LQG	Linear Quadratic Gaussian
LQR	Linear Quadratic Regulator
LMI	Linear Matrix Inequality
MADB	Maximum Allowable Delay Bound
NCS	Networked Control System
PID	Proportional-Integral-Derivative Controller
PROFIBUS	Process Field Bus
PSS	Power System Stabilizer
SCADA	Supervisory Control And Data Acquisition
UPS	Uninterruptable Power Supply
VSI	Voltage Source Inverter

List of Symbols

$\mathbf{A}$ State matrix ($n \times n$ matrix).

$\mathbf{A}_c$ The controller state matrix ($n_c \times n_c$ matrix).

$\mathbf{A}_{ds}$ State matrix of the discrete system ($n \times n$ matrix).

$\mathbf{A}_d$ Delayed states matrix ($n \times n$ matrix).

$\mathbf{A}_{ij}$ A matrix describes how the dynamics of the i^{th} unit can be influenced by the j^{th} unit.

$\mathbf{A}_{ii}$ State matrix of the i^{th} unit.

$\mathbf{A}_p$ The plant state matrix ($n_p \times n_p$ matrix).

$\overline{\mathbf{A}}$ The augmented state matrix.

$\mathbf{A}_{cl}$ The augmented state matrix of the closed loop Markovian jump system.

$\mathbf{B}$ Input matrix ($n \times m$ matrix).

$\mathbf{B}_c$ The controller input matrix ($n_c \times r$ matrix).

$\mathbf{B}_{ds}$ Input matrix of the discrete system ($n \times m$ matrix).

$\mathbf{B}_i$ The input matrix of the i^{th} plant.

$\mathbf{B}_p$ The plant input matrix ($n_p \times m$ matrix).

$\overline{\mathbf{B}}$ The augmented input matrix.

$\mathbf{C}$ Output matrix ($p \times n$ matrix).

$\mathbf{C}_c$ The controller output matrix ($m \times n_p$ matrix).

$\mathbf{C}_p$ The plant output matrix ($r \times n_p$ matrix).

$\overline{\mathbf{C}}_{r_s(k)}$ The output matrix of the augmented state vector.

$\mathbf{C}_{xi}$ The output matrix of the i^{th} plant.

$\mathbf{C}_{zi}$ The output matrix of the i^{th} controller.

$\mathbf{D}$ Direct transmission matrix ($p \times m$ matrix).

$\mathbf{D}_c$ The controller direct transmission matrix ($m \times r$ matrix).

d The number of dropouts.

d_k The data dropouts at the instant *k*.

d_{sc} The number of dropouts between the sensor and the controller.

d_{ca} The number of dropouts between the controller and the actuator.

d_s The finite delay bound.

$\mathbf{F}$ The controller state matrix.

$\mathbf{F}_{ii}$ The state matrix of the i^{th} controller.

$\mathbf{F}_{ij}$ A matrix represents how the dynamic of the j^{th} controller affects the dynamics of the i^{th} controller

$\overline{\mathbf{F}}$ The controller augmented state matrix.

$\mathbf{G}$ The controller input matrix.

$\mathbf{G}_i$ The i^{th} controller input matrix.

$\overline{\mathbf{G}}$ The controller augmented input matrix.

h The sampling period.

$\mathbf{H}$ The controller output matrix.

$\mathbf{H}_i$ The i^{th} controller output matrix.

$\overline{\mathbf{H}}$ The controller augmented output matrix.

$\mathbf{h}(t, \mathbf{x})$ A piecewise-continuous function of both *t* and **x**.

$\mathbf{I}_{n \times n}$ The identity matrix ($n \times n$ matrix).

I_s The reference current.

i_{Li} The inductor current of the i^{th} converter.

$\mathbf{J}$ The controller feed-forward matrix.

K The controller gain.

$\mathbf{K}$ The controller state feedback gain matrix.

K_v The voltage controller gain.

K_i The current controller gain.

k The output voltage feedback gain.

k_1 Constant derived from the electric torque.

k_2 Constant derived from the electric torque.

k_3 Constant derived from field voltage.

k_4 Constant derived from field voltage.

k_5 Constant derived from terminal voltage.

k_6 Constant derived from terminal voltage.

k_A The voltage regulator gain.

$\overline{\mathbf{K}}$ The controller augmented feed-forward matrix.

M The inertia moment coefficient.

$m^{(i)}$ The number of the messages.

N_{node} The number of the nodes in the network.

$\mathbf{P}$ A positive definite symmetric matrix.

P_0 The initial transition probability.

p_{ij} The probability of the jump from mode *i* to mode *j*.

P_{sc} The probability transition matrix for the sensor to the controller time delay.

P_{ca} The probability transition matrix for the controller to the actuator time delay.

$\mathbf{Q}$ A positive definite symmetric matrix.

R_A The domain of attraction.

$\Re$ The set of real numbers.

$\Re^{m\times n}$ The vector space of $m\times n$ real matrices.

$r_s(k)$ A bounded random integer sequence governed by Markov Chain.

$r_{ca}(k)$ A bounded random integer sequence governed by Markov Chain.

$\mathbf{S}_i$ A positive symmetric constant matrix.

T_A The voltage regulator time constant.

T_{total} The total time delay induced in the network.

T_{pre} The pre processing time delay.

T_{dn} The network time delay.

T_{d0} The *d*-axis transient open circuit time constant.

T_{post} The post processing time delay.

T_w The waiting time delay.

T_{tr} The transmission time delay.

T_{retr} The retransmission time delay.

$T_{tr}^{(i,j)}$ The time required to transmit the $(i,j)^{\text{th}}$ message from node *i* to node *j*.

$T_{retr}^{(i,j)}$ The time required to retransmit the $(i,j)^{\text{th}}$ message if a collision has been detected.

$T_{\max}$ The period of messages transmission.

T_s The sampling time.

U_T The utilization.

$\mathbf{u}(t)$ The control input vector (m-vector).

u_E The excitation control input.

$\mathbf{u}^{(i)}$ The control input vector of the i^{th} plant.

$\mathbf{u}_l^{\mathbf{i}}$ The local control input vector.

$\mathbf{u}_g^i$ The global control input vector.

$\mathbf{u}(k)$ The control input vector at instant k.

$\mathbf{u}_p(t)$ The input vector of the plant (m-vector).

V_m The amplitude of the pulse width modulator signal.

V_{ref} The reference voltage.

$\mathbf{V}(x)$ Lyapunov function.

$\mathbf{v}(k)$ The controller output vector at instant k.

$\mathbf{x}(k)$ The state vector at instant k.

$\mathbf{x}(t)$ State vector (n-vector) or state variable.

$\mathbf{x}_c(t)$ The state vector of the controller (n_c-vector).

$\mathbf{x}^{(i)}$ The state vector of the i^{th} plant.

$\mathbf{x}_p(t)$ The state vector of the plant (n_p-vector).

$\bar{\mathbf{x}}(k)$ The augmented state vector ((d_s+1)n-vector).

$\tilde{\mathbf{x}}(k)$ The augmented state vector for the system with dynamic controller.

$\mathbf{y}(k)$ The output vector at the instant k.

$\mathbf{y}(t)$ The output vector (p-vector).

$\mathbf{y}_p(t)$ The output vector of the plant (r-vector).

$\mathbf{y}_x^{(i)}$ The output vector of the i^{th}.

$\mathbf{z}(k)$ The controller state vector at instant k.

$\mathbf{z}^{(i)}(t)$ The controller state vector of the i^{th} controller.

$\bar{\mathbf{z}}(k)$ The controller augmented state vector.

α A positive number.

β The decay rate of the DSTMJLS.

δ_i The duty cycle of the i^{th} converter.

$\Delta\omega$ The angular velocity.

$\Delta\delta$ The torque angle.

Δe_q The quadrature transient voltage.

Δe_{FD} The exciter output variation.

ε A small positive number.

$\mathbf{\Phi}$ The closed-loop system matrix ($(n_p + n_c)\times(n_p + n_c)$ matrix).

$\mathbf{\Gamma}$ The closed-loop matrix.

φ A small positive number.

γ A positive scalar.

η A postive number.

$\mathbf{\Lambda}$ The closed-loop system matrix ($(n_p + n_c)\times(n_p + n_c)$ matrix).

λ_i The i^{th} eigenvalue of a matrix.

μ A small positive number.

$\mathbf{\Pi}_i$ A positive definite matrix of appropriate dimension, where i = 1,2,3.

$\mathbf{\Theta}$ The closed-loop system matrix ($(n_p + n_c)\times(n_p + n_c)$ matrix).

ρ A small positive number.

$\mathbf{\Sigma}_i$ A real nonsingular matrix with appropriate dimension.

τ The time delay.

τ_c The controller time delay.

$\tau_s(k)$ The time delay at the instant k.

τ_{sc} The time delay between the sensor and the controller including the data dropouts.

τ_{scm} The maximum bound for the sensor to the controller time delay.

τ'_{sc} The time delay between the sensor and the controller.

τ_{ca} The time delay from the controller to the actuator including the data dropouts.

τ'_{ca} The time delay from the controller to the actuator.

τ_{cam} The maximum bound for the controller to the actuator time delay.

τ_k The time delay at instant *k*.

ω_z The compensator zero.,

ω_p The compensator pole.

$\mathbf{\Omega}$ A nonsingular real matrix.

$\mathbf{\Omega}_{11}$ A square matrix.

$\mathbf{\Omega}_{12}$ Block matrix.

$\mathbf{\Omega}_{22}$ Block matrix.

Ω_c The estimate of the domain of attraction

ξ A small positive number.

$\xi(t)$ The state vector for the parallel DC/DC buck converter system.

$\bar{\xi}(t)$ The augmented state vector for the parallel DC/DC buck converter system.

$\mathbf{\Xi}_i$ A positive definite matrix of appropriate dimension, where i = 1,2,3.

$\mathbf{\Psi}$ The closed-loop system matrix ($n \times n$ matrix).

$\in$ A small positive number.

$\|\mathbf{A}\|$ The induced 2-norm of a matrix **A**.

$\|\mathbf{x}\|$ The norm of a vector **x**.

$\forall$ for all.

$\Rightarrow$ implies.

CHAPTER ONE: INTRODUCTION

Networked control systems (NCS) refer to the system in which the information of sensors, commands, control signals are transmitted through a network. The NCS is a multidisciplinary subject area that integrates control engineering, communication, computer science and physical plants together. Networked control system is a very promising and challenging new control technology and very active research area. NCS applications include many research areas such as manufacturing plants, automobiles and aircrafts. Because of the widespread of the shared networks, for example the Internet and the Ethernet, NCS attracted many researchers especially for large systems with distributed structure such as the power systems and the distributed energy systems. The classical control view that relies on point-to-point control connection can face many obstacles for large and complex distributed energy systems. In the last decade, many researchers have reported that NCS can be used to enhance the stability and the performance of the distributed energy systems (Vesely et al. 2011; Casavola et al. 2008; Shaobu et al. 2012; Yang 2006).

In the next section, the research motivation and the literature review are given. The literature review is devoted to distributed energy systems that have already started to implement control strategies over a shared network. One section in the chapter is dedicated to define and describe the main fundamental issues in NCSs which are the time delay and the data dropouts. In the last section of this chapter, the outline of the thesis and the main contributions are given.

1.1 Motivation of the Research

Distributed energy systems have emerged as alternative energy sources for conventional power generation. In the distributed energy system, a number of distributed energy sources are dispersed on a geographical area and interconnected to supply a specific amount of energy to clustered or dispersed loads. As the number of the installed energy sources and the number of the loads is increasing, these systems are evolving in a way that will make them large and complex systems. The control of such large and complex systems brought many challenges. Implementing the ideal centralized control strategy will not achieve the future energy system requirements such as the flexibility, expandability and high reliability.

For example, if we look at the power system, it used to be an ideal centralized control system before the 1970s (Yang 2006). The supervisory control and data acquisition system (SCADA) is used to fuse the sensors' information in the large network into the centralized controller where they are processed and the proper commands are sent back to the widespread system actuators (Mak et al. 2002). As the system is becoming more complex, the pure centralized control strategy is no longer a suitable choice for many reasons:

1) Collecting large quantity of data spread on a large physical area through communication links takes a long processing time that affects the global stability of the system; 2) The reliability concerns: the main feature in any centralized system is the single point of failure. The number of the blackouts around the world where the cost was billions of pounds is the evidence that highlighted the weaknesses of the centralization control. 3) Another reason is the market driving force which requires an efficient system operation where the system has to supply the loads according to the market prices. Due to these reasons, the power system started to move toward the decentralization in the early 1970s (Yang 2006). The decentralized control is one of the solutions of the problem of the control system complexity because the interconnections between the distributed units are neglected, but the stability of the overall system cannot be guaranteed.

Both centralized and decentralized systems have their own unique advantages and disadvantages so the proposed system control architecture should take the benefits of the both (Beccuti et al. 2006). Among many possible applications, quasi-decentralized control is particularly attractive to distributed energy systems (Yang et al. 2006). The quasi-decentralized control provides a compromise between the centralized and the decentralized control (Yang et al. 2000;Sun et al. 2008). The term quasi-decentralized control refers to a situation in which part of information used for control are collected and processed locally although some information needs to be transferred between local plants and/or controllers through the network connection, in which the total number of such signal transmission is kept at the minimum (Yang 2006). The block diagrams for centralized, decentralized and quasi-decentralized control systems are shown in Figure 1.1, 1.2, and 1.3, respectively (Yang 2006).

With the advances in the network technology and in the networked control system, the quasi-decentralized control strategy can be implemented where the control signals are exchanged over the shared networks. This can reduce the complexity caused by the complicated and space taking wiring.

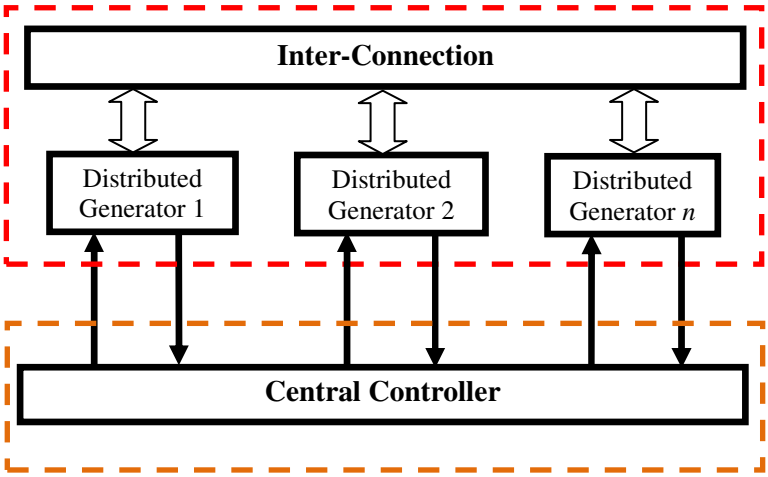

Figure 1.1 A Fully Centralized Controller

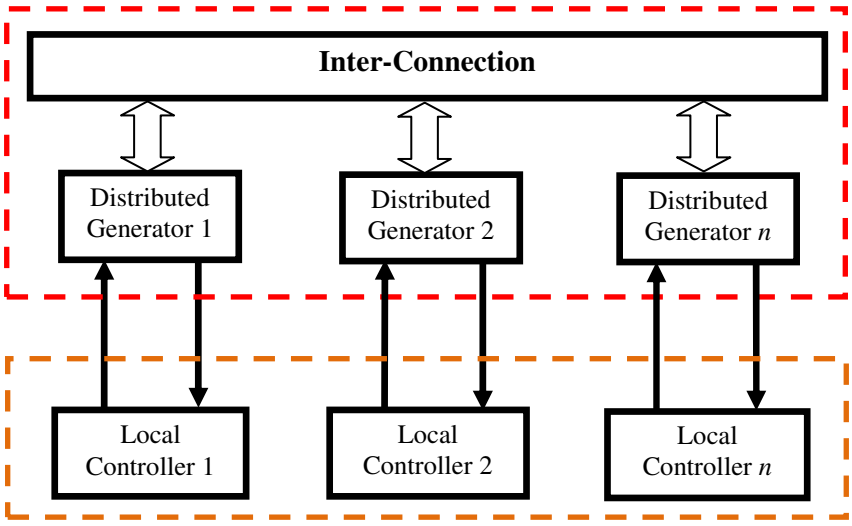

Figure 1.2 A Decentralized Control System

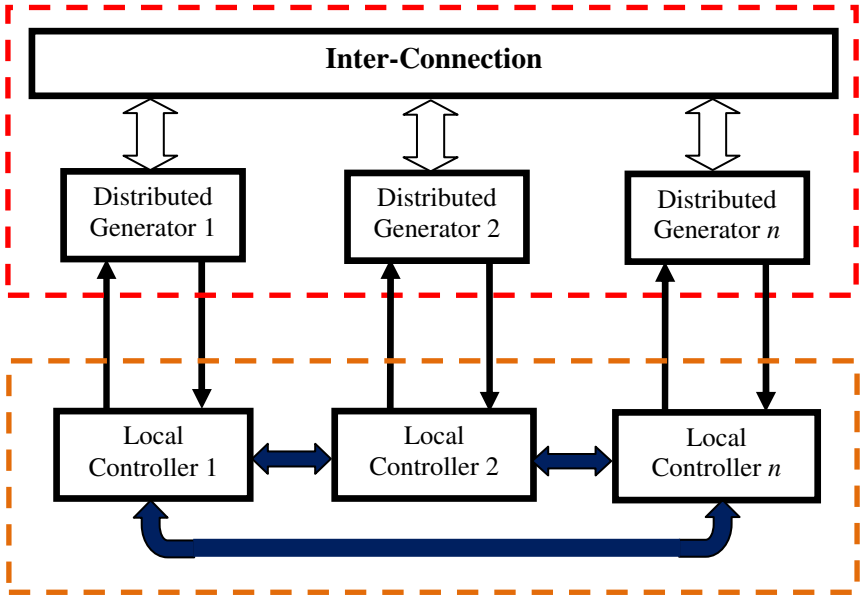

Figure 1.3 A Quasi-Decentralized Control System

Recently, many researchers pointed out the challenges arise from the distributed energy systems evolution and discussed the future communication requirement and specially the relying on the shared networks, see for example, (Beccuti et al. 2006;Bhowmik et al. 2004;Bose 2004;Bose 2005;Chenine et al. 2007;Cory et al. 1993;Ericsson 1998;Fardanesh 2002;Guerrero et al. 2006;Hauser et al. 2005;Holbert et al. 2005;Kok et al. 2005;Mak et al. 2002;Lachs et al. 1996;Mazumder et al. 2005;Moore et. al 1999;Naduvathuparambil et al. 2002;Sidhu et al. 2004;St Iliescu et al. 2008;Tomsovic et al. 2005;Xiaoyang et al. 2005;Ukai et al. 2003;Yongqing et al. 2008;Wu et al. 2005;Zhu et al. 2007;Sun et al. 2008;Wei 1993).

Using shared networks reduces the installation time, maintenance time, the cost and makes the system flexible, easy to diagnose and to reconfigure. In addition to that both the control performance and the reliability will be enhanced. When these systems use the shared networks for control coordination, they become multi-units interconnected networked control

system. Replacing the point to point control strategy with shared network will bring up new challenging problems that must be solved in order to exploit all benefits of using the shared network. Sending the control signals through a shared network will introduce time delay, and some of the data will be lost. The time delay degrades the performance of the system, or it may at the worse lead to instability. When using a shared network rather than a point-to-point communication, it is important either to design a stabilizing controller that takes the time delay into account or to estimate the maximum allowable delay bound (MADB) under which the system is stable and then the network is scheduled to do not exceed the MADB. Even though these two approaches have been used in the literature, there is no relatively simple method to be used in practice for large interconnected system because most of the recent methods concentrate on reducing the conservativeness of the results while the complexity is increased dramatically. The thesis proposes a new method for estimating the MADB in networked control systems with application to the distributed energy systems. The method is based on using the finite difference approximation for the delay term. The proposed method is simpler than the recent published methods while giving comparable results.

1.2 Review of the Previous Research in NCSs

The current trend in distributed energy system control strategies is moving toward implementing the quasi-decentralized control strategy where the control signals are exchanged over communication networks. In the following, we will describe some distributed energy systems that have already started to implement the quasi-decentralized control strategy over a shared communication network.

The power system stabilizer (PSS) implements the decentralized control where the interactions between the units are neglected, and the local controller relies only on the local data (Yang et al. 2006). In order to achieve more robust stability control under a wide range of operating conditions, the quasi decentralized control structure using the available network technology is proposed (Yang et al. 2006). In (Ganjefar et al. 2009) the authors proposed the use of the Internet to improve the dynamic stability of the power system. In their proposal, the PSSs are communicating through the Internet and the problem of the Internet disruption is discussed. The maximum time delay guarantees the stability of the system is estimated through the simulation to be 0.72 sec. The system they are studying is really a NCS but the authors do not use the available methods in the literature for analyzing the NCSs in order to analyze the stability of the proposed control system.

The load frequency is one of the classical centralized power system control problems. The load frequency is achieved by the Automatic Generation Control (AGC) where the frequency deviation is used to sense the change in the load demand. In the AGC, a dedicated communication link is used to send the AGC signals as shown in Figure 1.4. In the case of fault in the dedicated communication link, other communication links are used usually the telephone lines. Because of the increased number of ancillary services, the need for a duplex and distributed communication links becomes more pronounced (Bhowmik et al. 2004).

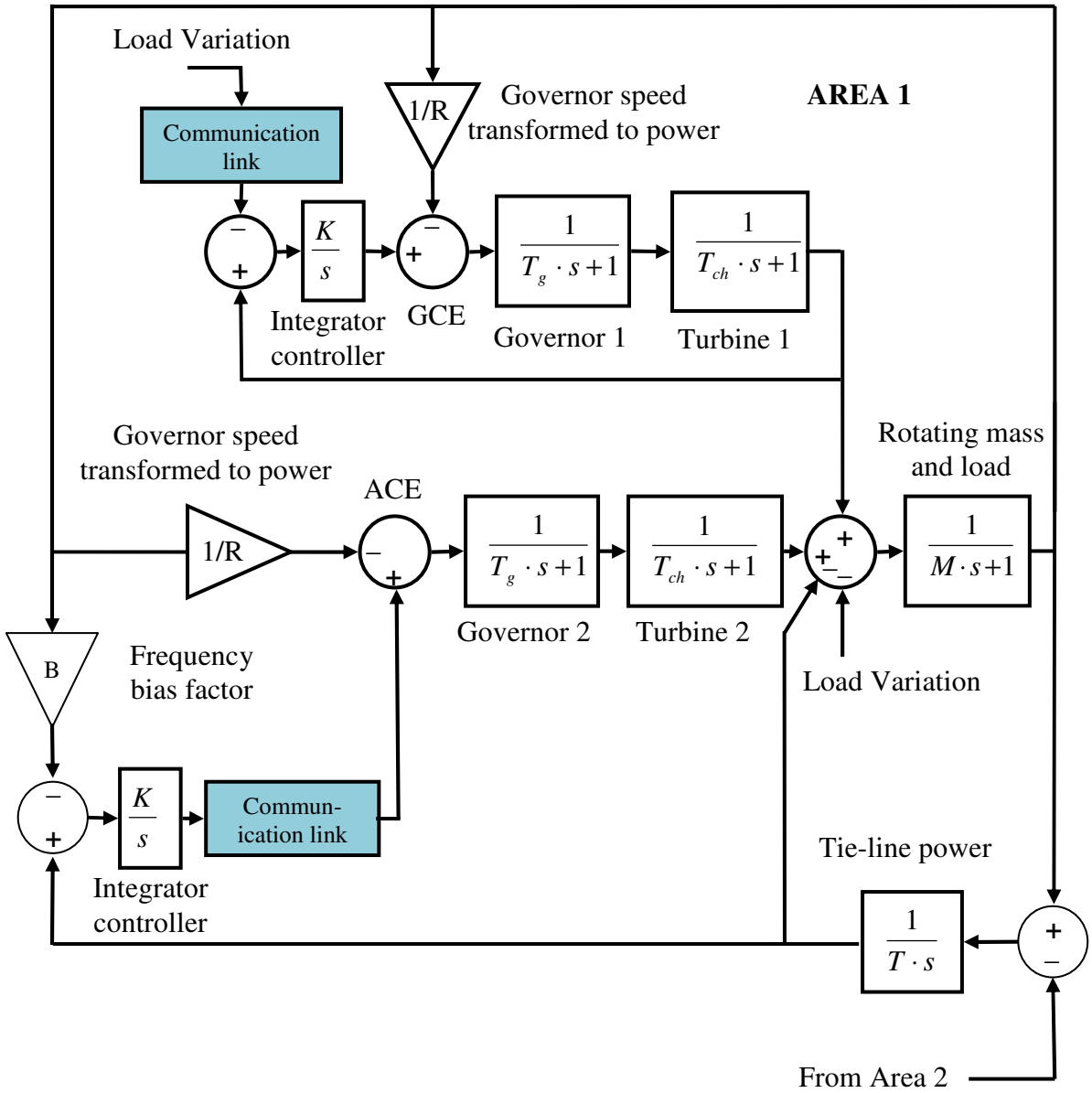

Figure 1.4 The AGC with bilateral contract (Bhowmik et al. 2004).

The system shown in Figure 1.4 consists of three areas with bilateral contracts between the different areas. To guarantee that the frequency is within the limited range the Area Control Error (ACE) and the Generator Control Error (GCE) signals are distributed between the different areas as shown in Figure 1.4. The ACE and the GCE are used to increase or decrease the generated power. Sending these signals through the communication link will introduce time delay and some of these data will be lost. The authors in (Yu et al. 2004)

used a simple stability criteria but rather conservative that was reported in the 1980s and introduced in (Mori 1985;Mori et al. 1989). In (Bhowmik et al. 2004) the authors used the simulation to study the effect of the time delay on the load frequency control system. They considered constant and random time delay and studied the effects of the time delay on the stability of the system although they do not give any method to estimate the control system requirements in terms of the maximum time delay. In (Yu et al. 2004) the problem of the load frequency control is formulated as a general time delay problem which is then solved in Linear Matrix Inequality (LMI) form, but it is only applicable to constant time delays.

Power electronic systems are among the distributed energy systems that the use of shared network can reduce the complexity in the control interconnections. With the advances in power electronic and the hybrid vehicles these systems will become complex systems and hence the use of the wiring will be complex, expensive, less reliable and bulky. In addition to that a failure in one connection may lead to the failure of the whole system, and hence a suitable communication method is a mandatory. In power electronic system usually many converters are connected in parallel. The main reason for paralleling many converters is to increase the output power while increasing the reliability and reducing the cost and the size of the system. The main issue is to maintain regulated output voltage while achieving a good current sharing. Many control strategies have been proposed and implemented in real applications. These methods can be put under two categories; 1) Communication less methods, 2) Communication based methods. In the communication less method, there is no information transfer between the local converters' controllers, and the controllers are fully decentralized. These methods cannot guarantee an equal active current sharing between the modules. In the communication based method such as the master-slave control strategy, the modules communicate with each other, and the control tasks

are distributed between the local controllers. In large-scale systems, the most complex task is the wiring, and the use of shared network can solve this problem, but the stability of the system must be first analyzed. The most widely used control strategy is the master-slave control strategy which is implemented in (Lai et al. 2009;Mazumder et al. 2005;Mazumder et al. 2008) for a parallel DC/DC buck converter system where a communication network is used to transfer the control signals. Parallel DC/DC buck converter can be found in many applications such as the UPS (Uninterruptible Power Supply) (Shanxu et al. 1999). In parallel DC/DC converters, all the converters should share the load current equally by control connections between the converters. To achieve the active current sharing the reference current signal is broadcast to all the slaves in the system, and hence no direct control connection is required (Lai et al. 2009;Mazumder et al. 2005;Mazumder et al. 2008). The wireless communication is used in an interactive power network in (Acharya et al. 2006) where the authors studied the effects of the network characteristics on the stability and performance of the control system. They proposed that the power network could have three states, which are; nominal, rerouting and clustered state. In the nominal mode, the power modules communicate through the network. When a fault occurs in one of the channels, the signals are rerouted, if the rerouting cannot achieve the stability; then the units enter the clustered mode that implements the decentralized control. In (Zhang et al. 2007) the authors are trying to treat the power electronic modules as communication nodes. The required bandwidth for the different control tasks is estimated, and they are classified into fast, medium-speed and eruptive control loop and depending on these estimations the suitable network is chosen. The authors mentioned that there is a trend towards the integration of both the power electronic and the communication.

The Microgrid is one of the possible forms of the power system evolution (Katiraei et al. 2008;Lasseter 2001;Lasseter et al. 2004;Markvart 2006). The Microgrid can be a system of parallel DC/DC converters or parallel DC/AC inverters. In the AC Microgrid in addition to the current sharing requirement the synchronization between the parallel inverters is necessary to eliminate the circulating currents. A good survey on the control techniques and the problem of the communication in parallel three-phase inverters is given in (Mohd et al. 2010;Prodanovic et al. 2000). In the Microgrid there are three different views, two of these views adopt the use of the communication while the other view adopts the decentralized control (Prodanovic et al. 2006). The authors in (Pogaku et al. 2007) claims that the communications based methods can be implemented if the microsources are in close proximity, and the communication link must meet the system bandwidth requirement with a good reliability. With the advances in the network theory and the network technology, the assumption of the small area or close proximity is not required. The communication problem in the Microgrid is discussed in (Green et al. 2007) where the communication link is used for power sharing and synchronization, and the required bandwidth is estimated to be around 100 kbit/s. In the parallel inverters, both the current sharing signal and the synchronization signals are sent through the communication link. Because of the complexity in the wiring, some researchers suggested control strategies without any communication between the converters. All of these methods depend on the so-called droop control method where the active power is used to modulate the voltage and the frequency is modified through the real power (De Brabandere et al. 2004;Ju et al. 2007;Tuladhar et al. 1997). The main drawbacks are the slow dynamic, sharing error, and the method cannot be implemented if the loads are nonlinear. Moreover, since the droop control is a fully decentralized control method it is not superior to the centralized control method because of the slow dynamic

and the sharing error. Some researchers suggested the use of low bandwidth communication links to reduce this error, which makes the control system quasi-decentralized. For example, in (Marwali et al. 2004) two control loops are used; one implements the droop control, which is local, and the other loop implements the average power control through a low bandwidth communication link. In the recent years, the Microgrid attracted more attention and the use of shared networks has been considered in many papers. In (Yongqing et al. 2008) a system of two parallel three-phase inverters driving a motor is controlled over CAN (Controlled Area Network) bus where the master-slave control strategy is used to distribute the control tasks between the different inverters.

When the distributed energy system implements the quasi-decentralized control strategy over a shared network, it will form a networked control system. From the previous literature, I found that either no method for the stability of the system is given or the authors use some stability analysis methods that are rather complex. In the following section, the basic definitions and issues in NCSs are briefly described.

1.3 Description of Networked Control Systems

When a traditional feedback control system is closed via a communication channel, which may be shared with other nodes outside the control system, then the control system is called an NCS (Networked Control System). An NCS can also be defined as a feedback control system wherein the control loops are closed through a real-time network (Wang, F. Y et al. 2008). The defining feature of an NCS is that information (reference input, plant output, control input, etc.) is exchanged using a network among control system components (sensors, controllers, actuators, etc., as shown in Figure 1.5).

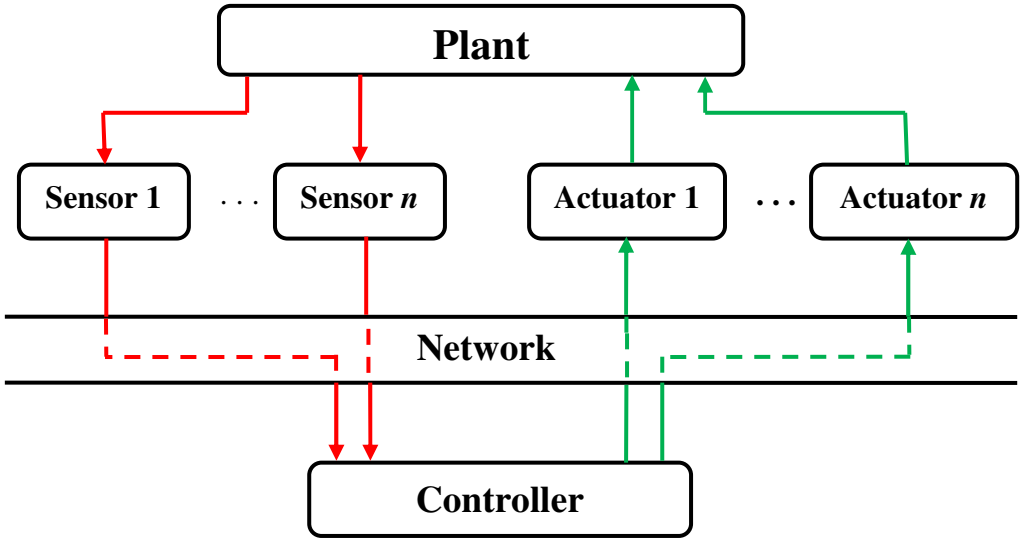

Figure 1.5 A Typical Networked Control System

The NCS notation used for the first time by Gregory C. Walsh (Walsh al. 1999). Some researchers refer to NCSs as distributed real-time control systems (Nilsson 1998). Because NCS integrates control systems, communication networks, information theory and computer science, some references refer to NCSs as Integrated Communication and Control Systems ICCSs (Ling et al. 2007) but the NCS notation is used in this thesis.

In NCS, the information exchange has various time delays, which are defined as the *networked induced delay*. This delay may be constant, varied or even random and the time delay modelling is a very challenging research area. This induced delay may degrade the performance of the system or may destabilize the control system. Another point that should be pointed out is the *Packet Dropouts* which means some data may not have the chance to reach their destination and the question that should be asked here is to *what extent can the distributed system survive in the cases of time delay or losing some data?*

Closing the loop through the shared communication network makes the analysis and design of NCSs complex and the conventional control theory assumptions (such as

zero time delay from the sensor to the controller and from the controller to the actuator) became void.

Communication networks have been utilized in real-world applications for about thirty years (Baillieul et al. 2007). The main difference between these systems and the networked control systems is that the communication networks were dedicated, while in NCSs they are general-purpose, and the new concepts in communications and networks have been merged with the control concepts, and it became a complete system (single entity) (Wang, F. Y. et al. 2007).

NCS is not only a multidisciplinary area closely affiliated with computer networking, communication, signal processing, robotics, information technology, and control theory, but it also puts all these together beautifully to achieve a single system which can efficiently work over a network (Wang, F. Y. et al. 2008). In addition, NCS has many advantages such as modularity, low costs, reduced weight, decentralization of control, integrated diagnosis, simple installation, quick and easy maintenance, and expandability (it is easy to add/remove sensor, actuator or controller with low cost). NCS can be easily modified or upgraded. NCSs are able to fuse global information to make intelligent decisions over large physical spaces. These points make the NCSs suitable for distributed energy system applications. On the other hand, we have communication constraints, delay, which may be fixed, varied or even random. The absence of a universal clock makes the assumption of constant sampling intervals unrealistic (Ling et al. 2007). Losing some data and the latency of arriving the data due to the network nature makes the system stochastic (Ling et al. 2007).

In the classical control theory, the control signals and the sensor signals are point-to-point connected. In the NCS, the situation is quite different because both the actuator and the sensor signals are transmitted through a communication network, and the control system performance will depend strongly on the characteristics of the communication network. The random time delay may cause another problem in the control system which is the packets-out-of-order. The researchers in the last few years concentrated on the following issues:

1- NCS analysis and design.
2- Network architecture, protocols and scheduling.
3- Experimental and simulation studies.
4- NCS modelling (especially time-delay and data dropout modelling).
5- Stability analysis.

Non-linear NCS has not been studied extensively (Jiang et al. 2008b). Furthermore, the study of NCSs for a particular application and the use of a specific communication network have not been considered in many papers. The time delay and packet dropouts are characteristics of the network, and even if they can be kept very low with good scheduling and reducing network traffic they cannot be totally eliminated. Therefore, new methods for compensating these two imperfections are very important research areas.

There are also other issues such as protocols, scheduling, communication constraints, etc., but these issues affect the time delay and packet dropouts so from control system view point our interest will be in the time delay and data dropouts. In the following section, a brief description of the basic problems concerning NCS is given.

1.3.1 Network-Induced Delays in Networked Control Systems:

As we discussed previously the network-induced delay may degrade the performance of the system and even may lead to system instability. In the analysis of the NCS, the assumption of constant sampling is not always valid (Ling et al. 2007). Figure 1.6 shows a system with varying time delays.

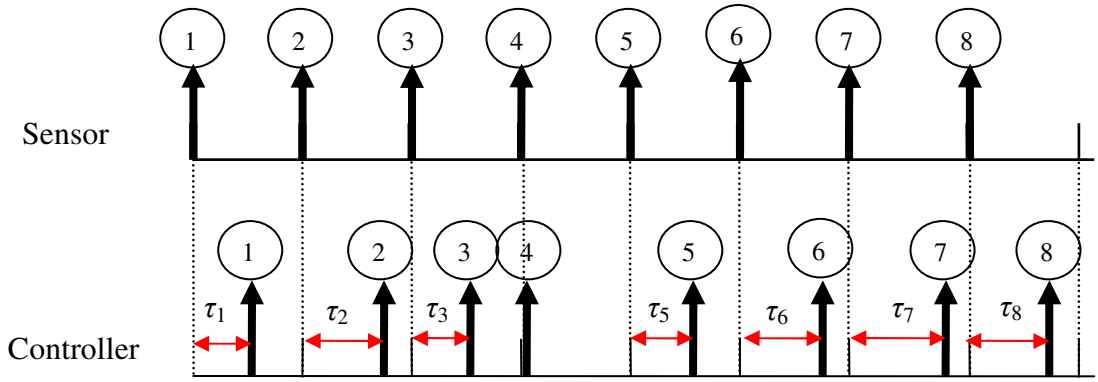

Figure 1.6 Time Delay in NCS

Time delay can be made small and deterministic by good scheduling and giving some signals high priority, and the system can be treated as an ordinary deterministic time delay system (Nilsson 1998). Time delay affects the performance and the stability. The factors that affect the time delay are: the network load, the network scheduling, the network bandwidth, the message size and the message priority.

The time delay in NCSs can be modelled based on the statistics of the time delay. A model that exactly characterizes the network induced delay is difficult to obtain but generally, a good and reliable model can be obtained. Time delay can be dealt with as a constant if the delay introduced by the network is less than the application's delay (Nilsson 1998).

Many researchers proposed control methods to compensate the time delay effects. In (Sadeghzadeh et al. 2008) they solve the time delay problem by using a variable sampling period approach, and a neural network was developed to estimate the time delay. Next, this estimated time delay is taken as the sampling period. However, they restricted their models to time delays less than one sampling period, and they assumed that the time delay is governed by some function. In (Liu et al. 2005) the authors consider random time delay governed by Markov Chains. Some papers proposed fuzzy compensators for the time delays, for example, in (Jiang et al. 2008b) they use T-S fuzzy model for the NCS. Also the model predictive control and the Markovian jump system approach are addressed in many papers. A detailed review on the time delay problem in NCS is presented in Chapter 3.

1.3.2 Packets Dropouts:

In some cases due to bandwidth or communication constraints, the message may not be transmitted in a single packet but split into multiple packets. Due to the network nature, these packets may be delayed, or they may be even lost as shown in Figure 1.7 or may arrive but out-of-order as shown in Figure 1.8. Packet dropouts may be considered as a special case of an infinite time delay.

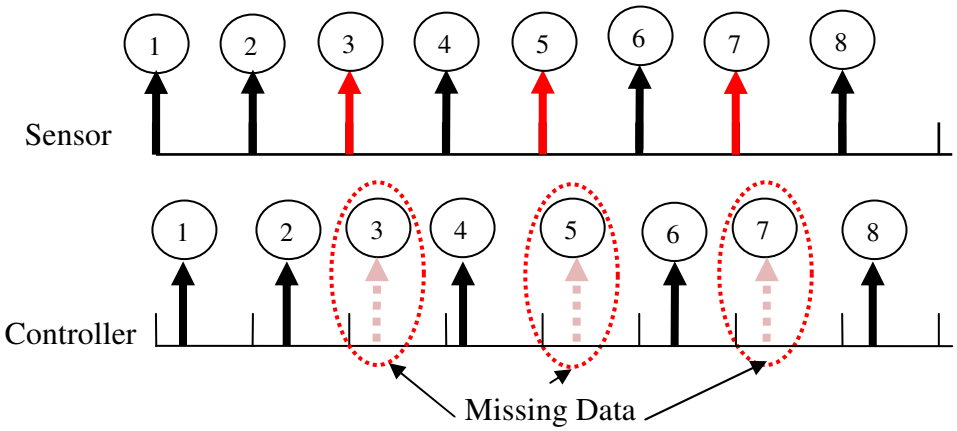

Figure 1.7 Packets Dropouts in NCS

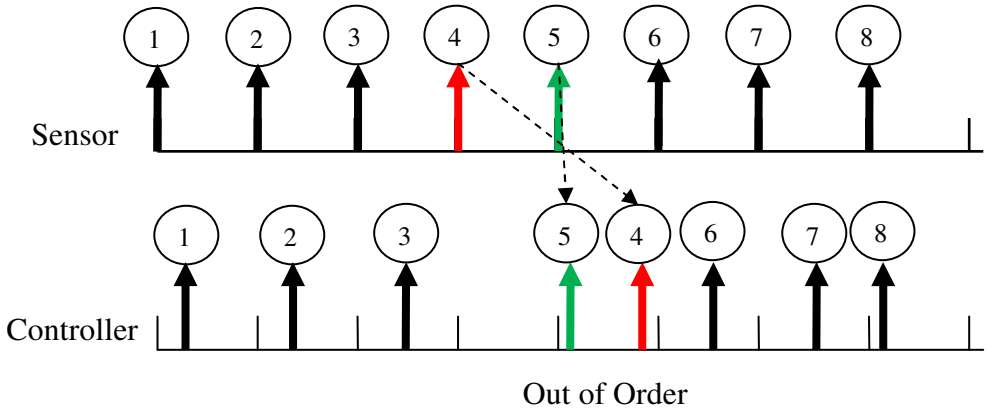

Figure 1.8 Packets out-of-order in NCS

When a packet is lost there is no need to retransmit it again, an acknowledgement must be sent to transmit a new data. In (Wang, Y.-L et al. 2008) the design of a networked control system based on Lyapunov function is addressed where they took the packet out-of-order into account. In (Millan et al. 2008) the development of a generalized predictive control scheme to overcome the high dropout levels is presented.

1.3.3 NCSs Structures:

Networked control system can have one of the following structures (Wang F. Y et al 2008) as shown in Figure 1.9: Direct Structure and Hierarchical Structure. These two structures are found in many distributed energy systems. In the direct structure, the sensors and the actuators are directly connected to the network (and the plant), but the controller is connected to them through the network. Using shared network to transfer the measurements, from sensors to controllers and control signals from controllers to actuators, can greatly reduce the complexity of the connections.

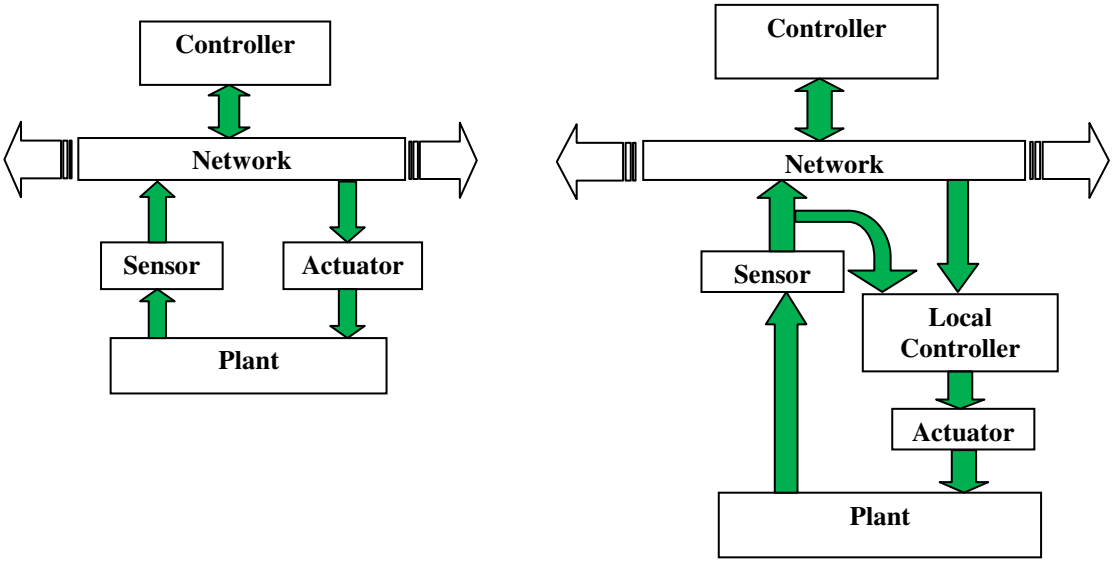

Figure 1.9 (a) Direct Structure of NCS, (b) Hirarchical Structure of NCS

In the hierarchical structure, the system is divided into subsystems; with each subsystem has sensor, actuator and controller in a hierarchical structure. In this structure, the local controllers can communicate with each other and with the central controller to achieve the global goals of the system. This structure can be found in parallel DC/DC and parallel DC/AC converters in Microgrid.

1.3.4 Networked Control System Stability:

The stability is a crucial part in designing any control system. In NCS, the main causes of instability are the time delay and the data dropouts. The stability analysis is very complex in the presence of the time delay because the latter introduces an exponential term in the characteristics equation which replaces the algebraic equation with transcendental equation.

The control system designer should take the induced time delay and packet dropouts effects into account. An accurate model for the time delay should be obtained in order to incorporate its effect in the control system performance. The time delay depends on many

factors such as the network type; the protocol used, the bandwidth and the packet size and as a result the time delay may have one of the following forms; *Constant (Fixed) Time Delay*, *Varied Time Delay* and *Random Time Delay*. In designing NCSs a stability criterion has to be made to ensure system stability under some time delay conditions. The stability theory that has to be applied depends on the network characteristics and hence on the time delay.

If the sampling time is equal or larger than the maximum time delay, then the time delay can be treated as a constant time delay and the existing time delay control methodology can be used. The simple stability theories for discrete systems can be applied in this case. In some networks, the time delay may be time varied but periodic and in this case more difficult methods have to be applied.

In some cases, the time delay may be random due to the network and protocol characteristics. These random time delays can be modelled based on probabilistic methods, and Markov Chains is one of these methods. The stability analysis of this type of time delay is the most challenging because more advanced and sophisticated techniques must be used to formulate the random delay and nonlinear control theories must be applied. Nilsson (Nilsson 1998) proposed an optimal stochastic control method to control NCSs with random time delay, which is modelled using Markov Chains. Also the Markovian Jump Linear System approach and the model predictive control have been reported in many papers (Liu, Lei-Ming et al. 2005;Liu et al. 2008;Xiao et al. 2000;Yu et al. 2008; Zhang, Guofeng et al. 2008;Wu et al. 2009;Jing et al. 2007).

In most of the stability and stabilization control problems, the final stability or controller design is in the form of Linear Matrix Inequality (LMI) which has to be solved numeri-

cally. The LMI arises in many control design and stability problems. The applications of LMI in control theory are reported in (Boyd et al. 1995). The LMI has the following form:

$$\mathbf{S}(x) = \mathbf{S}_0 + \sum_{i=1}^{m} \mathbf{x}_i \mathbf{S}_i > 0 \qquad (1.2)$$

where $\mathbf{x} \in R^m$ is the variable and $\mathbf{S}_i = \mathbf{S}_i^T > 0$ is a positive symmetric constant matrix. The strict LMI in (1.2) is a set of polynomial inequalities in the variable $\mathbf{x}$. The LMI (1.2) is a convex problem that can be solved efficiently using the Matlab toolbox. This form appears in many control problems (Boyd et al. 1995). The advances in convex optimization algorithms made the LMI a powerful design tool. The Matlab developed the LMI toolbox (Gahinet et al. 1995) that implements interior-point algorithms for solving the LMI problems. If the LMI problem can be solved, we say that the LMI is feasible if not it is infeasible. The solution of (1.2) is called the feasible set.

1.4 Main Contributions of the Thesis

The contributions of the thesis can be summarized into the following:

- For NCSs with bounded time delays, a new stability and maximum allowable delay bound estimation method has been proposed. The method adopts the finite difference approximation for the delay term in the analysis. A theorem is derived for estimation of the maximum allowed time delay to maintain the system stability. A further derived corollary (Corollary 3.1) has a simple structure in a scalar inequality form for MADB estimation. The results of the estimated MADB obtained through Theorem 3.1 and Corollary 3.1 are comparable with the results obtained through

the methods in the previous published literature, however, the method proposed in this thesis has a much simpler procedure in applications. Furthermore, the method links the controller parameters to the MADB and can be used to guide in the process of choosing the controller parameters. The same methodology has been applied to NCS with dynamic controller. Theorem 3.4 and Corollary 3.5 are derived while neglecting the actuator to the controller time delay. While Theorem 3.5 and Corollary 3.6 are derived when the actuator to the controller time delay is not neglected. Theorem 3.7 is proposed for multi-units interconnected system and applied to three generator power system, and the value of the MADB is estimated. It is found that the MADB can be achieved with the current network technology.

- The proposed method has been extended to study the stability and maximum allowable delay bound for a class of nonlinear NCS. A new stability criterion is derived for a class of nonlinear NCS with norm bounded nonlinearity. The theorem is based on writing the norm bounded constraint as LMI and use of the finite difference approximation for the delay term and then the quadratic Lyapunov function is used to derive theorem in LMI form. The results of the theorem have been compared with some of the published results, and the method is simpler while giving comparable results.
- Due to the component aging, noise in measurements, and slowly time varying parameters all the system performances are subject to uncertainties. A new stability theorem for uncertain NCS with norm bounded uncertainties has been derived. Again, the proposed method is much simpler in applications than those previously published methods.

- When the time delay is governed by Markov Chains the NCS can be modelled as discrete-time Markovian jump system and the stability of the system is formulated as Bilinear Matrix Inequality (BMI). The BMI is not a convex problem and cannot be solved directly. In this thesis, the V-K iteration algorithm is used to solve the BMI where the BMI is divided into three basic LMI problems that can be solved using the Matlab LMI toolbox. The problems to be solved can be considered as three types: feasibility problem, eigenvalue problem and generalized eigenvalue problem. We proposed improved V-K algorithm by maximizing the decay rate in both the V- and K-iteration loops.
- A parallel DC/DC buck converter system implements master-slave control strategy through a shared network is modelled as NCS, and it is used as one of the case studies. The stability of the system in the presence of the time delay is analyzed. The MADB is estimated, and it is found that the parameters that affect the MADB strongly are the voltage controller gain, the output feedback gain factor, and the load resistance. The stochastic stability of the parallel DC/DC buck converters is analyzed. The range of the voltage controller parameters that achieves the stochastic parameters is determined.

The list of the published papers is given below:

[1] A. F. Khalil and J. Wang, “Time Delay Tolerance Estimation for Linear Control System Stability Analysis using a Finite Difference Method”, In the Proceedings of the 15th International Conference on Automation and Computing, 2009, Luton, UK, pp. 70-75.

[2] A. F. Khalil and W. Jihong, "A new stability and time-delay tolerance analysis approach for Networked Control Systems," In the Proceeding of the 49th IEEE conference on Control and Decision 2010, pp. 4753-4758.

[3] A. F. Khalil and J. Wang, "A New Stability Analysis and Time-Delay Tolerance Estimation Approach for Output Feedback Networked Control Systems," In the Proceeding of the United Kingdom International Control Conference, 2010 pp. 4753-4758.

[4] A. F. Khalil and J. Wang, "A New Method for Estimating the Maximum Allowable Delay in Networked Control of bounded nonlinear systems," The 17th International Conference on Automation and Computing (IEEE), Huddersfield, UK 2011, pp. 80-85.

1.5 Thesis Outline

The thesis is organised into seven chapters. Chapter 1 is an introductory chapter, and the rest of the thesis chapters are summarized below:

Chapter 2 is dedicated to time delay analysis in two control networks which are the CAN and the Ethernet. The time delay modelling is based on the time delay analysis and is crucial part in studying the stability of NCS. We chose the CAN and the Ethernet because they are among the widely used computer networks for control systems. The description of the CAN and the Ethernet with a brief review on the control networks is given in this chapter. The time delay simulation analysis has been carried out using the TrueTime 1.5 simulator whose basic blocks are briefly summarized. A simulation study has been carried out to study the characteristics of the time delay in the CAN and the Ethernet. Different scenarios have been simulated with different message priority, message length, bit rate and network load.

Chapter 3 reports the proposed new method for stability analysis and MADB estimation for NCS. The chapter starts with literature review on the time delay problem in NCS. Then the mathematical model for NCS with state feedback controller is represented, and Theorem 3.1 and Corollary 3.1 are derived. Theorem 3.1 and Corollary 3.1 are used to estimate the MADB. Many examples are picked-up from the literature, and the results are compared

with those obtained using the proposed method. The same methodology for the NCS with state feedback controller has been applied to NCS with dynamic controller and to multi-units interconnected NCS. For the NCS with dynamic controller, two cases are studied; the first with neglecting the time delay between the controller and the actuator and the second case when the time delay from the controller to the actuator is considered. The results of the theorem and the corollary derived for the multi-units interconnected systems have been applied to a power system consist of three synchronous generators. The MADB for the three generators system is estimated, and the simulation results for the system are carried out to show that the MADB lies within the stability margin.

Chapter 4 deals with the stochastic stability of NCS when the time delay is modelled using Markov Chains. At first the jump system is described with a short review on its application in NCS. Then the NCS with both state feedback and dynamic controller are modelled as a Markovian jump system. The sufficient conditions for the stability of the system are given, and the problem is formulated as BMI. The V-K iteration algorithm for solving the BMI is described with the details of solving the three basic problems in the V-K algorithm using the LMI matlab toolbox. The V-K iteration algorithm is applied to the cart and the inverted pendulum problem.

Chapter 5 reports the stability analysis and MADB estimation for parallel DC/DC buck converter controlled through a shared network. The model of the parallel DC/DC buck converter is presented in this chapter, and the master-slave control strategy is explained. Then a case study system consists of three parallel DC/DC buck converters is analyzed where the MADB is estimated. The proposed method is compared with one of the published methods. Using the proposed method in chapter 3 the parameters that affect the MADB are studied. Under the bounded time delay assumption, the proposed method for

estimating the MADB is used to find the range of the voltage controller gain that gives MADB larger than the worst-case time delay in the CAN and the Ethernet with constant, periodic, and random but bounded time delay. The last section of this chapter is devoted to design a stochastic stabilizing controller for the parallel converters system when the time delay is modelled using Markov Chains.

Chapter 6 proposes two new stability and MADB estimation methods, one for a class of NCS with norm bounded nonlinearity and the second method for uncertain NCS. The mathematical model for a class of nonlinear NCS is presented in the chapter, and two stability criteria are derived. The first stability theorem is in LMI form and is based on using the finite difference approximation for the time delay term and writing the nonlinear constraint as LMI. Another stability criterion in scalar inequality form is derived, and the results of the estimated MADB are compared with the results available in the literature. Then the stability of uncertain NCS is studied and a method for estimating the MADB for the uncertain NCS is presented. The stability theorem is in LMI form, and many examples picked from the literature for comparison.

Chapter 7 is the concluding chapter where the conclusions drawn from this research are summarized along with some suggested future projects.

1.6 Summary

This chapter introduces the thesis from its background, motivation, and main contributions to review of the concepts and current methods. The chapter serves a preparation and overview to the whole thesis.

CHAPTER TWO: TIME DELAYS IN SHARED NETWORKS

2.1 Introduction

Control networks are the backbone for any networked control system, for instance, a distributed energy system is controlled through a shared network. The induced time delay in a network can degrade the performance of the system or destabilize the system. In networked control systems, the control network is defined as the medium by which the sensors, the actuators and the controllers can exchange their information. The main difference between control networks and data networks is that the control networks can support real-time constraint (the guarantee of receiving the message within a bounded time) which may not be achieved in data networks. Another difference that can designate between these two networks is that both the message length and the bit rate are high in data networks while in control networks, the messages are bursted and short. In this chapter, the time delay is analysed in two candidate control networks, the CAN and the Ethernet. The CAN implements a deterministic protocol where the time delay can be made constant or bounded. On the other hand, the Ethernet is a non deterministic protocol because the network cannot be pri-

oritized. In this study TrueTime 1.5 simulator is used. The TrueTime 1.5 simulator operates in Matlab/Simulink environment but m-files for configuring the blocks must be written. A brief description of the simulator is presented in this chapter. The features associated with the time delays in these two networks are studied with different message length, priority, and load. Furthermore, the time delay characteristics are investigated for transmitting either periodic or random messages.

2.2 Time Delays

The time delay is defined as the difference between the time of receiving the message and the time of sending the message (Lian et al. 2001). The total time delay, T_{total} , consists of pre processing time delay, T_{pre} , network time delay, T_{dn} , and post processing time delay, T_{post} . The pre-processing time delay is composed of analogue to digital conversion, computation time and encoding time. The post processing time delay is composed of digital to analogue conversion, computation time delay and decoding time delay. The network time delay is the time when the data are ready for transmission until the data are received by the designated destination. The network time delay consists mainly of 1) Waiting time delay, T_w, the sending node has to wait a specific time until the network becomes idle then it starts transmission. 2) Retransmission time delay, T_{retr} , if a collision occurs the sending node should wait for a random time then it starts retransmission. 3) Transmission time delay, T_{tr} , the time required to transmit the message and it depends on the message length and the bit rate. The time delay is given by:

$$T_{dn} = T_{tr} + T_{retr} + T_w \tag{2.1}$$

$$T_{total} = T_{pre} + T_{dn} + T_{post} \tag{2.2}$$

To understand the time delay in computer networks a statistical analysis should be conducted in order to derive the time delay characteristics from their probabilistic distribution. According to (Lian et al. 2001) the parameters that affect the time delay are the access delay, transmission time, response time, message delay, message collisions, message throughput, packet size, network utilization, and determinism boundaries. In this work, we use simple models for the time delay and the network utilization to estimate the time delay and network load. In this case, the time queuing and buffering time delay are represented by the waiting time delay.

2.2.1 Network Schedule

Scheduling algorithms are constructed to handle the flow of messages among the network nodes. The performance of the NCS depends strongly on the network scheduling (Branicky et al. 2002). This means to assign a time schedule for all the components in the control systems, which are the sensors, the actuators and the plants. The network scheduling algorithm assigns the message priorities in the network. The NCS can be schedulable if all the tasks within the NCS can be accomplished before the deadline (Branicky et al. 2002).

2.2.2 Network Utilization

The network utilization can be defined as the percentage of the total message lengths over the period time or running time, the utilization is given by (Lian et al. 2001):

$$U_T = \frac{\sum_{i \in N_{node}} \sum_{j=1}^{m^{(i)}} \left(T_{tr}^{(i,j)} + T_{retr}^{(i,j)} \right)}{T_{\max}} \tag{2.3}$$

where $T_{tr}^{(i,j)}$ is the time required to transmit the $(i,j)^{\text{th}}$ message from node i to node j. $T_{retr}^{(i,j)}$ is the time required to retransmit the $(i,j)^{\text{th}}$ message if a collision has been detected. $T_{\max}$ is the period of messages transmission. U_T is the utilization. $m^{(i)}$ is the number of the messages to be sent by the i^{th} node. The utilization is used to describe the network load level. Under low load the utilization approaches zero and when the utilization approaches one or larger than one then the network is said to be saturated or overloaded. Different networks can show different time delay characteristics under high utilization load.

2.3 Control Networks

Computer networks can be classified into data networks and control networks. Data networks are intended for transmitting data messages such as video, audio, text messages, etc. The Internet and the Ethernet are two of the most well-known examples of data networks. The data networks implement protocols that do not support real time control tasks but intended for transmitting long messages with high bit rate. Although the data networks are characterized by high bit rates and long messages, the receiving of the message within a bounded time slot is not guaranteed. On contrast, control networks implement protocols that support real time constraints and in many cases, the network can be made deterministic. The control networks such as the CAN, Field buses (FIB), and PROFIBUS (Process Field Bus) are found in the industry, and the messages are bursted with relatively slow data rates.

Due to the availability of data networks almost in everywhere they gathered a lot of attention to be used as a communication medium for NCS (Montestruque et al. 2004;Chow et

al. 2001). One of the candidate networks is the Ethernet that implements the CSMA/CD (carrier-sense multiple access with collision detection) protocol set by the IEEE 802.3 network standard and can support real time constraints.

2.3.1 Controller Area Network (CAN)

The motive for developing CAN was from the car industry in order to reduce the cost, weight and complexity in the wiring in a vehicle (Baillieul et al. 2007). The CAN is a serial communication bus developed in 1983 at Robert Bosch GmbH and realized in 1986 (Baillieul et al. 2007). The CAN implements the carrier-sense multiple access protocol with arbitration on message priority (CSMA/AMP) where each node must listen to the network before trying to transmit. The CSMA/AMP is a prioritized deterministic protocol where the nodes or the messages can be assigned to a priority, and the arbitration is used to win the access to the network. The message of the CAN is shown Figure 2.1. The CAN message or frame can be divided into the data frame (broadcast a message to the CAN bus), remote frame (Requests transmission of message), error frame (Signals error condition) and overload frame (Special error frame). The total overhead is 47 bits, and the data message can be from zero to 8 bytes. The identifier in the arbitration field is 11-bit in the standard CAN while it is 29-bit in the extended CAN, which allows 2^{29} priority levels. The abbreviations in Figure 2.1 are: SOF (Start of Frame), RTR (Remote Transmission Request), the DLC (Data Length Code) and the two bits r_0 and r_1 forms the control field, CRC (Cycling Redundant Code), ACK (Acknowledgement), EOF (End of Frame), int (Interface Space). For more detailed description for the CAN frame the reader can refer to (Bosch 1991).

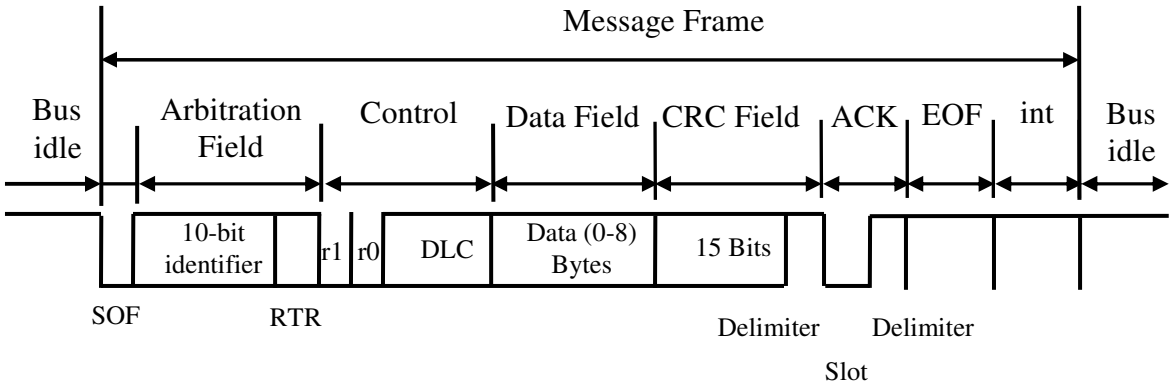

Figure 2.1 The message frame format of CAN (Lian et al. 2001)

When a node tries to transmit it listens to the network if it is idle, then the node starts to transmit directly. If many nodes are trying to transmit at the same time the arbitration is used to gain access to the network. When two nodes are transmitting at the same time the identifiers are sent if one node receives the same bit it has sent, then that node will win the arbitration. Depending on the bus length the maximum bit rate in the CAN can be up to 1 Mbit/s. The bit rate with different bus lengths is given in Table 2.1. The number of the nodes in the CAN depends on the network utilization and for a higher number of nodes; the multilevel network approach can be used. However, the CAN is a deterministic protocol that guarantees a fixed time delay for the highest priority node; the bit rate is low compared to other networks such as the Ethernet.

Table 2.1 The bit rate with different bus lengths (Corrigan 2008)

Bus Length/ m	25	50	100	250	500	1000	2500	5000
Bit Rate Mbit/s	1	0.8	0.5	0.25	0.125	0.05	0.02	0.01

2.3.2 Ethernet

The Ethernet is one of the most widely used local area networks (LANs). The Ethernet is mainly intended for transmitting large data messages and was introduced in beginning of the 1980s. In contrast to the CAN, the Ethernet is not a deterministic protocol because it

implements the carrier-sense multiple access with collision detection (CSMA/CD). The bit rate in the Ethernet can be ranged from the standard 10 Mbit/s up to 100 Gbit/s. The Ethernet message is shown in Figure 2.2. The Preamble bits for synchronization and the start of delimiter are 8 bytes, and the minimum message length is 64 bytes.

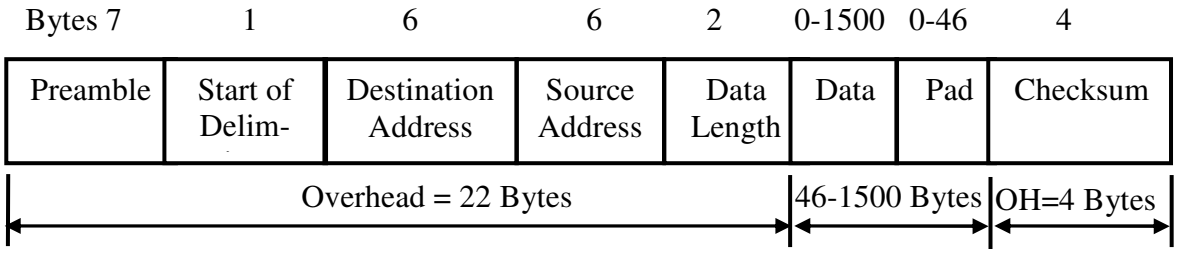

Figure 2.2 The message frame format of Ethernet (Lian et al. 2001)

The minimum packet size in the Ethernet is 46 bytes and if the data message is less than 46 bytes padded bits are automatically added to make the data message 46 bytes. Including the overhead and checksums bits, the minimum Ethernet message is 72 bytes. When any node starts to initiate a transmission, it listens to the network if a collision is detected the node waits for a random time specified by the binary exponential back of algorithm (BEF) (Lian et al. 2001). This random time is randomly chosen between zero and (2^n-1) slot time (Ethernet message transmission time), where n is the number of collisions detected by the node. For a 10 Mbit/s Ethernet the slot time is 51.2 μs (=512/10,000,000). After ten collisions the retransmission time is fixed to 1023 slot time (Lian et al. 2001). As the number of the collisions exceeds sixteen, the network reports transmission error to the sending node. The main disadvantage in the Ethernet is the unfairness in the Ethernet protocol. Under heavy load the number of collisions will be high, and the protocol cannot guarantee an equal chance to all the nodes, and the time delay in this case may not be bounded which violates one of the networked control system requirements.

2.4 TrueTime 1.5 Simulator

TrueTime 1.5 is a software based on Matlab/Simulink, and it is dedicated to the simulation of real-time control systems (Andersson et al. 2005;Henriksson et al. 2004;Henriksson et al. 2006;Sui et al. 2010). The software is based on Matlab/Simulink but source code programs in Matlab or C++ (needs a compiler) must be written to initialize the TrueTime blocks and to be executed during the run. TrueTime 1.5 simulator is freeware developed in Lund University and can be downloaded free from http://www.control.lth.se/truetime. The TrueTime Library is shown in Figure 2.3. The TrueTime 1.5 simulator contains six basic blocks, which are the kernel, the network, the wireless network, the battery, the sending and the receiving blocks.

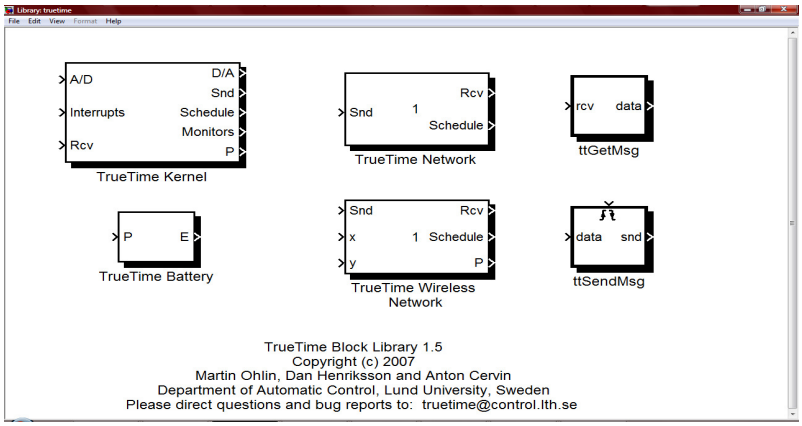

Figure 2.3 The TrueTime Block Library.

The TrueTime 1.5 simulator blocks are connected with the ordinary Simulink blocks to form a real-time control system such as the networked control system. Before a simulation can be run, however, it is necessary to initialize kernel blocks and network blocks, and to create tasks, interrupt handlers, timers, events, monitors, etc., for the simulation. The TrueTime 1.5 supports networked control system simulation. In the following section, the time delay is studied in the CAN and the Ethernet using the TrueTime 1.5 simulator.

2.5 Simulation Results for the CAN and the Ethernet

Different scenarios have been implemented in the TrueTime 1.5 simulator to study the time delay in two popular control networks, which are the Ethernet and the CAN. The simulator supports only packet level simulation so the parameters that will be considered are the bit rate, the message size, the priority and the utilization.

2.5.1 The Time Delay Analysis in the CAN

The CAN is a deterministic protocol intended for short messages. In this simulation study, the CAN has seven nodes that represent the load and the system nodes. Three nodes represent the system while the other four simulate the load on the network. The parameters that affect the time delay are investigated; these are the priority, the bit rate, the message length, the utilization, and the message type (periodic messages or random messages). The TrueTime 1.5 Simulink implementation of the CAN with seven nodes is shown in Figure 2.4. The system node has middle priority on the network, but the system nodes are the only active nodes in the network. The system nodes are actuator1, actuator2 and the sensor. This simulates a distributed energy system implementing the master-slave control strategy. The following cases are considered:

- **Under no Load**: The system nodes are the only active nodes in the network.
- **Periodic Load:** All the nodes in the network are periodic.
- **Random Load:** The load nodes are random.

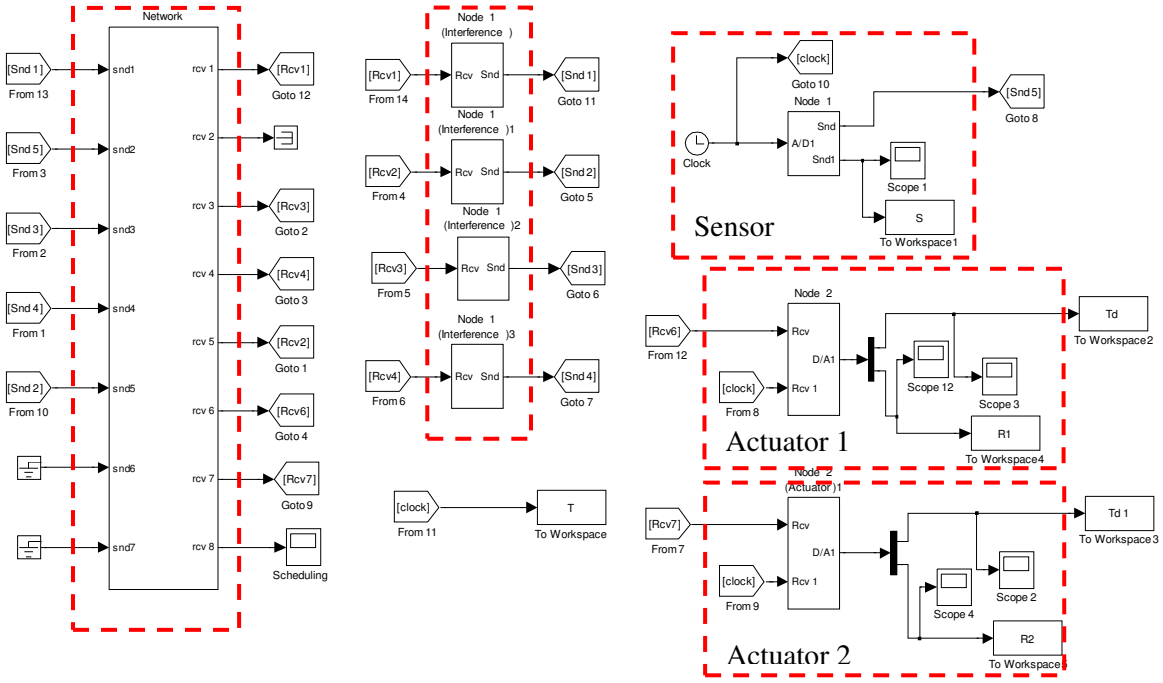

Figure 2.4 The CAN with seven nodes

1) *Under no load condition*:

The sampling period for the system node is 0.01 s and only the system node is active on the network. The time delay with four byte and eight byte messages is shown in Figure 2.5. The bit rate is 100 Kbit/s and the total message length is 94 bits for the four bytes message and 128 bits for the eight byte message. As can be seen from Figure 2.5 the time delay is almost constant under low load condition. With four byte message, the time delay consists of the transmission time which is 0.94 ms in addition to 0.1 ms analogue to digital conversion time delay and actuator time delay, then the total time delay is 1.04 ms. With eight byte message the total time delay is 1.38 ms because the waiting time delay, and the retransmission time delay are also zero.

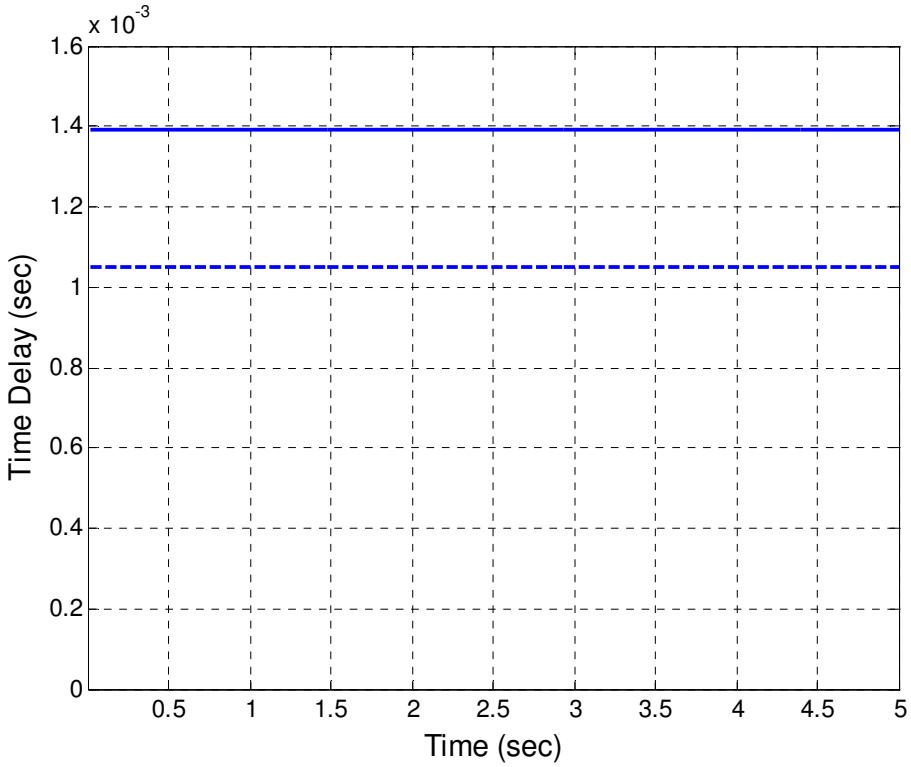

Figure 2.5 The time delay in the CAN with low load, solid-line 94 bit message, dashed-line 128 bit message.

The network schedule in Figure 2.6 shows that the system node is the only active node in the network, and it has the second priority in the network. Since only the system node is active then the utilization with 128 bits message is given by:

$$U_T = \frac{128/100{,}000}{0.01} = 0.0128$$

This shows very low network utilization. Two different simulations with the system node has a high and low priority, and we observed no change to the time delay characteristics, and it is almost constant.

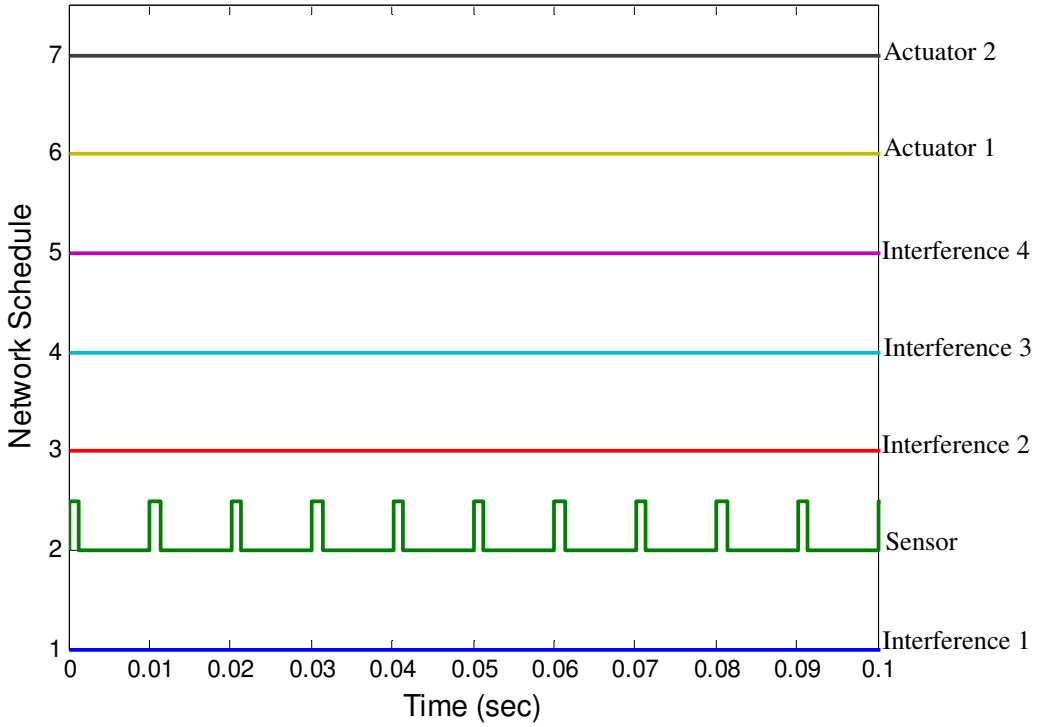

Figure 2.6 The Network Schedule

2) *The Load is Periodic*:

In the second scenario, all the activities on the network are periodic. The system nodes use 5 ms period for the transmission while the period of the load messages is 0.1 s. As expected the time delay will be periodic because all the activities on the network are periodic, and the CAN implements a deterministic protocol. The time delay is shown in Figure 2.7. From Figure 2.7 the time delay is periodic with 0.1 s period. The time delay has three different values, which are 1.48 ms, 1.58 ms and 5.2 ms. The time delay behaviour can be explained by looking at the scheduling in Figure 2.8.

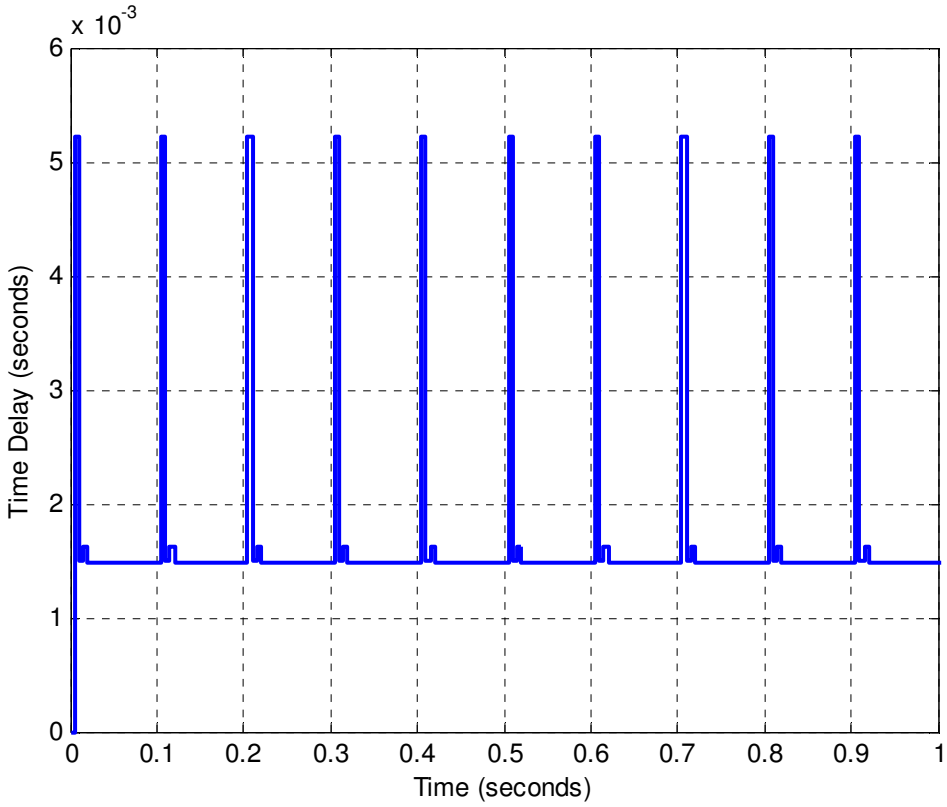

Figure 2.7 The time delay with periodic load messages

Since the system node has a middle priority on the network, there are mainly three possible states for the network. The first state is when the system node starts to transmit, the network is idle and so the time delay will only have transmission time delay component which is 1.48 ms (in addition to the pre, and post processing time delay). The second state occurs as the system node starts to broadcast, the lower-priority node that has already occupied the network and hence the system node will wait until that node finishes the transmission. Then it starts to transmit and in this case we will have a small waiting time delay component in addition to the transmission time delay, and the total time delay in this case is 1.58 ms.

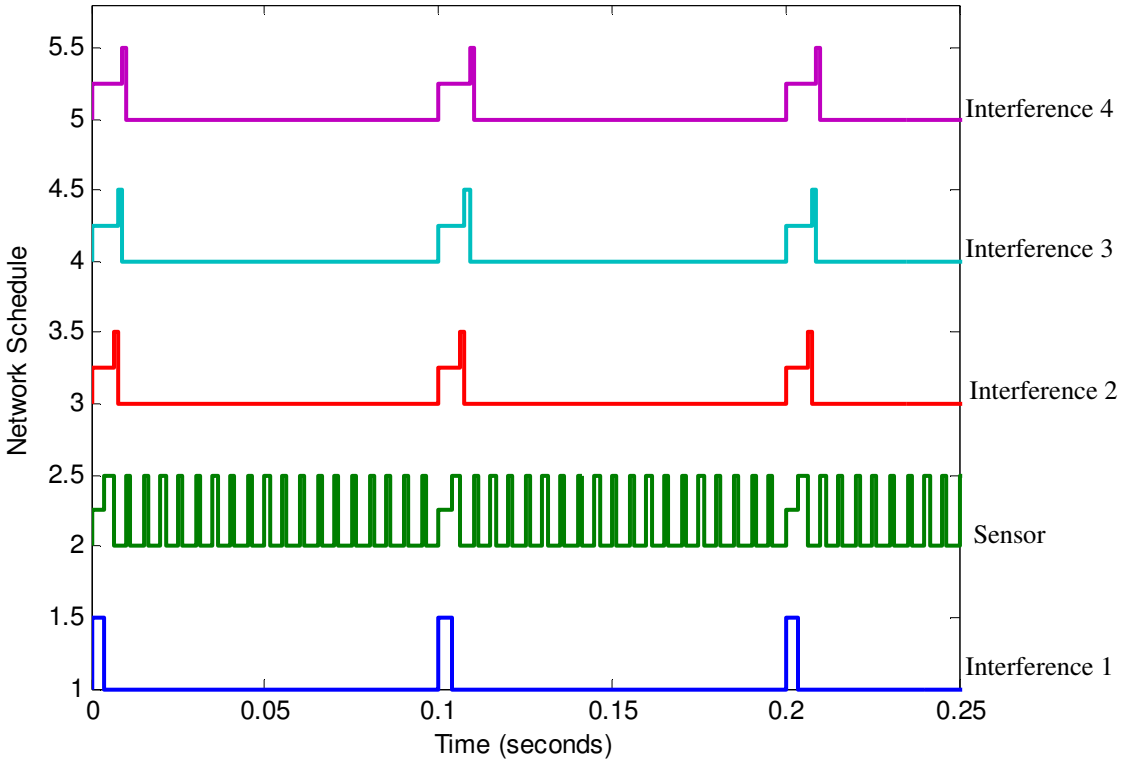

Figure 2.8 The network schedule with periodic messages load.

The sensor scheduling signal has three different values, which are low, medium and high. When the signal is low, the sensor node is idle and when it is medium then the sensor node is waiting for the network to become idle. The signal becomes high when it is already occupied the network. The last state has a time delay of 5.2 ms, in this case the system node will wait for the higher-priority node to finish its activity in the network, and the system node should wait until the network becomes idle, the total time delay is then:

$$T_d = T_{tr} + T_{retr} + T_w = T_{tr} + 0 + T_w = \frac{128}{100{,}000} + 0 + \frac{3 \cdot 128}{100{,}000} = 5.1ms$$

In addition to 0.1 ms pre- and post-processing time delay, the total time delay is 5.2 ms as shown in Figure 2.8. The network utilization is given by:

$$U_T = \frac{\sum_{i \in N_{node}} \sum_{j=1}^{m^{(i)}} \left(T_{tr}^{(i,j)} + T_{retr}^{(i,j)} \right)}{T_{\max}}$$
$$= \frac{3 \cdot 128/100{,}000}{0.1} + \frac{128/100{,}000}{0.005} + \frac{3 \cdot 128/100{,}000}{0.1} = 0.3328$$

The network utilization is still medium. With different priorities, we noticed that with increasing the load with periodic messages the time delay is periodic with different periodic forms even with high utilization. As the network utilization is less than one then the receiving of the message is guaranteed, and this is the advantage of the deterministic protocol.

3) *The Load is Random*

When all the messages are random, the time delay is expected to be random even with deterministic network. In this scenario, we have a CAN with seven nodes; three are assigned as the system nodes and four as the load nodes which are random. In (Nilsson 1998) the message length is chosen to have a uniform distribution but in our case, the activities of the four nodes are random with constant message length, which simulates the non periodic activity on the network. The bit rate is 500 kbit/s and the message's length is 94 bits. The load messages have 0.01 s period while the system node has 5 ms period. The time delay when the system node has a middle priority is shown in Figure 2.9. The time delay has three different states, which are 0.1 ms, 5 ms and 9.8 ms. The histogram of the time delay in Figure 2.9 is shown in Figure 2.10. The time delay has three states that can be modelled using Markov Chain. The network schedule is shown in Figure 2.11.

In many simulations with different message lengths and priorities, the time delay is random with different distribution functions due to the random messages in the network.

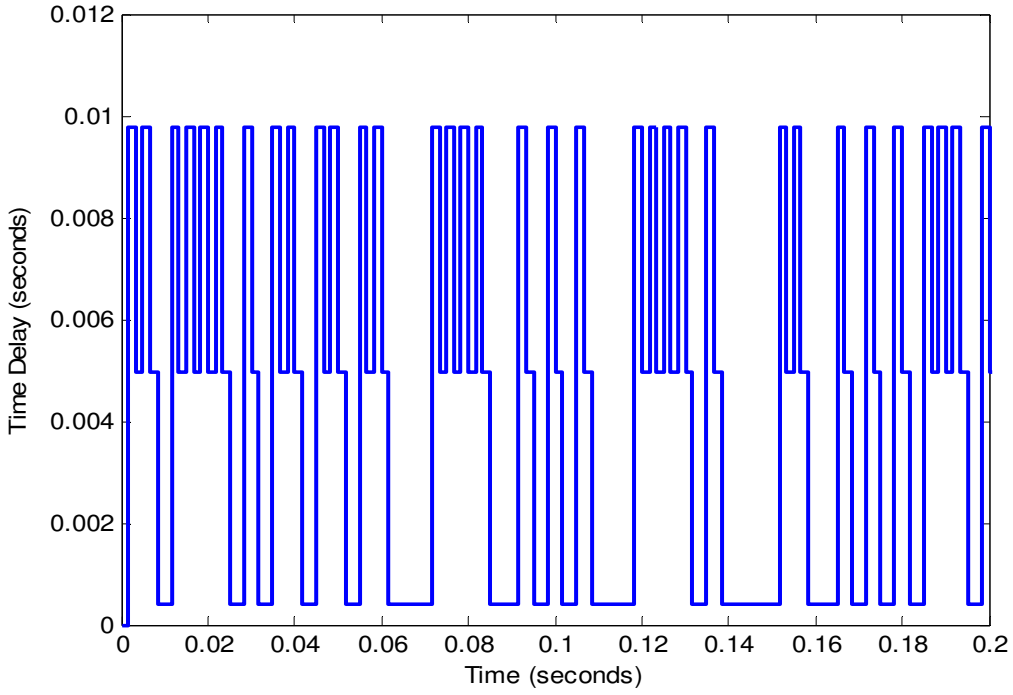

Figure 2.9 The time delay with random messages and middle priority

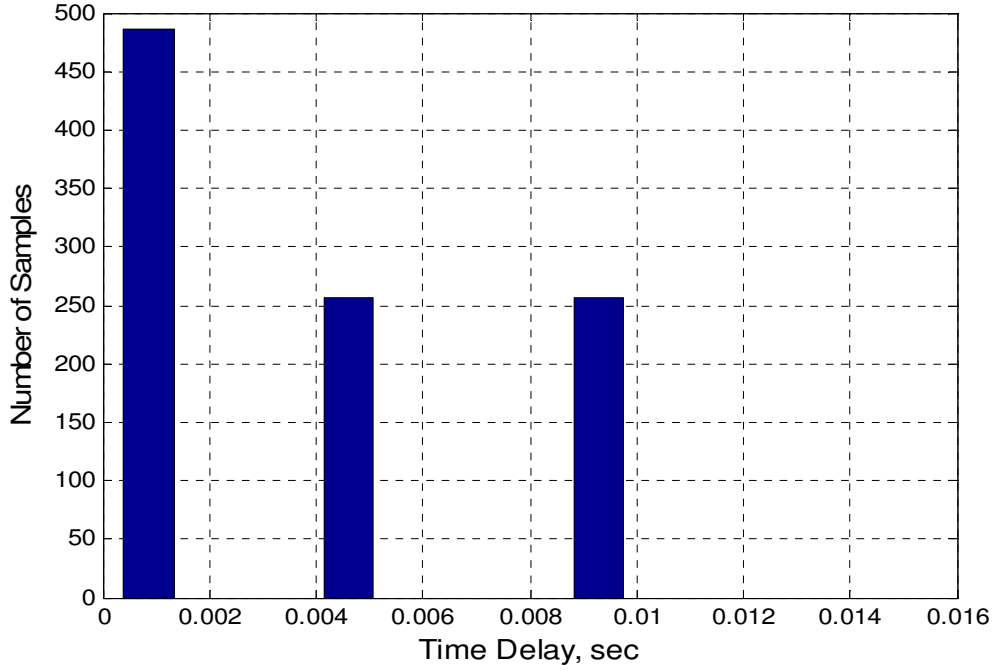

Figure 2.10 The histogram of the time delay in Figure 2.9

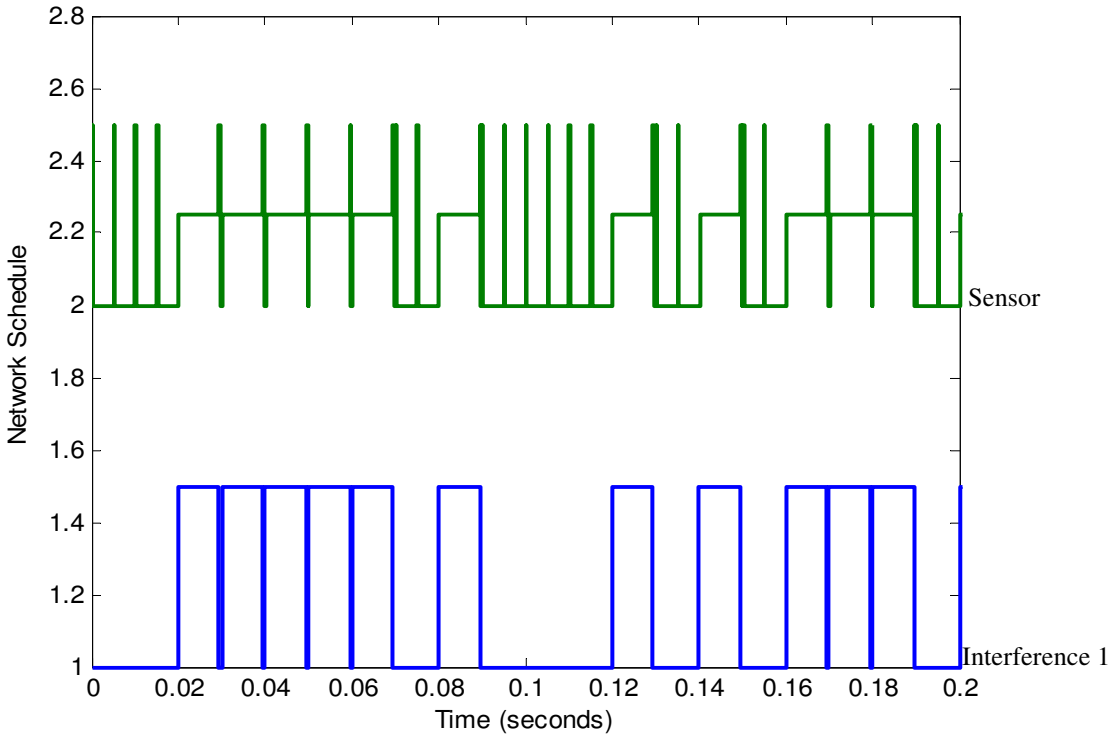

Figure 2.11 The network schedule with random messages load.

From the network schedule in Figure 2.11 we noticed in many cases when the sensor node starts to transmit the network is idle, and the time delay will only have transmission time delay component. The idle network can represent the low state in Markov chain. Another interesting property is that when the current state is the low state then the next state will be either the high state or the low state as can be seen from Figure 2.9. In the medium state when the sensor node starts to transmit the higher priority is already occupied the network.

The time delay when the load message has a period of 0.012 s is shown in Figure 2.12, and the distribution function is shown in Figure 2.13. We found that in some cases the time delay can be modelled using Markov Chains.

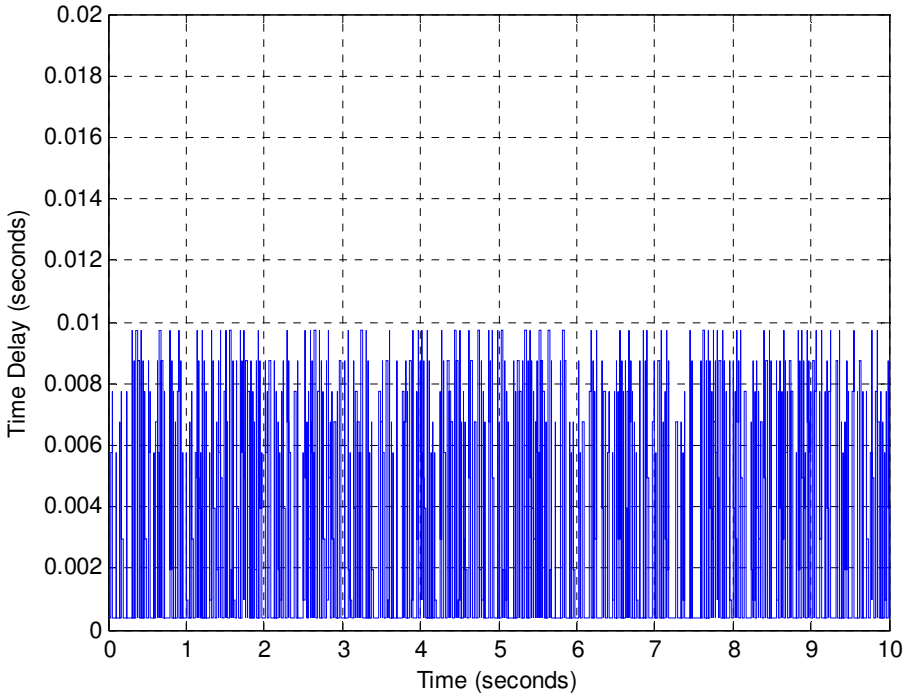

Figure 2.12 The time delay with random messages and middle priority and 0.012 s load message

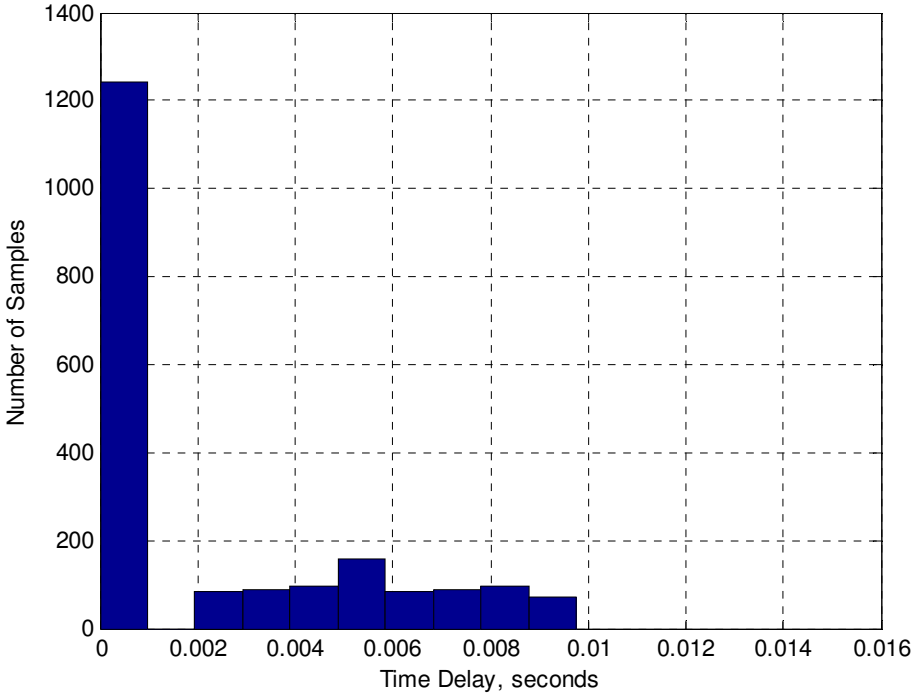

Figure 2.13 The histogram of the time delay in Figure 2.12

From the distribution in Figure 2.13 it can be seen that the time delays are mostly distributed around 1 ms with some time delays are uniformly distributed in the interval [2 ms, 9 ms]. The average time delay is 2.5 ms and the maximum time delay is 9.8 ms, this can be explained by looking at the scheduling in Figure 2.14.

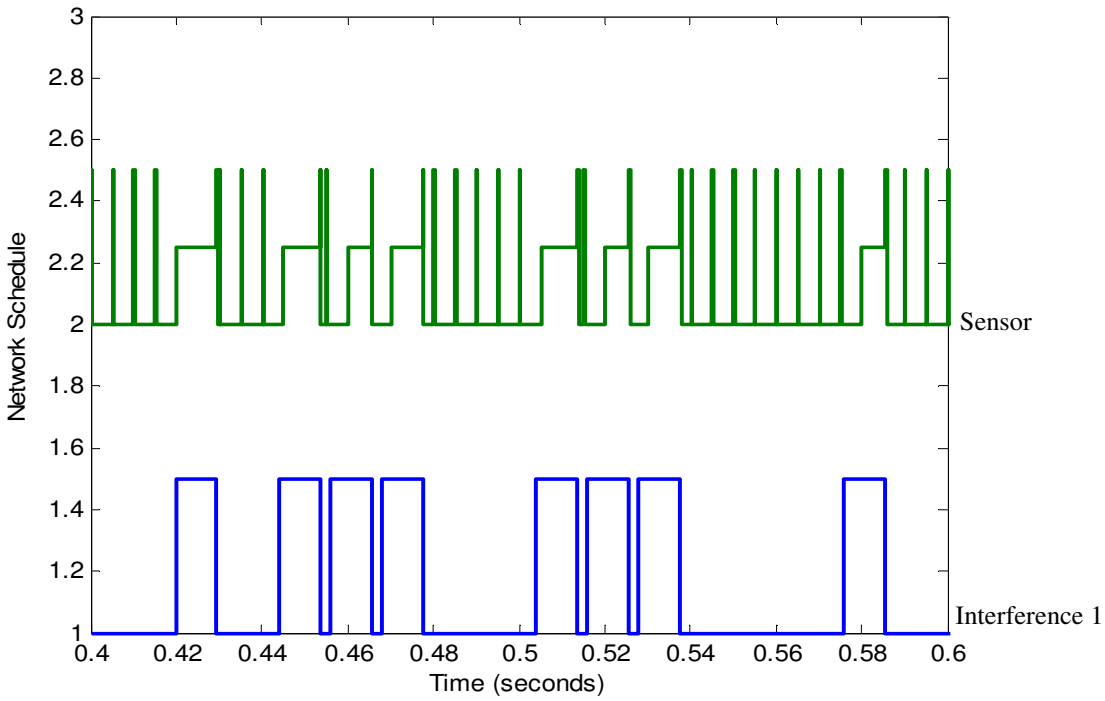

Figure 2.14 The network schedule with random messages load.

In most of the time, the network is idle and there is no waiting time delay and hence the time delay will have only transmission time delay, which is 1.04 ms and this explains the large distribution around 1 ms. The load message is a random signal with 9.5 ms width. In some cases when the sensor node is trying to transmit, the load message is already occupied the network which causes the time delay to be distributed between 2 ms and 9 ms. The time delay and the distribution function when the load message has 0.009 s period are shown in Figure 2.15 and Figure 2.16.

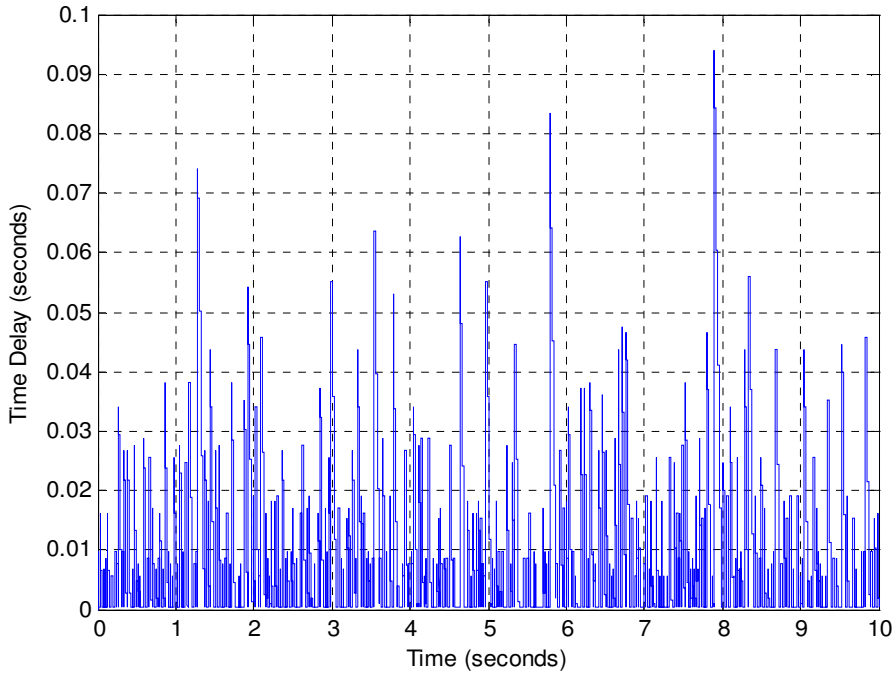

Figure 2.15 The time delay with random messages and middle priority with 0.009 s load message

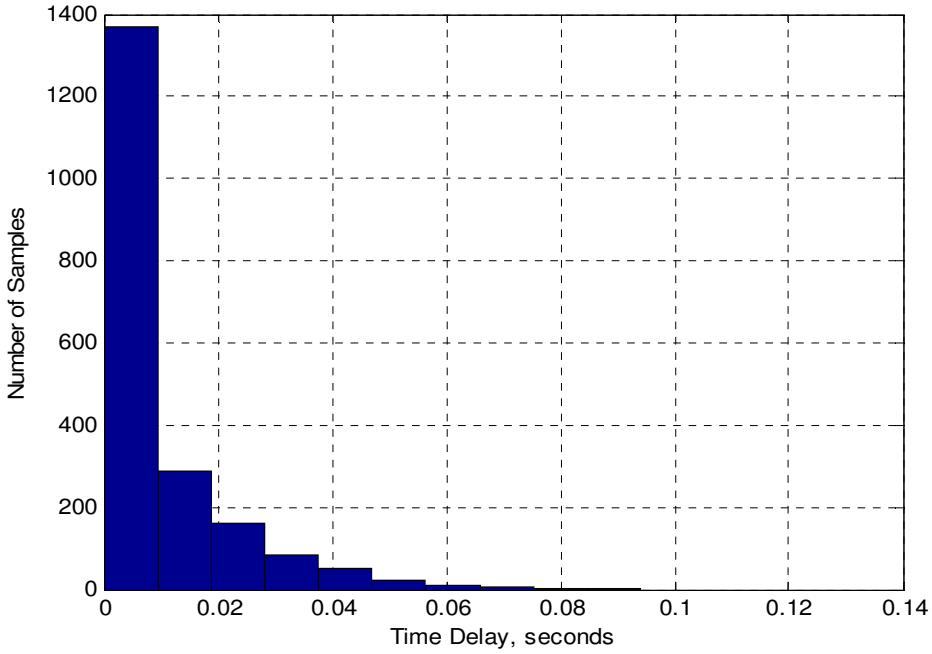

Figure 2.16 The histogram of the time delay in Figure 2.15

From the distribution in Figure 2.16 the time delay distribution has a Dirac shape with 9.8 ms average values. The network scheduling is shown in Figure 2.17.

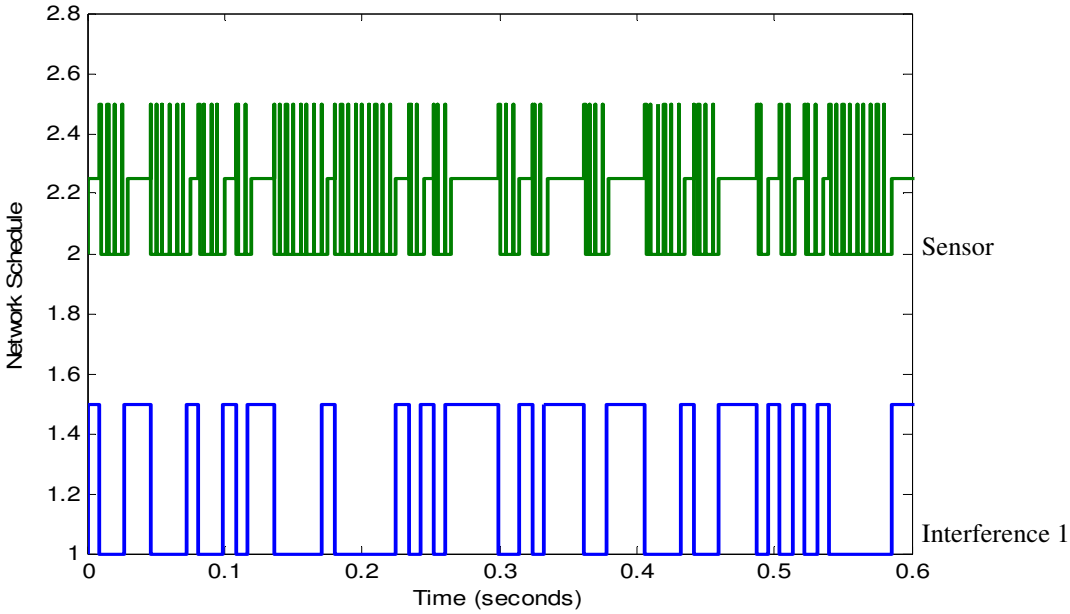

Figure 2.17 The network schedule with random messages load.

It can be seen from Figure 2.17 that the load occupies the network most of the time which increases the time delay. With different priorities we found that the priority affects the average time delay. Increasing the priority reduces the average time delay.

2.5.2 The Time Delay Analysis in the Ethernet

The Ethernet is a non deterministic protocol and even with periodic messages on the network the time delay is not expected to show any periodicity. The simulated Ethernet consists of seventeen nodes three of which are the system nodes while the other fourteen nodes are assigned as the load nodes. The TrueTime 1.5 Simulink implementation of the network is shown in Figure 2.18.

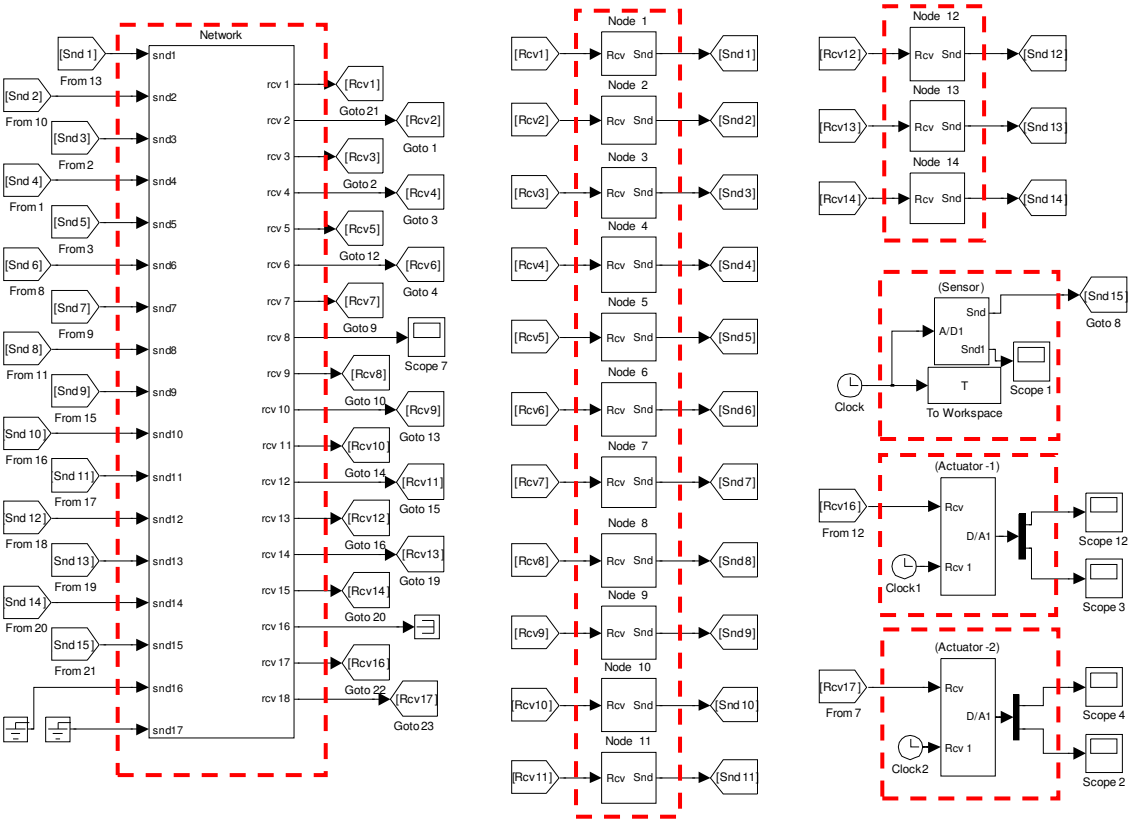

Figure 2.18 The Ethernet with seventeen nodes

The bit rate is the standard 10 Mbits/s bit rate, and the system message length is 576 bits with 5 ms period. All the load messages are periodic with different message lengths. The time delay under low load is shown in Figure 2.19. The periods of the messages are 5 ms, which makes the utilization 0.1728. The network schedule is shown in Figure 2.20, which shows that the system node has assigned the number fifteen because the Ethernet does not support any prioritization. Since the protocol is nondeterministic we can see that under low load, there are no collisions in the network and hence the time delay is constant and can be calculated as:

$$T_{dn} = T_{tr} + T_{retr} + T_w = T_{tr} + 0 + T_w = \frac{567}{10{,}000{,}000} + 0 + 0 = 5.67 \cdot 10^{-5}$$

$$T_{total} = T_{pre} + T_{dn} + T_{post} = 0.00001 + 5.67 \cdot 10^{-5} + 0.0001 = 1.676 \cdot 10^{-4} \text{ sec}$$

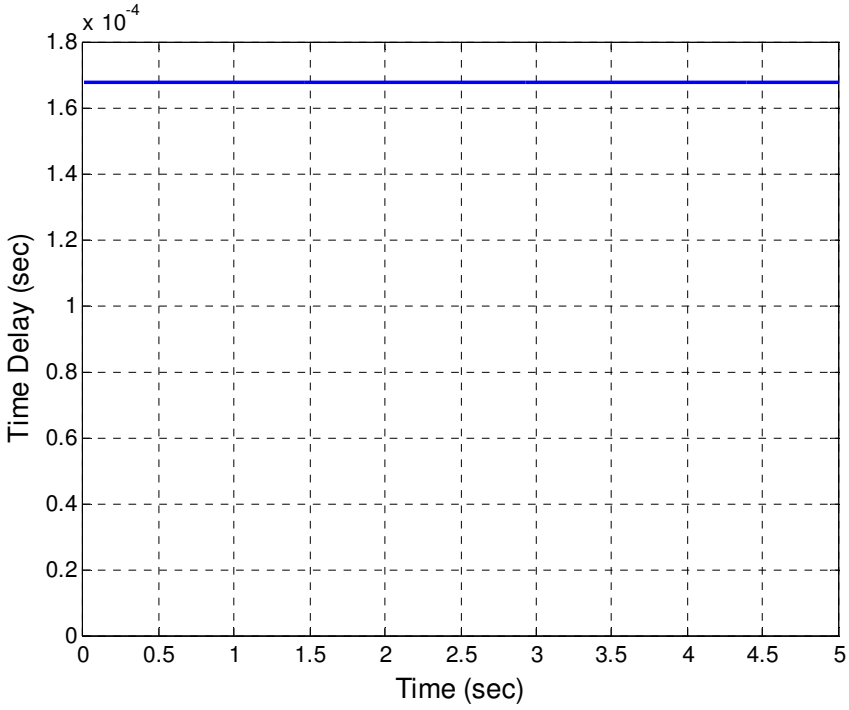

Figure 2.19 The time delay in the Ethernet with low load

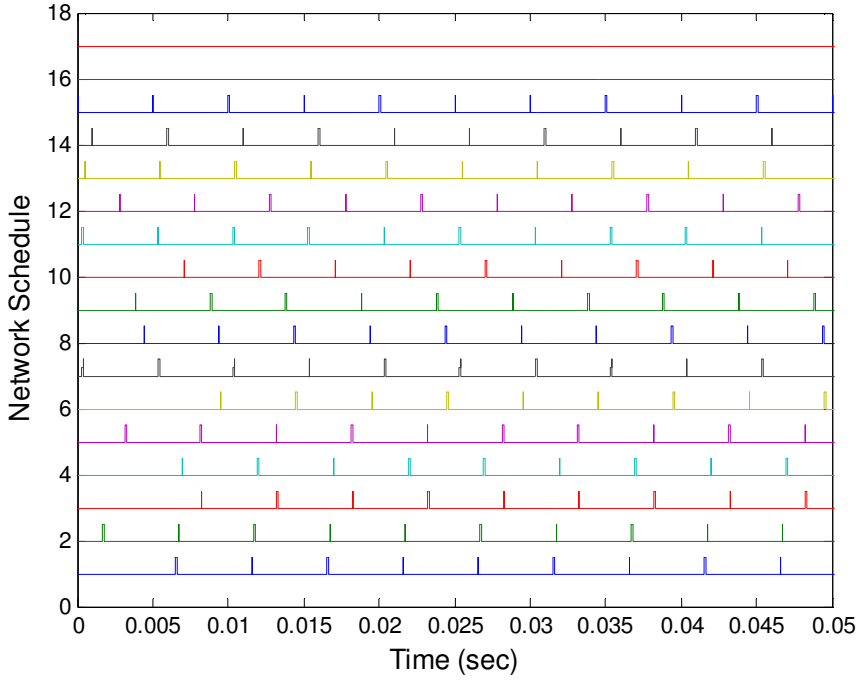

Figure 2.20 The network schedule in the Ethernet with low load

When the load messages have a period of 2 ms, the utilization is 0.4147 s. At this utilization level the time delay and the histogram are shown in Figure 2.21 and Figure 2.22. When the network is loaded, we can see that there is a considerable time delay because many messages are trying to transmit at the same time. Both the time delay and the histogram proves that the time delay is random but bounded and in this case, we have not observed any correlation between the previous, current and next time delay.

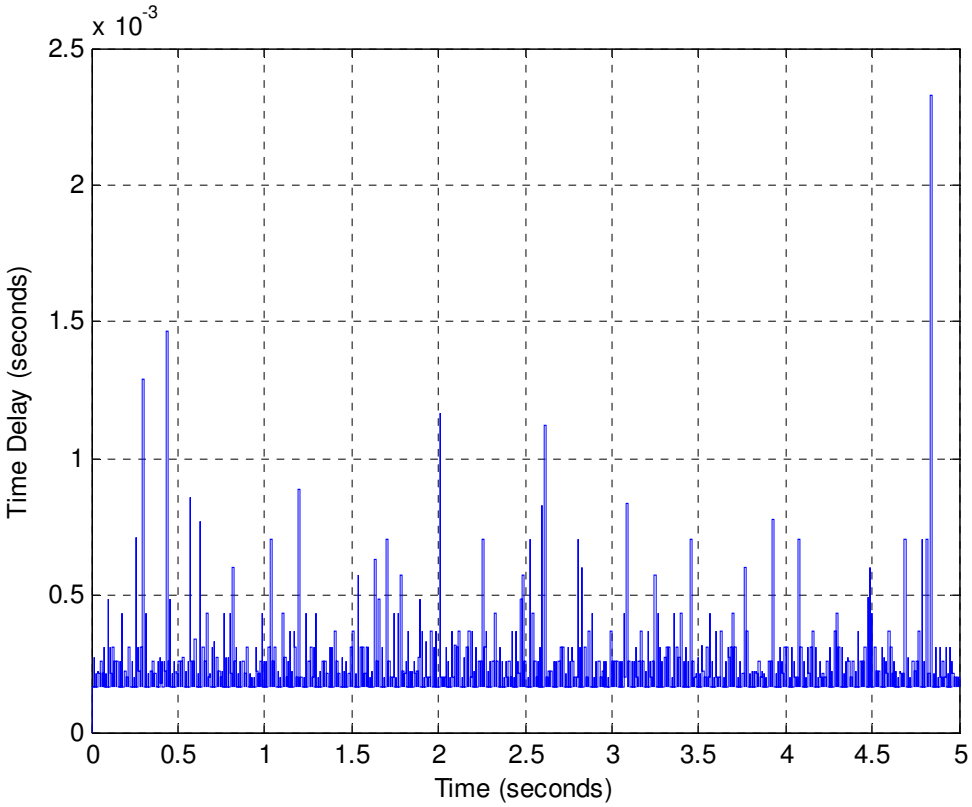

Figure 2.21 The time delay in the Ethernet with medium load

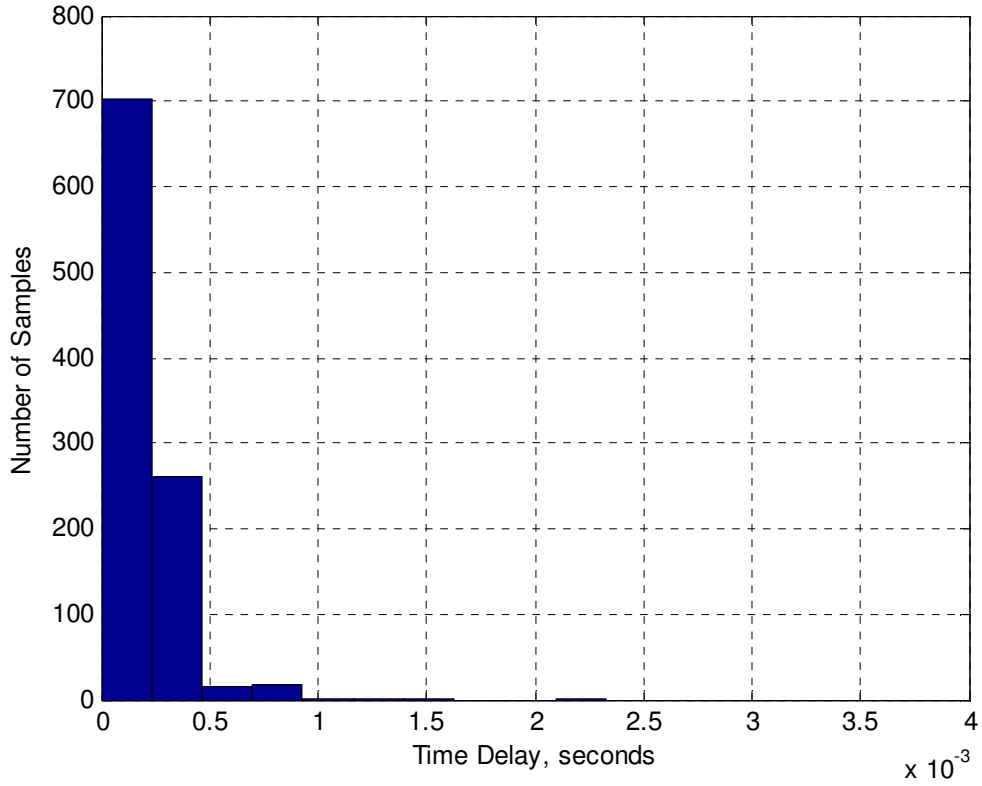

Figure 2.22 The histogram of the time delay in Figure 2.21

The main disadvantage in the Ethernet appears when the network is nearly loaded. With 1 ms load period the utilization is 0.8179 and the time delay is shown in Figure 2.23. In this case, the time delay may not be bounded because the network is loaded. Due to the large number of collisions at this utilization level the retransmission time is increasing dramatically, and the Ethernet protocol cannot guarantee a fair bandwidth distribution between the nodes. When a collision occurs in the Ethernet, the node waits for a random time after ten collisions the waiting time is fixed and after sixteen collisions, a transmission error is sent back to the sending node. The main disadvantage for this protocol is that it cannot guarantee receiving the messages within a bounded time.

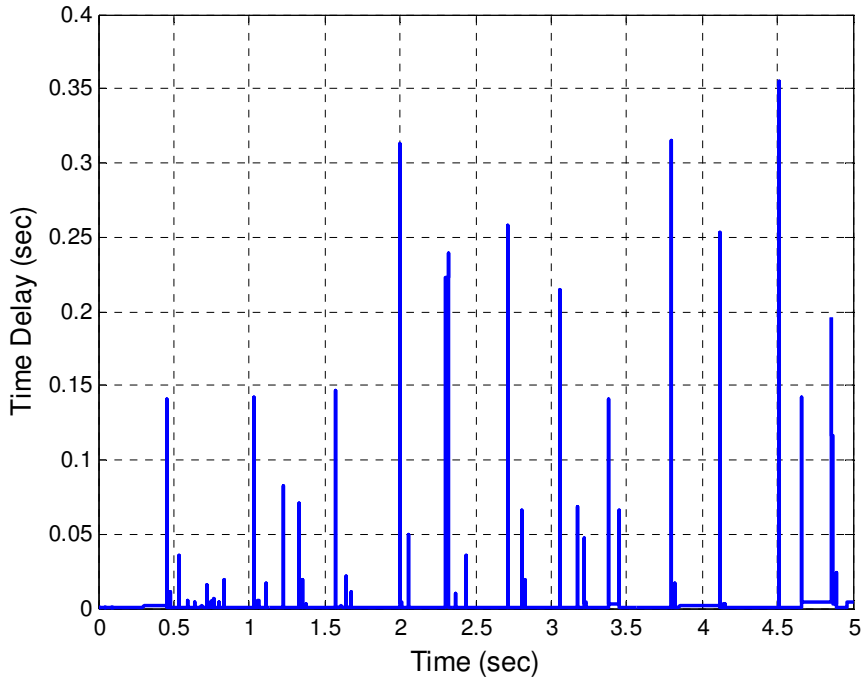

Figure 2.23 The time delay in the Ethernet with medium utilization

2.6 Discussions

In both the Ethernet and the CAN under very low load conditions, the time delay is almost constant and depends only on the message length and the network bit rate. With prioritized network even when a node has a low priority the time delay is constant under low network utilization levels. When all the activities on the network are periodic, the time delay will also be periodic in a deterministic network. The node priority does not affect the characteristics of the time delay but when the network is overloaded the node with the higher priority will have a guaranteed transmission while the transmission of the lower-priority nodes will not be guaranteed. In the CAN with random messages the time delay is random, and in some cases it can be governed by Markov Chain when the network utilization is low or medium. When the messages are random in the CAN, the time delay can show different

probability distribution functions. Increasing the utilization increases the average time delay, and reducing the priority increases the average time delay.

Although the Ethernet protocol is not a deterministic protocol, the time delay is constant with periodic messages under very low load condition. Under the condition of low network utilization the time delay becomes periodic even though the protocol is random because the number of collisions is still very low. At the medium and high utilization the time delay is random. When the network is nearly overloaded, the transmission is not guaranteed.

From the previous discussion, the following can be concluded:

- The time delay has five different patterns: Constant, Periodic, Random but bounded, Random governed by Markov Chains and random but unbounded. The constant time delay model can be used if the maximum time delay of the system is much larger than the worst-case time delay.
- The time delay can be affected by the bit rate, message length, priority and utilization.

Depending on the time delay analysis in this chapter two proposed methods will be introduced in the next chapters. In the first method, the time delay is assumed to be bounded and this is the case when the time delay is constant, periodic or random. The worst-case time delay is used to model the time delay under the assumption that the time delay is constant, and this can be achieved through using a buffer. On the other hand, when the time delay is random and governed by Markov Chain the discrete time Markovian jump system approach is used to study the stochastic stability of the system.

2.7 Summary

In this chapter, a brief introduction to control networks was given. Mainly, two candidates of control networks are discussed; they are the CAN, which is a deterministic network, and the Ethernet, which is a non deterministic network. As the Ethernet was originally intended for data transmission, it is characterized by long data message and high bit rate compared to the CAN. Control networks are the backbone for all the networked control systems and in order to design a networked control system the time delay induced with these networks needs to be pre-analyzed. To characterize the time delay TrueTime 1.5 Simulator is used, which is intended for real time control systems simulation. Different scenarios have been simulated, and it is found that the time delay can be constant, periodic and bounded, random and bounded, random governed by Markov Chain and in some cases, the time delay can be random and unbounded. The main difference between the CAN and the Ethernet appears under high utilization where the time delay can be unbounded in the Ethernet. Depending on these models for the time delay, two analysis methods for NCSs have been proposed in this thesis. The first method is introduced in Chapter 3 and is based on the assumption that the time delay is either constant or bounded. The second method in Chapter 4 can be used whenever the time delay is random and governed by Markov chain.

CHAPTER 3: MAXIMUM ALLOWABLE DELAY ESTIMATION FOR NETWORKED CONTROL SYSTEMS

3.1 Introduction

Time delays may degrade the performance of NCSs or may lead to system instability. There are many methods reported in the literature for analyzing the stability of time delay systems. However, most of them are very complex to use in practice. Therefore, there is a need for a simple and easy method in terms of engineering design and using by practical engineers. From the analysis in Chapter 2 the time delay can be constant, periodic, or random but bounded. This chapter presents a new method for analyzing the stability of NCSs that can be used as a guideline tool for designing the controller. The detailed description of the proposed method for estimating the maximum time delay in NCSs is presented in this chapter. At first, the method is applied to a single-unit NCS with a state feedback controller (Khalil et al. 2010a). A few examples are illustrated, and the results are compared with that proposed in the previously published literature. The method is then extended to an NCS with a dynamic controller (Khalil et al. 2010b) with an application to a multi-units

distributed interconnected NCS, which are used in many distributed energy system application cases such as electrical power systems, parallel DC/DC converters, parallel DC/AC inverters, and Microgrids. A small-scale power system consisting of three generators is studied as a demonstration example and the MADB for the system is estimated using the proposed method.

3.2 Time delays in networked control systems

A typical organization of an NCS is shown in Figure 3.1. As the control loop is closed through a communication network, the time delay and data dropout are unavoidable. This may degrade the performance of the NCS or even destabilize the system. In general, the control systems with time delays can be classified into time delay independent (where the stability is not affected by the time delay) and time delay dependent (where the time delay does affect the stability) (Mahmoud 2000). Time delay, no doubt, increases complexity in the process of analysis and design of NCSs. Conventional control theories built on a number of standing assumptions, including synchronized control and non delayed sensing and actuation must be re-evaluated before they can be applied for NCSs (Mahmoud et al. 2003). Analytical and graphical methods have been studied in (Marshall et al. 1992). The stability criteria for NCSs based on Lyapunov-Krasovskii functional approach has been reported in (Tang et al. 2008;Yue et al. 2004a;Yue et al. 2004b;Liu 2003).

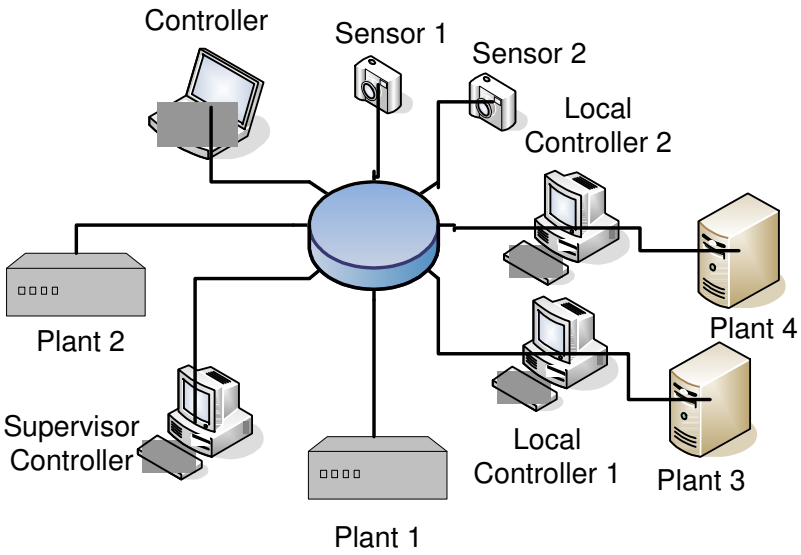

Figure 3.1 A Typical Networked Control System

The main goal of the most-recent work in this field is to reduce the conservativeness of the stability region by using Lyapunov-Krasovskii functional approach with improved algorithms for solving the Linear Matrix Inequality (LMI) set although, at expense of increased complexity and computation time. In (Yue et al. 2004a;Yue et al 2004b), a Lyapunov-Krasovskii function is used to derive a set of LMIs and the stability problem is then formalized as a feasibility LMI problem. In many of the previously reported works, the controller is designed in the absence of the time delay. In (Jian et al. 2008), an improved Lyapunov-Krasovskii function is used with triple integral terms. The LMI methods require that the closed-loop system to be Hurwitz (De Souza et al. 1995;Liu 2003;Zhang et al. 2001). In (Wu et al. 2007)**,** a modified Cone Complementary linearization algorithm based on the Lyapunov-Krasovskii approach is implemented. The method reported in (Zhu et al. 2008) is claimed to be less conservative, and the computational complexity is reduced. An LMI method in the frequency domain is derived in (Jun et al. 2000), which is then transformed on to an equivalent non-frequency domain LMI by applying Kalman-Yakubovich-Popov Lemma. It has been reported that the ordinary Lyapunov stability analysis is linked

by a suggested variable to state vectors through convolution (Kim 2005), and the stability analysis is simplified to only require solving a nonlinear algebraic matrix equation.

In (Zhang et al. 2001), the hybrid system technique is used to derive a stability region, and an upper bound is derived for the time delay in an inequality form. Comparing with the other published results, the results are rather conservative. The hybrid system stability analysis technique has also been used in (Branicky et al. 2000). A simple analytical relation is derived between the sampling period, the time delay and the controller gains. The same approach is used in (Xei et al. 2002) with more conservative stability region results. The model-based approach for deriving necessary and sufficient conditions for the stability is presented in (Montestruque et al. 2004). The stability criteria are derived in terms of the update time and the parameters of the model. The model-based approach is then extended to study the stability of a distributed interconnected NCS in (Sun et al. 2008). The optimal stochastic control was studied in (Nilsson 1998) with a discrete time system model where the random time delays are modelled using Markov Chains, and the controller uses the knowledge of the past state time delays by involving time stamping.

Most of the previously developed approaches require excessive load of computations, and also for higher-order systems; the load of computations will increase dramatically. In practice, engineers may find it difficult to apply those available methods in control systems design because of the complexity of the methods and lack of a guideline in linking the design parameters to the system performance. Almost all the design procedures highly depend on the post-design simulation to determine the design parameters. So there is a demand for a simple design approach with clear guidance for practical applications. In this chapter, a new stability analysis and controller design method is proposed, in which the design approach is simpler and a clearer design procedure is given.

3.3 Maximum allowable delay bound estimation for NCSs

Although the issues involved with time delays in control systems have been studied for a long time, it is difficult to find a method simple enough to be accepted by control system design engineers in industry. It is found that the most previously reported methods rely on LMI techniques, and they are generally too complicated for practical engineers to use and also involve heavy load of numerical calculations and computation time. A new method is proposed in this chapter, which has a simple structure and is used for estimating the maximum time delay allowed while the system stability can still be maintained. In control systems, the sampling time is preferred to be small (Park et al. 2002). The Maximum Allowable Delay Bound (MADB) (Yang et al. 2007;Khalil et al. 2010a;Khalil et al. 2010b;Khalil et al. 2011;Kim et al. 2003;Cheng et al. 2007) can be defined as the maximum time delay presented to the system while the system stability is retained if without considering the system performance.

3.3.1 The mathematical model of a single unit NCS

A continuous-time invariant linear system is given by:

$$\begin{aligned} \dot{\mathbf{x}}(t) &= \mathbf{A}\mathbf{x}(t) + \mathbf{B}\mathbf{u}(t) \\ \mathbf{y}(t) &= \mathbf{C}\mathbf{x}(t) + \mathbf{D}\mathbf{u}(t) \end{aligned} \tag{3.1}$$

where $\mathbf{x}(t) \in \Re^n$ is the system state vector, $\mathbf{u}(t) \in \Re^m$ is the system control input and $\mathbf{y}(t) \in \Re^p$ is the system output. $\mathbf{A} \in \Re^{n\times n}$, $\mathbf{B} \in \Re^{n\times m}$, $\mathbf{C} \in \Re^{p\times n}$ and $\mathbf{D} \in \Re^{p\times m}$ are constant matrices with appropriate dimensions.

Suppose that the control signals are connected to the control plant through a kind of network, so the time delay is inevitable to be involved in the feedback loop as shown in Figure 3.2. The state feedback can therefore be written as:

$$\mathbf{u}(t) = \mathbf{K}\mathbf{x}(t-\tau) \tag{3.2}$$

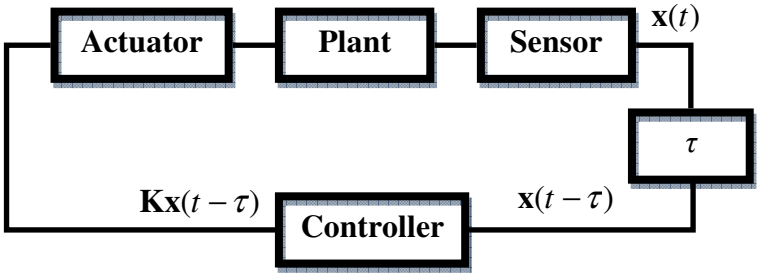

Figure 3.2 An NCS with time delay between the sensor and the controller

where τ is the equivalent time delay and $\mathbf{K}$ represents the feedback control gains with appropriate size. The time delay may be constant, variable or even random. In NCSs, the time delay is composed of delays from sensors to controllers, in controller and controllers to actuators, which can be expressed by:

$$\tau = \tau_{sc} + \tau_c + \tau_{ca} \tag{3.3}$$

where τ_{sc} is the time delay between the sensor and the controller, τ_c is the time delay in the controller, τ_{ca} is the time delay from the controller to the actuator. For a general formulation, the packet dropouts can be incorporated into (3.3):

$$\tau = \tau_{sc} + \tau_c + \tau_{ca} + dh \tag{3.4}$$

where d is the number of dropouts and h is the sampling period. In (3.4) the data dropouts can be considered as a special case of time delay (Zhang et al. 2008a;Zhang et al. 2008b). It is supposed that the following hypotheses hold.

Hypothesis 3.1 (H 3.1):

- **i.** Sensors are clock driven.
- **ii.** The controllers and the actuators are event driven.
- **iii.** The data are transmitted as a single packet.
- **iv.** The old packets are discarded.
- **v.** The matrix $(\mathbf{I}_{n\times n} + \tau\mathbf{BK})^{-1}$ is non-singular.
- **vi.** All the states are available for the measurement and hence for the transmission.

Hypothesis 3.2 (H 3.2):

The time delay τ is small enough for the finite difference approximation to be held.

Definition 1 (D1):

For a function $f(t)$, the n^{th} order reminder for its Taylor's series expansion is defined by (Meyer 2000)

$$R_n(f(\mathbf{x}), \tau) = \sum_{n}^{\infty} \frac{f^{(n)}(\mathbf{x})}{n!}\tau^n$$

3.3.2 Maximum allowable delay bound estimation in the time domain

Applying the state feedback proposed in (3.2) to the system (3.1), we have:

$$\dot{\mathbf{x}}(t) = \mathbf{A}\mathbf{x}(t) + \mathbf{BK}\mathbf{x}(t-\tau) \tag{3.5}$$

Equation (3.5) can be rearranged as:

$$\dot{\mathbf{x}}(t) = (\mathbf{A} + \mathbf{BK})\mathbf{x}(t) + \mathbf{BK}[\mathbf{x}(t-\tau) - \mathbf{x}(t)] \tag{3.6}$$

Theorem 3.1:

Suppose that H 3.1 and H 3.2 hold. For System (3.1) with the feedback control of (3.2), the closed-loop system is globally asymptotically stable if $\lambda_i(\mathbf{\Psi}) \in \mathrm{C}^-$ for $i = 1, 2, \cdots, n$ and all the state variables' 2nd order reminders are small enough for the given value of τ, where $\mathbf{\Psi}$ is given by:

$$\mathbf{\Psi} = [(\mathbf{I}_{n\times n} + \tau\mathbf{BK})^{-1}(\mathbf{A} + \mathbf{BK})] \tag{3.7}$$

Proof:

The expression for $\mathbf{x}(t-\tau)$ can be obtained by Taylor Expansion as (Meyer 2000):

$$\mathbf{x}(t-\tau) = \sum_{n=0}^{\infty} (-1)^n \frac{\tau^n}{n!} \mathbf{x}^{(n)}(t) \tag{3.8}$$

or $$\mathbf{x}(\mathbf{t}-\tau) = \mathbf{x}(t) - \tau\dot{\mathbf{x}}(t) + \mathbf{R}_2(\mathbf{x}, \tau) \tag{3.9}$$

From (3.9) it can be seen that $\mathbf{R}_2(\mathbf{x}, \tau)$ depends on the time delay, τ, and the higher-order derivatives of $\mathbf{x}(t)$. If τ is small enough, all the elements of $\mathbf{R}_2(x, \tau)$ are small enough to be ignored. Then we have:

$$\mathbf{x}(t-\tau) - \mathbf{x}(t) \cong -\tau\dot{\mathbf{x}}(t) \tag{3.10}$$

Substituting (3.10) into (3.6), the following can be derived:

$$\dot{\mathbf{x}}(t) \approx (\mathbf{A} + \mathbf{BK})\mathbf{x}(t) - \tau\mathbf{BK}\dot{\mathbf{x}}(t) \tag{3.11}$$

$$(\mathbf{I} + \tau\mathbf{BK})\dot{\mathbf{x}}(t) \approx (\mathbf{A} + \mathbf{BK})\mathbf{x}(t)$$

$$\dot{\mathbf{x}}(t) \approx [(\mathbf{I} + \tau\mathbf{BK})^{-1}(\mathbf{A} + \mathbf{BK})]\mathbf{x}(t) \tag{3.12}$$

$$\mathbf{\Psi} = [(\mathbf{I} + \tau\mathbf{BK})^{-1}(\mathbf{A} + \mathbf{BK})] \tag{3.13}$$

Therefore, the system (3.12) will be globally asymptotically stable if

$\lambda_i(\mathbf{\Psi}) \in \mathrm{C}^-$ for $i = 1, 2, \cdots, n$ □

Corollary 3.1:

Suppose H 3.1 and H 3.2 hold. For the control system (3.1) with the control law (3.2), the closed-loop system is globally asymptotically stable if

$$\tau < \frac{1}{\|\mathbf{BK}\|}$$

Proof:

For System (3.1), suppose that the state feedback has been designed to ensure $\lambda_i(\mathbf{A} + \mathbf{BK}) \in \mathrm{C}^-$ for $i = 1, 2, \cdots, n$. Therefore, for a chosen positive definite matrix $\mathbf{P} = \mathbf{P}^T$, it will find a positive definite matrix $\mathbf{Q} = \mathbf{Q}^T$ to have:

$$\mathbf{P}(\mathbf{A} + \mathbf{BK}) + (\mathbf{A} + \mathbf{BK})^{\mathbf{T}}\mathbf{P} = -\mathbf{Q} \tag{3.14}$$

Choosing a Lyapunov functional candidate as:

$$\mathbf{V}(x) = \mathbf{x}^{\mathbf{T}}\mathbf{P}\mathbf{x} > 0 \qquad \forall \ \mathbf{x} \neq \mathbf{0} \tag{3.15}$$

The objective for the next step is to find the range of τ that will ensure $\dot{\mathrm{V}}(x) < 0$, $\forall \ \mathbf{x} \neq \mathbf{0}$ (Goodall et al. 2001;Wang et al. 1998;Wang, J. et al. 2007). Taking the derivative of (3.15) along with the trajectory (3.12),

$$
\begin{aligned}
\dot{\mathbf{V}}(x) &= \dot{\mathbf{x}}^{\mathbf{T}}\mathbf{P}\mathbf{x} + \mathbf{x}^{\mathbf{T}}\mathbf{P}\dot{\mathbf{x}} \\
&\cong \mathbf{x}^{\mathbf{T}}[(\mathbf{A}+\mathbf{BK})^{\mathbf{T}}\mathbf{P}\mathbf{P}^{-1}(\mathbf{I}+\tau\mathbf{BK})^{-\mathbf{T}}\mathbf{P} + \mathbf{P}(\mathbf{I}+\tau\mathbf{BK})^{-1}\mathbf{P}^{-1}\mathbf{P}(\mathbf{A}+\mathbf{BK})]\mathbf{x} \\
&\quad - \mathbf{x}^{\mathbf{T}}[\mathbf{P}(\mathbf{A}+\mathbf{BK}) + (\mathbf{A}+\mathbf{BK})^{\mathbf{T}}\mathbf{P}]\mathbf{x} + \mathbf{x}^{\mathbf{T}}[\mathbf{P}(\mathbf{A}+\mathbf{BK}) + (\mathbf{A}+\mathbf{BK})^{\mathbf{T}}\mathbf{P}]\mathbf{x} \\
&\cong \mathbf{x}^{\mathbf{T}}[(\mathbf{A}+\mathbf{BK})^{\mathbf{T}}\mathbf{P}\mathbf{P}^{-1}(\mathbf{I}+\tau\mathbf{BK})^{-\mathbf{T}}\mathbf{P} - (\mathbf{A}+\mathbf{BK})^{\mathbf{T}}\mathbf{P} \\
&\quad + \mathbf{P}(\mathbf{I}+\tau\mathbf{BK})^{-1}\mathbf{P}^{-1}\mathbf{P}(\mathbf{A}+\mathbf{BK}) - \mathbf{P}(\mathbf{A}+\mathbf{BK})]\mathbf{x} - \mathbf{x}^{\mathbf{T}}\mathbf{Q}\mathbf{x}
\end{aligned}
$$

Rearranging the terms in the above equation, then we have

$$
\begin{aligned}
\dot{\mathbf{V}}(\mathbf{x}) \cong \mathbf{x}^{\mathbf{T}}\{&(\mathbf{A}+\mathbf{BK})^{\mathbf{T}}\mathbf{P}[\mathbf{P}^{-1}(\mathbf{I}+\tau\mathbf{BK})^{-\mathbf{T}}\mathbf{P} - \mathbf{I}] \\
&+ [\mathbf{P}(\mathbf{I}+\tau\mathbf{BK})^{-1}\mathbf{P}^{-1} - \mathbf{I}]\mathbf{P}(\mathbf{A}+\mathbf{BK})]\}\mathbf{x} - \mathbf{x}^{\mathbf{T}}\mathbf{Q}\mathbf{x}
\end{aligned}
\tag{3.16}
$$

If $\mathbf{P}(\mathbf{I}+\tau\mathbf{BK})^{-1}\mathbf{P}^{-1} - \mathbf{I} = \mathbf{I}$ then (3.16) will become

$$
\mathbf{x}^{\mathbf{T}}[\mathbf{P}(\mathbf{A}+\mathbf{BK}) + (\mathbf{A}+\mathbf{BK})^{\mathbf{T}}\mathbf{P}]\mathbf{x} - \mathbf{x}^{\mathbf{T}}\mathbf{Q}\mathbf{x} = 0
$$

Move the last term to the right hand side, the following will be derived:

$$
\mathbf{x}^{\mathbf{T}}[\mathbf{P}(\mathbf{A}+\mathbf{BK}) + (\mathbf{A}+\mathbf{BK})^{\mathbf{T}}\mathbf{P}]\mathbf{x} = \mathbf{x}^{\mathbf{T}}\mathbf{Q}\mathbf{x}
$$

So $\left\|\mathbf{P}(\mathbf{A}+\mathbf{BK}) + (\mathbf{A}+\mathbf{BK})^{\mathbf{T}}\mathbf{P}\right\| \cdot \|\mathbf{x}\|^{\mathbf{2}} = \|\mathbf{Q}\| \cdot \|\mathbf{x}\|^{2}$

Assuming that we can find a positive number to make the following hold:

$$
\left\|\mathbf{P}(\mathbf{A}+\mathbf{BK}) + (\mathbf{A}+\mathbf{BK})^{\mathbf{T}}\mathbf{P}\right\| = 2\gamma\left\|(\mathbf{A}+\mathbf{BK})^{\mathbf{T}}\mathbf{P}\right\| = \|\mathbf{Q}\|
$$

Then γ is the norm of $\mathbf{P}^{-1}(\mathbf{I}+\tau\mathbf{BK})^{-1}\mathbf{P} - \mathbf{I}$. Therefore, we have

$$
\begin{aligned}
&\mathbf{x}^{\mathbf{T}}[(\mathbf{A}+\mathbf{BK})^{\mathbf{T}}\mathbf{P}[\mathbf{P}^{-1}(\mathbf{I}+\tau\mathbf{BK})^{-\mathbf{T}}\mathbf{P} - \mathbf{I}] \\
&+ [\mathbf{P}(\mathbf{I}+\tau\mathbf{BK})^{-1}\mathbf{P}^{-1} - \mathbf{I}]\mathbf{P}(\mathbf{A}+\mathbf{BK})]]\mathbf{x} \\
&\le 2\left\|(\mathbf{P}^{-1}(\mathbf{I}+\tau\mathbf{BK})^{-\mathbf{T}}\mathbf{P} - \mathbf{I})\mathbf{P}(\mathbf{A}+\mathbf{BK})\right\| \cdot \|\mathbf{x}\|^{2}
\end{aligned}
$$

Choose

$$\left\|\mathbf{P}^{-1}(\mathbf{I}+\tau\mathbf{BK})^{-1}\mathbf{P}-\mathbf{I}\right\| \le 1 \tag{3.17}$$

Using Neumann Series formula for the inverse of the sum of two matrices (Meyer 2000):

$$(\mathbf{I}+\tau\mathbf{BK})^{-1} = \mathbf{I}-\tau\mathbf{BK}+\tau^2(\mathbf{BK})^2-\tau^3(\mathbf{BK})^3+\ldots- \tag{3.18}$$

If τ is small enough then (3.18) can be given as:

$$(\mathbf{I}+\tau\mathbf{BK})^{-1} \approx \mathbf{I}-\tau\mathbf{BK} \tag{3.19}$$

Applying (3.19) into (3.17) then we have,

$$\left\|\mathbf{P}^{-1}(\mathbf{I}+\tau\mathbf{BK})^{-1}\mathbf{P}-\mathbf{I}\right\| \approx \left\|\mathbf{P}^{-1}(\mathbf{I}-\tau\mathbf{BK})\mathbf{P}-\mathbf{I}\right\| = \left\|\tau\mathbf{BK}\right\| < 1$$

And finally we get

$$\tau < \frac{1}{\left\|\mathbf{BK}\right\|} \tag{3.20}$$

That is, for any $\tau < 1/\left\|\mathbf{BK}\right\|$, $\dot{\mathrm{V}}(x) < 0$, the system will be globally asymptotically stable. □

Theorem 3.1 and Corollary 3.1 give us a much simpler tool compared to other methods published previously in estimating the maximum allowable time delay for NCSs. Further analysis using the Frequency Domain method is described in the next subsection.

3.3.3 Maximum allowable delay bound estimation in the *s*-domain

Taking Laplace Transform of (3.11), we have:

$$[s\mathbf{I}-(\mathbf{A}+\mathbf{BK})+\tau s\mathbf{BK}]\mathbf{X}(s) = 0 \tag{3.21}$$

The characteristics equation is defined as:

$$[s\mathbf{I} - (\mathbf{A} + \mathbf{BK}) + \tau s\mathbf{BK}] = 0 \tag{3.22}$$

For a stable system the roots of the characteristics equation (3.22) must lie in the left hand side of the *s*-plane. From the characteristics equation, it is clear that the term $\tau s\mathbf{BK}$ influences the system performance and the stability, as the term of $\tau s\mathbf{BK}$ may push the closed-loop system poles towards the right hand side of the s-plane. As we have seen the system characteristic is determined by the term $\tau\mathbf{BK}\dot{\mathbf{x}}(t)$ in a certain level, this term can be regarded as a differentiator in the feedback loop; in turn it will introduce extra zeros to the closed-loop system and the time delay can be considered to have resulted in a variable gain to the feedback path. When we use the second-order difference approximation (3.22) becomes:

$$[s\mathbf{I} - (\mathbf{A} + \mathbf{BK}) + \tau s\mathbf{BK} - (\tau^2 s^2 / 2)\mathbf{BK}] = 0$$

Preliminary 3.1 (Meyer 2000): **(**Inverse Eigenvalues Theorem**)**

Given a matrix $\mathbf{\Omega}$ *that is nonsingular, with eigenvalues* $\lambda_1, \cdots, \lambda_n > 0$. *Then* $\lambda_1, \cdots, \lambda_n$ *are eigenvalues of* $\mathbf{\Omega}$ *if and only if* $\lambda_1^{-1}, \cdots, \lambda_n^{-1}$ *are eigenvalues of* $\mathbf{\Omega}^{-1}$.

Corollary 3.2

If the system (3.1) with the controller (3.2) is asymptotically stable for $\tau < 1/|\lambda_{\min}(\mathbf{BK})|$, where $\lambda_{\min}(\mathbf{BK}) = Tr(\mathbf{BK})$, then $\lambda_i[(\mathbf{I} + \tau\mathbf{BK})^{-1}] \in \mathbb{C}^+$, for $i = 1, 2, \cdots, n$.

Proof:

From Corollary 3.2 we can see that if Corollary 3.1 is satisfied, then all the eigenvalues of $(\mathbf{I}_{n\times n} + \tau\mathbf{BK})^{-1}$ are positive.

From Preliminary 3.1, the signs of the eigenvalues of $(\mathbf{I}_{n\times n} + \tau\mathbf{BK})^{-1}$ and $(\mathbf{I}_{n\times n} + \tau\mathbf{BK})$ are the same. For a single-input-single-output control system the matrix $\mathbf{BK}$ can be written as:

$$\mathbf{BK} = \begin{bmatrix} b_1 \\ b_2 \\ \vdots \\ b_n \end{bmatrix} \begin{bmatrix} k_1 & k_2 & \cdots & k_n \end{bmatrix} = \begin{bmatrix} b_1k_1 & b_1k_2 & \cdots & b_1k_n \\ b_2k_1 & b_2k_2 & \cdots & b_2k_n \\ \vdots & \vdots & \ddots & \vdots \\ b_nk_1 & b_nk_2 & \cdots & b_nk_n \end{bmatrix} \tag{3.23}$$

The interesting property of $\mathbf{BK}$ is that it is singular. The eigenvalues of $\mathbf{BK}$ are given by:

$$\mathbf{BK} - \lambda\mathbf{I}_{n\times n} = \begin{bmatrix} b_1k_1 - \lambda & b_1k_2 & \cdots & b_1k_n \\ b_2k_1 & b_2k_2 - \lambda & \cdots & b_2k_n \\ \vdots & \vdots & \ddots & \vdots \\ b_nk_1 & b_nk_2 & \cdots & b_nk_n - \lambda \end{bmatrix} \tag{3.24}$$

The characteristics equation of $\mathbf{BK}$ is given by the determinant of (3.24):

$$\begin{aligned} &\lambda^2 - Tr(\mathbf{BK})\lambda + \frac{1}{2}\left[Tr(\mathbf{BK}^2) - Tr(\mathbf{BK})^2\right] \\ &\quad \cdots \\ &\lambda^n - Tr(\mathbf{BK})\lambda^{n-1} + \frac{1}{2}\left[Tr(\mathbf{BK}^2) - Tr(\mathbf{BK})^2\right]\lambda^{n-2} + \cdots + \frac{1}{2}\left[Tr(\mathbf{BK}^2) - Tr(\mathbf{BK})^2\right] \end{aligned} \tag{3.25}$$

Because $\mathbf{BK}$ is singular $\det(\mathbf{BK}) = 0$ and hence;

$$\det(\mathbf{BK}) = \frac{1}{2}\left[Tr(\mathbf{BK}^2) - Tr(\mathbf{BK})^2\right] = 0$$

$$Tr(\mathbf{BK}^2) = Tr(\mathbf{BK})^2 \tag{3.26}$$

Substituting (3.26) into (3.25) then (3.25) becomes:

$$\begin{aligned} &\lambda^2 - Tr(\mathbf{BK})\lambda \quad \rightarrow \quad \lambda(\lambda - Tr(\mathbf{BK})) \\ &\quad \cdots \qquad\qquad\qquad\quad \cdots \end{aligned}$$

$$(-1)^n \lambda^n - Tr(\mathbf{BK})\lambda^{n-1} \quad \rightarrow \quad (-1)^n \lambda^{n-1}(\lambda - Tr(\mathbf{BK})) \tag{3.27}$$

Finally, the eigenvalues of $\mathbf{BK}$ are:

$$\lambda_1, \cdots, \lambda_{n-1} = 0 \qquad \lambda_n = Tr(\mathbf{BK}) < 0 \tag{3.28}$$

Equation (3.28) shows that the minimum eigenvalue of $\mathbf{BK}$ equals $Tr(\mathbf{BK})$. If the eigenvalues of $(\mathbf{I}_{n\times n} + \tau\mathbf{BK})$ are: $s_1, \cdots, s_n$. Then the eigenvalues of $(\mathbf{I}_{n\times n} + \tau\mathbf{BK})^{-1}$ are: $\frac{1}{s_1}, \cdots, \frac{1}{s_n}$. The eigenvalues of $(\mathbf{I}_{n\times n} + \tau\mathbf{BK})$ are given by:

$$\tau \cdot \mathbf{BK} + \mathbf{I}_{n\times n} - s\mathbf{I}_{n\times n} = \begin{bmatrix} \tau b_1 k_1 + 1 - s & \tau b_1 k_2 & \cdots & \tau b_1 k_n \\ \tau b_2 k_1 & \tau b_2 k_2 + 1 - s & \cdots & \tau b_2 k_n \\ \vdots & \vdots & \ddots & \vdots \\ \tau b_n k_1 & \tau b_n k_2 & \cdots & \tau b_n k_n + 1 - s \end{bmatrix} \tag{3.29}$$

The characteristics equation is given by the determinant of (3.29), after solving the characteristics equation it can be found that;

$$s_1, \cdots, s_{n-1} = 1 \qquad s_n = 1 + \tau \cdot Tr(\mathbf{BK}) = 1 + \tau \cdot \lambda_{\min}(\mathbf{BK})$$

$$\text{If } \tau < \frac{1}{|Tr(\mathbf{BK})|} \quad \rightarrow \quad s_n > 0 \quad \rightarrow \quad s_1, \cdots, s_n > 0$$

$$(\mathbf{I}_{n\times n} + \tau\mathbf{BK}) > 0 \quad \rightarrow \quad (\mathbf{I}_{n\times n} + \tau\mathbf{BK})^{-1} > 0 \qquad \square$$

From Corollary 3.2 a simpler stability criterion can be derived as follows.

Corollary 3.3

Suppose that H 3.1 and H 3.2 hold. For system (3.1) with the control law (3.2), the closed-loop system is globally asymptotically stable if

$$\tau < \frac{1}{abs(\mathbf{KB})}$$ (where *abs* is the absolute value)

Proof:

Corollary 3.3 can be easily proved by using the following Preliminary:

Preliminary 3.2: (Mahmoud 2000)

For any nonsingular matrices, $\mathbf{\Sigma}_1$, $\mathbf{\Sigma}_3$ *and real matrices* $\mathbf{\Sigma}_2$, $\mathbf{\Sigma}_4$ *with appropriate dimensions, it follows that*

$$\left(\mathbf{\Sigma}_1 + \mathbf{\Sigma}_2\mathbf{\Sigma}_3\mathbf{\Sigma}_4\right)^{-1} = \mathbf{\Sigma}_1^{-1} - \mathbf{\Sigma}_1^{-1}\mathbf{\Sigma}_2\left[\mathbf{\Sigma}_3^{-1} + \mathbf{\Sigma}_4\mathbf{\Sigma}_1^{-1}\mathbf{\Sigma}_2\right]^{-1}\mathbf{\Sigma}_4\mathbf{\Sigma}_1^{-1}$$

Choosing $\mathbf{\Sigma}_1 = \mathbf{I}$, $\mathbf{\Sigma}_2 = \mathbf{B}$, $\mathbf{\Sigma}_3 = \tau$ and $\mathbf{\Sigma}_4 = \mathbf{K}$, then:

$$(\mathbf{I} + \tau\mathbf{BK})^{-1} = \mathbf{I}^{-1} - \mathbf{I}^{-1}\mathbf{B}\left[1/\tau + \mathbf{K}\cdot\mathbf{I}^{-1}\cdot\mathbf{B}\right]^{-1}\mathbf{K}\cdot\mathbf{I}^{-1} = \mathbf{I} - \mathbf{B}\left[1/\tau + \mathbf{KB}\right]^{-1}\mathbf{K}$$

$$(\mathbf{I} + \tau\mathbf{BK})^{-1} = \mathbf{I} - \frac{1}{1/\tau + \mathbf{KB}}\mathbf{BK} \qquad (3.30)$$

For $(\mathbf{I} + \tau\mathbf{BK})^{-1}$ to be positive definite, $\tau < 1/abs(\mathbf{KB})$ ($\mathbf{KB} = Tr(\mathbf{KB})$). Equation (3.30) can be used as a simple and fast tool for estimating the MADB in NCS.

3.3.4 Numerical examples for estimating the maximum allowable delay bound

In general, two approaches are applied to controller design for NCSs. The first approach is to design a controller without considering the time delay and then the MADB for the system is estimated in the second step. Based on the estimated MADB, a communication protocol will be designed or chosen to guarantee that the induced time delay is less than the

MADB (Kim et al. 2003). The second approach is to design the controller while taking the time delay and data dropouts into account from the very first step of design (Yang et al. 2007;Zhang et al. 2001). In this section, a number of examples are studied to demonstrate the approach proposed and compare it with the previously published methods. In particular, the results derived using the method proposed in this thesis have been compared with the results using the LMI method given in (Zhang et al. 2008b).

In the comparisons in the following examples, the fourth-order pade approximation is used for the delay term in the s-domain, and is defined as (Golub et al. 1989):

$$e^{-\tau s} \approx P_d(s) = \frac{N_d(s)}{D_d(s)} = \left(\sum_{k=0}^{n}(-1)^k c_k \tau^k s^k\right) / \left(\sum_{k=0}^{n} c_k \tau^k s^k\right) \tag{3.31}$$

The coefficients are given by:

$$c_k = \left((2n-k)!n!\right)/\left(2n!k!(n-k)!\right) \quad k = 0,1,...,n \quad (n=6) \tag{3.32}$$

With the fourth-order Pade approximation, the truncation error in the time delay is less than 0.0001. The LMI based method, which has been used for the comparisons is based on using Lyapunov-Krasovskii functional and can be summarized as follows:

Corollary 3.4: (Yue et al. 2004a)

For a given scalar τ *and a matrix* $\mathbf{K}$*, if there exist matrices* $\mathbf{P}>0$, $\mathbf{Q}>0$, $\mathbf{\Pi}_i>0$ *and* $\mathbf{\Xi}_i>0 \quad (i=1,2,3)$ *) of appropriate dimension such that:*

$$\begin{bmatrix} \mathbf{\Xi}_1+\mathbf{\Xi}_1^T-\mathbf{\Pi}_1\mathbf{A}-\mathbf{A}^T\mathbf{\Pi}_1^T & \mathbf{\Xi}_2^T-\mathbf{\Xi}_1-\mathbf{A}^T\mathbf{\Pi}_2^T-\mathbf{\Pi}_1\mathbf{BK} & \mathbf{\Xi}_3^T-\mathbf{A}^T\mathbf{\Pi}_3^T+\mathbf{\Pi}_1+\mathbf{P} & \tau\mathbf{\Xi}_1 \\ * & -\mathbf{\Xi}_2-\mathbf{\Xi}_2^T-\mathbf{\Pi}_2\mathbf{BK}-(\mathbf{BK})^T\mathbf{\Pi}_2^T & -\mathbf{\Xi}_3^T+\mathbf{\Pi}_2-(\mathbf{BK})^T\mathbf{\Pi}_3^T & \tau\mathbf{\Xi}_2 \\ * & * & \mathbf{\Pi}_3+\mathbf{\Pi}_3^T+\tau\mathbf{Q} & \tau\mathbf{\Xi}_3 \\ * & * & * & -\tau\mathbf{Q} \end{bmatrix} < 0$$

$$(i_{k+1} - i_k)h + \tau_{k+1} \le \eta \quad k = 1,2,\cdots \tag{3.33}$$

Then the system (3.1)- (3.2) is exponentially asymptotically stable.

With a given controller gain $\mathbf{K}$, solving (3.33) using the LMI Matlab Toolbox the maximum time delay can be computed.

Example 3.1:

The system in this example is most widely used in the literature and is described by the following equation:

$$\dot{x}(t) = \begin{bmatrix} 0 & 1 \\ 0 & -0.1 \end{bmatrix} x(t) + \begin{bmatrix} 0 \\ 0.1 \end{bmatrix} u(t)$$

In previously reported work (Yue et al. 2004b;Jiang et al. 2008a), the feedback control was chosen as:

$$u(t) = \begin{bmatrix} -3.75 & -11.5 \end{bmatrix} x(t)$$

From Corollary 3.1, $1/\|\mathbf{BK}\| = 0.8695$, Theorem 3.1 and Corollary 3.3 both give 0.8696 s, so the MADB is estimated to be 0.8695 s. The same result can be obtained through Corollary 3.4 as reported in (Yue et al. 2004b;Naghshtabrizi 2007;Zhang et al. 2008a;Zhang et al. 2008b). In (Branicky et al. 2000;Zhang et al. 2001), the value reported for the MADB is 4.5×10^{-4} s and in (Park et al. 2002) it is 0.0538 s. In (Yang et al. 2007), the MADB is 0.785 s. It has been reported in (Jian et al. 2008), where an improved Lyapunov-Krasovskii approach has been used, that the MADB is 1.0551 s, also 1.05 s reported in (Zhang et al. 2008a;Zhang et al. 2008b) with improved algorithm for solving the LMI. In (Jiang et al.

2008a), the MADB is 1.0081 s. Using the proposed method with second order finite difference approximation we can obtain 1.13 s as the MADB.

Example 3.2: (Ogata 1996)

$$\dot{x}(t) = \begin{bmatrix} 0 & 1 & 0 \\ 0 & 0 & 1 \\ 0 & -2 & -3 \end{bmatrix} x(t) + \begin{bmatrix} 0 \\ 0 \\ 1 \end{bmatrix} u(t)$$

$$u(t) = \begin{bmatrix} -160 & -54 & -11 \end{bmatrix} x(t)$$

For this third-order system, using either the LMI method or the method specified in Theorem 3.1 and Corollary 3.3, 0.0909 s can be obtained as the MADB.

Example 3.3: (Ogata 1996)

$$\dot{x}(t) = \begin{bmatrix} 0 & 1.000 & 0 & 0 \\ 20.601 & 0 & 0 & 0 \\ 0 & 0 & 0 & 1 \\ -0.4905 & 0 & 0 & 0 \end{bmatrix} x(t) + \begin{bmatrix} 0 \\ -1 \\ 0 \\ 0.5 \end{bmatrix} u(t)$$

$$u(t) = \begin{bmatrix} 298.1504 & 60.6972 & 163.0989 & 73.3945 \end{bmatrix} x(t)$$

This is the fourth-order model of the inverted pendulum which, in many papers, is reduced to a second-order description in order to verify the stability of NCSs. Using the LMI method the MADB is 0.0416 s and Theorem 3.1 gives 0.0416 s while Corollary 3.3 gives 0.0147 s. It is noticed that there is good agreement between our method and the LMI method because τ is small enough to make the finite difference approximation hold.

Many examples have been studied to compare the results obtained using the proposed method with the results obtained using the LMI method (Yue et al. 2004a) and the fourt-order Pade approximation method. The calculation results for eleven examples are summarized in Table 3.1. The examples are given in Appendix A.

Table 3.1The MADB (seconds) using the proposed method with 1st, 2nd, 3rd order finite difference approximation for the delay term, the LMI method, the fourth-order Pade Approximation method and the simulation based method.

	The Finite Difference Method			The LMI	Pade Approximation	Simulation Based
	1st Order	2nd Order	3rd Order			
1	0.8695	0.8427	1.1321	0.8696	1.1672	1.180
2	0.1000	0.0995	0.1421	0.1000	0.1475	0.149
3	0.0100	0.0099	0.0149	0.0100	0.0156	0.0157
4	0.1428	0.1385	0.1808	0.1429	0.1855	0.1860
5	0.8217	0.8489	0.9085	0.8217	0.9091	0.9140
6	0.5000	0.4816	0.6303	0.5000	0.6474	0.6510
7	0.9940	0.9940	0.9960	0.9940	0.9960	0.9970
8	0.0856	0.0854	0.1192	0.0856	0.1230	0.1230
9	0.0909	0.0919	0.1251	0.0909	0.1284	0.1285
10	0.0416	0.0400	0.0496	0.0416	0.0505	0.0505
11	∞ *	∞ *	∞ *	3.0934	∞ *	∞ *

Remark:

* The system is time delay independent with our method the system is stable for any positive time delay while the LMI gives 3.0934 s, which shows that the resutls of the proposed method are less conservative.

From Table 3.1, it can be seen that the proposed new method can give values of MADB similar to the values obtained using the LMI method and the other methods, however, the method proposed in this thesis has a much simpler procedure, and it should have no difficulties for practical design engineers to accept this approach. Clearly, the MADB with the first-order finite difference approximation is comparable with the LMI method. Furthermore, we found good agreement between the third-order finite difference approximation and the fourth-order Pade approximation. The simulation based results for the MADB show that the estimated MADB through the proposed method sufficiently achieves the system stability.

3.4 Maximum allowable delay bound estimation for NCSs with dynamic controllers

3.4.1 The mathematical model of NCSs with dynamic controllers

A continuous-time networked control system is shown in Figure 3.3; the continuous-time invariant linear plant model is given by:

$$\begin{cases} \dot{\mathbf{x}}_p(t) = \mathbf{A}_p \mathbf{x}_p(t) + \mathbf{B}_p \hat{\mathbf{u}}_p(t) \\ \mathbf{y}_p(t) = \mathbf{C}_p \mathbf{x}_p(t) \end{cases} \tag{3.34}$$

where $\mathbf{x}_p(t) \in \Re^{n_p}$, $\hat{\mathbf{u}}_p(t) \in \Re^m$ and $\mathbf{y}_p(t) \in \Re^r$ are the state of the plant, the input of the plant and the output respectively. $\mathbf{A}_p \in \Re^{n_p \times n_p}$, $\mathbf{B}_p \in \Re^{n_p \times m}$, $\mathbf{C}_p \in \Re^{r \times n_p}$ are factor matrices.

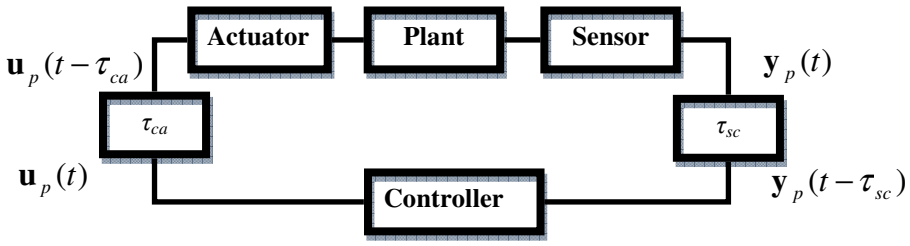

Figure 3.3 A Networked Control System

As shown in Figure 3.3 the time delay from the controller output to the plant (τ_{ca}) is inevitable to be involved in the feedback loop. Also, there is a time delay between the measured feedback signals to the controller input (τ_{sc}). The dynamic controller is given by:

$$\begin{cases} \dot{\mathbf{x}}_c(t) = \mathbf{A}_c \mathbf{x}_c(t) + \mathbf{B}_c \hat{\mathbf{y}}_p(t) \\ \mathbf{u}_p(t) = \mathbf{C}_c \mathbf{x}_c(t) + \mathbf{D}_c \hat{\mathbf{y}}_p(t) \end{cases} \tag{3.35}$$

where $\mathbf{x}_c(t) \in \Re^{n_c}$, $\mathbf{u}_p(t) \in \Re^m$ and $\hat{\mathbf{y}}_p(t) \in \Re^r$ are the state of the controller, the input of the controller and the output respectively. $\mathbf{A}_c \in \Re^{n_c \times n_c}$, $\mathbf{B}_c \in \Re^{n_c \times r}$, $\mathbf{C}_c \in \Re^{m \times n_c}$ and $\mathbf{D}_c \in \Re^{m \times r}$ are factor matrices. Both the controller and the plant will receive a delayed version as follows:

$$\hat{\mathbf{y}}_p(t) = \mathbf{y}_p(t - \tau_{sc})$$

$$\hat{\mathbf{u}}_p(t) = \mathbf{u}_p(t - \tau_{ca}) \tag{3.36}$$

For a general formulation, the packet dropouts can be incorporated in (3.4):

$$\tau_{sc} = \tau'_{sc} + d_{sc}h$$

$$\tau_{ca} = \tau'_{ca} + d_{ca}h \tag{3.37}$$

where d_{sc} and d_{ca} are the number of dropouts between the sensor and the controller, and between the controller and the actuator. h is the sampling period. For the following analysis it is supposed that H 3.1 and H 3.2 hold. Two cases are considered in the discussion, one with neglecting the controller to actuator time delay and in the second case the controller to the actuator time delay is taken into account.

3.4.2 Case I: Neglecting τ_{ca}

A simplification can be made by considering only the sensor to the controller time delay. In this simplified model, we assume that all the delays and dropouts are lumped between the sensor and the controller (Yue et al. 2004b). Applying the dynamic controller proposed in (3.35) to the plant (3.34) and setting $\tau_{ca} = 0$, and $\tau_{sc} = \tau$, we have:

$$\dot{\mathbf{x}}_p(t) = \mathbf{A}_p\mathbf{x}_p(t) + \mathbf{B}_p\hat{\mathbf{u}}_p(t)$$

$$\dot{\mathbf{x}}_p(t) = \mathbf{A}_p\mathbf{x}_p(t) + \mathbf{B}_p[\mathbf{C}_c\mathbf{x}_c(t) + \mathbf{D}_c\hat{\mathbf{y}}_p(t)]$$

$$\dot{\mathbf{x}}_p(t) = \mathbf{A}_p\mathbf{x}_p(t) + \mathbf{B}_p\mathbf{C}_c\mathbf{x}_c(t) + \mathbf{B}_p\mathbf{D}_c\mathbf{y}_p(t-\tau)$$

$$\dot{\mathbf{x}}_p(t) = \mathbf{A}_p\mathbf{x}_p(t) + \mathbf{B}_p\mathbf{C}_c\mathbf{x}_c(t) + \mathbf{B}_p\mathbf{D}_c\mathbf{C}_p\mathbf{x}_p(t-\tau) \tag{3.38}$$

The controller dynamic is given by:

$$\dot{\mathbf{x}}_c(t) = \mathbf{A}_c\mathbf{x}_c(t) + \mathbf{B}_c\hat{\mathbf{y}}_p(t)$$

$$\dot{\mathbf{x}}_c(t) = \mathbf{A}_c\mathbf{x}_c(t) + \mathbf{B}_c\mathbf{y}_p(t-\tau)$$

$$\dot{\mathbf{x}}_c(t) = \mathbf{A}_c\mathbf{x}_c(t) + \mathbf{B}_c\mathbf{C}_p\mathbf{x}_p(t-\tau) \tag{3.39}$$

The plant and the controller then become:

$$\begin{bmatrix}\dot{\mathbf{x}}_p(t)\\ \dot{\mathbf{x}}_c(t)\end{bmatrix} = \begin{bmatrix}\mathbf{A}_p & \mathbf{B}_p\mathbf{C}_c\\ 0 & \mathbf{A}_c\end{bmatrix}\begin{bmatrix}\mathbf{x}_p(t)\\ \mathbf{x}_c(t)\end{bmatrix} + \begin{bmatrix}\mathbf{B}_p\mathbf{D}_c\mathbf{C}_p & 0\\ \mathbf{B}_c\mathbf{C}_p & 0\end{bmatrix}\begin{bmatrix}\mathbf{x}_p(t-\tau)\\ \mathbf{x}_c(t-\tau)\end{bmatrix} \tag{3.40}$$

Theorem 3.4:

Suppose that H 3.1 and H 3.2 hold. For system (3.34) with the dynamic controller of (3.35), the closed-loop system is globally asymptotically stable if $\lambda_i(\mathbf{\Lambda}) \in \mathbb{C}^-$, for $i = 1, 2, \cdots, n$ and all the state variables' 2nd order reminders are small enough for the given value of τ, where $\mathbf{\Lambda}$ is given by:

$$\mathbf{\Lambda} = \left(\mathbf{I} + \begin{bmatrix}\tau_{sc}\mathbf{B}_p\mathbf{D}_c\mathbf{C}_p & 0\\ \tau_{sc}\mathbf{B}_c\mathbf{C}_p & 0\end{bmatrix}\right)^{-1}\begin{bmatrix}\mathbf{A}_p + \mathbf{B}_p\mathbf{D}_c\mathbf{C}_p & \mathbf{B}_p\mathbf{C}_c\\ \mathbf{B}_c\mathbf{C}_p & \mathbf{A}_c\end{bmatrix} \tag{3.41}$$

Proof:

Recall; $\mathbf{x}(t) = \begin{bmatrix} \mathbf{x}_p(t) \\ \mathbf{x}_c(t) \end{bmatrix}$ $\mathbf{A} = \begin{bmatrix} \mathbf{A}_p & \mathbf{B}_p\mathbf{C}_c \\ 0 & \mathbf{A}_c \end{bmatrix}$ $\mathbf{A}_d = \begin{bmatrix} \mathbf{B}_p\mathbf{D}_c\mathbf{C}_p & 0 \\ \mathbf{B}_c\mathbf{C}_p & 0 \end{bmatrix}$ Then (3.40) becomes:

$$\dot{\mathbf{x}}(t) = \mathbf{A}\mathbf{x}(t) + \mathbf{A}_d\mathbf{x}(t-\tau) \tag{3.42}$$

Substituting (3.10) into (3.42), the following can be derived:

$$\dot{\mathbf{x}}(t) = (\mathbf{A} + \mathbf{A}_d)\mathbf{x}(t) - \tau\ \mathbf{A}_d\dot{\mathbf{x}}(t) \tag{3.43}$$

$$\dot{\mathbf{x}}(t) = [(\mathbf{I} + \tau\ \mathbf{A}_d)^{-1}(\mathbf{A} + \mathbf{A}_d)]\mathbf{x}(t) \tag{3.44}$$

$$\mathbf{\Lambda} = [(\mathbf{I} + \tau\ \mathbf{A}_d)^{-1}(\mathbf{A} + \mathbf{A}_d)] \tag{3.45}$$

$$\mathbf{\Lambda} = \left(\mathbf{I} + \begin{bmatrix} \tau\ \mathbf{B}_p\mathbf{D}_c\mathbf{C}_p & 0 \\ \tau\ \mathbf{B}_c\mathbf{C}_p & 0 \end{bmatrix}\right)^{-1} \begin{bmatrix} \mathbf{A}_p + \mathbf{B}_p\mathbf{D}_c\mathbf{C}_p & \mathbf{B}_p\mathbf{C}_c \\ \mathbf{B}_c\mathbf{C}_p & \mathbf{A}_c \end{bmatrix} \tag{3.46}$$

The system (3.40) will be globally asymptotically stable if

$\lambda_i(\mathbf{\Lambda}) \in \mathrm{C}^-$, for $i = 1, 2, \cdots, n$. □

Corollary 3.5:

Suppose H 3.1 and H 3.2 hold. For the control system (3.34) and (3.35) the closed-loop system is globally asymptotically stable if

$$\tau < 1/(\left\|\mathbf{B}_p\mathbf{D}_c\mathbf{C}_p\right\| + \left\|\mathbf{B}_c\mathbf{C}_p\right\|).$$

Proof: *Straight forward as Corollary 3.1.*

3.4.3 Case II: Taking τ_{ca} into consideration:

In this case, the controller to actuator time delay has been taken into consideration. Applying the dynamic controller proposed in (3.35) to the plant (3.34), we have:

$$\dot{\mathbf{x}}_p(t) = \mathbf{A}_p\mathbf{x}_p(t) + \mathbf{B}_p\mathbf{C}_c\mathbf{x}_c(t-\tau_{ca}) + \mathbf{B}_p\mathbf{D}_c\mathbf{C}_p\mathbf{x}_p(t-\tau)$$

$$\dot{\mathbf{x}}_c(t) = \mathbf{A}_c\mathbf{x}_c(t) + \mathbf{B}_c\mathbf{C}_p\mathbf{x}_p(t-\tau_{sc}) \tag{3.47}$$

Theorem 3.5:

Suppose that H 3.1 and H 3.2 hold. For system (3.34) with the dynamic controller of (3.35), the closed-loop system is globally asymptotically stable if $\lambda_i(\mathbf{\Phi}) \in \mathbb{C}^-$, for $i = 1, 2, \cdots, n$ and all the state variables' 2nd order reminders are small enough for the given value of τ_{sc} and τ_{ca}, where $\mathbf{\Phi}$ is given by:

$$\mathbf{\Phi} = \left(\mathbf{I} + \begin{bmatrix} (\tau_{sc}+\tau_{ca})\mathbf{B}_p\mathbf{D}_c\mathbf{C}_p & \tau_{ca}\mathbf{B}_p\mathbf{C}_c \\ \tau_{sc}\mathbf{B}_c\mathbf{C}_p & 0 \end{bmatrix} \right)^{-1} \begin{bmatrix} \mathbf{A}_p + \mathbf{B}_p\mathbf{D}_c\mathbf{C}_p & \mathbf{B}_p\mathbf{C}_c \\ \mathbf{B}_c\mathbf{C}_p & \mathbf{A}_c \end{bmatrix}$$

Proof: *Straight forward as Theorem 3.1.*

Corollary 3.6:

Suppose H 3.1 and H 3.2 hold. For the plant (3.34) with controller (3.35) the closed-loop system is globally asymptotically stable if

$$\tau_{sc}\left(\left\|\mathbf{B}_p\mathbf{D}_c\mathbf{C}_p\right\| + \left\|\mathbf{B}_c\mathbf{C}_p\right\|\right) + \tau_{ca}\left(\left\|\mathbf{B}_p\mathbf{D}_c\mathbf{C}_p\right\| + \left\|\mathbf{B}_p\mathbf{C}_c\right\|\right) < 1$$

Proof: *Straight forward as Corollary 3.1.*

Substituting with $\tau_{sc} = \tau$ and $\tau_{ca} = 0$ in either Theorem 3.5 or Corollary 3.6 they are reduced to Theorem 3.4 or Corollary 3.5 respectively.

3.4.4 Maximum allowable delay bound estimation in the s-domain

Corollary 3.7

If system (3.34) with controller (3.35) is asymptotically stable for $\tau < 1/\left|\lambda_{\min}(\mathbf{A}_d)\right|$ then $\lambda_i[(I+\tau\mathbf{A}_d)^{-1}] \in \mathrm{C}^+, \text{for} \quad i = 1,2,\cdots,n$. This means:

$$\tau < \frac{1}{\left|\lambda_{\min}(\mathbf{A}_d)\right|} \qquad \rightarrow \qquad \lambda_i(\mathbf{I}_{n\times n} + \tau\mathbf{A}_d)^{-1} > 0$$

Proof:

For more general case for time delay systems with dynamic controller, multi-Input-multi-output systems and system with delayed states. These systems can be modelled as:

$$\dot{\mathbf{x}}(t) = \mathbf{A}\mathbf{x}(t) + \mathbf{A}_d\mathbf{x}(t-\tau) \tag{3.48}$$

The main assumption is that the eigenvalues of $\mathbf{A}_d$ are all negative, $s_1 < 0, \cdots, s_n < 0$, and are given by;

$$\mathbf{A}_d - s\mathbf{I}_{n\times n} = \begin{bmatrix} a_{11}-s & a_{12} & \cdots & a_{1n} \\ a_{21} & a_{22}-s & \cdots & a_{2n} \\ \vdots & \vdots & \ddots & \vdots \\ a_{n1} & a_{n2} & \cdots & a_{nn}-s \end{bmatrix} \tag{3.49}$$

The characteristic equation is the determinant of the above equation. Assume that the eigenvalues are given by:

$$s_1 = \alpha_1, \cdots, s_n = \alpha_n \qquad \alpha_1 < 0, \cdots, \alpha_n < 0 \tag{3.50}$$

The eigenvalues of $(\mathbf{I}_{n\times n} + \tau\mathbf{A}_d)$ are given by:

$$\tau \cdot \mathbf{A}_d + \mathbf{I}_{n\times n} - \lambda \mathbf{I}_{n\times n} = \begin{bmatrix} \tau a_{11} + 1 - \lambda & \tau a_{12} & \cdots & \tau a_{1n} \\ \tau a_{21} & \tau a_{22} + 1 - \lambda & \cdots & \tau a_{2n} \\ \vdots & \vdots & \ddots & \vdots \\ \tau a_{n1} & \tau a_{n2} & \cdots & \tau a_{nn} + 1 - \lambda \end{bmatrix} \tag{3.51}$$

The characteristic equation is the determinant of (3.51);

$$\begin{aligned} &\det\left(\begin{bmatrix} \tau a_{11} + 1 - \lambda & \tau a_{12} & \cdots & \tau a_{1n} \\ \tau a_{21} & \tau a_{22} + 1 - \lambda & \cdots & \tau a_{2n} \\ \vdots & \vdots & \ddots & \vdots \\ \tau a_{n1} & \tau a_{n2} & \cdots & \tau a_{nn} + 1 - \lambda \end{bmatrix}\right) \\ &= \tau^n \det\left(\begin{bmatrix} a_{11} + (1-\lambda)/\tau & a_{12} & \cdots & a_{1n} \\ a_{21} & a_{22} + (1-\lambda)/\tau & \cdots & a_{2n} \\ \vdots & \vdots & \ddots & \vdots \\ a_{n1} & a_{n2} & \cdots & a_{nn} + (1-\lambda)/\tau \end{bmatrix}\right) = 0 \end{aligned} \tag{3.52}$$

Replacing $(\lambda - 1)/\tau$ by $-s$ in (3.52) we get;

$$= \tau^n \det\left(\begin{bmatrix} a_{11} - s & a_{12} & \cdots & a_{1n} \\ a_{21} & a_{22} - s & \cdots & a_{2n} \\ \vdots & \vdots & \ddots & \vdots \\ a_{n1} & a_{n2} & \cdots & a_{nn} - s \end{bmatrix}\right) \tag{3.53}$$

From (3.53) we can find that:

$$(\lambda_1 - 1)/\tau = \alpha_1, \cdots, (\lambda_n - 1)/\tau = \alpha_n \qquad \alpha_1 < 0, \cdots, \alpha_n < 0$$

$$\lambda_1 = 1 + \tau\alpha_1, \cdots, \lambda_n = 1 + \tau\alpha_n \qquad \alpha_1 < 0, \cdots, \alpha_n < 0 \tag{3.54}$$

If $\tau < 1/|\alpha_{\min}|$ then all the eigenvalues are positive, and if $\tau > 1/|\alpha_{\min}|$ at least one of the eigenvalues will be negative so if $\tau < \dfrac{1}{|\lambda_{\min}(\mathbf{A}_d)|}$ then $(\mathbf{I} + \tau\mathbf{A}_d)^{-1}$ is positive definite.

Example 3.4:

$$\mathbf{A}_p = \begin{bmatrix} 0 & 1 \\ 0 & -0.1 \end{bmatrix} \mathbf{B}_p = \begin{bmatrix} 0 \\ 0.1 \end{bmatrix} \quad \mathbf{C}_p = \begin{bmatrix} 1 & 0 \\ 0 & 1 \end{bmatrix} \mathbf{A}_c = \begin{bmatrix} 0 & 0 \\ 0 & 0 \end{bmatrix} \mathbf{B}_c = \begin{bmatrix} 0 & 0 \\ 0 & 0 \end{bmatrix} \mathbf{C}_c = \begin{bmatrix} 2 & 3 \end{bmatrix}$$

$$\mathbf{D}_c = \begin{bmatrix} -3.75 & -11.5 \end{bmatrix}$$

This example appeared in (Zhang et al. 2008a;Zhang et al. 2008b). The MADB using Theorem 3.4 is 0.869 s. Using Corollary 3.5 we have; $\left\|\mathbf{B}_p\mathbf{D}_c\mathbf{C}_p\right\| = 1.2096$ and $\left\|\mathbf{B}_c\mathbf{C}_p\right\| = 0$, so the MADB is 0.827 s. The same result can be obtained using the LMI method reported in (Yue et al. 2004b ;Naghshtabrizi 2007;Zhang et al. 2008a;Zhang et al. 2008b). In (Branicky et al. 2000;Zhang et al. 2001), the value reported for MADB is 4.5×10^{-4} s and in (Park et al. 2002) it is 0.0538 s. In (Yang et al. 2007), the MADB is 0.785 s. It has been reported in (Jian et al. 2008), where an improved Lyapunov-Krasovskii approach has been used, that the MADB is 1.0551 s, also 1.05 s reported in (Zhang et al. 2008b) with improved algorithm for solving the LMI. In (Jiang et al. 2008a), the MADB is 1.0081 s. Using the proposed method with second-order finite difference approximation we can obtain 1.13 s as the MADB.

Example 3.5:

$$\mathbf{A}_p = \begin{bmatrix} 0 & 1 \\ -2 & -3 \end{bmatrix} \mathbf{B}_p = \begin{bmatrix} 0 \\ 1 \end{bmatrix} \mathbf{C}_p = \begin{bmatrix} 0 & 1 \end{bmatrix} \mathbf{A}_c = \begin{bmatrix} 0 & 1 \\ -0.1 & -0.1 \end{bmatrix} \mathbf{B}_c = \begin{bmatrix} 0 \\ -0.01 \end{bmatrix}$$

$$\mathbf{C}_c = \begin{bmatrix} 0.02 & 0.01 \end{bmatrix} \mathbf{D}_c = 0$$

This system appeared in (Xue et al. 2008), where they used a variable-sampling approach for analyzing the NCS. The MADB using Theorem 3.4 is 6002 s. The eigenvalues of the open-loop system are -2 and -1 and with the controller they are -2, -0.9999,

-0.0501±j0.3123. We can see that the controller does not affect the system stability nor the performance and the system is expected to withstand very long time delay. Using Corollary 3.5 we have $\left\|\mathbf{B}_p\mathbf{D}_c\mathbf{C}_p\right\| = 0$ and $\left\|\mathbf{B}_c\mathbf{C}_p\right\| = 0.01$ so $\tau_{sc} < 100$. We can see that Corollary 3.5 gives more conservative result.

Example 3.6:

This example is unstable batch reactor (Antunes et al. 2009;Nesic et al. 2004). The two-input-two-output linearized model of an unstable batch reactor is given by:

$$\mathbf{A}_p = \begin{bmatrix} 1.38 & -0.2077 & 6.715 & -5.676 \\ -0.5814 & -4.29 & 0 & 0.675 \\ 1.067 & 4.273 & -6.654 & 5.893 \\ 0.048 & 4.273 & 1.343 & -2.104 \end{bmatrix} \mathbf{B}_p = \begin{bmatrix} 0 & 0 \\ 5.679 & 0 \\ 1.136 & -3.146 \\ 1.136 & 0 \end{bmatrix}$$

$$\mathbf{C}_p = \begin{bmatrix} 1 & 0 & 1 & -1 \\ 0 & 1 & 0 & 0 \end{bmatrix} \mathbf{A}_c = \begin{bmatrix} 0 & 0 \\ 0 & 0 \end{bmatrix} \mathbf{B}_c = \begin{bmatrix} 0 & 1 \\ 1 & 0 \end{bmatrix} \mathbf{C}_c = \begin{bmatrix} -2 & 0 \\ 0 & 8 \end{bmatrix} \mathbf{D}_c = \begin{bmatrix} 0 & -2 \\ 5 & 0 \end{bmatrix}$$

The MADB using Theorem 3.4 is 0.0635 s. With different protocols and Theorems (Nesic et al. 2004) obtained 0.01, 0.0082 and 0.0657 as the MADB and the simulation based actual MADB is 0.089 s. In (Naghshtabrizi 2007) with a sampling-data approach the MADB is 0.0405 s. Also 0.0279 s and 0.0517 s are reported in (Antunes et al. 2009). In (Tabbara et al. 2007), the MADB is 0.0123 s. Although our method still gives more conservative results than some published ones, it is much simpler. Using Corollary 3.5 we have; $\left\|\mathbf{B}_p\mathbf{D}_c\mathbf{C}_p\right\| = 27.3603$ and $\left\|\mathbf{B}_c\mathbf{C}_p\right\| = 1.7321$, so the MADB is 0.0344 s. With Corollary 3.6 and assuming $\tau_{sc} = \tau_{ca}$ the MADB is 0.0122 s. It is noticed that using Corollary 3.6 more conservative results are produced.

Example 3.7:

The last example is the CH-47 tandem-rotor helicopter (Tabbara et al. 2005);

$$\mathbf{A}_p = \begin{bmatrix} -0.02 & 0.005 & 2.4 & -32 \\ -0.14 & 0.44 & -1.3 & -30 \\ 0 & 0.018 & -1.6 & 1.2 \\ 0 & 0 & 1 & 0 \end{bmatrix} \mathbf{B}_p = \begin{bmatrix} 0.14 & -0.12 \\ 0.36 & -8.6 \\ 0.35 & 0.009 \\ 0 & 0 \end{bmatrix} \mathbf{C}_p = \begin{bmatrix} 0 & 1 & 0 & 0 \\ 0 & 0 & 0 & 57.3 \end{bmatrix}$$

$$\mathbf{A}_c = \begin{bmatrix} 0 & 0 \\ 0 & 0 \end{bmatrix} \mathbf{B}_c = \begin{bmatrix} 0 \\ 0 \end{bmatrix} \quad \mathbf{C}_c = \begin{bmatrix} 0 & 0 \end{bmatrix} \mathbf{D}_c = \begin{bmatrix} -12.7177 & -45.0824 \\ 63.5123 & 25.9144 \end{bmatrix}$$

The maximum time delay using Theorem 3.4 is 1.81×10^{-3} s. Using Corollary 3.5 we have $\left\|\mathbf{B}_p\mathbf{D}_c\mathbf{C}_p\right\| = 13751$ and $\left\|\mathbf{B}_c\mathbf{C}_p\right\| = 0$ then the MADB is 7.272×10^{-5} s. In (Antunes, et al. 2009) the values reported for MADB are 8.02×10^{-4}, 1.48×10^{-3} and 6.21×10^{-4} s. The MADB reported in (Tabbara et al. 2005) is 4.23×10^{-5} s. In (Tabbara et al. 2007) after some improvements to their method the MADB values are 2.81×10^{-4} s and 5.4×10^{-5} s with different protocols. Through the simulation the system is stable even with 0.002 s. The system output; vertical velocity (x_2) and pitch altitude (x_4) are shown in Figure 3.4 with 0.0018 s time delay. In this example our method gives less conservative results than the published ones.

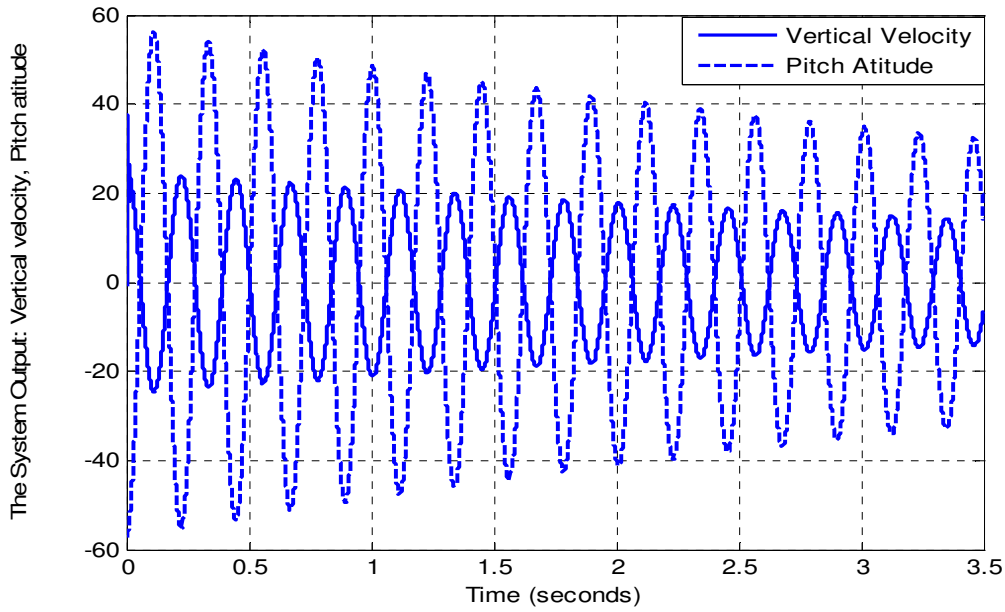

Figure 3.4 The response of the CH-47 with 0.0018 s time delay

3.5 Controller design using the finite difference approximation:

The previous theorems and corollaries can be used to estimate the MADB in NCS or in other words, to study the stability of the NCS. In this section, we will present a controller design method assuming that H 3.1 and H 3.2 hold and both Corollary 3.1 and Corollary 3.2 are satisfied.

Theorem 3.6

The system (3.1) with the linear controller (3.2) is asymptotically stable for small $\tau > 0$ if there exist $\mathbf{Q} = \mathbf{Q}^T > 0$ such that the following LMI is feasible:

$$\begin{bmatrix} -2\mathbf{Q} - \tau \cdot \mathbf{Y}^T\mathbf{B}^T - \tau \cdot \mathbf{B}\mathbf{Y} & \mathbf{0} \\ \mathbf{0} & \mathbf{A}\mathbf{Q} + \mathbf{B}\mathbf{Y} + \mathbf{Q}\mathbf{A}^T + \mathbf{Y}^T\mathbf{B}^T \end{bmatrix} < 0$$

where $\mathbf{Y} = \mathbf{K}\mathbf{Q}$

Proof

Since the system without the time delay must be stable for $\mathbf{P} = \mathbf{P}^T > 0$, we have the Lyapunov functional candidate as:

$$\mathbf{V}(x) = \mathbf{x}^{\mathbf{T}}\mathbf{P}\mathbf{x} \qquad \mathbf{x} \neq \mathbf{0} \tag{3.55}$$

Taking derivative of (3.55), then we have:

$$\dot{\mathbf{V}}(x) = \mathbf{x}^{\mathbf{T}}[(\mathbf{A}+\mathbf{BK})^{\mathbf{T}}\mathbf{P} + \mathbf{P}(\mathbf{A}+\mathbf{BK})]\mathbf{x}$$

Then $\dot{\mathrm{V}}(x) < 0$ if:

$$(\mathbf{A}+\mathbf{BK})^{\mathbf{T}}\mathbf{P} + \mathbf{P}(\mathbf{A}+\mathbf{BK}) < 0$$

$$\mathbf{P}^{-1}(\mathbf{A}+\mathbf{BK})^{\mathbf{T}} + (\mathbf{A}+\mathbf{BK})\mathbf{P}^{-1} < 0$$

$$\mathbf{Q}(\mathbf{A}+\mathbf{BK})^{\mathbf{T}} + (\mathbf{A}+\mathbf{BK})\mathbf{Q} < 0 \tag{3.56}$$

If (3.56) is satisfied, then $\lambda_i(\mathbf{A}+\mathbf{BK}) \in \mathrm{C}^-$, for $i = 1,2,\cdots,n$. For the time delay system to be asymptotically stable $\lambda_i[(I+\tau\mathbf{BK})^{-1}(\mathbf{A}+\mathbf{BK})] \in \mathrm{C}^-$, for $i = 1,2,\cdots,n$ and from Corollary 3.2, $\lambda_i[(I+\tau\mathbf{BK})^{-1}] \in \mathrm{C}^+$, for $i = 1,2,\cdots,n$, then we must have:

$$\mathbf{P}(\mathbf{I}+\tau\mathbf{BK})^{-1} + (\mathbf{I}+\tau\mathbf{BK})^{-T}\mathbf{P} > 0 \tag{3.57}$$

$$\mathbf{P}(\mathbf{I}+\tau\mathbf{BK})^{-1}(\mathbf{I}+\tau\mathbf{BK}) + (\mathbf{I}+\tau\mathbf{BK})^{-T}\mathbf{P}(\mathbf{I}+\tau\mathbf{BK}) > 0$$

$$(\mathbf{I}+\tau\mathbf{BK})^{T}\mathbf{P}(\mathbf{I}+\tau\mathbf{BK})^{-1}(\mathbf{I}+\tau\mathbf{BK}) + (\mathbf{I}+\tau\mathbf{BK})^{T}(\mathbf{I}+\tau\mathbf{BK})^{-T}\mathbf{P}(\mathbf{I}+\tau\mathbf{BK}) > 0$$

$$(\mathbf{I}+\tau\mathbf{BK})^{T}\mathbf{P} + \mathbf{P}(\mathbf{I}+\tau\mathbf{BK}) > 0$$

$$\mathbf{P}^{-1}(\mathbf{I}+\tau\mathbf{BK})^T\mathbf{P}\mathbf{P}^{-1}+\mathbf{P}^{-1}\mathbf{P}(\mathbf{I}+\tau\mathbf{BK})\mathbf{P}^{-1}>0$$

$$\mathbf{P}^{-1}(\mathbf{I}+\tau\mathbf{BK})^T+(\mathbf{I}+\tau\mathbf{BK})\mathbf{P}^{-1}>0$$

$$\mathbf{Q}(\mathbf{I}+\tau\mathbf{BK})^T+(\mathbf{I}+\tau\mathbf{BK})\mathbf{Q}>0 \tag{3.58}$$

Choosing $\mathbf{Y}=\mathbf{KQ}$, $\mathbf{Y}^T=\mathbf{QK}^T$, and applying in (3.56) we have;

$$\mathbf{QA}^T+\mathbf{QK}^T\mathbf{B}^T+\mathbf{AQ}+\mathbf{BKQ}<0$$

$$\mathbf{QA}^T+\mathbf{Y}^T\mathbf{B}^T+\mathbf{AQ}+\mathbf{BY}<0 \tag{3.59}$$

Then (3.58) becomes;

$$\mathbf{Q}+\tau\mathbf{QK}^T\mathbf{B}^T+\mathbf{Q}+\tau\mathbf{BKQ}>0$$

$$2\mathbf{Q}+\tau\mathbf{Y}^T\mathbf{B}^T+\tau\mathbf{BY}>0 \tag{3.60}$$

Finally the system with given time delay to be stable for $\mathbf{Q}=\mathbf{Q}^T>0$, we must have;

$$\mathbf{QA}^T+\mathbf{Y}^T\mathbf{B}^T+\mathbf{AQ}+\mathbf{BY}<0$$

$$2\mathbf{Q}+\tau\mathbf{Y}^T\mathbf{B}^T+\tau\mathbf{BY}>0 \tag{3.61}$$

The LMIs (3.61) can be written as single LMI as follows:

$$\begin{bmatrix}-2\mathbf{Q}-\tau\cdot\mathbf{Y}^T\mathbf{B}^T-\tau\cdot\mathbf{BY} & \mathbf{0}\\ \mathbf{0} & \mathbf{AQ}+\mathbf{BY}+\mathbf{QA}^T+\mathbf{Y}^T\mathbf{B}^T\end{bmatrix}<0$$

Example 3.8:

$\mathbf{A}=\begin{bmatrix}0 & 1\\ 0 & -0.1\end{bmatrix}$ $\mathbf{B}=\begin{bmatrix}0\\ 0.1\end{bmatrix}$ The time delay is 0.2 s.

Using Theorem 3.6 and solving the LMI we get;

$$\mathbf{Y} = \begin{bmatrix} -10.0642 & -7.6449 \end{bmatrix} \qquad \mathbf{Q} = \begin{bmatrix} 1.0273 & -0.1854 \\ -0.1854 & 1.0273 \end{bmatrix} \qquad \mathbf{K} = \begin{bmatrix} -11.3952 & -8.8524 \end{bmatrix}$$

The response of the system with 0.2 s time delay is shown in Figure 3.5 which shows the system is stable.

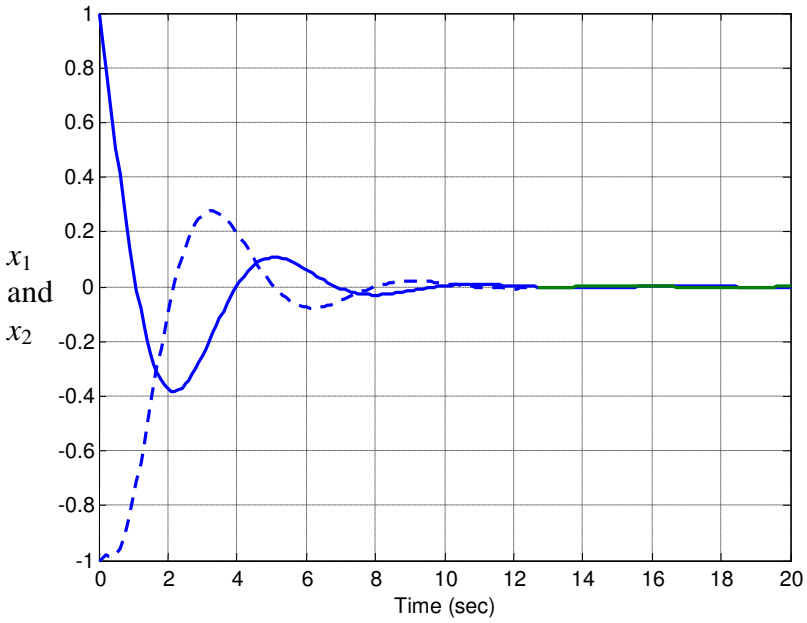

Figure 3.5 The system response with 0.2 s time delay.

3.6 Networked Control of Distributed Interconnected Units

The distributed systems, such as power systems, Microgrids, parallel DC/DC and DC/AC converters are composed of *n* interconnected subsystems. Each subsystem can be modelled by a continuous-time linear or non-linear system, the *n* networked subsystems are shown in Figure 3.6.

3.6.1 Mathematical model of n-connected networked control systems

The mathematical model of n linear connected systems is given by (Sun et al. 2008):

$$\begin{aligned}
\dot{\mathbf{x}}^{(1)} &= \mathbf{A}_{11}\mathbf{x}^{(1)} + \mathbf{B}_1\mathbf{u}^{(1)} + \sum_{\mathbf{j=2}}^{\mathbf{n}} \mathbf{A}_{1\mathbf{j}}\mathbf{x}^{(\mathbf{j})} \\
\dot{\mathbf{x}}^{(2)} &= \mathbf{A}_{22}\mathbf{x}^{(2)} + \mathbf{B}_2\mathbf{u}^{(2)} + \sum_{\mathbf{j=1,j\neq i}}^{\mathbf{n}} \mathbf{A}_{2\mathbf{j}}\mathbf{x}^{(\mathbf{j})} \\
&\vdots \\
\dot{\mathbf{x}}^{(\mathbf{n})} &= \mathbf{A}_{\mathbf{nn}}\mathbf{x}^{(\mathbf{n})} + \mathbf{B}_{\mathbf{n}}\mathbf{u}^{(n)} + \sum_{\mathbf{j=1}}^{\mathbf{n-1}} \mathbf{A}_{\mathbf{nj}}\mathbf{x}^{(\mathbf{j})}
\end{aligned} \tag{3.62}$$

where: $\mathbf{x}^{(1)}$, $\mathbf{x}^{(2)}$, . . ., $\mathbf{x}^{(n)}$ are the states vectors. $\mathbf{u}^{(1)}$, $\mathbf{u}^{(2)}$, . . . , $\mathbf{u}^{(n)}$ are control input vectors. $\mathbf{x}^{(i)} := \left[\mathbf{x}_1^{(i)} \quad \mathbf{x}_2^{(i)} \quad . \quad . \quad . \quad \mathbf{x}_{\mathbf{n_i}}^{(i)}\right]^{\mathbf{T}} \in \Re^{\mathbf{n_i}}$ and $\mathbf{u}^{(i)} := \left[\mathbf{u}_1^{(i)} \quad \mathbf{u}_2^{(i)} \quad . \quad . \quad . \quad \mathbf{u}_{\mathbf{n_i}}^{(i)}\right]^{\mathbf{T}} \in \Re^{\mathbf{n_i}}$, n_i is the number of states in the i^{th} subsystem. $\mathbf{A}_{ij}$ (where $i \neq j$) describes how the dynamics of the i^{th} subsystem can be influenced by the j^{th} subsystem. Equation (3.62) can be written in general form as:

$$\dot{\mathbf{x}}^{(\mathbf{i})} = \mathbf{A}_{\mathbf{ii}}\mathbf{x}^{(\mathbf{i})} + \mathbf{B}_{\mathbf{i}}\mathbf{u}^{(\mathbf{i})} + \sum_{\mathbf{j=1,j\neq i}}^{\mathbf{n}} \mathbf{A}_{\mathbf{ij}}\mathbf{x}^{(\mathbf{j})} \qquad i = 1,2,\cdots,n \tag{3.63}$$

With quasi-decentralized control law consists of global and local controller and given by:

$$\mathbf{u}^{\mathbf{i}} = \mathbf{u}_l^{\mathbf{i}} + \mathbf{u}_g^{i} = \mathbf{K}_{\mathbf{ii}}\mathbf{x}^{(\mathbf{i})} + \sum_{\mathbf{j=1,j\neq i}}^{\mathbf{n}} \mathbf{K}_{\mathbf{ij}}\mathbf{x}^{(\mathbf{j})}(t - \tau_{ji}) \tag{3.64}$$

If $\mathbf{K}_{\mathbf{ij}} = 0$, then we have full decentralized control system.

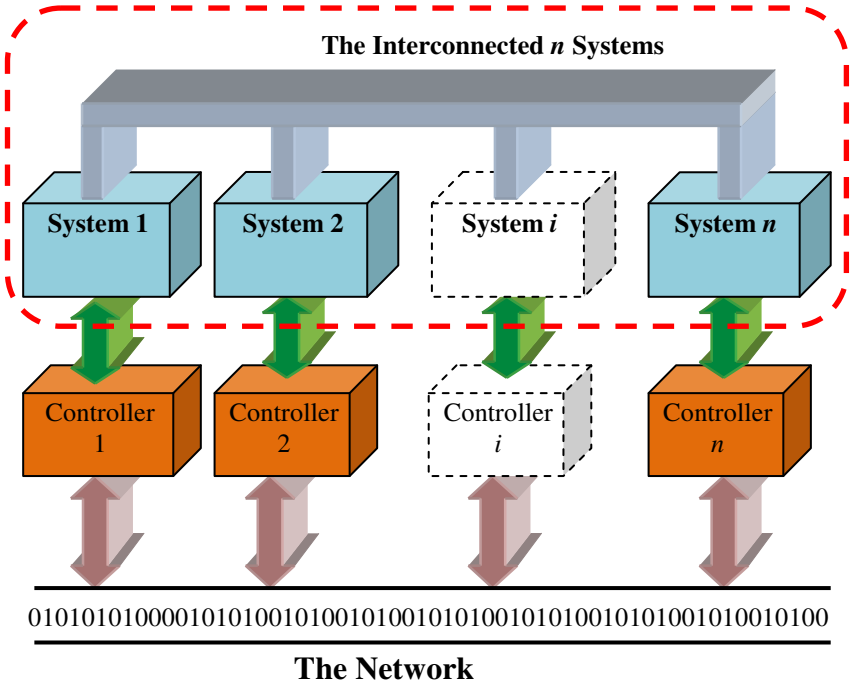

Figure 3.6 A networked system consists of *n* sub-systems.

Theorem 3.7:

Suppose that H 3.1 and H 3.2 hold. For the system (3.62) with the controllers of (3.63), the closed-loop system is globally asymptotically stable if $\lambda_i(\boldsymbol{\Theta}) \in \mathbb{C}^-$, for $i = 1, 2, \cdots, n$ and all the state variables' 2^{nd} order reminders are small enough for the given value of τ, where $\boldsymbol{\Theta}$ is given by:

$$\boldsymbol{\Theta} = \left(\mathbf{I}_{n\times n} + \tau \begin{bmatrix} \mathbf{0} & \mathbf{B}_1\mathbf{K}_{12} & \cdots & \mathbf{B}_1\mathbf{K}_{1n} \\ \mathbf{B}_2\mathbf{K}_{21} & \mathbf{0} & \cdots & \mathbf{B}_2\mathbf{K}_{2n} \\ \vdots & \vdots & \ddots & \vdots \\ \mathbf{B}_n\mathbf{K}_{n1} & \mathbf{B}_n\mathbf{K}_{n3} & \cdots & \mathbf{0} \end{bmatrix} \right)^{-1} \begin{bmatrix} \mathbf{A}_{11}+\mathbf{B}_1\mathbf{K}_{11} & \mathbf{A}_{12}+\mathbf{B}_1\mathbf{K}_{12} & \cdots & \mathbf{A}_{1n}+\mathbf{B}_1\mathbf{K}_{1n} \\ \mathbf{A}_{21}+\mathbf{B}_2\mathbf{K}_{21} & \mathbf{A}_{22}+\mathbf{B}_2\mathbf{K}_{22} & \cdots & \mathbf{A}_{2n}+\mathbf{B}_2\mathbf{K}_{2n} \\ \vdots & \vdots & \cdots & \vdots \\ \mathbf{A}_{n1}+\mathbf{B}_n\mathbf{K}_{n1} & \mathbf{A}_{n2}+\mathbf{B}_n\mathbf{K}_{n2} & \cdots & \mathbf{A}_{nn}+\mathbf{B}_n\mathbf{K}_{nn} \end{bmatrix}$$

Proof:

Substituting (3.64) into (3.62) we get:

$$\begin{aligned}
\dot{\mathbf{x}}^{(1)} &= \mathbf{A_{11}}\mathbf{x}^{(1)} + \mathbf{B_1}\mathbf{K}_{11}\mathbf{x}^{(1)} + \sum_{\mathbf{j=2}}^{\mathbf{n}} \mathbf{A_{1j}}\mathbf{x}^{(\mathbf{j})}(\mathbf{t}) + \sum_{\mathbf{j=1,j\neq i}}^{\mathbf{n}} \mathbf{B_1}\mathbf{K}_{1\mathbf{j}}\mathbf{x}^{(\mathbf{j})}(t-\tau_{j1}) \\
\dot{\mathbf{x}}^{(2)} &= \mathbf{A_{22}}\mathbf{x}^{(2)} + \mathbf{B_2}\mathbf{K}_{22}\mathbf{x}^{(2)} + \sum_{\mathbf{j=1,j\neq i}}^{\mathbf{n}} \mathbf{A_{2j}}\mathbf{x}^{(\mathbf{j})}(\mathbf{t}) + \sum_{\mathbf{j=1,j\neq i}}^{\mathbf{n}} \mathbf{B_2}\mathbf{K}_{2\mathbf{j}}\mathbf{x}^{(\mathbf{j})}(t-\tau_{j2}) \\
&\vdots \\
\dot{\mathbf{x}}^{(\mathbf{n})} &= \mathbf{A_{nn}}\mathbf{x}^{(\mathbf{n})} + \mathbf{B_n}\mathbf{K}_{nn}\mathbf{x}^{(n)} + \sum_{\mathbf{j=1}}^{\mathbf{n-1}} \mathbf{A_{nj}}\mathbf{x}^{(\mathbf{j})}(\mathbf{t}) + \sum_{\mathbf{j=1,j\neq i}}^{\mathbf{n}} \mathbf{B_n}\mathbf{K}_{n\mathbf{j}}\mathbf{x}^{(\mathbf{j})}(t-\tau_{jn})
\end{aligned} \tag{3.65}$$

At the node *i,* using the following finite difference approximation:

$$\mathbf{x}^{(\mathbf{j})}(t-\tau_{ji}) = \mathbf{x}^{(\mathbf{j})}(t) - \tau_{ji}\dot{\mathbf{x}}^{(\mathbf{j})}(t) \tag{3.66}$$

Substituting (3.66) into (3.65):

$$\begin{aligned}
\dot{\mathbf{x}}^{(1)} &= (\mathbf{A_{11}} + \mathbf{B_1}\mathbf{K}_{11})\mathbf{x}^{(1)} + \sum_{\mathbf{j=1,j\neq i}}^{\mathbf{n}} (\mathbf{A_{1j}} + \mathbf{B_1}\mathbf{K}_{1\mathbf{j}})\mathbf{x}^{(\mathbf{j})}(t) - \sum_{\mathbf{j=1,j\neq i}}^{\mathbf{n}} \tau_{j1}\mathbf{B_1}\mathbf{K}_{1\mathbf{j}}\dot{\mathbf{x}}^{(\mathbf{j})}(t) \\
\dot{\mathbf{x}}^{(2)} &= (\mathbf{A_{22}} + \mathbf{B_2}\mathbf{K}_{22})\mathbf{x}^{(2)} + \sum_{\mathbf{j=1,j\neq i}}^{\mathbf{n}} (\mathbf{A_{2j}} + \mathbf{B_2}\mathbf{K}_{2\mathbf{j}})\mathbf{x}^{(\mathbf{j})}(t) - \sum_{\mathbf{j=1,j\neq i}}^{\mathbf{n}} \tau_{j2}\mathbf{B_2}\mathbf{K}_{2\mathbf{j}}\dot{\mathbf{x}}^{(\mathbf{j})}(t) \\
&\vdots \\
\dot{\mathbf{x}}^{(\mathbf{n})} &= (\mathbf{A_{nn}} + \mathbf{B_n}\mathbf{K}_{nn})\mathbf{x}^{(n)} + \sum_{\mathbf{j=1,j\neq i}}^{\mathbf{n}} (\mathbf{A_{nj}} + \mathbf{B_n}\mathbf{K}_{n\mathbf{j}})\mathbf{x}^{(\mathbf{j})}(t) - \sum_{\mathbf{j=1,j\neq i}}^{\mathbf{n}} \tau_{jn}\mathbf{B_n}\mathbf{K}_{n\mathbf{j}}\dot{\mathbf{x}}^{(\mathbf{j})}(t)
\end{aligned} \tag{3.67}$$

Writing (3.67) in matrix form:

$$\begin{bmatrix} \dot{\mathbf{x}}^{(1)}(\mathbf{t}) \\ \dot{\mathbf{x}}^{(2)}(\mathbf{t}) \\ . \\ . \\ . \\ \dot{\mathbf{x}}^{(n)}(\mathbf{t}) \end{bmatrix} = \left(\mathbf{I}_{n\times n} + \begin{bmatrix} \mathbf{0} & \tau_{21}\mathbf{B_1}\mathbf{K_{12}} & . & . & . & \tau_{n1}\mathbf{B_1}\mathbf{K}_{1n} \\ \tau_{12}\mathbf{B_2}\mathbf{K_{21}} & \mathbf{0} & . & . & . & \tau_{n2}\mathbf{B_2}\mathbf{K}_{2n} \\ . & . & \mathbf{0} & . & . & . \\ . & . & . & \mathbf{0} & . & . \\ . & . & . & . & \mathbf{0} & . \\ \tau_{n1}\mathbf{B}_n\mathbf{K}_{n1} & \tau_{n2}\mathbf{B}_n\mathbf{K}_{n3} & . & . & . & \mathbf{0} \end{bmatrix} \right)^{-1} *$$

$$\begin{bmatrix} \mathbf{A}_{11}+\mathbf{B}_1\mathbf{K}_{11} & \mathbf{A}_{12}+\mathbf{B}_1\mathbf{K}_{12} & . & . & . & \mathbf{A}_{1n}+\mathbf{B}_1\mathbf{K}_{1n} \\ \mathbf{A}_{21}+\mathbf{B}_2\mathbf{K}_{21} & \mathbf{A}_{22}+\mathbf{B}_2\mathbf{K}_{22} & . & . & . & \mathbf{A}_{2n}+\mathbf{B}_2\mathbf{K}_{2n} \\ . & . & . & . & . & . \\ . & . & . & . & . & . \\ . & . & . & . & . & . \\ \mathbf{A}_{n1}+\mathbf{B}_n\mathbf{K}_{n1} & \mathbf{A}_{n2}+\mathbf{B}_n\mathbf{K}_{n2} & . & . & . & \mathbf{A}_{nn}+\mathbf{B}_n\mathbf{K}_{nn} \end{bmatrix} \begin{bmatrix} \mathbf{x}^{(1)}(\mathbf{t}) \\ \mathbf{x}^{(2)}(\mathbf{t}) \\ . \\ . \\ . \\ \mathbf{x}^{(n)}(\mathbf{t}) \end{bmatrix} \tag{3.68}$$

Assuming $\tau_{ij} = \tau$, where $i \neq j$, $i = 1,2,\cdots,n$ and $j = 1,2,\cdots,n$

$$\begin{bmatrix} \dot{\mathbf{x}}^{(1)}(\mathbf{t}) \\ \dot{\mathbf{x}}^{(2)}(\mathbf{t}) \\ . \\ . \\ . \\ \dot{\mathbf{x}}^{(n)}(\mathbf{t}) \end{bmatrix} = \left(\mathbf{I}_{n\times n} + \begin{bmatrix} \mathbf{0} & \tau\mathbf{B}_1\mathbf{K}_{12} & . & . & . & \tau\mathbf{B}_1\mathbf{K}_{1n} \\ \tau\mathbf{B}_2\mathbf{K}_{21} & \mathbf{0} & . & . & . & \tau\mathbf{B}_2\mathbf{K}_{2n} \\ . & . & \mathbf{0} & . & . & . \\ . & . & . & \mathbf{0} & . & . \\ . & . & . & . & \mathbf{0} & . \\ \tau\mathbf{B}_n\mathbf{K}_{n1} & \tau\mathbf{B}_n\mathbf{K}_{n3} & . & . & . & \mathbf{0} \end{bmatrix} \right)^{-1} *$$

$$\begin{bmatrix} \mathbf{A}_{11}+\mathbf{B}_1\mathbf{K}_{11} & \mathbf{A}_{12}+\mathbf{B}_1\mathbf{K}_{12} & . & . & . & \mathbf{A}_{1n}+\mathbf{B}_1\mathbf{K}_{1n} \\ \mathbf{A}_{21}+\mathbf{B}_2\mathbf{K}_{21} & \mathbf{A}_{22}+\mathbf{B}_2\mathbf{K}_{22} & . & . & . & \mathbf{A}_{2n}+\mathbf{B}_2\mathbf{K}_{2n} \\ . & . & . & . & . & . \\ . & . & . & . & . & . \\ . & . & . & . & . & . \\ \mathbf{A}_{n1}+\mathbf{B}_n\mathbf{K}_{n1} & \mathbf{A}_{n2}+\mathbf{B}_n\mathbf{K}_{n2} & . & . & . & \mathbf{A}_{nn}+\mathbf{B}_n\mathbf{K}_{nn} \end{bmatrix} \begin{bmatrix} \mathbf{x}^{(1)}(\mathbf{t}) \\ \mathbf{x}^{(2)}(\mathbf{t}) \\ . \\ . \\ . \\ \mathbf{x}^{(n)}(\mathbf{t}) \end{bmatrix} \tag{3.69}$$

Equation (3.69) can be used as a fast and easy tool to analyze the stability of a large NCS.

3.6.2 Example: A three synchronous generators controlled over network

In power systems, there are two types of controllers. One is the local controller that is responsible for optimizing the performance of the system without taking the interaction from the network transmitted information into consideration (Hardiansyah et al. 2000). Another type is the global controller that is used to co-ordinate the interactions between the subsystems and hence improves the performance of the overall system. These two types of controllers are applied in a centralized architecture (Hardiansyah et al. 2000). In this study, a

quasi-decentralized control is applied to the system where there exists a transfer of information between the subsystems through a network. As the power system is a huge system dispersed over a large geographical area and relies on the communication for its control it can be viewed as a large NCS. A power system with three machines interconnected through a network is studied to demonstrate how this newly proposed method can be used in the analysis and design of multi-units interconnected distributed NCS.

A networked connection of three generators is shown in Figure 3.7. The three generators rely on the information transferred over the network to meet load demands and for control coordination, the use of the network can mimic the scenario of fault in the central controller. In this manner, the three generators exchange their states through the network.

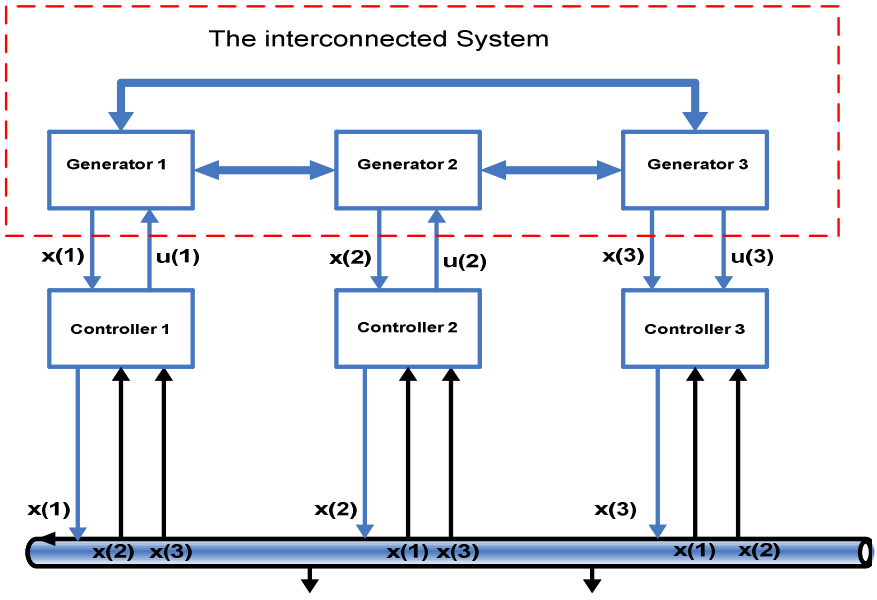

Figure 3.7 Three synchronous generators controlled over network

The interconnected power system shown in Figure 3.8 is a typical three-machine/infinite busbar system (Chen et al. 1987;Fleming et al. 1981;Hanmandlu et al. 1993;Chan et al.

1983). The system consists of one thermal power plant and two hydropower plants, which are rated 360MVA, 503MVA and 1673MVA, respectively. The model used is the linearized 3rd order linear mathematical description equipped with 1st order exciter.

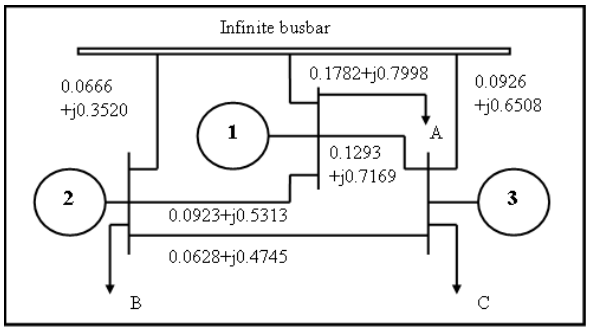

Figure 3.8 Three machine interconnected power system

The small signal mathematical model for a synchronous generator has four state variables $\mathbf{x}^T = \begin{bmatrix} \Delta\omega & \Delta\delta & \Delta e_q & \Delta e_{FD} \end{bmatrix}$, which are the angular velocity, the torque angle, the quadrature transient voltage and the exciter output variation, respectively (Lee et al. 1998). The system model is presented below:

$$\Delta\dot{\omega}(t) = \frac{k_1}{M}\Delta\delta(t) - \frac{k_2}{M}\Delta e_q(t)$$

$$\Delta\dot{\delta}(t) = \omega_0 \Delta\omega(t)$$

$$\Delta\dot{e}_q(t) = -\frac{k_4}{T_{d0}}\Delta\delta(t) - \frac{1}{T_{d0}k_3}\Delta e_q(t) + \frac{1}{T_{d0}}\Delta e_{FD}(t)$$

$$\Delta\dot{e}_{FD}(t) = -\frac{k_4 k_5}{T_A}\Delta\delta(t) - \frac{k_6}{T_A}\Delta e_q(t) - \frac{1}{T_A}\Delta e_{FD}(t) + \frac{k_A}{T_A}u_E \qquad (3.70)$$

where k_1 and k_2 are constants derived from the electric torque, k_3 and k_4 are constants derived from field voltage, k_5 and k_6 are constants derived from terminal voltage, T_A is

the voltage regulator time constant, k_A represents voltage regulator gain, T_{d0} is the *d*-axis transient open circuit time constant, M is the inertia moment coefficient, and u_E represents the excitation control input. The three generators are modelled as three plants with local quasi-decentralized controllers that exchange their states information through a network. The states of the three generators and their state vectors are chosen as follows:

$$x^{(i)} = \begin{bmatrix} x_1^{(i)} & x_2^{(i)} & x_3^{(i)} & x_4^{(i)} \end{bmatrix}^T = \begin{bmatrix} \Delta\omega_i & \Delta\delta_i & \Delta e_{qi} & \Delta e_{FDi} \end{bmatrix}^T \qquad \text{where } i = 1,2,\cdots,3$$

The controller for the i^{th} generator is composed of a local controller that dependens on the states of the i^{th} system and a global controller which depends on the states of the other generators, which are transmitted through the network.

$\mathbf{A}_{11}, \mathbf{A}_{12}, \mathbf{A}_{13}, \mathbf{A}_{21}, \mathbf{A}_{22}, \mathbf{A}_{23}, \mathbf{A}_{31}, \mathbf{A}_{32}$ and $\mathbf{A}_{33}$ are 4-by-4 system state matrices. $\mathbf{B}_1, \mathbf{B}_2$ and $\mathbf{B}_3$ are 4-by-1 vectors. These matrices are listed below (Chen et al. 1987;Fleming et al. 1981;Hanmandlu et al. 1993;Chan et al. 1983):

$$\mathbf{A}_{11} = \begin{bmatrix} 0 & 377 & 0 & 0 \\ -0.147 & -0.039 & -0.013 & 0 \\ -0.266 & -0.393 & -0.922 & 1 \\ -30.1 & -309.14 & -60.943 & -20 \end{bmatrix} \quad \mathbf{A}_{12} = \begin{bmatrix} 0 & 0 & 0 & 0 \\ 0.022 & 0.004 & 0 & 0 \\ -0.087 & 0.754 & 0.024 & 0 \\ 24.599 & -91.99 & -3.501 & 0 \end{bmatrix}$$

$$\mathbf{A}_{13} = \begin{bmatrix} 0 & 0 & 0 & 0 \\ 0.046 & 0.02 & 0.003 & 0 \\ -0.025 & 1.131 & 0.072 & 0 \\ 62.051 & -1675 & -10.194 & 0 \end{bmatrix} \quad \mathbf{A}_{21} = \begin{bmatrix} 0 & 0 & 0 & 0 \\ 0.004 & -0.034 & -0.087 & 0 \\ 0.121 & 1.131 & 0.021 & 0 \\ -18.48 & -64.47 & -12.55 & 0 \end{bmatrix}$$

$$\mathbf{A}_{22} = \begin{bmatrix} 0 & 377 & 0 & 0 \\ -0.149 & 0.032 & -0.008 & 0 \\ -1.6 & -1.885 & -0.21 & 1 \\ 106.09 & -516.11 & -21.67 & -20 \end{bmatrix} \quad \mathbf{A}_{23} = \begin{bmatrix} 0 & 0 & 0 & 0 \\ 0.079 & -0.028 & 0 & 0 \\ 0.46 & 0.754 & 0.06 & 0 \\ 16.99 & -171.91 & -11.41 & 0 \end{bmatrix}$$

$$\mathbf{A}_{31}=\begin{bmatrix} 0 & 0 & 0 & 0 \\ 0.001 & -0.017 & -0.003 & 0 \\ 0.083 & 0 & -0.002 & 0 \\ -10.1 & -33.93 & -6.78 & 0 \end{bmatrix} \qquad \mathbf{A}_{32}=\begin{bmatrix} 0 & 0 & 0 & 0 \\ 0.017 & -0.01 & 0 & 0 \\ 0.22 & 0 & 0.011 & 0 \\ 1.7 & -46.37 & -2.1 & 0 \end{bmatrix}$$

$$\mathbf{A}_{33}=\begin{bmatrix} 0 & 377 & 0 & 0 \\ -0.056 & -0.017 & -0.009 & 0 \\ -1.2 & -1.131 & -0.197 & 1 \\ 70.1 & -893.49 & -54.4 & -20 \end{bmatrix} \quad \mathbf{B}_1=\begin{bmatrix} 0 \\ 0 \\ 0 \\ 800 \end{bmatrix} \mathbf{B}_2=\begin{bmatrix} 0 \\ 0 \\ 0 \\ 900 \end{bmatrix} \mathbf{B}_3=\begin{bmatrix} 0 \\ 0 \\ 0 \\ 1000 \end{bmatrix}$$

Choosing the matrices $\mathbf{Q}$ and $\mathbf{R}$ as in (Hanmandlu et al. 1993):

$$\mathbf{Q}=diag(1.0,\ 1.0,\ 1.0,\ 0.001,\ 4.0,\ 10.0,\ 10.0,\ 0.001,\ 10.0,\ 10.0,\ 10.0,\ 0.001)$$

$$\mathbf{R}=diag(1000,\ 1000,\ 1000)$$

Following the procedure of LQR controller design, the controller gain matrix can be derived, and they are listed in Table 3.2. With Theorem 3.7, the maximum allowable time delay between the plants communications can be estimated as 0.1823 s. Using the LMI method the solution takes longer time. Furthermore, the solution gives a very conservative result with MADB of 0.0946 s.

Table 3.2 The Optimal Control Gains

	The controller gains			
$\mathbf{K}_{11}$	0.016816	-1.248700	-0.112220	-0.005098
$\mathbf{K}_{12}$	-0.107890	4.871900	-0.000435	0.000079
$\mathbf{K}_{13}$	-0.042185	11.53600	-0.014631	-0.000649
$\mathbf{K}_{21}$	0.006097	0.000017	0.004761	0.000089
$\mathbf{K}_{22}$	-0.036174	-0.756290	-0.074018	-0.003454
$\mathbf{K}_{23}$	-0.023896	-0.11324	0.003539	0.0001204
$\mathbf{K}_{31}$	0.0035432	-0.48189	0.020087	-0.000811
$\mathbf{K}_{32}$	0.0063483	1.5655	0.0023165	0.00013378
$\mathbf{K}_{33}$	-0.064655	-7.2562	0.069285	-0.0032193

With the optimal controller designed in the above subsection, simulation studies have been carried out. The responses of the three networked generators for different values of time delays are shown in Figures 3.9-3.14. A disturbance of 5 % has been imposed onto the mechanical torque in the first generator.

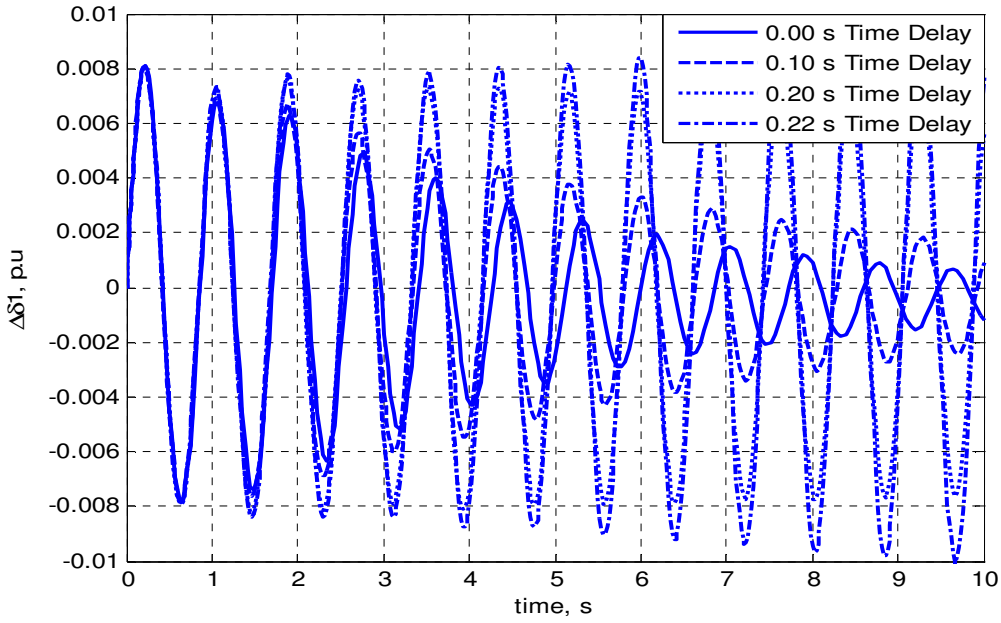

Figure 3.9 The rotor angle deviation of the first generator.

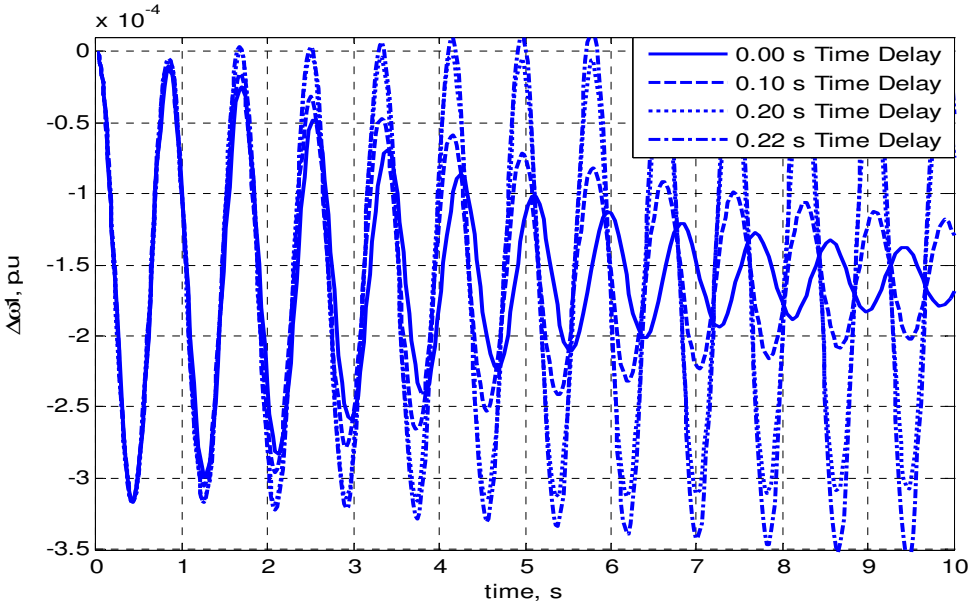

Figure 3.10 The speed deviation of the first generator.

From the simulation results in Figure 3.9-3.14, it is clearly shown that the system is stable if the time delay is within the estimated boundary range. When the time delay is near to or over the estimated boundary, the system responses are either unstable or critically stable.

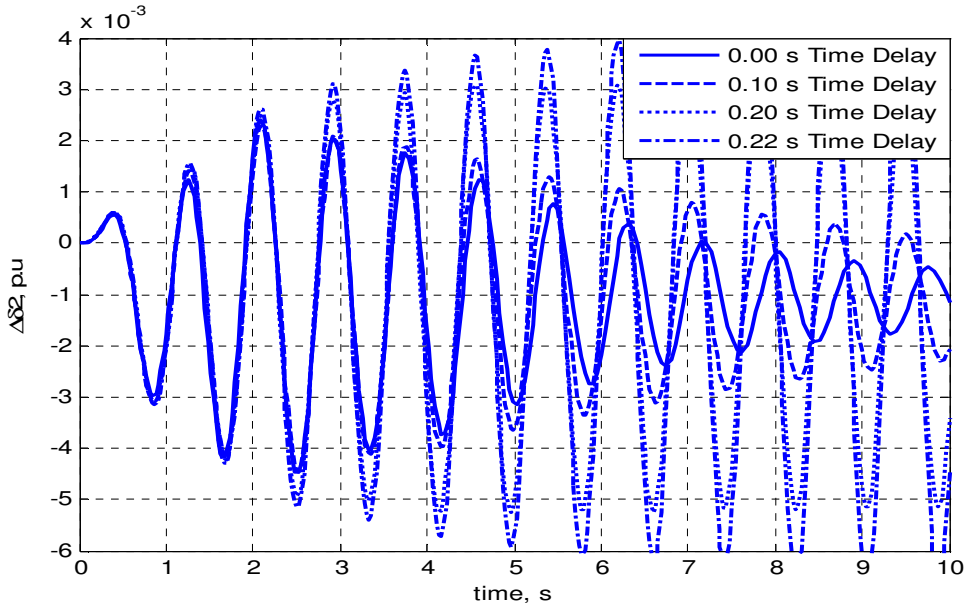

Figure 3.11 The rotor angle deviation of the second generator.

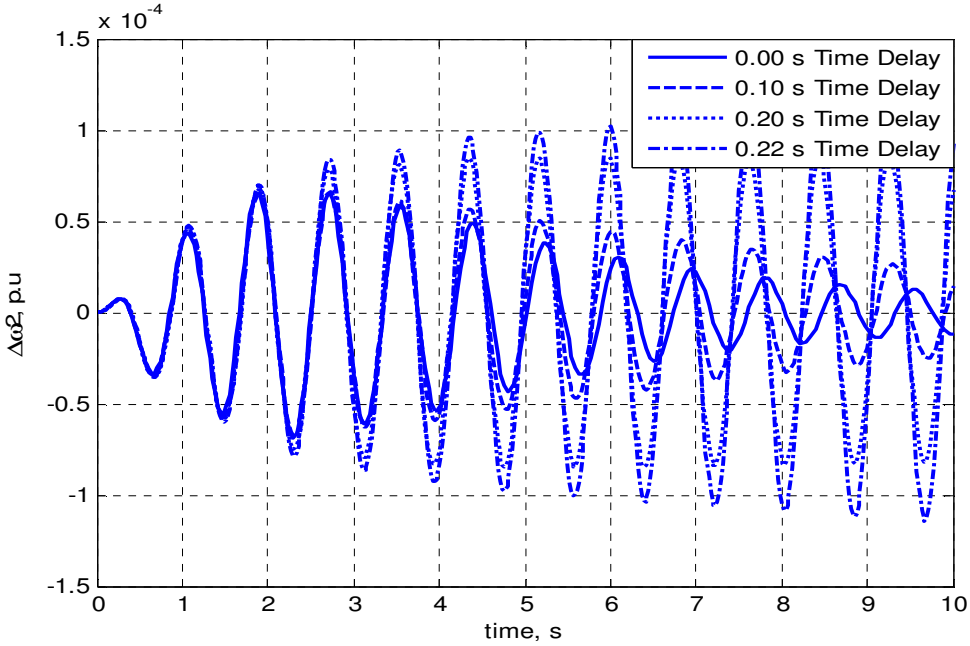

Figure 3.12 The speed deviation of the second generator.

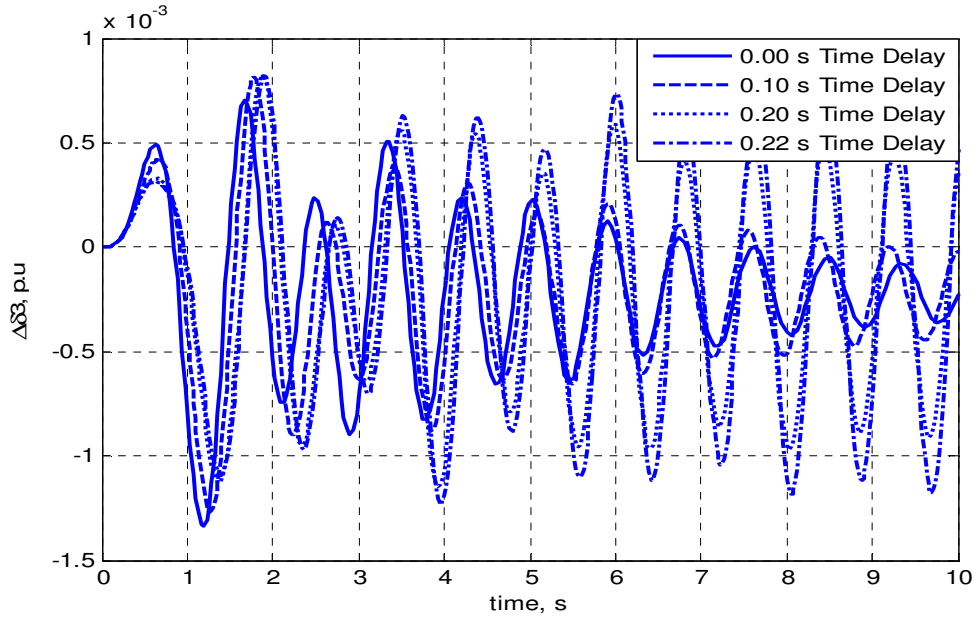

Figure 3.13 The rotor angle deviation of the third generator.

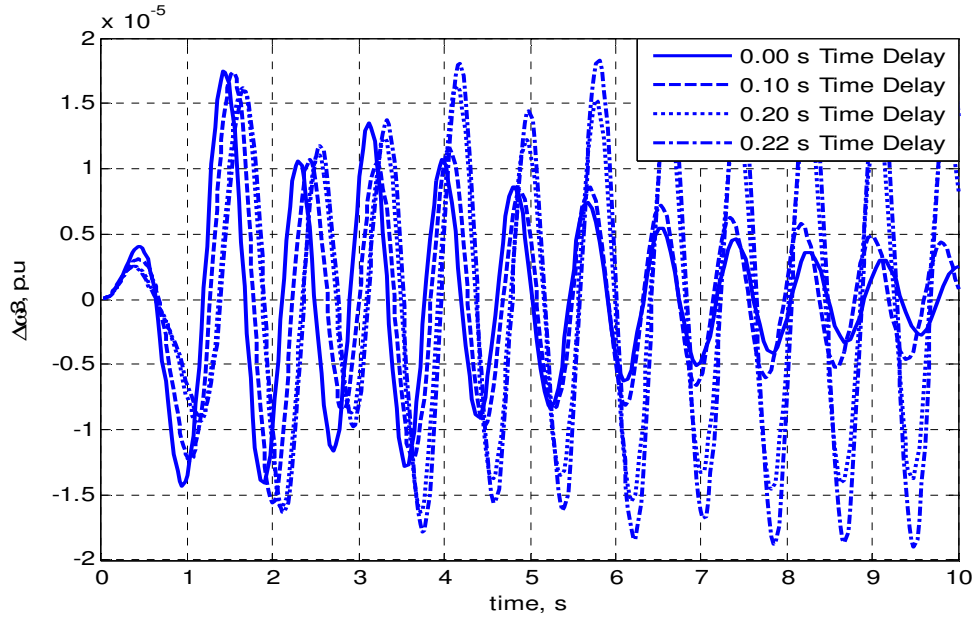

Figure 3.14 The speed deviation of the third generator.

It can be seen from all the figures that the MADB obtained with our method is still conservative because the system is still stable even with 0.2 s time delay, however, the dynamical performance is not acceptable. From the figures, the system is stable with 0.1 s time delay. In power systems, the time delay for the feedback signals is in the order of 100 ms (Holbert et al. 2005). The time delays in the communication links induced into the power systems is

within the range from few milliseconds to hundred milliseconds depending on the communication network type used, the transmission protocol, network load and other factors (Holbert et al. 2005;Naduvathuparambil et al. 2002). A time delay in the order of few microseconds can be attained in a small geographical area in control networks, e.g. the time delays in control networks such as Ethernet, ControlNet and DeviceNet is in the order of microseconds for the area with few kilometers (Lian et al. 2001). From the results of the estimated MADB for the three generators system and the values of the time delays in real communication networks, the networked control is applicable to control the three generators power system described in this example. It has been mentioned in (Naduvathuparambil et al. 2002), that the time delay in the current communication links used in the power system can stabilize almost all real-time power system applications.

3.7 Summary

In this chapter, a new method for estimating the MADB in NCSs is presented. Three types of NCSs are studied; single-unit NCS, NCS with dynamic controller, and multi-units interconnected distributed NCS. The method is simple and easy to use and involves less computation while gives comparable results with the methods published in the literature. An example system consists of three generators has been analyzed in the case the system is controlled over a network. The MADB value obtained for the three generators is feasible with the current network and communication technology. The work in this chapter can be applied to a network with a constant time delay and slowly time varying time delay or if the scheduling can guarantee that the time delay in the network does not exceed the MADB for the system, and this is not always the case. The time delay can be random, which makes the system stochastic and the following chapter deals with designing a stochastic controller for NCS under random time delay governed by Markov Chains.

CHAPTER 4: ROBUST STABILIZATION OF NETWORKED CONTROL SYSTEM USING MARKOVIAN JUMP SYSTEM APPROACH

4.1 Introduction

The time delay in real-time networks may be constant, varied or even random. In Chapter 3, the stability analysis and controller design problem for a class of networked control systems with constant time delay or with schedulable networks were discussed. In the approach proposed in Chapter 3 the MADB is used to schedule the network to do not exceed this threshold or when the time delay is bounded. In this chapter, the stability and controller design for networked control systems with a random time delay is studied where the random time delay is modelled using Markov Chains. The controller is designed while taking the stochastic nature of the network into account. The random time delay is assumed to be governed by Markov Chains, and the system is modelled as a discrete-time jump linear system. Both the time delay from sensors to controllers and from controllers to actuators

are considered for both state feedback and dynamic controllers. The controller can be switching (mode-dependent) or non-switching (mode-independent). The controller design problem is an output feedback problem in a bilinear matrix inequality (BMI) form. The BMI problem is not convex, which can only be solved using iterative algorithms such as the V-K iteration algorithm. In the V-K iteration algorithm, the BMI is divided into Eigenvalue Problem (EVP) and Generalized Eigenvalue Problem (GEVP) which are iterated to achieve the mean square stability and hence to derive the stabilizing controllers. The EVP and GEVP are solved using the Matlab LMI Toolbox. The controller design method has been applied to the cart and the inverted pendulum; the derived controller was tested on the nonlinear model. In this chapter, a brief review on the jump linear system and their applications in NCS is given, and the discrete-time model of the networked control system is explained. The mean square stability is usually used to study the stability and stabilization of discrete-time Markovian Jump Linear System (DTMJLS). The sufficient and necessary conditions for the mean square stability of the DTMJLS are also reviewed. The V-K iteration algorithm for solving the BMI is explained. The controller design method is applied to the cart and the inverted pendulum problem.

4.2 Jump Linear Systems

The Jump Linear System (JLS) is mostly used to study the stability and stabilization of a system with abrupt changes due to the variations in the system structure or partly system failure. In this way, the system will have a number of models or modes and jumps from one mode to another in a random fashion and in many cases, the jump parameter can be modelled using Markov Chains. The first report for the Jump Linear System (JLS) in a

continuous-time form was introduced in 1961. There are many papers in the literature discussing the stability and controller design for the Markovian Jump Linear Systems (Ait-Rami et al. 1995;Boukas et al. 1997;De Souza 2003;De Souza et al. 1997;Shi et al. 1998). In (Liu, Lei-Ming et al. 2005) the robust stabilization of the continuous and discrete JLS is addressed where the controller design problem is solved via the LMIs. The probability distribution function is time-varying but bounded. In (De Souza et al. 1997) the problem of H_∞ filtering for DTMJLS is presented where the robust controller design problem is formulated as the problem of solving the LMI, and they assumed that the Markovian Jump parameter is accessible. In (De Souza 2003) the mode-independent H_∞ filter design for DTMJLS is studied where the jump parameter is not accessible. The transition probability is unknown but belongs to a given polytope. The controller design for a DTMJLS with uncertain parameters is studied in (Boukas et al. 1997;Shi et al. 1998). The authors in (Boukas et al. 1997) took the structural linear uncertainty, norm-bounded nonlinear uncertainty and fractional form uncertainty into consideration. The published work focused on the general DTMJLS, in the following the application of the DTMJLS in NCSs will be our main focus.

In networked control systems, as discussed in Chapter 2, the time delay can be random and because there is a correlation between the preceding, current and next time delay, the time delay can be modelled as a Markov Chain. The time delay changes as a result of the change in the network load or in the other factors, which are usually random. The network state changes from one to another in a random manner governed by Markov Chain. An example for a network with different three load states is shown in Figure 4.1. The network load changes from low to medium to high and the time delay is a Markovian process

and jumps between these three modes in a random manner. The jump system will have three modes of operations.

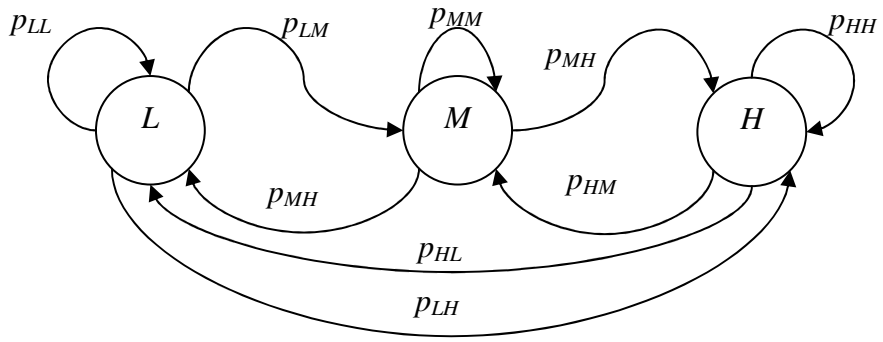

Figure 4.1 An example of a Markov chain load modelling, the three network loads: low (L), medium (M), and high (H). p_{ij} **where** $i, j \in U = \{L, M, H\}$ **is the probability of the transition from mode *i* to *j***

As an example, the time delay has three different values depending on the network load, and the transition probability is given by:

$$P = \begin{bmatrix} p_{LL} & p_{LM} & p_{LH} \\ p_{ML} & p_{MM} & p_{MH} \\ p_{HL} & p_{HM} & p_{HH} \end{bmatrix}$$

$$p_{ij} = \mathbf{Prob}\{\tau^{k+1} = j \mid \tau^{k} = i\}\, i, j \in U = \{L, M, H\}$$

where p_{ij} is the probability of the jump from mode *i* to mode *j*. In the Jump system theory literature, the mode means the model, i.e., if the system is said to have two modes, it means that the system has one jump parameter with two modes. In networked control systems, the use of this concept is different. If the system has one mode, it means that the system has one jump parameter, which is usually the sensor to the controller time delay. When both the sensor to the controller and the controller to the actuator time delays are considered the

system is said to have two modes, or it has two jump parameters. The controllers are classified into switching (mode-dependent) and non-switching (mode-independent). In the switching controller the controller changes with the jump parameter, which is the time delay, and hence the time delay must be accessed at the controller node. The time delay can be accessed through time stamping and clock synchronization, which requires the sensor and the actuator nodes to be smart and embedded processors must be installed. On the other hand, the system analysis becomes complex and the packet length with the time stamping will be larger and hence the time stamping increases the network load and in some networks it cannot be achieved. The non-switching controller is easy to be implemented because it does not change with the jump parameter and hence the time stamping is not required. In networked control systems where the time delay is governed by Markov Chains the controller can be classified into: Non-switching (Mode-independent), switching with one mode (mode-dependent), and switching with two modes (mode-dependent). In all the three types one or two of the time delays are considered in the design. The difference in the performance between the switching and non-switching controller is reported to be small (Xiao et al. 2000). The application of the discrete-time jump system in networked control systems has been addressed in many papers, see, for example (Liu, Lei-Ming et al. 2005;Liu et al. 2008;Xiao et al. 2000;Yu et al. 2008). In (Liu, Lei-Ming et al. 2005;Liu et al. 2008;Xiao et al. 2000) the discrete-time model is augmented, and the generated output feedback problem is formulated as Bilinear Matrix Inequality, which is solved using the V-K iteration algorithm to derive the controller. In this work, we adopt the algorithm in (Xiao et al. 2000) with some modification to the V-K iteration loop. The method in (Xiao et al. 2000) is limited to time delays less than the sampling period and in (Liu, Lei-Ming et al. 2005;Liu et al. 2008) the method is extended to time delays larger than the sampling pe-

riod. From the control point of view when the system is controlled over a network with time delay larger than the sampling time the system performance is not acceptable. In (Zhang et al. 2005a) the authors use the discrete model for the plant and both the time delay from the sensor to the controller, and from the controller to the actuator are considered. The discrete mode dependent Lyapunov function has been used to derive a stabilizing switching controller. In (Yu et al. 2008) the authors concentrate on the problem of the random data dropouts, and the sufficient conditions for the mean square stability are derived. The stability analysis and controller design with two random time delays are studied in (Yu, Bo et al. 2008;Shi et al. 2009a;Shi et al 2009b;Zhang et al. 2005). In (Shi et al. 2009a;Shi et al. 2009b) the NCS is modelled where both the time delays are considered. The controller depends on the current sensor to controller time delay and the previous controller to actuator time delay and hence the controller depends on the three random variables, τ_k, d_k, $d_{k-\tau_{k+1}}$, which are interdependent. The resulting system cannot be regarded as the standard DTMJLS. The derived theorem is in a set of LMI with nonlinear matrix inequalities constraints, which are non-convex and can be solved by iterative algorithms such as the Cone Complementary Linearization (CCL) (Product Reduction). The optimal stochastic control is studied in (Nilsson 1998) where the optimal stochastic controller is derived when the time delay is random. The use of the model predictive control in NCS has been studied in (Zhang, Guofeng et al. 2007;Jing et al. 2007;Wu et al. 2009) where both the sensor to the controller and the controller to the actuator time delays are considered.

4.3 Mathematical Modelling of NCSs with Time Delay

4.3.1 Modelling of a Class of Networked Control Systems

a) NCS Systems with State Feedback Controller

The model of a single loop networked control system is shown in Figure 4.2. The plant is in continuous-time and the sensors sample the plant states. The measured signals are transmitted through the network in a discrete form. These data will suffer random time delays, and some of them may be lost when they are transmitted through the network. The presence of the random time delay makes the system to have the nature of a stochastic hybrid system. The discrete time-invariant plant model is given by:

$$\mathbf{x}(k+1) = \mathbf{A}_d \mathbf{x}(k) + \mathbf{B}_d \mathbf{u}(k) \tag{4.1}$$

where $\mathbf{x}(k) \in \Re^n$ is the system state vector, $\mathbf{u}(k) \in \Re^m$ is the system control input, and the matrices $\mathbf{A}_d$ and $\mathbf{B}_d$ are given by:

$$\mathbf{A}_d = e^{\mathbf{A}h} \qquad \mathbf{B}_d = \int_0^h e^{\mathbf{A}(h-s)} \mathbf{B} ds \tag{4.2}$$

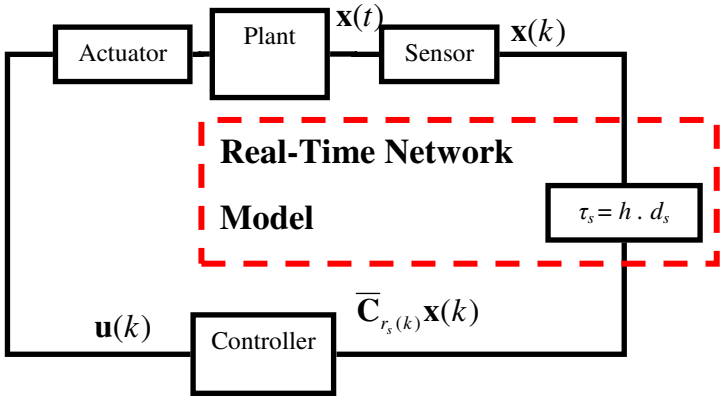

Figure 4.2 The Networked Control System

In the model shown in Figure 4.2 the time delays are lumped together between the sensor and the controller. In many of the published works in the literature, the time delay between the controller and the actuator is neglected. For the next analysis, the following assumptions are required and are made:

Assumption 4.1:

- The sensors are clock driven. The actuator and the controller are event driven; which means that the sensors samples the plant states periodically and the actuators and the controllers use the data, as soon as they arrive.
- The data are sent as a single packet.
- The data are received in chronological order, which means that old data are disregarded.

The mode-dependent switching state feedback control law is given by:

$$\mathbf{u}(k) = \mathbf{K}(r_s(k))\mathbf{x}(k - r_s(k)) \tag{4.3}$$

where $\tau(k) = r_s(k) \cdot h$, h is the sampling period and $r_s(k)$ is a bounded random integer sequence governed by Markov Chain with $0 \le r_s(k) \le d_s < \infty$, and d_s is the finite delay bound. By augmenting the state variable:

$$\bar{\mathbf{x}}(k) = \left[\mathbf{x}(k)^T \quad \mathbf{x}(k-1)^T \quad \cdots \quad \mathbf{x}(k-d_s)^T\right]^T$$

where $\bar{\mathbf{x}}(k) \in R^{(d_s+1)n}$, applying the controller (4.3) into (4.1) the closed-loop system becomes:

$$\bar{\mathbf{x}}(k+1) = (\bar{\mathbf{A}} + \bar{\mathbf{B}}\mathbf{K}(r_s(k))\bar{\mathbf{C}}(r_s(k)))\bar{\mathbf{x}}(k) \tag{4.4}$$

where;

$$\overline{\mathbf{A}} = \begin{bmatrix} \mathbf{A} & \mathbf{0} & \cdots & \mathbf{0} & \mathbf{0} \\ \mathbf{I} & \mathbf{0} & \cdots & \mathbf{0} & \mathbf{0} \\ \mathbf{0} & \mathbf{I} & \cdots & \mathbf{0} & \mathbf{0} \\ \vdots & \vdots & \ddots & \vdots & \vdots \\ \mathbf{0} & \mathbf{0} & \cdots & \mathbf{I} & \mathbf{0} \end{bmatrix} \overline{\mathbf{B}} = \begin{bmatrix} \mathbf{B} \\ \mathbf{0} \\ \mathbf{0} \\ \vdots \\ \mathbf{0} \end{bmatrix} \qquad \overline{\mathbf{C}}(r_s(k)) = \begin{bmatrix} \mathbf{0} & \cdots & \mathbf{0} & \mathbf{I} & \mathbf{0} & \cdots & \mathbf{0} \end{bmatrix}$$

$\overline{\mathbf{C}}(r_s(k))$ incorporates the time delay into the model, $\overline{\mathbf{C}}(r_s(k))$ has all the elements being zero except for the $r_s(k)^{\text{th}}$ block being an identity matrix. The closed-loop system (4.4) can be re-written as;

$$\overline{\mathbf{x}}(k+1) = \mathbf{A}_{cl}(r_s(k))\overline{\mathbf{x}}(k) \tag{4.5}$$

b) NCS with Dynamic Output Feedback Controller

Stabilizing the plant (4.1) with a dynamic controller as shown in Figure 4.3, the dynamic controller model is given by:

$$\mathbf{z}(k+1) = \mathbf{F}\mathbf{z}(k) + \mathbf{G}\mathbf{y}(k)$$

$$\mathbf{v}(k) = \mathbf{H}\mathbf{z}(k) + \mathbf{J}\mathbf{y}(k) \tag{4.6}$$

In the case of the dynamic controller, both the time delay from the sensors to the controller, and from the controller to the actuators are considered, which are illustrated in Figure 4.3. Augmenting the controller states as;

$$\overline{\mathbf{z}}(k) = \begin{bmatrix} \mathbf{z}(k)^T & \mathbf{v}(k)^T & \cdots & \mathbf{v}(k-d_{ca})^T \end{bmatrix}^T$$

The controller model with the augmented states is then given by:

$$\overline{\mathbf{z}}(k+1) = \overline{\mathbf{F}}\overline{\mathbf{z}}(k) + \overline{\mathbf{G}}\mathbf{y}(k)$$

$$\mathbf{u}(k) = \overline{\mathbf{H}}(r_{ca}(k))\bar{\mathbf{z}}(k) + \overline{\mathbf{K}}(r_{ca}(k))\mathbf{y}(k) \tag{4.7}$$

where;

$$\overline{\mathbf{F}} = \begin{bmatrix} \mathbf{F} & \mathbf{0} & \cdots & \mathbf{0} & \mathbf{0} \\ \mathbf{H} & \mathbf{0} & \cdots & \mathbf{0} & \mathbf{0} \\ \mathbf{0} & \mathbf{I} & \cdots & \mathbf{0} & \mathbf{0} \\ \vdots & \vdots & \ddots & \vdots & \vdots \\ \mathbf{0} & \mathbf{0} & \cdots & \mathbf{I} & \mathbf{0} \end{bmatrix} \qquad \overline{\mathbf{G}} = \begin{bmatrix} \mathbf{G} \\ \mathbf{J} \\ \mathbf{0} \\ \vdots \\ \mathbf{0} \end{bmatrix}$$

$$\overline{\mathbf{H}}(r_{ca}(k)) = \begin{cases} [\mathbf{H} \quad \mathbf{0} \quad \cdots \quad \mathbf{0} \quad \mathbf{0} \quad \cdots \quad \mathbf{0}] & \text{if} \quad r_{ca}(k) = 0 \\ [\mathbf{0} \quad \cdots \quad \mathbf{0} \quad \mathbf{I} \quad \mathbf{0} \quad \cdots \quad \mathbf{0}] & \text{if} \quad r_{ca}(k) \neq 0 \end{cases}$$

$$\overline{\mathbf{K}}(r_{ca}(k)) = \begin{cases} \mathbf{J} & \text{if} \quad r_{ca}(k) = 0 \\ \mathbf{0} & \text{if} \quad r_{ca}(k) \neq 0 \end{cases}$$

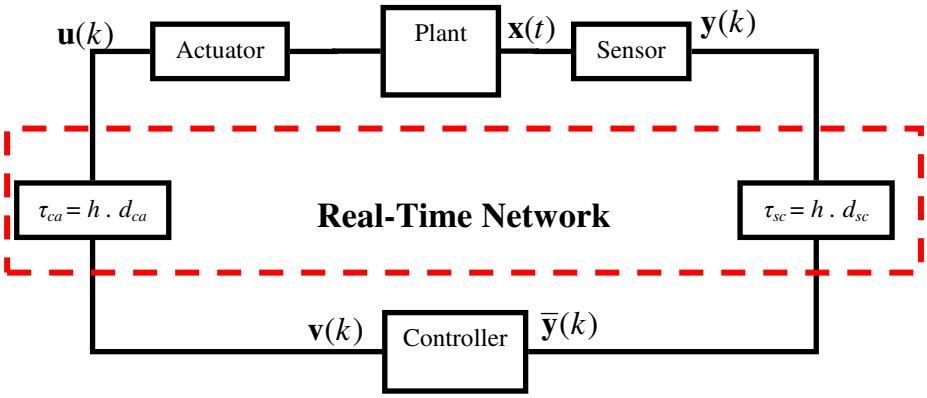

Figure 4.3 Networked Control System with both time delays from the sensor to the controller and from the controller to the actuator are taking into account

When the time stamping is used, $\mathbf{F}$, $\mathbf{G}$, $\mathbf{H}$ and $\mathbf{J}$ are replaced by $\mathbf{F}(\tau_{sc})$, $\mathbf{G}(\tau_{sc})$, $\mathbf{H}(\tau_{sc})$, and $\mathbf{J}(\tau_{sc})$. The augmented plant model with output feedback can be described by:

$$\tilde{\mathbf{x}}(k+1) = \tilde{\mathbf{A}}\tilde{\mathbf{x}}(k) + \tilde{\mathbf{B}}\mathbf{u}(k)$$

$$\mathbf{y}(k) = \mathbf{C}\tilde{\mathbf{C}}(r_{sc}(k))\tilde{\mathbf{x}}(k) \tag{4.8}$$

Augmenting both the plant states and controller states as: $\bar{\mathbf{x}}(k) = \left[\tilde{\mathbf{x}}(k)^T \quad \tilde{\mathbf{z}}(k)^T\right]^T$. The closed-loop system with the plant (4.8) and the controller (4.7) becomes;

$$\bar{\mathbf{x}}(k+1) = (\bar{\mathbf{A}} + \bar{\mathbf{B}}\mathbf{K}(r_{ca}(k))\bar{\mathbf{C}}(r_{sc}(k)))\bar{\mathbf{x}}(k) \tag{4.9}$$

where;

$$\bar{\mathbf{A}} = \begin{bmatrix} \tilde{\mathbf{A}} & \mathbf{0} \\ \mathbf{0} & \mathbf{0} \end{bmatrix} \bar{\mathbf{B}} = \begin{bmatrix} \tilde{\mathbf{B}} & \mathbf{0} \\ \mathbf{I} & \mathbf{0} \end{bmatrix}$$

$$\bar{\mathbf{C}}(r_{sc}(k)) = \begin{bmatrix} \mathbf{0} & I \\ \mathbf{C}\tilde{\mathbf{C}}(r_{sc}(k)) & \mathbf{0} \end{bmatrix} \mathbf{K}(r_{ca}(k)) = \begin{bmatrix} \tilde{\mathbf{F}} & \tilde{\mathbf{G}} \\ \tilde{\mathbf{H}}(r_{ca}(k)) & \tilde{\mathbf{K}}(r_{ca}(k)) \end{bmatrix}$$

Equation (4.9) can be written as;

$$\bar{\mathbf{x}}(k+1) = \mathbf{A}_{cl}(r_{sc}(k), r_{ca}(k))\bar{\mathbf{x}}(k) = \mathbf{A}_{cl}(r_s(k))\bar{\mathbf{x}}(k) \tag{4.10}$$

The two time delays are random and bounded, $\tau_{scm} \geq \tau_{sc} \geq 0$ and $\tau_{cam} \geq \tau_{ca} \geq 0$. These can be modelled as two homogeneous Markov Chains, and they jump from mode to mode according to their transition probabilities P_{sc} and P_{ca} respectively. The random variable τ_{sc} and τ_{ca} can be converted to a single random variable given by $r_s(k) = (r_{sc}(k), r_{ca}(k))$, where the transition probability, P, is given by the Kronecker product of the sensor to the controller time delay transition probability, and the time delay from the controller to the actuator transition probability as;

$$P = P_{sc} \otimes P_{ca} \tag{4.11}$$

For simplicity (4.10) can be written as:

$$\mathbf{x}(k+1) = \mathbf{A}(r(k))\mathbf{x}(k) \tag{4.12}$$

Equations (4.5) and (4.10) are standard DTMJLS. Equation (4.5) is a jump system with one mode, which is the sensor to the controller time delay while (4.10) represents a jump system with two modes, which are the sensor to the controller, and the controller to the actuator time delays.

According to the Markovian integer jump parameter, $r(k) \in \{0,1,...,d\}$, the system matrix will be $\mathbf{A}_{cl}(r(k)) \in \{\mathbf{A}_{cl}(0), \mathbf{A}_{cl}(1), ..., \mathbf{A}_{cl}(d)\}$. The system jumps between the different modes, $\mathbf{A}_{cl}(0), \mathbf{A}_{cl}(1), ..., \mathbf{A}_{cl}(d)$, in a random manner. In order to stabilize the system with mode-independent or mode-dependent controller the mean square stability must be established.

4.3.2 Modelling Time Delays Using Markov Chains

The random time delay is modelled as a finite state Markov process with the following properties:

$$P\{r_s(k+1) = j \mid r_s(k) = i\} = p_{ij} \qquad 0 \le i, j \le d_s$$

$$0 \le p_{ij} \le 1 \qquad \sum_{j=0}^{d} p_{ij} = 1 \tag{4.13}$$

where d_s is the number of modes and $r_s(k)$ is the Markovian process. The general transition probability matrix is given by:

$$P = \begin{bmatrix} p_{00} & p_{01} & 0 & 0 & \cdots & 0 \\ p_{10} & p_{11} & p_{12} & 0 & \cdots & 0 \\ \vdots & \vdots & \vdots & \vdots & \ddots & \vdots \\ \vdots & \vdots & \vdots & \vdots & \vdots & 0 \\ p_{d0} & p_{d1} & p_{d2} & p_{d3} & \cdots & p_{d_s d_s} \end{bmatrix} \tag{4.14}$$

The constraint (4.13) means the summation of the probabilities in every row is one. The assumption made is that the data are received in chronological order, which means that the old data are discarded. Suppose that at instant *k*, we received $\mathbf{x}(k)$, at $k+1$ if there is no new data, then the old data will be used by the controller, but if we receive $\mathbf{x}(k-1)$ at $k+1$, then it will be older than $\mathbf{x}(k)$ and hence $\mathbf{x}(k-1)$ must be discarded, this can be interpreted as;

$$P\{r_s(k+1) > r_s(k)+1\} = 0 \tag{4.15}$$

From (4.15) the time delay can increase only at one step, but it can decrease as many steps as can be seen from (4.14). The diagonal elements in (4.14) represent the probability of successive equal time delays or in other words, the probability that the network remains in the same state. The upper diagonal elements represent the possibility of receiving longer delays or increasing the network load. The zero elements represent the discard of the old data.

4.4 The Stability of Linear Jump System

The Mean Square stability is the stability criteria used to study the stability of Markovian Jump Systems, which is equivalent to the Asymptotic Wide Sense Stationary Stability (AWSS) (Costa 1993). For the jump system the stochastic stability, mean square stability and the exponential mean square stability are all equivalent, and every condition implies the almost sure (asymptotic) stability.

Definition 4.1: (Liu, Lei-Ming et al. 2005)

The system (4.12) is mean square stable if for every initial condition state, $(\mathbf{x}_0, r_0)$,

$$\lim_{k\to\infty} \mathrm{E}\left[\left\|\mathbf{x}(k)\right\|^2\right] = 0 \tag{4.16}$$

Definition 4.2: (Liu, Lei-Ming et al. 2005)

The system (4.12) is mean square stable with decay rate β (El Ghaoui et al. 1996) if for every initial condition state, $(\mathbf{x}_0, r_0)$,

$$\lim_{k\to\infty} \beta^k \mathrm{E}\left[\left\|\mathbf{x}(k)\right\|^2\right] = 0 \qquad \beta > 1 \tag{4.17}$$

The necessary and sufficient conditions for mean square stability for the jump system are derived in (Costa 1993), and they are given in the following theorem.

Theorem 4.1: (Costa 1993) *The mean square stability of system (4.12) is equivalent to the existence of symmetric positive definite matrices* $\mathbf{Q}_0, \mathbf{Q}_1, \cdots, \mathbf{Q}_d$ *satisfying any one of the following 4 conditions*:

$$\mathbf{A}_i\left(\sum_{j=0}^{d} p_{ji}\mathbf{Q}_\mathbf{j}\right)\mathbf{A}_i^T < \mathbf{Q}_i, \qquad i = 0,\cdots,d$$

$$\mathbf{A}_j^T\left(\sum_{j=0}^{d} p_{ji}\mathbf{Q}_i\right)\mathbf{A}_j < \mathbf{Q}_j, \qquad i = 0,\cdots,d$$

$$\sum_{j=0}^{d} p_{ji}\mathbf{A}_j\mathbf{Q}_j\mathbf{A}_i^T < \mathbf{Q}_i, \qquad i = 0,\cdots,d$$

$$\sum_{j=0}^{d} p_{ji}\mathbf{A}_i^T\mathbf{Q}_j\mathbf{A}_i < \mathbf{Q}_j, \qquad i = 0,\cdots,d$$

where $j = 0,\cdots,d$ represents the number of the modes. An interesting property is that the stability of each mode is neither sufficient nor necessary for the mean square stability.

4.5 The V-K Iteration

Theorem 4.1 is essential for studying the DTMJLS. The conditions 1-4 are equivalent for studying the stability of the DTMJLS but for the controller design, each condition will lead to a different controller. Choosing condition (4) in Theorem 4.1 the closed-loop system becomes:

$$\sum_{j=0}^{d} p_{ji}(\mathbf{A}_i + \mathbf{B}_i\mathbf{K}_i\mathbf{C}_i)^T \mathbf{Q}_j (\mathbf{A}_i + \mathbf{B}_i\mathbf{K}_i\mathbf{C}_i) < \mathbf{Q}_j, \qquad i = 0,\cdots,d \tag{4.18}$$

A lower bound for the decay rate (Lyapunov Exponent), $\beta = 1/\alpha$, ($\lim_{k\to\infty} \beta^k E\left(\|\mathbf{x}(k)\|^2\right)$), can be obtained by replacing $\mathbf{Q}_i$ with $\alpha\mathbf{Q}_i$ on the right hand side of (4.18).

$$\sum_{j=0}^{d} p_{ji}(\mathbf{A}_i + \mathbf{B}_i\mathbf{K}_i\mathbf{C}_i)^T \mathbf{Q}_j (\mathbf{A}_i + \mathbf{B}_i\mathbf{K}_i\mathbf{C}_i) < \alpha\mathbf{Q}_j, \qquad j = 0,\cdots,d \tag{4.19}$$

The coupled equations (4.19) are Bilinear Matrix Inequalities, which are non convex and finding a global optimal solution is very difficult. However, many control problems are formulated as BMIs, there are a few methods for solving the BMIs. For example, the path-following linearization method reported in (Hassibi et al. 1999) can be used, where each matrix is perturbed, and the higher-order terms are neglected. The most widely used technique for the solution is by iteration methods such the D-K, G-K and V-K iteration algorithms (Banjerdpongchai 1997). As these are considered as Coupled Bilinear Matrix Inequalities (BMI's) in α, $\mathbf{K}_i$ and $\mathbf{Q}_i$, they can be formulated into two problems as:

1. If we fix $\mathbf{K}_i$ ($i = 0,\cdots,d$), then we have a Generalized Eigenvalue Problem (GEVP) which is quasi-convex.

2. If we fix $\mathbf{Q}_i$ ($i = 0,\cdots,d$), then we have Eigenvalue Problem, which is convex.

Both of these problems can be solved very efficiently using the Convex Optimization. The BMI problem solution can be summarized as follows:

Equation (4.19) can be written as:

$$\alpha\mathbf{Q}_j - \begin{bmatrix}\overline{\mathbf{A}}_0^T & \overline{\mathbf{A}}_1^T & \cdots & \overline{\mathbf{A}}_d^T\end{bmatrix}\begin{bmatrix} p_{j0}\mathbf{Q}_0 & & 0 \\ & \ddots & \\ 0 & & p_{jd}\mathbf{Q}_d\end{bmatrix}\begin{bmatrix}\overline{\mathbf{A}}_0 \\ \overline{\mathbf{A}}_1 \\ \vdots \\ \overline{\mathbf{A}}_d\end{bmatrix} > 0 \qquad j = 0,\cdots,d \qquad (4.20)$$

Using Schur complement to (4.20) then we have:

$$\begin{bmatrix} \alpha\mathbf{Q}_j & \overline{\mathbf{A}}_0^T & \cdots & \overline{\mathbf{A}}_d^T \\ \overline{\mathbf{A}}_0 & p_{j0}^{-1}\mathbf{Q}_0^{-1} & \cdots & 0 \\ \vdots & \vdots & \ddots & \vdots \\ \overline{\mathbf{A}}_d & 0 & \cdots & p_{jd}^{-1}\mathbf{Q}_d^{-1}\end{bmatrix} > 0$$

$$\begin{bmatrix} \alpha\mathbf{Q}_j & (\mathbf{A}_0 + \mathbf{B}_0\mathbf{K}_0\mathbf{C}_0)^T & \cdots & (\mathbf{A}_d + \mathbf{B}_d\mathbf{K}_d\mathbf{C}_d)^T \\ (\mathbf{A}_0 + \mathbf{B}_0\mathbf{K}_0\mathbf{C}_0) & p_{j0}^{-1}\mathbf{Q}_0^{-1} & \cdots & 0 \\ \vdots & \vdots & \ddots & \vdots \\ (\mathbf{A}_d + \mathbf{B}_d\mathbf{K}_d\mathbf{C}_d) & 0 & \cdots & p_{jd}^{-1}\mathbf{Q}_d^{-1}\end{bmatrix} > 0 \qquad (4.21)$$

As it is mentioned above, (4.21) is a bilinear matrix inequality which is difficult to be solved. A few methods were reported for solving this problem, and the method reported in (Xiao et al. 2000) is adopted in this thesis, which is to divide the BMI into two LMIs and by solving these two LMIs a local optimal solution can be found. The problem solution process is divided to three basic problems, which are: Feasibility Problem, Eigenvalue Problem, and Generalized Eigenvalue Problem which are described in the next sub-sections.

4.5.1 The Feasibility Problem (FP)

The first step is to find an initial feasible solution to (4.19). The initial solution is to set $\alpha = 1,\ \mathbf{K}_0 = \mathbf{K}, \cdots, \mathbf{K}_d = \mathbf{K}$ and the initial transition probability, $P = P_0$, then solve for $\mathbf{Q}_0, \cdots, \mathbf{Q}_d$. The Matlab feasp function in the LMI Matlab Toolbox is used to solve this problem; a brief description of this function is given below:

Syntax: [tmin,xfeas] = feasp(lmisys,options,target)

This function finds whether the LMI system is feasible or not, if the solution is feasible the function returns tmin as 0 or negative (strictly feasible) and gives xfeas (called the decision variables), which contains the LMI variables that are $\mathbf{Q}_0, \cdots, \mathbf{Q}_d$. If tmin is a small positive number, then the LMI system is marginally feasible, which means it may be feasible. A more detailed description of this function is given in (Gahinet etal. 1995).

4.5.2 The Eigenvalue Problem (EVP)

Fix $\mathbf{Q}_i\ (i = 0, \cdots, d)$, then (4.21) becomes LMIs in α and $\mathbf{K}_i\ (i = 0, \cdots, d)$, but (4.21) is not in the solvable form, and by changing the variables it can be solved efficiently using the Matlab LMI Toolbox:

$$\mathbf{Y}_0 = \mathbf{K}_0\mathbf{C}_0 \cdots \mathbf{Y}_d = \mathbf{K}_d\mathbf{C}_d \qquad \mathbf{Y}_0{}^T = \mathbf{C}_0{}^T\mathbf{K}_0{}^T \cdots \mathbf{Y}_d{}^T = \mathbf{C}_d{}^T\mathbf{K}_d{}^T$$

Then (4.21) becomes;

$$\begin{bmatrix} \alpha\mathbf{Q}_j & (\mathbf{A}_0 + \mathbf{B}_0\mathbf{Y}_0)^T & \cdots & (\mathbf{A}_d + \mathbf{B}_d\mathbf{Y}_d)^T \\ (\mathbf{A}_0 + \mathbf{B}_0\mathbf{Y}_0) & p_{j0}^{-1}\mathbf{Q}_0{}^{-1} & \cdots & 0 \\ \vdots & \vdots & \ddots & \vdots \\ (\mathbf{A}_d + \mathbf{B}_d\mathbf{Y}_d) & 0 & \cdots & p_{jd}^{-1}\mathbf{Q}_d{}^{-1} \end{bmatrix} > 0$$

$$\begin{bmatrix} \alpha\mathbf{Q}_j & \mathbf{A}_0^T + \mathbf{Y}_0^T\mathbf{B}_0^T & \cdots & \mathbf{A}_d^T + \mathbf{Y}_d^T\mathbf{B}_d^T \\ \mathbf{A}_0 + \mathbf{B}_0\mathbf{Y}_0 & p_{j0}^{-1}\mathbf{Q}_0^{-1} & \cdots & 0 \\ \vdots & \vdots & \ddots & \vdots \\ \mathbf{A}_d + \mathbf{B}_d\mathbf{Y}_d & 0 & \cdots & p_{jd}^{-1}\mathbf{Q}_d^{-1} \end{bmatrix} > 0 \quad j = 0,\cdots,d \tag{4.22}$$

If we fix $\mathbf{Q}_i$ ($i = 0,\cdots,d$) and α, then we have a set of LMIs in $\mathbf{K}_i$ ($i = 0,\cdots,d$).

The Eigenvalue Problem EVP:

For a given $\mathbf{Q}_i$ ($i = 0,\cdots,d$), solve the following LMIs for α and $\mathbf{Y}_i$ ($i = 0,\cdots,d$).

$$\begin{bmatrix} \alpha\mathbf{Q}_j & \mathbf{A}_0^T + \mathbf{Y}_0^T\mathbf{B}_0^T & \cdots & \mathbf{A}_d^T + \mathbf{Y}_d^T\mathbf{B}_d^T \\ \mathbf{A}_0 + \mathbf{B}_0\mathbf{Y}_0 & p_{j0}^{-1}\mathbf{Q}_0^{-1} & \cdots & 0 \\ \vdots & \vdots & \ddots & \vdots \\ \mathbf{A}_d + \mathbf{B}_d\mathbf{Y}_d & 0 & \cdots & p_{jd}^{-1}\mathbf{Q}_d^{-1} \end{bmatrix} > 0 \qquad j = 0,\cdots,d$$

This problem can be solved using mincx matlab function in the LMI toolbox. This function minimizes a linear objective under LMI constraints; the function syntax is:

Syntax: [copt,xopt] = mincx(lmisys,c,options,xinit,target)

The optimization variables xopt which are in our case $\mathbf{K}_0 \cdots \mathbf{K}_d$ and α are stored in the variable vector $\mathbf{x}$. The decision variables are minimized through the linear objective $\mathbf{c}$. The mincx minimizes the linear objective $\mathbf{c}^T\mathbf{x}$ over the LMI. The variable vector is: $\mathbf{x} = \begin{bmatrix}\mathbf{K}_0 & \cdots & \mathbf{K}_d & \alpha\end{bmatrix}^T$ and the linear objective is given by: $\mathbf{c} = \begin{bmatrix}0 & \cdots & 0 & 1\end{bmatrix}^T$, then:

$$\mathbf{c}^T\mathbf{x} = \begin{bmatrix}0 & \cdots & 0 & 1\end{bmatrix} \cdot \begin{bmatrix}\mathbf{K}_0 & \cdots & \mathbf{K}_d & \alpha\end{bmatrix}^T = \alpha$$

It should be noted that the LMI system must be feasible before this function can be used. The detailed description of the mincx function is given in (Gahinet et al. 1995).

4.5.3 The Generalized Eigenvalue Problem (GEVP)

If we fix $\mathbf{K}_i$ $(i = 0,\cdots,d)$, then we have a set of BMIs in $\mathbf{Q}_i (i = 0,\cdots,d)$, and α. In (Liu, Lei-Ming et al. 2008;Xiao et al. 2000) this problem is solved by setting $\alpha = 1$ and solving the GEVP for $\mathbf{Q}_i (i = 0,\cdots,d)$. We suggest here to minimize α while solving for $\mathbf{Q}_i (i = 0,\cdots,d)$ by using the following new variables:

$$\mathbf{W}_0 = \mathbf{B}_0\mathbf{K}_0\mathbf{C}_0 = \mathbf{B}_0\mathbf{Y}_0 \cdots \mathbf{W}_d = \mathbf{B}_d\mathbf{K}_d\mathbf{C}_d = \mathbf{B}_d\mathbf{Y}_d$$
$$\mathbf{W}_0^{\,T} = \mathbf{C}_0^{\,T}\mathbf{K}_0^{\,T}\mathbf{B}_0^{\,T} = \mathbf{Y}_0^{\,T}\mathbf{B}_0^{\,T} \cdots \mathbf{W}_d^{\,T} = \mathbf{C}_d^{\,T}\mathbf{K}_d^{\,T}\mathbf{B}_d^{\,T} = \mathbf{Y}_d^{\,T}\mathbf{B}_d^{\,T}$$

Then (4.21) becomes:

$$\begin{bmatrix} \alpha\mathbf{Q}_j & (\mathbf{A}_0 + \mathbf{W}_0)^T\mathbf{Q}_0 & \cdots & (\mathbf{A}_d + \mathbf{W}_d)^T\mathbf{Q}_d \\ \mathbf{Q}_0(\mathbf{A}_0 + \mathbf{W}_0) & p_{j0}^{-1}\mathbf{Q}_0 & \cdots & 0 \\ \vdots & \vdots & \ddots & \vdots \\ \mathbf{Q}_d(\mathbf{A}_d + \mathbf{W}_d) & 0 & \cdots & p_{jd}^{-1}\mathbf{Q}_d \end{bmatrix} > 0 \quad j = 0,\cdots,d \qquad (4.23)$$

This is a BMI in $\mathbf{Q}_i (i = 0,\cdots,d)$, and α. The problem is to maximize the decay rate that is to minimize α for a given $\mathbf{K}_i$ $(i = 0,\cdots,d)$; the GEVP is summarized as:

The Generalized Eigenvalue Problem GEVP:

For a given $\mathbf{Y}_i$ $(i = 0,\cdots,d)$, solve the following optimization problem.

Minimize α

Subject to

$$\begin{bmatrix} \alpha\mathbf{Q}_j & (\mathbf{A}_0 + \mathbf{W}_0)^T\mathbf{Q}_0 & \cdots & (\mathbf{A}_d + \mathbf{W}_d)^T\mathbf{Q}_d \\ \mathbf{Q}_0(\mathbf{A}_0 + \mathbf{W}_0) & p_{j0}^{-1}\mathbf{Q}_0 & \cdots & 0 \\ \vdots & \vdots & \ddots & \vdots \\ \mathbf{Q}_d(\mathbf{A}_d + \mathbf{W}_d) & 0 & \cdots & p_{jd}^{-1}\mathbf{Q}_d \end{bmatrix} > 0$$

$$\mathbf{Q}_0, \mathbf{Q}_1, ..., \mathbf{Q}_d > 0$$

$$\sum_{j=0}^{d} p_{0i} (\mathbf{A}_i + \mathbf{B}_i \mathbf{K}_i \mathbf{C}_i)^T \mathbf{Q}_j (\mathbf{A}_i + \mathbf{B}_i \mathbf{K}_i \mathbf{C}_i) < \alpha \mathbf{Q}_0$$

$$\cdots$$

$$\cdots$$

$$\cdots$$

$$\sum_{j=0}^{d} p_{di} (\mathbf{A}_i + \mathbf{B}_i \mathbf{K}_i \mathbf{C}_i)^T \mathbf{Q}_j (\mathbf{A}_i + \mathbf{B}_i \mathbf{K}_i \mathbf{C}_i) < \alpha \mathbf{Q}_d$$

The main problem is that the first constraint is nonlinear in $\mathbf{Q}_i \, (i = 0, \cdots, d)$, and α and we suggest the following solution algorithm: Start with $\alpha_{old} = 1$ and solve the above GEVP then we will get α_{new}. The iteration is continuing until the decay rate error is less than a certain value; i. e, $\alpha_{old} - \alpha_{new} < \Delta\alpha$.

The problem can be solved using gevp matlab function in the LMI Matlab toolbox. The function syntax is given as:

Syntax: [lopt,xopt] = gevp(lmisys,nlfc,options,linit,xinit,target)

The function gevp solves the following optimization problem:

Minimize λ subject to:

$$\mathbf{C}(x) < \mathbf{D}(x)$$

$$0 < \mathbf{B}(x)$$

$$\mathbf{A}(x) < \lambda \mathbf{B}(x)$$

Where **x** is the decision variables vector which contains $\mathbf{Q}_i \, (i = 0, \cdots, d)$, and α. As with the mincx the LMI system and the LMI constraints must be feasible.

Another easy way is just to solve the following problem by iteration;

Minimize α

Subject to

$$\mathbf{Q}_0, \mathbf{Q}_1, ..., \mathbf{Q}_d > 0$$

$$\sum_{j=0}^{d} p_{0i} (\mathbf{A}_i + \mathbf{B}_i \mathbf{K}_i \mathbf{C}_i)^T \mathbf{Q}_j (\mathbf{A}_i + \mathbf{B}_i \mathbf{K}_i \mathbf{C}_i) < \alpha \mathbf{Q}_0$$

$$\cdots$$

$$\cdots$$

$$\cdots$$

$$\sum_{j=0}^{d} p_{di} (\mathbf{A}_i + \mathbf{B}_i \mathbf{K}_i \mathbf{C}_i)^T \mathbf{Q}_j (\mathbf{A}_i + \mathbf{B}_i \mathbf{K}_i \mathbf{C}_i) < \alpha \mathbf{Q}_d$$

4.5.4 The V-K Iteration Algorithm:

In the V-K algorithm, the problem is iterated between the EVP and the GEVP. The proof of the algorithm convergence is given in (Banjerdpongchai 1997). The detailed algorithm is shown in the flowchart in Figure 4.4, and the algorithm can be summarized as:

1. The Initialization: Design the controller for the free delay system, i.e., LQR or LQG and choose an appropriate initial probability transition matrix, P_0.

2. Set $\mathbf{K}_0 = \mathbf{K}, \cdots, \mathbf{K}_d = \mathbf{K}$ and $\alpha = 1$. Solve the Feasibility Problem (FP). If the set of the LMIs is feasible proceed to step (3) if not go back to step (1) and try to modify $\mathbf{K}$ or P_0.

3. With the given $\mathbf{K}_0 \cdots \mathbf{K}_d$ solve the Generalized Eigenvalue Problem (GEVP).

4. With the given $\mathbf{Q}_0, \cdots, \mathbf{Q}_d$ solve the Eigenvalue Problem (EVP).

5. Perturb the probability transition matrix that is: $P_{new} = P_{old} + \Delta P_i$, (if P_E is reached go to (6)), then go to step (3).

6. END.

The initial transition probability matrix is:

$$P_0 = \begin{bmatrix} 1 & 0 & \dots & 0 \\ 1 & 0 & \dots & 0 \\ \vdots & \vdots & \ddots & \vdots \\ 1 & 0 & \dots & 0 \end{bmatrix} \approx \begin{bmatrix} 1-d\in & \in & \dots & \in \\ 1-d\in & \in & \dots & \in \\ \vdots & \vdots & \ddots & \vdots \\ 1-d\in & \in & \dots & \in \end{bmatrix}$$

where d and $\in$ are small positive numbers. It should be noted that the initial controller is designed for the free delay system. To get an initial feasible solution we have to start from small time delays and perturb the transition probability matrix toward larger time delays. The perturbation $\in$ should be a very small positive number in the order of 0.005 or the next iteration will not be feasible. An example of the perturbation matrix is:

$$\Delta P_0 = \begin{bmatrix} -s & s & 0 & \dots & 0 \\ 0 & 0 & 0 & \dots & 0 \\ \vdots & \vdots & \vdots & \ddots & \vdots \\ 0 & 0 & 0 & \dots & 0 \end{bmatrix} \quad \Delta P_1 = \begin{bmatrix} 0 & 0 & 0 & \dots & 0 \\ -s & s & 0 & \dots & 0 \\ \vdots & \vdots & \vdots & \ddots & \vdots \\ 0 & 0 & 0 & \dots & 0 \end{bmatrix} \quad \Delta P_2 = \begin{bmatrix} 0 & 0 & 0 & \dots & 0 \\ -s & 0 & s & \dots & 0 \\ \vdots & \vdots & \vdots & \ddots & \vdots \\ 0 & 0 & 0 & \dots & 0 \end{bmatrix}$$

As can be seen, the sum of the perturbation through any row is zero. More aggressive initial transition probability matrix can be used if the solution is feasible. In (Liu, Lei-Ming et al. 2008;Xiao et al. 2000) the perturbation is around 0.01 but even this small perturbation sometimes does not usually work, and we need to use smaller perturbation around 0.005. Furthermore, for the two modes the two probability matrices are perturbed at the same time while in our algorithm, they are perturbed separately. The V-K iteration algorithm is shown in Figure 4.4.

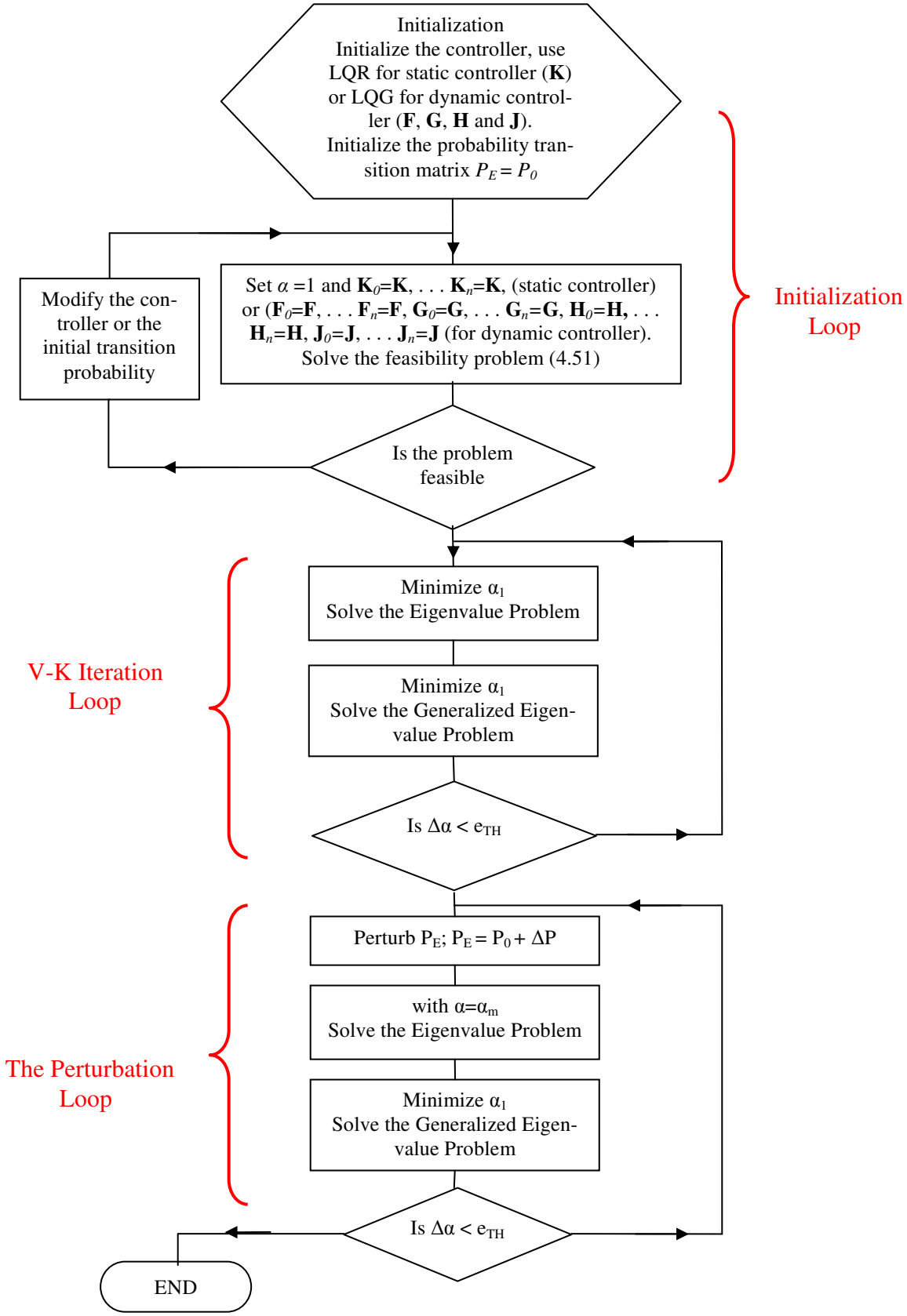

Figure 4.4 The V-K iteration algorithm

4.6 Example 4.1: The cart and inverted pendulum:

The inverted pendulum over a cart is one of the most widely used examples in control systems to demonstrate the new methods or algorithms. The system is shown in Figure 4.5; the pendulum mass is denoted by *m,* and the cart mass is *M*; the length of the pendulum rod is *L*.

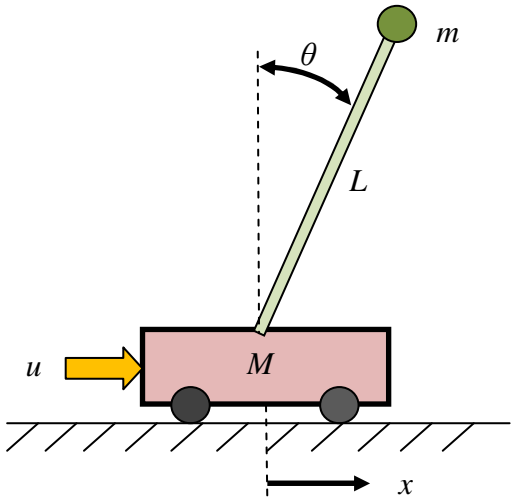

Figure 4.5 The cart and inverted pendulum

The model used is the fourth-order model. The open-loop system is unstable. The states are defined as $\mathbf{x} = \begin{bmatrix} x_1 & x_2 & x_3 & x_4 \end{bmatrix}^T = \begin{bmatrix} x & \dot{x} & \theta & \dot{\theta} \end{bmatrix}^T$ and the input as $u = F$. The nonlinear dynamic can be written as:

$$\dot{\mathbf{x}} = f(x,u) = \begin{bmatrix} x_2 \\ \dfrac{mg \sin x_3 \cos x_3 - mLx_4^2 \sin x_3 - u}{m\cos^2 x_3 - (M+m)} \\ x_4 \\ \dfrac{-(M+m)g \sin x_3 + mLx_4^2 \sin x_3 \cos x_3 + u\cos x_3}{mL\cos^2 x_3 - (M+m)L} \end{bmatrix}$$

After linearizing the system around the origin the linearized model can be given as:

$$\dot{\mathbf{x}} = \begin{bmatrix} x_2 \\ \dfrac{-mgx_3 + u}{M} \\ x_4 \\ \dfrac{(M+m)gx_3 - u}{ML} \end{bmatrix} = \begin{bmatrix} 0 & 1 & 0 & 0 \\ 0 & 0 & \dfrac{-mg}{M} & 0 \\ 0 & 0 & 0 & 1 \\ 0 & 0 & \dfrac{(M+m)g}{ML} & 0 \end{bmatrix} \mathbf{x} + \begin{bmatrix} 0 \\ \dfrac{1}{M} \\ 0 \\ \dfrac{-1}{ML} \end{bmatrix} u = \mathbf{A}\mathbf{x} + \mathbf{B}u$$

$$\mathbf{y} = \begin{bmatrix} x \\ \theta \end{bmatrix} = \begin{bmatrix} 1 & 0 & 0 & 0 \\ 0 & 0 & 1 & 0 \end{bmatrix} \mathbf{x} = h(x,u)$$

The parameters used are: $M = 1\ kg,\ m = 0.4\ kg,\ L = 0.7$ meters. The sampling time is $h = 0.1$ seconds. The time delay is bounded by 2: $r_s(k) \in \{0,1,2\}$.

After sampling the system with 0.1 s sampling rate, the system matrices are given by:

$$\mathbf{A} = \begin{bmatrix} 1 & 0.1 & -0.0199 & -0.0007 \\ 0 & 1 & -0.4049 & -0.0199 \\ 0 & 0 & 1.0996 & 0.1033 \\ 0 & 0 & 2.0247 & 1.0996 \end{bmatrix} \quad \mathbf{B} = \begin{bmatrix} 0.0050 \\ 0.1009 \\ -0.0073 \\ -0.1476 \end{bmatrix} \quad \mathbf{Q} = \mathbf{I}_4 \text{ and } \mathbf{R} = 1$$

It is assumed that the transition probability is given by:

$$P = \begin{bmatrix} 0.5 & 0.5 & 0 \\ 0.3 & 0.6 & 0.1 \\ 0.3 & 0.6 & 0.1 \end{bmatrix}$$

Using the LQR Matlab function, the controller is given by:

$$\mathbf{K}_{LQR} = \begin{bmatrix} 0.5943 & 1.4745 & 28.7321 & 6.7849 \end{bmatrix}$$

The required transition probability with the LQR controller does not stabilize the system with the time delay because the solution is infeasible. So the initial transition probability and the perturbation matrix are chosen as:

$$P_0 = \begin{bmatrix} 0.499 & 0.499 & 0.002 \\ 0.4 & 0.5 & 0.1 \\ 0.4 & 0.5 & 0.1 \end{bmatrix} \qquad \Delta P_i = \begin{bmatrix} 0 & 0 & 0 \\ -0.005 & 0.005 & 0 \\ -0.005 & 0.005 & 0 \end{bmatrix}$$

After 20 iterations, the desired transition matrix is reached, and the stabilizing controller is given as:

$$\mathbf{K} = \begin{bmatrix} 0.3181 & 0.7972 & 21.2058 & 5.4654 \end{bmatrix}$$

Note that the process can be started with any P and $\mathbf{K}_{LQR}$ as long as they give feasible solution. The Simulink implementation of the system is shown in Figure 4.6. In the simulation, we used the nonlinear dynamics of the system. In the simulations shown in Figure 4.7, comparison is made between the controller that takes the random time delay into consideration and the controller that does not take the random time delay into consideration. The initial condition is:

$$\begin{bmatrix} x & \dot{x} & \theta & \dot{\theta} \end{bmatrix} = \begin{bmatrix} 0 & 0 & 0.1 & 0 \end{bmatrix}$$

Using Theorem 3.1 the MADB with the LQR controller is 0.1210 s, while Corollary 3.1 gives 0.1217 s as the MADB. With the stabilizing controller that takes the random time delay into consideration, Theorem 3.1 gives 0.1420 s while Corollary 3.1 gives 0.1426 s. This shows an improvement in the stability margin with the new controller.

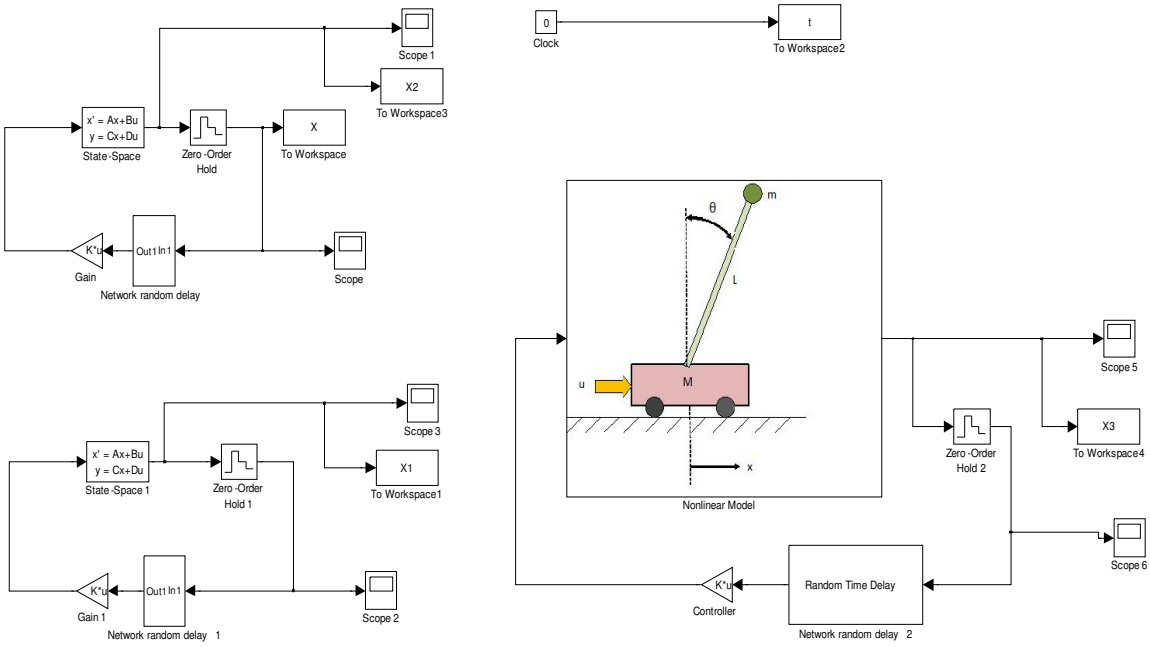

Figure 4.6 The Simulink implementation of example 4.1

The V-K iteration loop took 4-iterations, and the perturbation loop took 20 iterations; the minimum decay rate is 0.8837. By changing the Eigenvalue Problem loop by making an inner loop for minimizing α, the minimum attained decay rate is 0.8645. Moreover, using Theorem 3.1 the time delay margin increased to 0.1563 s. The system response is shown in Figure 4.8. The stabilizing controller with the improved algorithm is:

$$\mathbf{K} = \begin{bmatrix} 0.2823 & 0.7050 & 20.5227 & 4.9714 \end{bmatrix}$$

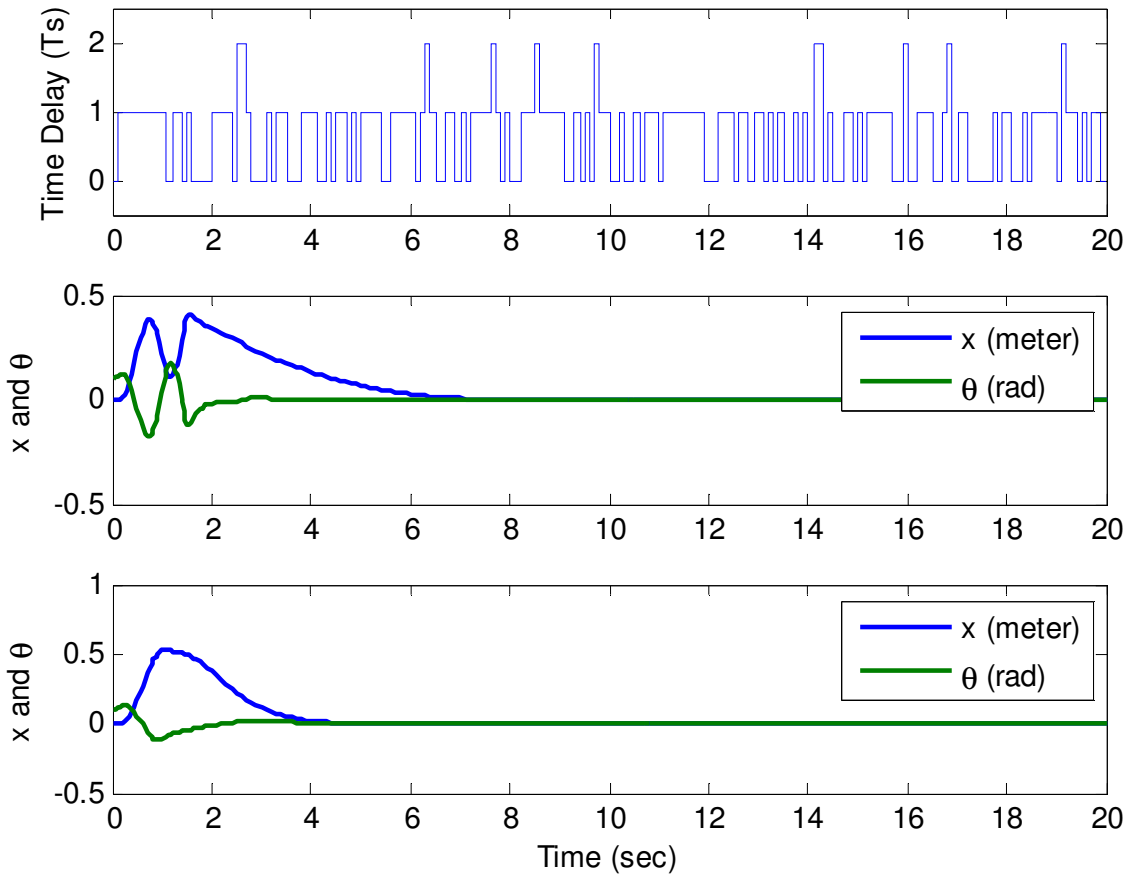

Figure 4.7 (a) The random time delay, (b) The response of the system in example 4.1 without time delay compensation (c) The response with time delay compensation

Even the system is stable in many simulation runs, with the controller that does not take the random time delay into account, in a few simulation runs the system is unstable.

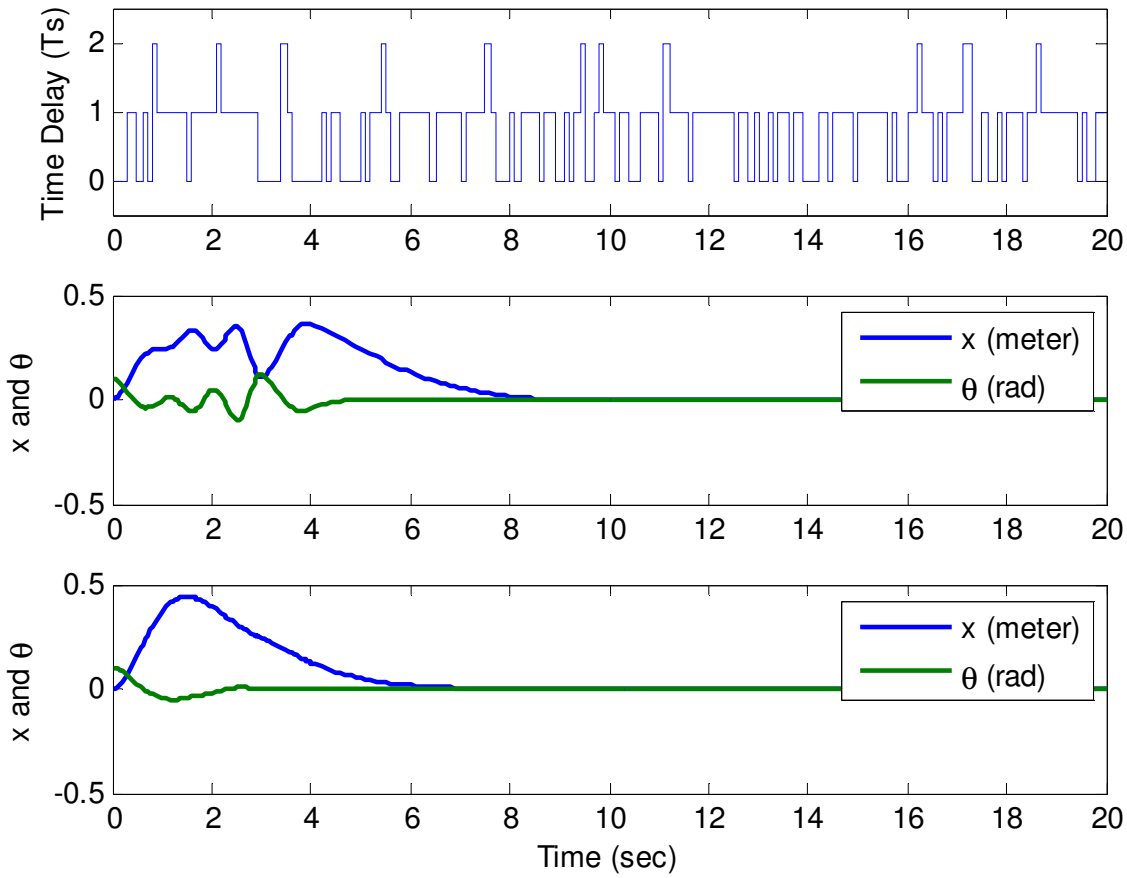

Figure 4.8 (a) The random time delay, (b) The response of the system in example 4.1 without time delay compensation (c) The response with time delay compensation

With a dynamic controller and the following transition probability matrix:

$$P = \begin{bmatrix} 0.34 & 0.65 & 0.01 \\ 0.34 & 0.33 & 0.33 \\ 0.34 & 0.33 & 0.33 \end{bmatrix}$$

The initial transition probability matrix and the perturbation matrix are given by:

$$P = \begin{bmatrix} 0.98 & 0.01 & 0.01 \\ 0.98 & 0.01 & 0.01 \\ 0.98 & 0.01 & 0.01 \end{bmatrix} \qquad \Delta P_i = \begin{bmatrix} -0.02 & 0.02 & 0 \\ -0.02 & 0.01 & 0.01 \\ -0.02 & 0.01 & 0.01 \end{bmatrix}$$

The sampling time is 0.05 s. The initial dynamic controller using the LQG is given by:

$$\mathbf{F} = \begin{bmatrix} -1.4684 & 2.0436 & 0.8454 & 0.0186 \\ -14.5396 & 4.7364 & 164.9275 & 7.1275 \\ 2.3599 & -0.0202 & -15.5496 & 2.8367 \\ 30.2555 & -7.2795 & -278.1537 & -6.9702 \end{bmatrix} \quad \mathbf{G} = \begin{bmatrix} 1.4598 & -1.0050 \\ 16.0342 & -108.0558 \\ -2.3303 & 16.2630 \\ -32.4070 & 224.5580 \end{bmatrix}$$

$$\mathbf{H} = \begin{bmatrix} 0.5969 & 1.5087 & 30.4620 & 7.1349 \end{bmatrix} \quad \mathbf{J} = \begin{bmatrix} 0 & 0 \end{bmatrix}$$

The controller does not stabilize the system with the given transition probability matrix. Starting with the initial transition probability matrix and after 32 iterations, the stabilizing dynamic controller is given by:

$$\mathbf{F} = \begin{bmatrix} 0.2876 & 0.0157 & -1.5549 & -0.0193 \\ -0.0900 & 1.1090 & 1.3934 & 0.4734 \\ 0.0619 & -0.0538 & 0.5468 & 0.0740 \\ 0.3277 & -0.1795 & -1.9525 & 0.3937 \end{bmatrix} \quad \mathbf{G} = \begin{bmatrix} 0.6565 & 0.6506 \\ 0.1624 & 0.2597 \\ -0.0932 & 0.9798 \\ -0.4077 & 1.3448 \end{bmatrix}$$

$$\mathbf{H} = \begin{bmatrix} 1.1084 & 1.5240 & 19.0996 & 4.0321 \end{bmatrix} \quad \mathbf{J} = \begin{bmatrix} 0.0217 & 0.8496 \end{bmatrix}$$

The system response with the initial controller and the stabilizing controller is shown in Figure 4.9, it is clear that the initial controller does not stabilize the system. Modifying the perturbation loop by maximizing the decay rate in the EVP, the controller is given as:

$$\mathbf{F} = \begin{bmatrix} 0.1863 & 0.0558 & -1.3769 & 0.0097 \\ -0.2237 & 1.0540 & 0.8079 & 0.3953 \\ 0.0686 & -0.0386 & 0.5959 & 0.1047 \\ 0.2257 & -0.0762 & -1.2304 & 0.5740 \end{bmatrix} \mathbf{G} = \begin{bmatrix} 0.7833 & 0.4623 \\ 0.2452 & 0.1856 \\ -0.0839 & 1.0353 \\ -0.2569 & 0.8785 \end{bmatrix}$$

$$\mathbf{H} = \begin{bmatrix} 0.5644 & 0.7883 & 13.7482 & 2.9918 \end{bmatrix} \quad \mathbf{J} = \begin{bmatrix} -0.1405 & 0.5738 \end{bmatrix}$$

The system response of the system with the initial controller and with the controller generated by the modified V-K iteration is shown in Figure 4.10.

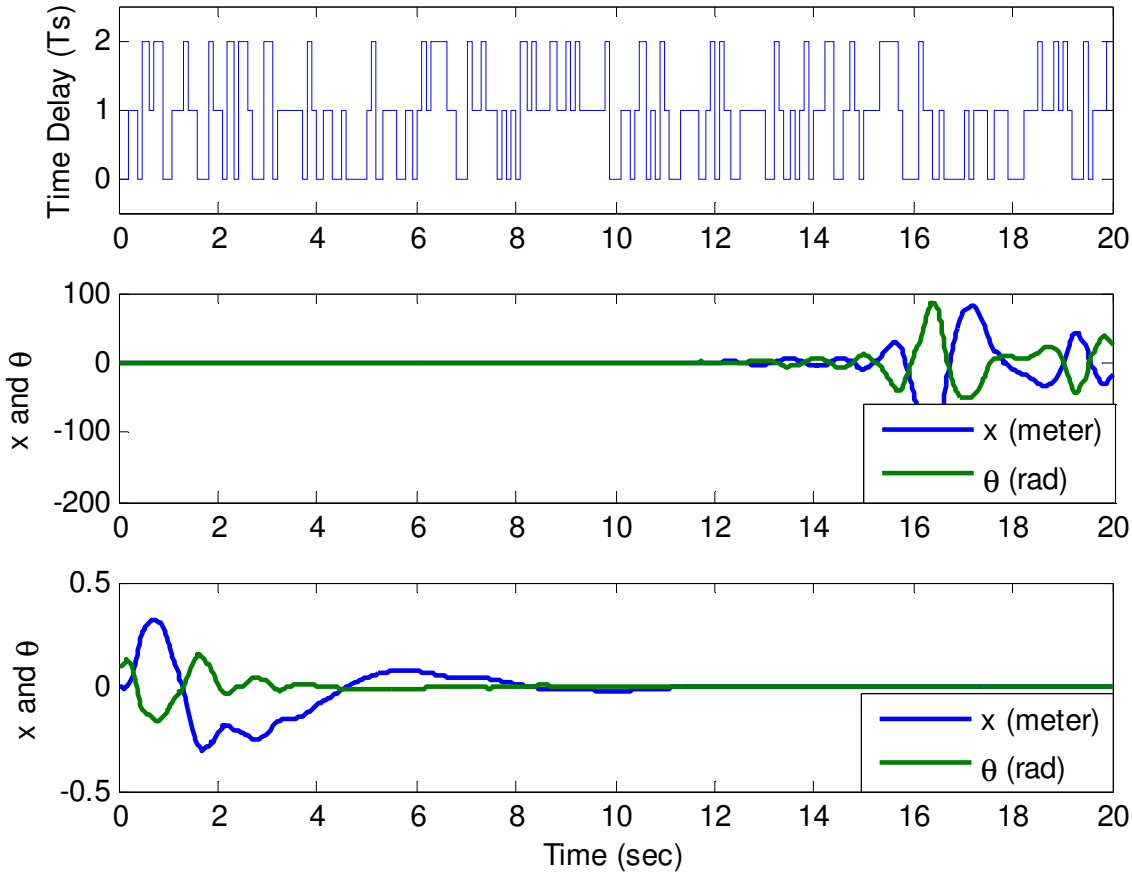

Figure 4.9 (a) The random time delay, (b) The response of the system in example 4.1 without time delay compensation (c) The response with time delay compensation

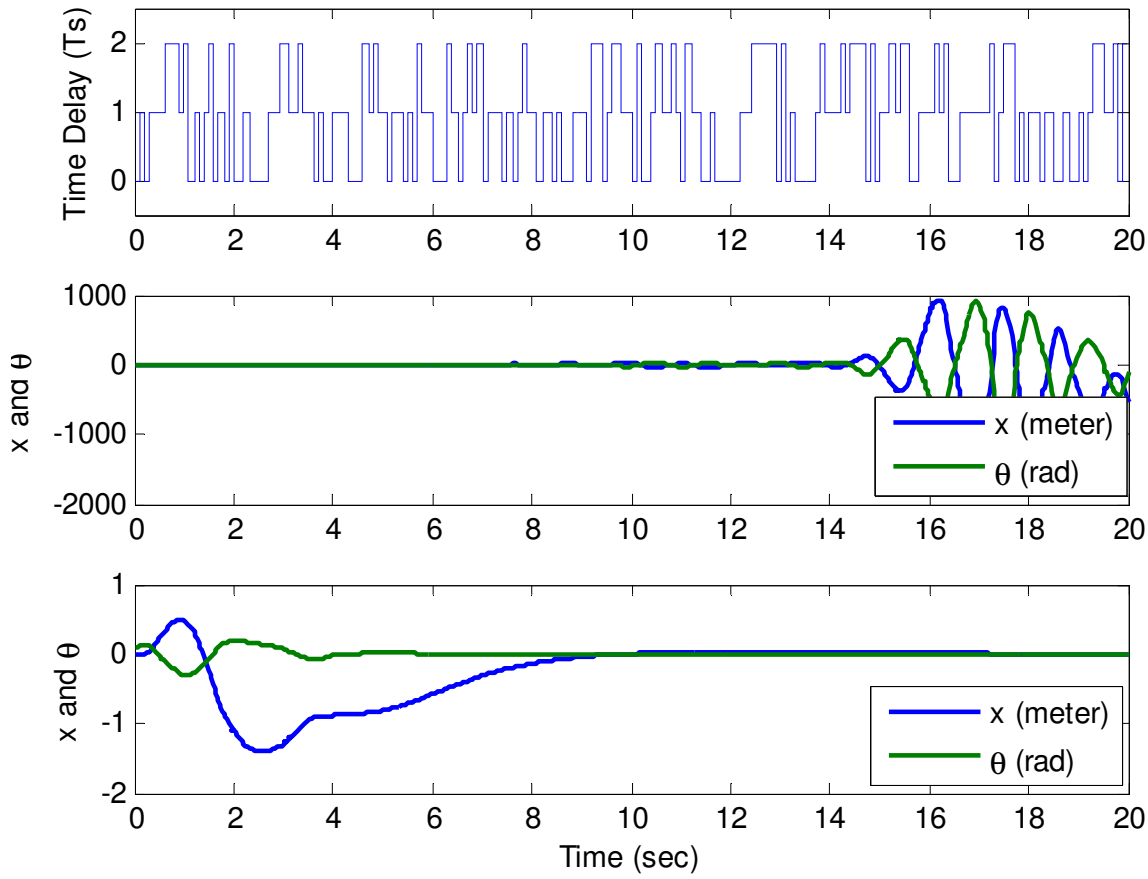

Figure 4.10 (a) The random time delay, (b) The response of the system in example 4.1 without time delay compensation (c) The response with time delay compensation

4.7 Summary

The issues of stability and controller design for networked control systems with random delays are discussed in this chapter. Both the time delays from the sensor to the controller, and from the controller to the actuator are modelled using Markov Chains. The resulting system is a standard Markovian Linear Jump System. The stability of the system is in the Bilinear Matrix Inequality form. A modified V-K iteration algorithm is proposed for deriving the stabilizing controller where we add another minimization loop for α instead of setting it to one, which gives higher decay rate.

CHAPTER FIVE: NETWORKED CONTROL OF PARALLEL DC/DC BUCK CONVERTERS

5.1 Introduction:

Connecting DC/DC converters in parallel offers many advantages such as increased power processing capabilities, improved reliability, easy maintenance, future expansion, and modularity (Siri et al. 1990;Zhang et al. 2004). Parallel DC/DC converters can be found in many industrial applications. The goal of the controller in parallel DC/DC converter systems is to maintain a regulated output voltage while achieving good load current sharing. Voltage regulation and current sharing are among the basic control issues in UPSs (Uninterruptible Power Supplies) and in parallel VSIs (Voltage Source Inverters) in Microgrids (Pogaku et al. 2007;Yongquin et al. 2008). There are a number of control strategies that are commonly used, which can be classified into centralized, master-slave and distributed control strategies (Prodanovic et al. 2000). In the centralized control strategy, all the information is sent to a centralized controller, and then the commands are sent back to the system. The main disadvantage of this strategy is the single point of failure and the complexity in

the controller design for large and complex interconnected systems. In the master-slave control strategy, one of the converters is known to be the master while the others are the slaves, the master controller contains the voltage controller while the slaves contain current controllers and have to track the master's reference current. In this control strategy there will be a transfer of information between the master controller and the slaves' controllers. Nowadays, there is an interest in controlling the DC/DC power converters through a shared communication network. Because it involves less information transfer, the master-slave control strategy is favoured for networked control system applications. In the following a brief review on controlling distributed power electronic systems through a shared network.

In the last few years, the applications of NCSs in power electronic systems have been frequently reported, see for example (Guerrero et al. 2006;Ren et al. 2009;Lai et al. 2009;Mazumder et al. 2005;Mazumder et al. 2008;Mazumder et al. 2010;Yongquing et al. 2008;Zhang et al. 2007). In (Yongquing et al. 2008), the control of parallel inverters based on CAN is introduced. The design is based on the maximum time delay that guarantees the stability, where the system composed of three three-phase DC/AC inverters driving a motor load. The authors allocated the required bandwidth based on the sampling time, and no method is given to estimate the MADB for the system. A new control strategy for controlling power electronic systems over a network was proposed in (Zhang et al. 2007). The work was to answer two questions: how to treat the power electronic module as communication node and how to estimate the time delay in different network types with different network topologies. In (Lai et al. 2009;Mazumder et al. 2005;Mazumder et al. 2008), the problem of controlling a parallel DC/DC converter over an RF communication interface is discussed. The authors in (Mazumder et al. 2005;Mazumder et al. 2008) use a method in the frequency domain to find the range of the system parameters and the controller parame-

ters that guarantee the stability of the system. There are a few publications on controlling these systems over control networks and most of them are complex to use. In this chapter, the control of parallel DC/DC Buck converters over a shared network is discussed. Two control networks are used for this study, which are the CAN and the Ethernet. As we discussed in Chapter 2, the CAN is a deterministic network while the Ethernet is not. Depending on the network load four different time delay types have been noticed. These are constant time delay, periodic time delay, random time delay with no correlation between the current and previous time delay and random time delay governed by Markov Chain. The method developed in Chapter 3 has been applied to the first three types, where the system is designed to have MADB larger than the worst-case time delay in the network. The proposed method in Chapter 3 is used for estimating the MADB in networked parallel DC/DC buck converter system and to link it with the system and the controller parameters. For the fourth case where the time delay is governed by Markov Chain, the Markovian jump system approach in Chapter 4 is used to design the controller that stochastically stabilizes the system.

In the following sections, the modelling of the parallel DC/DC converters is briefly described and then the master-slave control strategy, and the voltage and current controller's models are explained. A case study system consists of three parallel DC/DC converters is studied. The controller parameters that affect the MADB are investigated, and the controller parameters are used to modify the MADB to be larger than the worst-case network time delay. The design tools developed in Chapter 3 and Chapter 4 are used to design stabilizing controller under four different time delay cases, which is constant, periodic, random without correlation between the current and previous time delay and random governed by Markov Chains. The parallel DC/DC Buck converters system simulation is carried out with

the Matlab/SimPowerSystem while the network simulation is done using the TrueTime 1.5 simulator.

5.2 Parallel DC/DC Buck Converters

A system consists of *n* parallel connected DC/DC converters is shown in Figure 5.1. The converters are designed to supply power with a specified current and voltage to the load. These converters are expected to be identical. If these converters are not identical, a small difference between them can result in a large current sharing error between the converters (Siri et al. 1990), and hence a current sharing controller is necessary.

5.2.1 The Parallel DC/DC Buck Converters Mathematical Model

In order to design a controller, a model for the system must be provided. The most widely used approach for modelling power electronic systems is the time-average state-space approach (Middlebrook et al. 1976). The original model of the DC/DC Buck converters is nonlinear and time varying. In (Mazumder et al. 2005;Mazumder et al. 2008a;Mazumder et al. 2010;Mazumder et al. 2008b) the nonlinear model for the system is used and multiple Lyapunov functions are constructed to study the stability. In the time average model the nonlinear time varying model is perturbed and linearized around the equilibrium point and the higher-order derivatives are truncated. The state-space time average model of *n* parallel connected DC/DC converters is given by:

$$
\begin{aligned}
\frac{di_{L1}}{dt} &= \frac{-r_{L1}}{L_1} i_{L1} - \frac{1}{L_1} v + \frac{V_{in}}{L_1} \delta_1 \\
\frac{di_{L2}}{dt} &= \frac{-r_{L2}}{L_2} i_{L2} - \frac{1}{L_2} v + \frac{V_{in}}{L_2} \delta_2 \\
&\vdots \\
\frac{di_{Ln}}{dt} &= \frac{-r_{Ln}}{L_n} i_{Ln} - \frac{1}{L_n} v + \frac{V_{in}}{L_n} \delta_n \\
v &= \frac{1}{\sum_{i=1}^{n} C_i} i_{L1} + \frac{1}{\sum_{i=1}^{n} C_i} i_{L2} + \cdots + \frac{1}{\sum_{i=1}^{n} C_i} i_{Ln} - \frac{1}{R\sum_{i=1}^{n} C_i} v
\end{aligned}
\tag{5.1}
$$

where $i_{L1}, \cdots, i_{Ln}$ are the inductor currents and v is the output voltage, which are chosen as the state variables for the system. $\delta_1, \cdots, \delta_n$ are the duty cycles of the converters, which are chosen as the control inputs. The other parameters are shown in Figure 5.1.

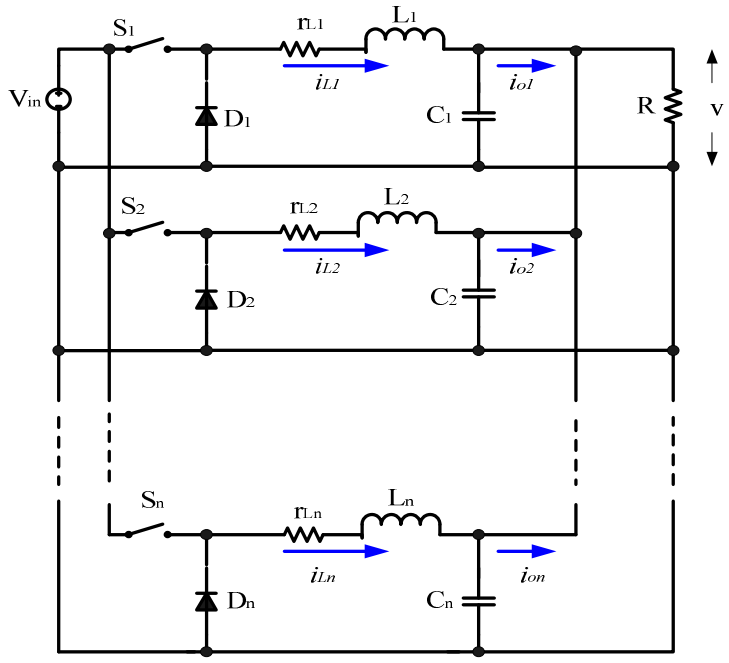

Figure 5.1 A parallel DC/DC Buck Converter system.

5.2.2 The Controller Model

A system consists of two DC/DC converters is shown in Figure 5.2. The master sends the reference current to the slave controller through a shared network. The slave converter will receive a delayed version of this signal, or it may not receive it at all where we consider the data loss or data dropout as a special case of the time delay. This time delay degrades the system performance, and it can even destabilize the system. The controller must be designed to guarantee the stability of the system in the presence of the time delay.

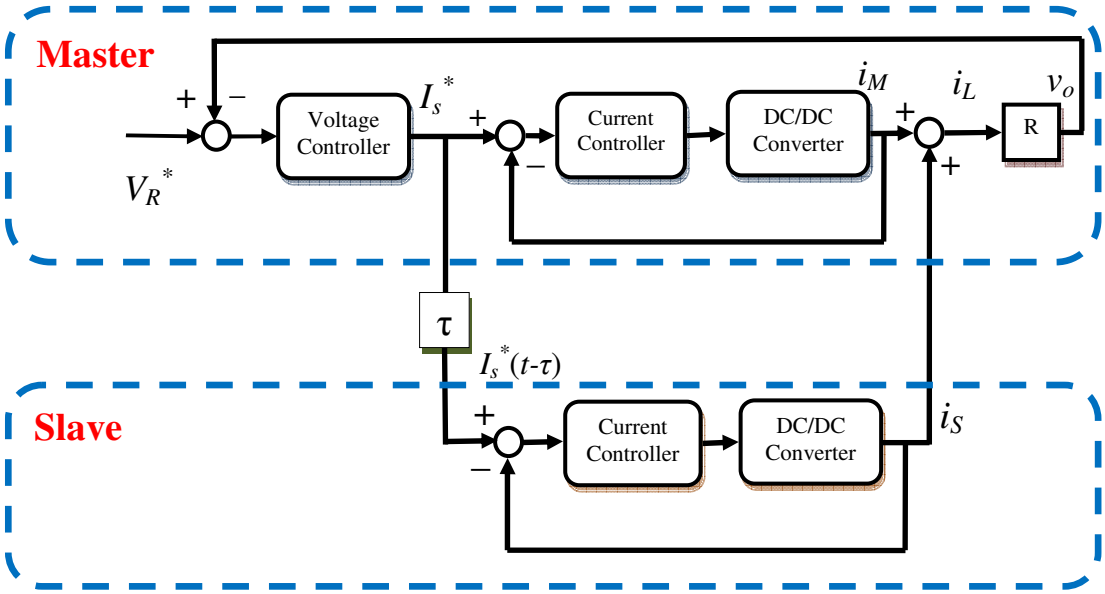

Figure 5.2 Master-slave control strategy for two DC/DC parallel converters

The voltage controller has to regulate the output voltage and to produce the reference current. The most widely used voltage and current compensator is the type II compensator with the following transfer function:

$$G(s) = K\frac{(s/\omega_z + 1)}{s(s/\omega_p + 1)} \tag{5.2}$$

where K is the controller gain, ω_z is the compensator zero, ω_p is the compensator pole. These parameters are tuned to give the system the required performance. This type of compensator is mainly used to track any changes in the input voltage or system load. The master controller contains both the voltage and the current controller and is shown in Figure 5.3.

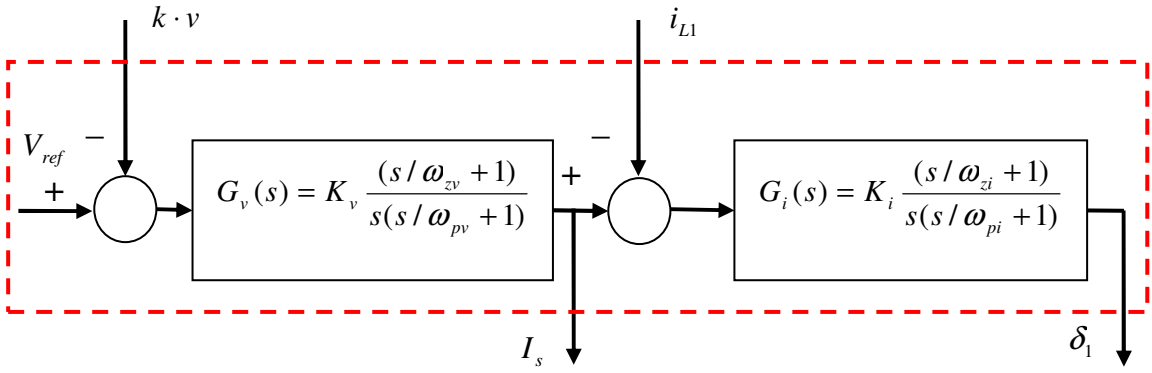

Figure 5.3 The master controller with both voltage and current controller

The state-space representation of the master controller is given as:

$$\begin{bmatrix} \dot{z}_1^{(1)} \\ \dot{z}_2^{(1)} \\ \dot{z}_3^{(1)} \\ \dot{z}_4^{(1)} \end{bmatrix} = \begin{bmatrix} -\omega_{pv} & 0 & 0 & 0 \\ 1 & 0 & 0 & 0 \\ \overline{K}_v & \overline{K}_v\omega_{zv} & -\omega_{p1} & 0 \\ 0 & 0 & 1 & 0 \end{bmatrix} \begin{bmatrix} z_1^{(1)} \\ z_2^{(1)} \\ z_3^{(1)} \\ z_4^{(1)} \end{bmatrix} + \begin{bmatrix} -k & 0 \\ 0 & 0 \\ 0 & -1 \\ 0 & 0 \end{bmatrix} \begin{bmatrix} v - k^{-1}V_{ref} \\ i_{L1} \end{bmatrix}$$

$$[I_s] = [\overline{K}_v \quad \overline{K}_v\omega_{zv} \quad 0 \quad 0] \cdot [z_1^{(1)} \quad z_2^{(1)} \quad z_3^{(1)} \quad z_4^{(1)}]^T$$

$$[\delta_1] = [0 \quad 0 \quad \overline{K}_1 \quad \overline{K}_1\omega_{z1}] \cdot [z_1^{(1)} \quad z_2^{(1)} \quad z_3^{(1)} \quad z_4^{(1)}]^T \qquad (5.3)$$

Where k is the feedback gain of the output voltage, V_{ref} is the reference voltage, I_s is the voltage controller output, which is the reference current, and $\overline{K}_v = K_v(\omega_{pv}/\omega_{zv})$.

The output of the voltage controller is used as the reference current for the master current controller and to all the parallel converters. The slaves' controllers will receive a delayed version of the master reference current. The model of the current controller in slave 1 is given by:

$$\begin{bmatrix} \dot{z}_1^{(2)} \\ \dot{z}_2^{(2)} \end{bmatrix} = \begin{bmatrix} -\omega_{p2} & 0 \\ 1 & 0 \end{bmatrix} \begin{bmatrix} z_1^{(2)} \\ z_2^{(2)} \end{bmatrix} + \begin{bmatrix} 1 \\ 0 \end{bmatrix} \left[I_s(t-\tau) - i_{L2}(t) \right]$$

$$\delta_2(t) = \begin{bmatrix} \overline{K}_2 & \overline{K}_2 \omega_{z2} \end{bmatrix} \begin{bmatrix} z_1^{(2)} \\ z_2^{(2)} \end{bmatrix} \tag{5.4}$$

where ω_{p2} and ω_{z2} are the pole and the zero of the slave controller and $\overline{K}_2 = K_2(\omega_{p2} / \omega_{z2})$. The main difference between the classical networked control system and the networked parallel DC/DC buck converter is that in the traditional networked control system the sensor, the actuator and the controller exchange their states through the network while in this system only the controllers exchange the information.

5.3 Networked Control of Parallel DC/DC Converters with Constant Time Delay

In many situations, the time delay may be constant, time varied or random but bounded and the worst-case time delay can be used as designing guide. In this case, we follow the analysis in Chapter 3 where the time delay is assumed either constant or bounded. The state-space model of a NCS consists of *n* parallel DC/DC converters is given as;

$$
\begin{aligned}
\dot{\mathbf{x}}^{(1)}(t) &= \mathbf{A}_{11}\mathbf{x}^{(1)}(t) + \sum_{j=2}^{n}\mathbf{A}_{1j}\mathbf{x}^{(j)}(t) + \mathbf{B}_1\mathbf{u}^{(1)}(t) \\
\dot{\mathbf{x}}^{(2)}(t) &= \mathbf{A}_{22}\mathbf{x}^{(2)}(t) + \sum_{j=1;\, j\neq 2}^{n}\mathbf{A}_{2j}\mathbf{x}^{(j)}(t) + \mathbf{B}_2\mathbf{u}^{(2)}(t) \\
&\vdots \\
\dot{\mathbf{x}}^{(n)}(t) &= \mathbf{A}_{nn}\mathbf{x}^{(n)}(t) + \sum_{j=1}^{n-1}\mathbf{A}_{nj}\mathbf{x}^{(j)}(t) + \mathbf{B}_n\mathbf{u}^{(n)}(t)
\end{aligned}
\tag{5.5}
$$

$$
\begin{aligned}
\mathbf{y}_x^{(1)} &= \mathbf{C}_{x1}\mathbf{x}^{(1)}(t) \\
\mathbf{y}_x^{(2)} &= \mathbf{C}_{x2}\mathbf{x}^{(2)}(t) \\
&\vdots \\
\mathbf{y}_x^{(n)} &= \mathbf{C}_{xn}\mathbf{x}^{(n)}(t)
\end{aligned}
\tag{5.6}
$$

where: $\mathbf{x}^{(1)}(t)$, $\mathbf{x}^{(2)}(t)$, . . ., $\mathbf{x}^{(n)}(t)$ are the states vectors of the converters. $\mathbf{u}^{(1)}(t)$, $\mathbf{u}^{(2)}(t)$, . . . , $\mathbf{u}^{(n)}(t)$ are the control input vectors of the converters. The state vector of the i^{th} converter is $\mathbf{x}^{(i)} := \left[\mathbf{x}_1^{(i)} \quad \mathbf{x}_2^{(i)} \quad . \quad . \quad . \quad \mathbf{x}_{n_i}^{(i)}\right]^T \in \Re^{n_i}$ and the control input vector is $\mathbf{u}^{(i)} := \left[\mathbf{u}_1^{(i)} \quad \mathbf{u}_2^{(i)} \quad . \quad . \quad . \quad \mathbf{u}_{m_i}^{(i)}\right]^T \in \Re^{n_i}$. n_i is the number of states in the i^{th} subsystem. m_i is the order of the i^{th} controller. $\mathbf{A}_{ij}$ (where $i \neq j$) describes how the dynamics of the i^{th} converter can be influenced by the j^{th} converter. The networked DC/DC converters implement the master-slave control strategy. The master controller contains both voltage controller and current controller. The master voltage controller sends the reference current to all the converters in the system through the shared network as shown in Figure 5.4.

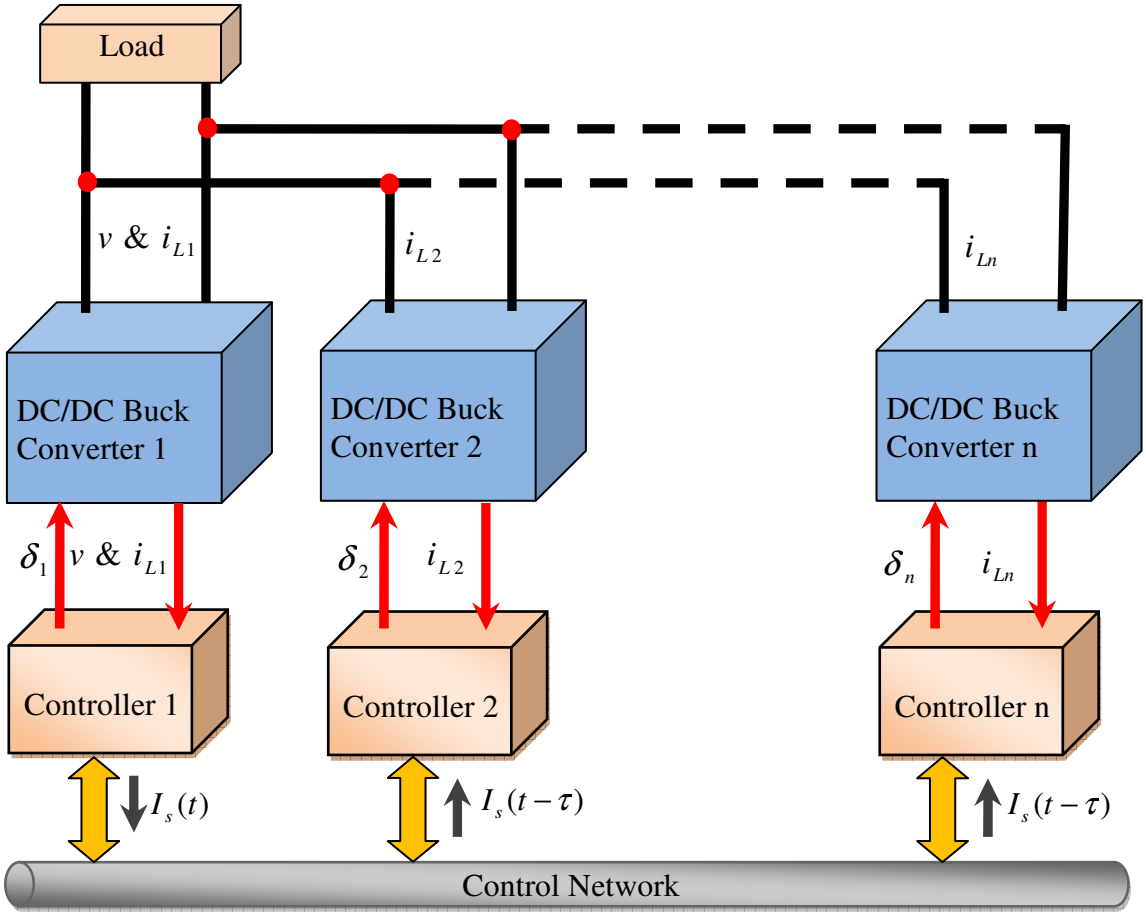

Figure 5.4 The parallel DC/DC converters communicating through control network.

Each slave controller has a current controller to track the master current, and they receive a delayed version of the reference current signal. The dynamic controllers are given by:

$$\dot{\mathbf{z}}^{(1)}(t) = \mathbf{F}_{11}\mathbf{z}^{(1)}(t) + \sum_{j=2}^{n}\mathbf{F}_{1j}\mathbf{y}_z^{(j)} + \mathbf{G}_1\mathbf{y}_x^{(1)} + \mathbf{R}_{ref}(t)$$

$$\dot{\mathbf{z}}^{(2)}(t) = \mathbf{F}_{22}\mathbf{z}^{(2)}(t) + \sum_{j=1;j\neq 2}^{n}\mathbf{F}_{2j}\mathbf{y}_z^{(j)} + \mathbf{G}_2\mathbf{y}_x^{(2)}$$

$$\vdots$$

$$\dot{\mathbf{z}}^{(n)}(t) = \mathbf{F}_{nn}\mathbf{x}^{(n)}(t) + \sum_{j=1}^{n-1}\mathbf{F}_{nj}\mathbf{y}_z^{(j)} + \mathbf{G}_n\mathbf{y}_x^{(n)}$$

$$
\begin{aligned}
\mathbf{v}^{(1)}(t) &= \mathbf{H}_1\mathbf{z}^{(1)}(t) & \mathbf{y}_z^{(1)} &= \mathbf{C}_{z1}\mathbf{z}^{(1)} \\
\mathbf{v}^{(2)}(t) &= \mathbf{H}_2\mathbf{z}^{(2)}(t) & \mathbf{y}_z^{(2)} &= \mathbf{C}_{z2}\mathbf{z}^{(2)} \\
&\vdots & &\vdots \\
\mathbf{v}^{(n)}(t) &= \mathbf{H}_n\mathbf{z}^{(n)}(t) & \mathbf{y}_z^{(n)} &= \mathbf{C}_{zn}\mathbf{z}^{(n)}
\end{aligned}
\tag{5.7}
$$

$\mathbf{F}_{ij}$ $(i \neq j)$ represents how the dynamic of the j^{th} controller affects the dynamics of the i^{th} controller. In the master controller $\mathbf{F}_{1j} = 0$ for $j = 2,\cdots,n$, because the master controller dynamics depend only on local information. τ_{ij} is the time delay from the j^{th} controller to the i^{th} controller. $\mathbf{G}_i$ is the input of the i^{th} controller. Since the controllers communicate directly with the plants, then $\mathbf{v}^{(i)}(t) = \mathbf{u}^{(i)}(t)$. Assuming constant or bounded time delay transfer from the master node to all slave nodes (Mazumder et al. 2008), we have;

$$
\tau_{j1} = \tau_{j2} = \cdots = \tau_{jn} = \tau_d \tag{5.8}
$$

Applying the controllers in (5.7) into the plants in (5.5)-(5.6), the complete system becomes:

$$
\begin{aligned}
\dot{\mathbf{x}}^{(1)}(t) &= \mathbf{A}_{11}\mathbf{x}^{(1)}(t) + \sum_{j=2}^{n}\mathbf{A}_{1j}\mathbf{x}^{(j)}(t) + \mathbf{B}_{11}\mathbf{H}_{11}\mathbf{z}^{(1)}(t) \\
\dot{\mathbf{x}}^{(2)}(t) &= \mathbf{A}_{22}\mathbf{x}^{(2)}(t) + \sum_{j=1;j\neq 2}^{n}\mathbf{A}_{2j}\mathbf{x}^{(j)}(t) + \mathbf{B}_{22}\mathbf{H}_{22}\mathbf{z}^{(2)}(t) \\
&\vdots \\
\dot{\mathbf{x}}^{(n)}(t) &= \mathbf{A}_{nn}\mathbf{x}^{(n)}(t) + \sum_{j=1}^{n-1}\mathbf{A}_{nj}\mathbf{x}^{(j)}(t) + \mathbf{B}_{nn}\mathbf{H}_{nn}\mathbf{z}^{(n)}(t) \\
\dot{\mathbf{z}}^{(1)}(t) &= \mathbf{F}_{11}\mathbf{z}^{(1)}(t) + \mathbf{G}_1\mathbf{C}_{x1}\mathbf{x}^{(1)}(t) + \sum_{j=2}^{n}\mathbf{F}_{1j}\mathbf{C}_{zj}\mathbf{z}^{(j)}(t-\tau) \\
\dot{\mathbf{z}}^{(2)}(t) &= \mathbf{F}_{22}\mathbf{z}^{(2)}(t) + \mathbf{G}_2\mathbf{C}_{x2}\mathbf{x}^{(2)}(t) + \sum_{j=1;j\neq 2}^{n}\mathbf{F}_{2j}\mathbf{C}_{zj}\mathbf{z}^{(j)}(t-\tau) \\
&\vdots \\
\dot{\mathbf{z}}^{(n)}(t) &= \mathbf{F}_{nn}\mathbf{z}^{(n)}(t) + \mathbf{G}_n\mathbf{C}_{xn}\mathbf{x}^{(n)}(t) + \sum_{j=1}^{n-1}\mathbf{F}_{nj}\mathbf{C}_{zj}\mathbf{z}^{(j)}(t-\tau)
\end{aligned}
\tag{5.9}
$$

We have here $\bar{\dot{\mathbf{z}}}(t) = \dot{\mathbf{z}}(t) - \mathbf{R}_{ref}(t)$, for simplicity we replaced $\bar{\dot{\mathbf{z}}}(t)$ by $\dot{\mathbf{z}}(t)$. Writing (5.9) in the matrix form:

$$\begin{bmatrix} \dot{\mathbf{x}}^{(1)}(t) \\ \dot{\mathbf{x}}^{(2)}(t) \\ \vdots \\ \dot{\mathbf{x}}^{(n)}(t) \\ \dot{\mathbf{z}}^{(1)}(t) \\ \dot{\mathbf{z}}^{(2)}(t) \\ \vdots \\ \dot{\mathbf{z}}^{(n)}(t) \end{bmatrix} = \begin{bmatrix} \mathbf{A}_{11} & \mathbf{A}_{12} & \cdots & \mathbf{A}_{1n} & \mathbf{B}_{11}\mathbf{H}_{11} & \mathbf{0} & \cdots & \mathbf{0} \\ \mathbf{A}_{21} & \mathbf{A}_{22} & \cdots & \mathbf{A}_{2n} & \mathbf{0} & \mathbf{B}_{22}\mathbf{H}_{22} & \cdots & \mathbf{0} \\ \vdots & \vdots & \ddots & \vdots & \vdots & \vdots & \ddots & \vdots \\ \mathbf{A}_{n1} & \mathbf{A}_{n2} & \cdots & \mathbf{A}_{nn} & \mathbf{0} & \mathbf{0} & \cdots & \mathbf{B}_{nn}\mathbf{H}_{nn} \\ \mathbf{G}_1\mathbf{C}_{x1} & \mathbf{0} & \cdots & \mathbf{0} & \mathbf{F}_{11} & \mathbf{0} & \cdots & \mathbf{0} \\ \mathbf{0} & \mathbf{G}_2\mathbf{C}_{x2} & \cdots & \mathbf{0} & \mathbf{0} & \mathbf{F}_{22} & \vdots & \mathbf{0} \\ \vdots & \vdots & \ddots & \vdots & \vdots & \vdots & \ddots & \vdots \\ \mathbf{0} & \mathbf{0} & \cdots & \mathbf{G}_n\mathbf{C}_{xn} & \mathbf{0} & \mathbf{0} & \cdots & \mathbf{F}_{nn} \end{bmatrix} \begin{bmatrix} \mathbf{x}^{(1)}(t) \\ \mathbf{x}^{(2)}(t) \\ \vdots \\ \mathbf{x}^{(n)}(t) \\ \mathbf{z}^{(1)}(t) \\ \mathbf{z}^{(2)}(t) \\ \vdots \\ \mathbf{z}^{(n)}(t) \end{bmatrix}$$

$$+ \begin{bmatrix} \mathbf{0} & \mathbf{0} & \cdots & \mathbf{0} & \mathbf{0} & \mathbf{0} & \cdots & \mathbf{0} \\ \mathbf{0} & \mathbf{0} & \cdots & \mathbf{0} & \mathbf{0} & \mathbf{0} & \cdots & \mathbf{0} \\ \vdots & \vdots & \ddots & \vdots & \vdots & \vdots & \ddots & \vdots \\ \mathbf{0} & \mathbf{0} & \cdots & \mathbf{0} & \mathbf{0} & \mathbf{0} & \cdots & \mathbf{0} \\ \mathbf{0} & \mathbf{0} & \cdots & \mathbf{0} & \mathbf{0} & \mathbf{F}_{12}\mathbf{C}_{z2} & \cdots & \mathbf{F}_{1n}\mathbf{C}_{zn} \\ \mathbf{0} & \mathbf{0} & \cdots & \mathbf{0} & \mathbf{F}_{21}\mathbf{C}_{z1} & \mathbf{0} & \vdots & \mathbf{F}_{2n}\mathbf{C}_{zn} \\ \vdots & \vdots & \ddots & \vdots & \vdots & \vdots & \ddots & \vdots \\ \mathbf{0} & \mathbf{0} & \cdots & \mathbf{0} & \mathbf{F}_{n1}\mathbf{C}_{z1} & \mathbf{F}_{n2}\mathbf{C}_{z2} & \cdots & \mathbf{0} \end{bmatrix} \begin{bmatrix} \mathbf{x}^{(1)}(t-\tau) \\ \mathbf{x}^{(2)}(t-\tau) \\ \vdots \\ \mathbf{x}^{(n)}(t-\tau) \\ \mathbf{z}^{(1)}(t-\tau) \\ \mathbf{z}^{(2)}(t-\tau) \\ \vdots \\ \mathbf{z}^{(n)}(t-\tau) \end{bmatrix} \tag{5.10}$$

The system in (5.10) can be written as:

$$\dot{\boldsymbol{\xi}}(t) = \mathbf{A}\boldsymbol{\xi}(t) + \mathbf{BK}\boldsymbol{\xi}(t-\tau) \tag{5.11}$$

The system matrices $\mathbf{A}$ and $\mathbf{BK}$ contains the system and the controller parameters, and we are going to estimate the MADB for a given set of parameters and to find the parameters that affect the MADB. Assuming Assumption 3.1 in Chapter 3 is valid the finite difference approximation can be used for the time delay term, and the following theorem can be easily derived.

Theorem 5.1

Suppose that H 3.1 and H 3.2 hold. For system (5.5)-(5.6) with the dynamic controller of (5.7), the closed-loop system is globally asymptotically stable if

$\lambda_i(\mathbf{\Gamma}) \in \mathrm{C}^-$ for $i = 1,2,\cdots,n$ and all the state variables' 2nd order reminders are small enough for the given value of τ, where $\mathbf{\Gamma}$ is given by:

$$\mathbf{\Gamma} = \left(\mathbf{I} + \tau \begin{bmatrix} \mathbf{0} & \mathbf{0} & \cdots & \mathbf{0} & \mathbf{0} & \mathbf{0} & \cdots & \mathbf{0} \\ \mathbf{0} & \mathbf{0} & \cdots & \mathbf{0} & \mathbf{0} & \mathbf{0} & \cdots & \mathbf{0} \\ \vdots & \vdots & \ddots & \vdots & \vdots & \vdots & \ddots & \vdots \\ \mathbf{0} & \mathbf{0} & \cdots & \mathbf{0} & \mathbf{0} & \mathbf{0} & \cdots & \mathbf{0} \\ \mathbf{0} & \mathbf{0} & \cdots & \mathbf{0} & \mathbf{0} & \mathbf{F}_{12}\mathbf{C}_{z2} & \cdots & \mathbf{F}_{1n}\mathbf{C}_{zn} \\ \mathbf{0} & \mathbf{0} & \cdots & \mathbf{0} & \mathbf{F}_{21}\mathbf{C}_{z1} & \mathbf{0} & \vdots & \mathbf{F}_{2n}\mathbf{C}_{zn} \\ \vdots & \vdots & \ddots & \vdots & \vdots & \vdots & \ddots & \vdots \\ \mathbf{0} & \mathbf{0} & \cdots & \mathbf{0} & \mathbf{F}_{n1}\mathbf{C}_{z1} & \mathbf{F}_{n2}\mathbf{C}_{z2} & \cdots & \mathbf{0} \end{bmatrix} \right)^{-1} \begin{bmatrix} \mathbf{A}_{11} & \mathbf{A}_{12} & \cdots & \mathbf{A}_{1n} & \mathbf{B}_{11}\mathbf{H}_{11} & \mathbf{0} & \cdots & \mathbf{0} \\ \mathbf{A}_{21} & \mathbf{A}_{22} & \cdots & \mathbf{A}_{2n} & \mathbf{0} & \mathbf{B}_{22}\mathbf{H}_{22} & \cdots & \mathbf{0} \\ \vdots & \vdots & \ddots & \vdots & \vdots & \vdots & \ddots & \vdots \\ \mathbf{A}_{n1} & \mathbf{A}_{n2} & \cdots & \mathbf{A}_{nn} & \mathbf{0} & \mathbf{0} & \cdots & \mathbf{B}_{nn}\mathbf{H}_{nn} \\ \mathbf{G}_1\mathbf{C}_{x1} & \mathbf{0} & \cdots & \mathbf{0} & \mathbf{F}_{11} & \mathbf{0} & \cdots & \mathbf{0} \\ \mathbf{0} & \mathbf{G}_2\mathbf{C}_{x2} & \cdots & \mathbf{0} & \mathbf{0} & \mathbf{F}_{22} & \vdots & \mathbf{0} \\ \vdots & \vdots & \ddots & \vdots & \vdots & \vdots & \ddots & \vdots \\ \mathbf{0} & \mathbf{0} & \cdots & \mathbf{G}_n\mathbf{C}_{xn} & \mathbf{0} & \mathbf{0} & \cdots & \mathbf{F}_{nn} \end{bmatrix}$$

From the matrix $\mathbf{\Gamma}$, it is clear that the controller interactions and the output of the controller can greatly affect the stability of the system under time delay.

5.4 Networked Control of the Parallel DC/DC Converters with Random Time Delay Governed by Markov Chains

Under random time delay the discrete-time model must be used to study the stability of the system. Assuming that the i^{th} node will broadcast its data to all the nodes in the network, then we have;

$$\begin{aligned} &\tau_{12}(k) = \tau_{13}(k) = \cdots = \tau_{1n}(k) = \tau_1(k) \\ &\tau_{21}(k) = \tau_{23}(k) = \cdots = \tau_{2n}(k) = \tau_2(k) \\ &\qquad \vdots \\ &\tau_{n1}(k) = \tau_{n2}(k) = \cdots = \tau_{nn-1}(k) = \tau_n(k) \end{aligned} \tag{5.12}$$

Digitizing the plant and the controller described by (5-5)-(5-7), then applying the controller into the plant and using the augmentation for both the system states and the controller states we get:

$$\bar{\xi}(k+1) = \bar{\mathbf{A}}\bar{\xi}(k) + \bar{\mathbf{B}}\mathbf{K}\tilde{\mathbf{C}}_i(\tau_i(k),\cdots,\tau_n(k))\bar{\xi}(k)$$

$$= (\bar{\mathbf{A}} + \bar{\mathbf{B}}\mathbf{K}\tilde{\mathbf{C}}_i(\tau_i(k),\cdots,\tau_n(k)))\bar{\xi}(k) \tag{5.13}$$

where;

$$\tilde{\mathbf{A}} = e^{\mathbf{A}h} \qquad \tilde{\mathbf{B}} = \int_0^h e^{\mathbf{A}(h-s)}\mathbf{B}ds \quad \bar{\mathbf{A}} = \begin{bmatrix} \tilde{\mathbf{A}} & \mathbf{0} & \cdots & \mathbf{0} & \mathbf{0} \\ \mathbf{I} & \mathbf{0} & \cdots & \mathbf{0} & \mathbf{0} \\ \mathbf{0} & \mathbf{I} & \cdots & \mathbf{0} & \mathbf{0} \\ \vdots & \vdots & \ddots & \vdots & \vdots \\ \mathbf{0} & \mathbf{0} & \cdots & \mathbf{I} & \mathbf{0} \end{bmatrix} \quad \bar{\mathbf{B}} = \begin{bmatrix} \tilde{\mathbf{B}} \\ \mathbf{0} \\ \mathbf{0} \\ \vdots \\ \mathbf{0} \end{bmatrix}$$

$$\bar{\mathbf{B}} = \begin{bmatrix} \mathbf{0} & \mathbf{0} & \cdots & \mathbf{0} & \mathbf{0} & \mathbf{0} & \cdots & \mathbf{0} \\ \mathbf{0} & \mathbf{0} & \cdots & \mathbf{0} & \mathbf{0} & \mathbf{0} & \cdots & \mathbf{0} \\ \vdots & \vdots & \ddots & \vdots & \vdots & \vdots & \ddots & \vdots \\ \mathbf{0} & \mathbf{0} & \cdots & \mathbf{0} & \mathbf{0} & \mathbf{0} & \cdots & \mathbf{0} \\ \mathbf{0} & \mathbf{0} & \cdots & \mathbf{0} & \mathbf{0} & \mathbf{F}_{12} & \cdots & \mathbf{F}_{1n} \\ \mathbf{0} & \mathbf{0} & \cdots & \mathbf{0} & \mathbf{F}_{21} & \mathbf{0} & \vdots & \mathbf{F}_{2n} \\ \vdots & \vdots & \ddots & \vdots & \vdots & \vdots & \ddots & \vdots \\ \mathbf{0} & \mathbf{0} & \cdots & \mathbf{0} & \mathbf{F}_{n1} & \mathbf{F}_{n2} & \cdots & \mathbf{0} \end{bmatrix} \mathbf{K} = \begin{bmatrix} \mathbf{0} & \mathbf{0} & \cdots & \mathbf{0} & \mathbf{0} & \mathbf{0} & \cdots & \mathbf{0} \\ \mathbf{0} & \mathbf{0} & \cdots & \mathbf{0} & \mathbf{0} & \mathbf{0} & \cdots & \mathbf{0} \\ \vdots & \vdots & \ddots & \vdots & \vdots & \vdots & \ddots & \vdots \\ \mathbf{0} & \mathbf{0} & \cdots & \mathbf{0} & \mathbf{0} & \mathbf{0} & \cdots & \mathbf{0} \\ \mathbf{0} & \mathbf{0} & \cdots & \mathbf{0} & \mathbf{C}_{z1} & \mathbf{0} & \cdots & \mathbf{0} \\ \mathbf{0} & \mathbf{0} & \cdots & \mathbf{0} & \mathbf{0} & \mathbf{C}_{z2} & \vdots & \mathbf{0} \\ \vdots & \vdots & \ddots & \vdots & \vdots & \vdots & \ddots & \vdots \\ \mathbf{0} & \mathbf{0} & \cdots & \mathbf{0} & \mathbf{0} & \mathbf{0} & \cdots & \mathbf{C}_{zn} \end{bmatrix}$$

$$\tilde{\mathbf{C}}_i(\tau_i(k),\cdots,\tau_n(k)) = \begin{bmatrix} \mathbf{0} & \mathbf{0} & \cdots & \mathbf{0} & \mathbf{0} & \mathbf{0} & \cdots & \mathbf{0} \\ \mathbf{0} & \mathbf{0} & \cdots & \mathbf{0} & \mathbf{0} & \mathbf{0} & \cdots & \mathbf{0} \\ \vdots & \vdots & \ddots & \vdots & \vdots & \vdots & \ddots & \vdots \\ \mathbf{0} & \mathbf{0} & \cdots & \mathbf{0} & \mathbf{0} & \mathbf{0} & \cdots & \mathbf{0} \\ \mathbf{0} & \mathbf{0} & \cdots & \mathbf{0} & \mathbf{C}_1(\tau_1(k)) & \mathbf{0} & \cdots & \mathbf{0} \\ \mathbf{0} & \mathbf{0} & \cdots & \mathbf{0} & \mathbf{0} & \mathbf{C}_2(\tau_2(k)) & \vdots & \mathbf{0} \\ \vdots & \vdots & \ddots & \vdots & \vdots & \vdots & \ddots & \vdots \\ \mathbf{0} & \mathbf{0} & \cdots & \mathbf{0} & \mathbf{0} & \mathbf{0} & \cdots & \mathbf{C}_n(\tau_n(k)) \end{bmatrix}$$

$\mathbf{C}_i(\tau_i(k)) = \begin{bmatrix} \mathbf{0} & \cdots & \mathbf{0} & \mathbf{I} & \mathbf{0} & \cdots & \mathbf{0} \end{bmatrix}$ has all the elements zero except the $\tau_i(k)^{\text{th}}$ is the identity matrix and h is the sampling period. The system in (5.13) is a generalized DTMJLS where it is assumed that all the controllers communicate over the network, but in

the master-slave control strategy only the master controller communicates with the slaves' controllers. The system in (5.13) is an *n* mode DTMJLS that can be written as:

$$\mathbf{x}(k+1) = \mathbf{A}(r(k))\mathbf{x}(k) \tag{5.14}$$

Using the design method in Chapter 4 the controller parameters can be selected to achieve the stochastic stability of the system in the presence of random time delay governed by Markov Chain.

5.5 Case Study: Three Parallel DC/DC Converters

The system consists of three DC/DC Buck converters connected in parallel. One of the converters is the master, and the others are the slaves. The mater contains the voltage controller which generates the current reference signal, which is then sent through the network to the other slaves' current controllers. The state vectors and control inputs are chosen as:

$$\mathbf{x}^{(1)} = \begin{bmatrix} i_{L1} & v \end{bmatrix}^T \; \mathbf{x}^{(2)} = \begin{bmatrix} i_{L2} \end{bmatrix} \mathbf{x}^{(3)} = \begin{bmatrix} i_{L3} \end{bmatrix} \mathbf{u}^{(1)} = \delta_1 \; \mathbf{u}^{(2)} = \delta_2 \; \mathbf{u}^{(3)} = \delta_3$$

Since the voltage controller is in the master converter, the voltage is used to be one of the master states. The system model matrices are given by;

$$\mathbf{A}_{11} = \begin{bmatrix} \dfrac{-r_{L1}}{L_1} & \dfrac{-1}{L_1} \\ \dfrac{1}{C_1 + C_2 + C_3} & \dfrac{-1}{R(C_1 + C_2 + C_3)} \end{bmatrix} \mathbf{A}_{12} = \mathbf{A}_{13} = \begin{bmatrix} 0 \\ \dfrac{1}{C_1 + C_2 + C_3} \end{bmatrix} \mathbf{A}_{21} = \begin{bmatrix} 0 & \dfrac{-1}{L_2} \end{bmatrix}$$

$$\mathbf{A}_{22} = \begin{bmatrix} \dfrac{-r_{L2}}{L_2} \end{bmatrix} \mathbf{A}_{23} = \mathbf{A}_{32} = \begin{bmatrix} 0 \end{bmatrix} \mathbf{A}_{31} = \begin{bmatrix} 0 & \dfrac{-1}{L_3} \end{bmatrix} \mathbf{A}_{33} = \begin{bmatrix} \dfrac{-r_{L3}}{L_3} \end{bmatrix} \mathbf{B}_1 = \begin{bmatrix} \dfrac{V_{in}}{L_1} \\ 0 \end{bmatrix} \mathbf{B}_2 = \begin{bmatrix} \dfrac{V_{in}}{L_2} \end{bmatrix}$$

$$\mathbf{B}_3 = \begin{bmatrix} \dfrac{V_{in}}{L_3} \end{bmatrix} \mathbf{C}_{x1} = \begin{bmatrix} 1 & 0 \\ 0 & 1 \end{bmatrix} \mathbf{C}_{x3} = \mathbf{C}_{x3} = \begin{bmatrix} 1 \end{bmatrix}$$

Combining both the voltage and the current controller, the master controller state is: $\mathbf{z}^{(1)} = \begin{bmatrix} z_1^{(1)} & z_2^{(1)} & z_3^{(1)} & z_4^{(1)} \end{bmatrix}$ and the slaves current controllers for the second and third converters are chosen as: $\mathbf{z}^{(2)} = \begin{bmatrix} z_1^{(2)} & z_2^{(2)} \end{bmatrix}$ and $\mathbf{z}^{(3)} = \begin{bmatrix} z_1^{(3)} & z_2^{(3)} \end{bmatrix}$. The matrices of the master voltage controller, master current controller and the current controllers for the slaves are given by;

$$\mathbf{G}_1 = \begin{bmatrix} 0 & -k \\ 0 & 0 \\ -1 & 0 \\ 0 & 0 \end{bmatrix} \quad \mathbf{G}_2 = \mathbf{G}_3 = \begin{bmatrix} -1 \\ 0 \end{bmatrix} \quad \mathbf{F}_{11} = \begin{bmatrix} -\omega_{pv} & 0 & 0 & 0 \\ 1 & 0 & 0 & 0 \\ K_v & K_v\omega_{zv} & -\omega_{p1} & 0 \\ 0 & 0 & 1 & 0 \end{bmatrix} \quad \mathbf{F}_{22} = \begin{bmatrix} -\omega_{p2} & 0 \\ 1 & 0 \end{bmatrix}$$

$$\mathbf{F}_{33} = \begin{bmatrix} -\omega_{p3} & 0 \\ 1 & 0 \end{bmatrix} \quad \mathbf{F}_{21} = \mathbf{F}_{31} = \begin{bmatrix} 1 \\ 0 \end{bmatrix} \qquad \mathbf{F}_{12} = \mathbf{F}_{13} = \begin{bmatrix} 0 \\ 0 \\ 0 \\ 0 \end{bmatrix} \quad \mathbf{F}_{23} = \mathbf{F}_{32} = \begin{bmatrix} 0 \\ 0 \end{bmatrix}$$

$$\mathbf{H}_1 = \begin{bmatrix} 0 & 0 & K_1 & K_1\omega_{z1} \end{bmatrix} \qquad \mathbf{H}_2 = \begin{bmatrix} K_2 & K_2\omega_{z2} \end{bmatrix} \quad \mathbf{H}_3 = \begin{bmatrix} K_3 & K_3\omega_{z3} \end{bmatrix}$$

$$\mathbf{C}_{z1} = \begin{bmatrix} K_v & K_v\omega_{zv} & 0 & 0 \end{bmatrix} \qquad \mathbf{C}_{z2} = \begin{bmatrix} 0 & 0 \end{bmatrix} \qquad \mathbf{C}_{z3} = \begin{bmatrix} 0 & 0 \end{bmatrix}$$

where k is the output voltage feedback gain, K_v is the voltage controller gain, ω_{zv} and ω_{pv} are the zero and the pole of the voltage controller, ω_{p1}, ω_{p2} and ω_{p3} are the poles of the master and the slaves current controllers respectively, ω_{z1}, ω_{z2} and ω_{z3} are the zeros of the master and the slaves current respectively K_1, K_2 and K_3 are the current controller gains of the master and the slave current controllers, V_m is the amplitude of the pulse width modulator signal. The simulation study has been conducted using the Mat-lab/SimPowerSystem Toolbox, and the models used in the simulation are the original nonlinear models. The Simulink implementation of the three parallel DC/DC Buck con-verters is shown in Figure 5.5.

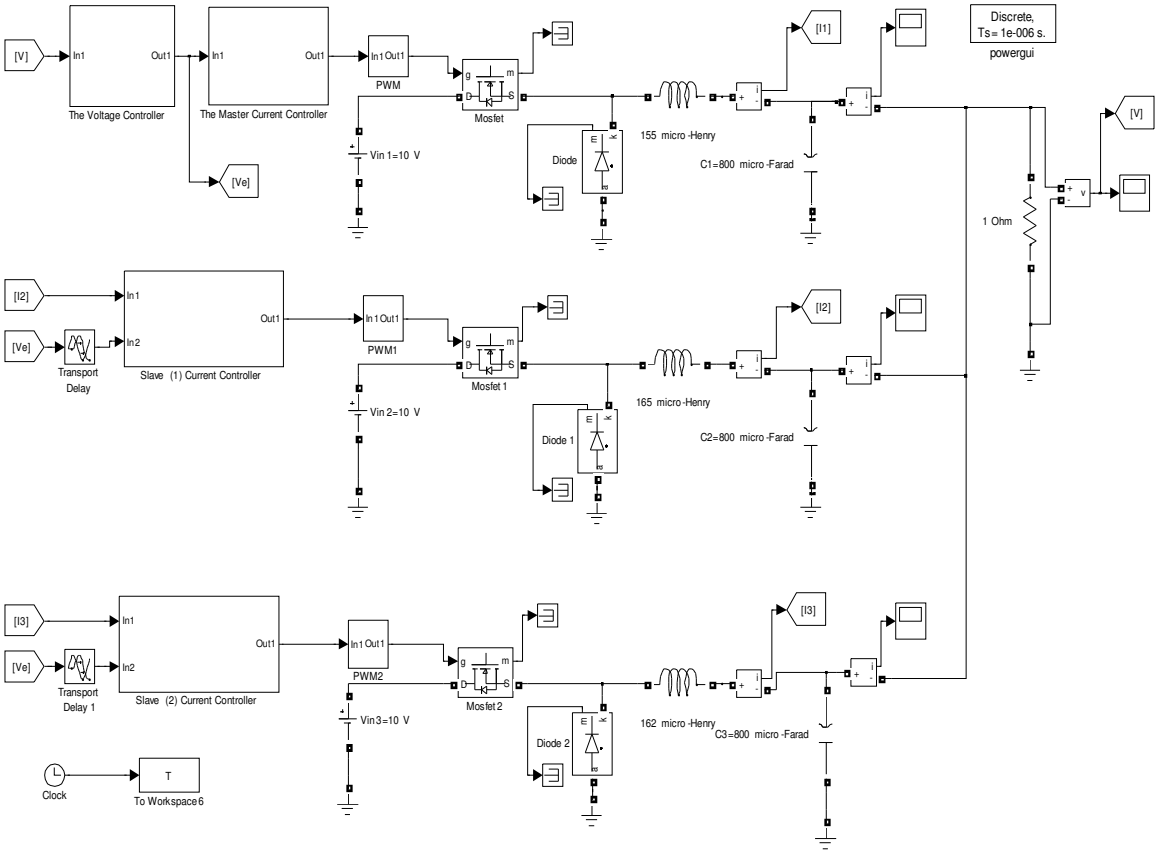

Figure 5.5 The Simulink implementation of the parallel DC/DC converters

5.5.1 Networked control of parallel DC/DC buck converter with the constant time delay model:

In control networks, the time delay in many cases can be constant or varied but bounded. In this case, the constant time delay assumptions made in Chapter 3 can be used. The system parameters are $L_1 = 155\mu H$, $L_3 = L_2 = 165\mu H$, $C_3 = C_2 = C_1 = 800\mu F$, $R = 1\Omega$ and $V_{in} = 10V$. The pulse-width modulator (PWM) uses a triangle signal with 4 V amplitude and 10 KHz switching frequency. The voltage controller has to regulate the output voltage at 5 V while shaping the frequency response to achieve a fast response to the change in the load or the input voltage, the voltage controller parameters are: $K_v = 50$,

$\omega_{zv} = 500 \quad rad \cdot s^{-1} \quad \omega_{pv} = 10 \quad Krad \cdot s^{-1}$. The current controllers parameters are:

$K_1 = K_2 = K_3 = 400$, $\omega_{z1} = \omega_{z2} = \omega_{z3} = 1000 \quad rad \cdot s^{-1}$, $\omega_{p1} = \omega_{p2} = \omega_{p3} = 10 \quad Krad \cdot s^{-1}$.

Using Theorem 5.1 the MADB is estimated as 14.1 ms. The output voltage of the system for different values of time delay is shown in Figure 5.6. The system is still stable even with 15 ms time delay, which means the results of Theorem 5.1 are still conservative. In addition, the master and slaves' currents with zero time delay are shown in Figure 5.7, which shows that the current controller achieved the current sharing between the parallel converters. Corollary 3.1 can give us a simple direct relation between the voltage controller gain and the MADB for the system as:

$$\|\mathbf{BK}\| = \sqrt{2K_v^2\omega_{z1}^2} = K_v\omega_{z1}\sqrt{2} \text{ so } \tau < 1/(K_v\omega_{z1}\sqrt{2}).$$

This relation shows that the MADB decreases with increasing the voltage controller gain.

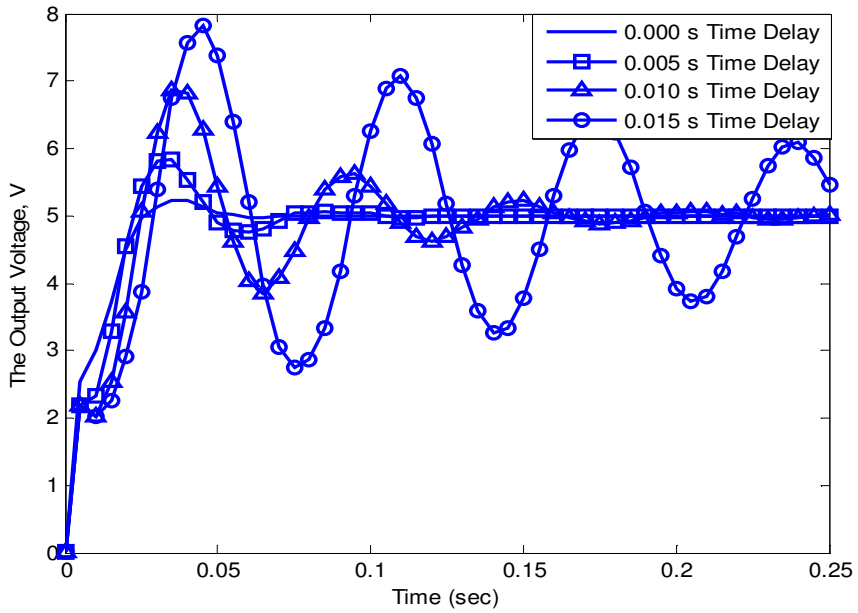

Figure 5.6 The output voltage with different values of time delay

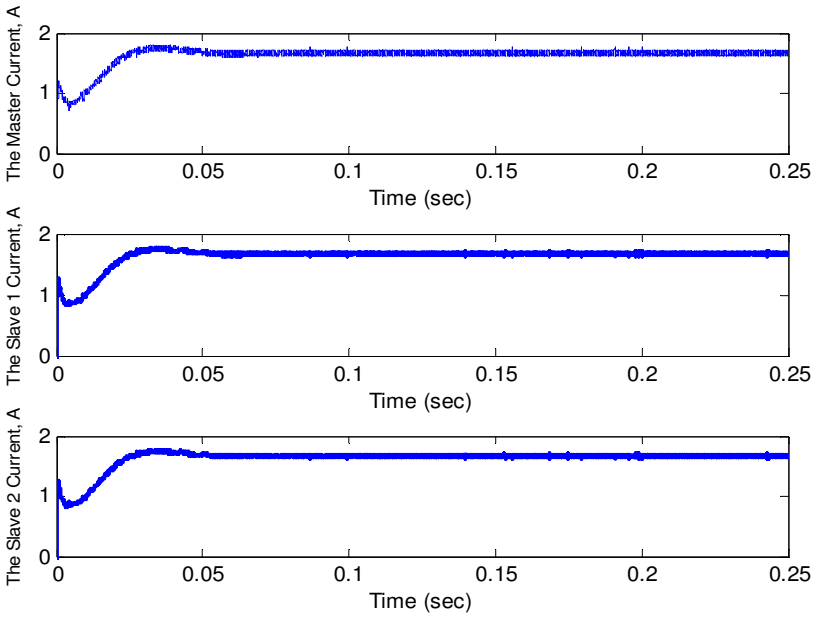

Figure 5.7 The master, slave (1) and slave (2) currents

From Figure 5.6 it can be seen that the system can be maintained stable when the time delay is within the estimated boundary range although the system dynamic performance is very much affected while the time delay is increased. Furthermore, the time delay estimated sufficiently ensures the system stability. As it can be seen from Figure 5.7 the current is shared equally between the converters but with increasing the time delay, we noticed that the slave converters will supply most of the current during the transient. The presence of the time delay in the reference current signals makes the slave converter slowly track the current reference signal.

As we have pointed out that the main feature in the proposed method is its simplicity. In the following, we compare our proposed method with one of the methods used in the literature. In (Mazumder et al. 2008a) the authors consider the problem of controlling parallel DC/DC converters system through an RF communication link where the time delay is assumed to be constant. The authors in (Mazumder et al. 2008a) use the following stability

method, which is given in (Gu et al. 2003), to study the stability of the system with the presence of time delay. For comparison, the theorem in (Gu et al. 2003) is summarized as follows;

Theorem 5.2: (Gu et al. 2003)

For the system (5.11) stable at $\tau_d = 0$, i.e., $\mathbf{A}+\mathbf{BK}$ is stable and $rank(\mathbf{BK}) = q$, we define

$$\bar{\tau}_i := \begin{cases} \min\limits_{1\le k\le n} \dfrac{\theta_k^i}{\omega_k^i}, & \textbf{if} \quad \lambda_i(j\omega_k^i I - \mathbf{A}, \mathbf{BK}) = e^{-j\theta_k^i} \\ & for \quad some \quad \omega_k^i \in (0,\infty), \theta_k^i \in [0, 2\pi] \\ \infty, & \underline{\rho}(j\omega I - \mathbf{A}, \mathbf{BK}) > 1 \quad \forall \omega \in (0,\infty) \end{cases} \tag{5.15}$$

Then $\bar{\tau} := \min_{1\le i\le q} \bar{\tau}_i$, and the system in (5.11) is stable for all $\tau_d \in [0, \bar{\tau})$ and becomes unstable at $\tau_d = \bar{\tau}$. We have $\underline{\rho}(\mathbf{A}, \mathbf{BK}) := \min\{|\lambda| \det(\mathbf{A} - \lambda\mathbf{BK}) = 0\}$, and $\lambda(\mathbf{A}, \mathbf{BK})$ is the generalized eigenvalue of the matrices $\mathbf{A}$ and $\mathbf{BK}$. The authors in (Mazumder et al. 2008a) use the following algorithm to find the maximum allowable time delay bound;

- First check if the system is time delay independent or not by checking the following condition

  $\underline{\rho}(j\omega I - \mathbf{A}, \mathbf{BK}) > 1 \quad \forall \omega \in (0,\infty)$

- If the above condition is satisfied, then the system is stable independent of the time delay, and if it is not satisfied for some value of ω, then they use this value of ω and solve $\lambda_i(j\omega I - \mathbf{A}, \mathbf{BK}) = e^{-j\theta}$ for θ and then (5.15) is used to calculate the corresponding time delay.

Using the data of the system given in (Mazumderet al. 2008a) for the three parallel DC/DC buck converter system, we have only one nonzero generalized eigenvalue:

$$\underline{\rho}(j\omega\mathbf{I}-\mathbf{A},\mathbf{BK}) := \min\{\lambda \| \det(j\omega\mathbf{I}-\mathbf{A}-\lambda\mathbf{BK})=0\}$$

We sweep ω from 0 to ∞ to find the value of ω that makes $\underline{\rho}(j\omega\mathbf{I}-\mathbf{A},\mathbf{BK}) \approx 1$, then we solve $\lambda_i(j\omega\mathbf{I}-\mathbf{A},\mathbf{BK}) = e^{-j\theta}$ for θ. For $\overline{K}_v = 3000$, sweeping ω from 0 to ∞ we find that $\underline{\rho}(j\omega\mathbf{I}-\mathbf{A},\mathbf{BK}) \approx 1$ at $\omega = 97.6$, and solving $\lambda_i(j\omega\mathbf{I}-\mathbf{A},\mathbf{BK}) = e^{-j\theta}$, we have $\lambda_i(j\omega\mathbf{I}-\mathbf{A},\mathbf{BK}) = 0.4220 - j0.9085$ then;

$$\lambda_i(j\omega\mathbf{I}-\mathbf{A},\mathbf{BK}) = 0.4220 - j0.9085 = 1.0017e^{-j1.1359} = e^{-j\theta} \rightarrow \theta = 1.1359$$

$$\tau_d = \frac{1.1359}{97.6} = 0.0116 = 11.6 \quad \text{ms}$$

Using Theorem 5.1 the maximum allowable time delay is 11 ms. The MADB verses the voltage controller gain with our method and the method in (Mazumder et al. 2008a) is shown in Figure 5.8. The good agreement between the two methods is extremely clear, especially at lower values for the MADB and this is because at very low values of the MADB, the truncation error in the finite difference approximation becomes very small and can be neglected.

Then the influences of the system and controller parameters onto the MADB are studied in this chapter. The system parameters are the values of the inductances, capacitances, and loads in addition to the voltage and current controllers' parameters. We found that the voltage controller parameters which are the output voltage feedback gain, *k*, the voltage con-

troller gain K_v and the load resistance all affect the MADB greatly as shown in Figures 5.9-5.15.

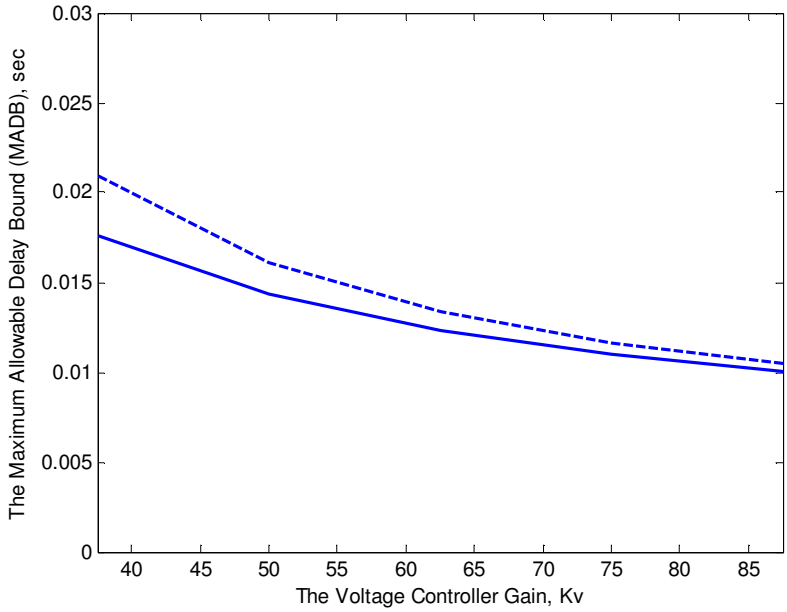

Figure 5.8 The Maximum allowable delay bound verses the voltage controller gain: dashed-line: the method in (Gu et al. 2003), solid-line: the proposed method

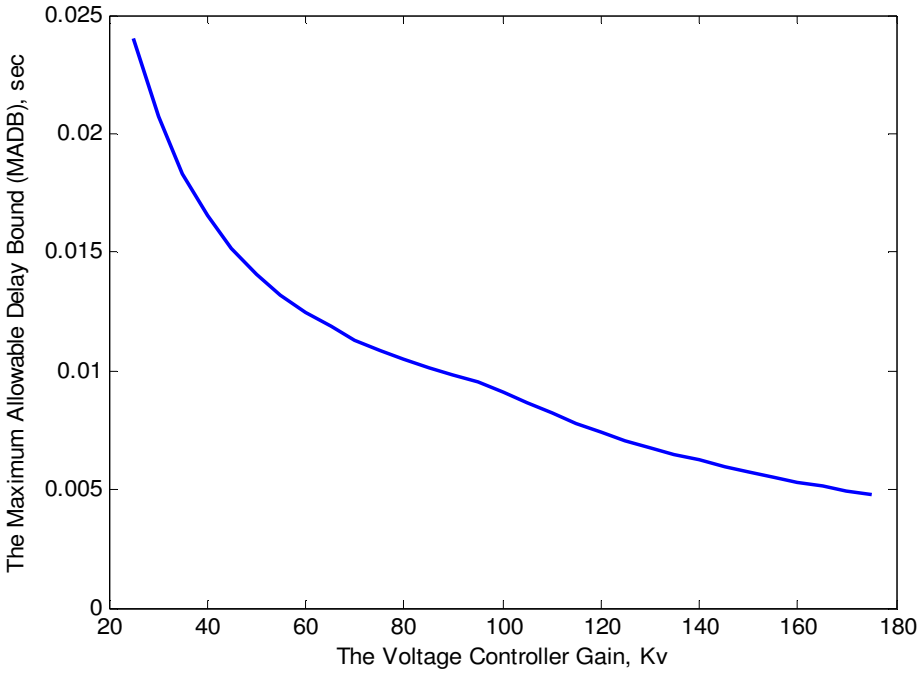

Figure 5.9 The MADB for different values of the voltage controller gain

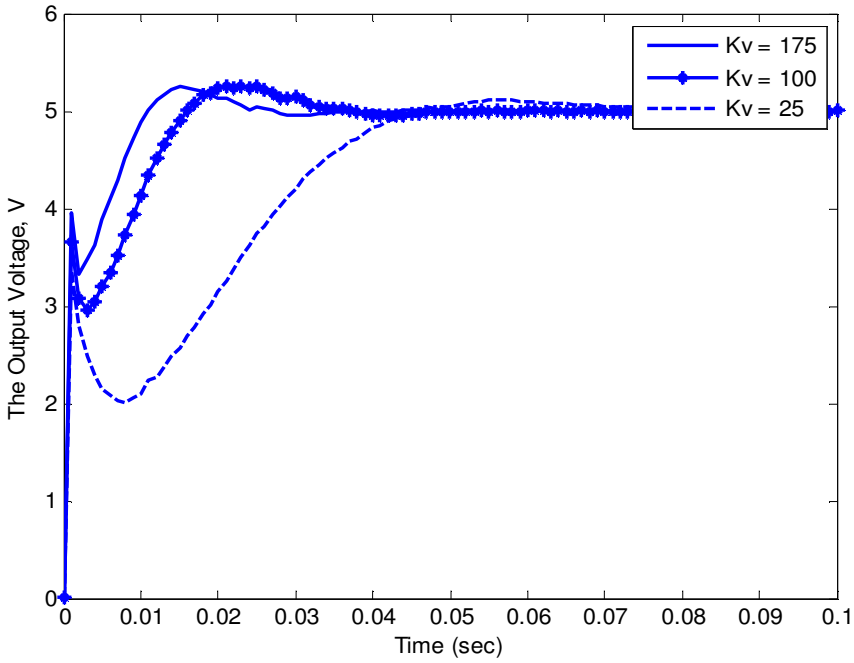

Figure 5.10 The Output Voltage Response with different voltage gains,

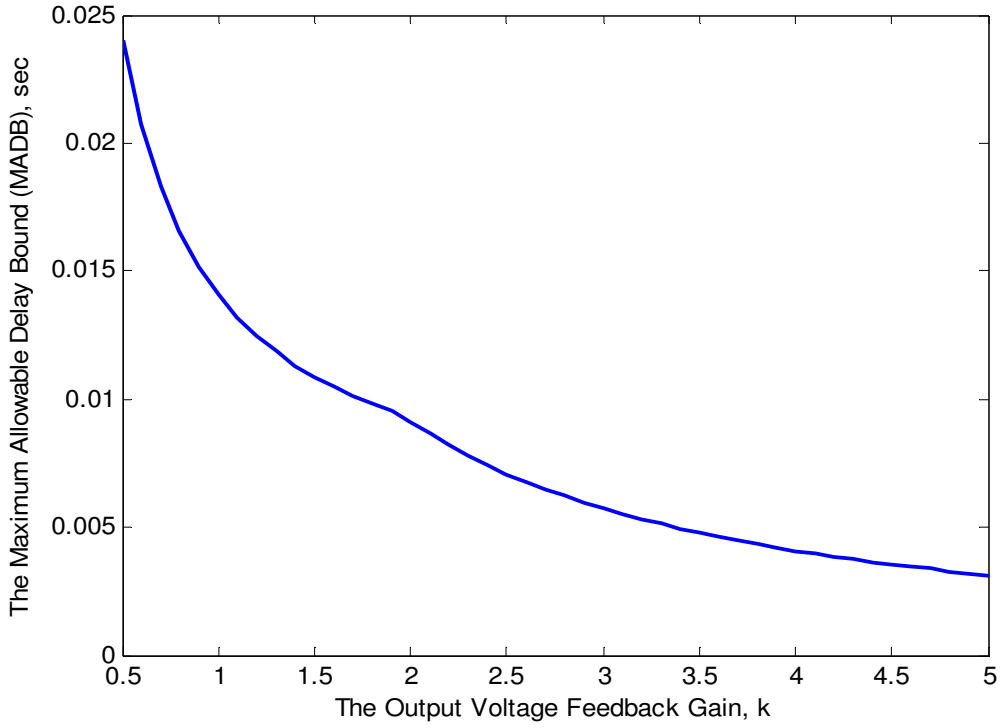

Figure 5.11 The MADB for different values of the output voltage feedback factor *k*

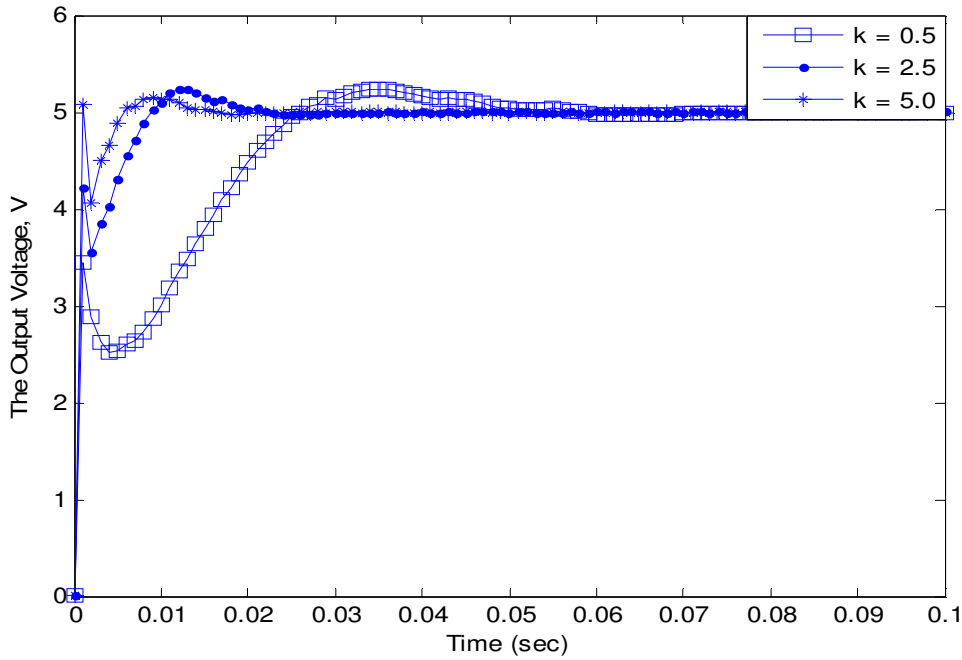

Figure 5.12 The Output Voltage Responses with different values of the output voltage feedback factors, *k*

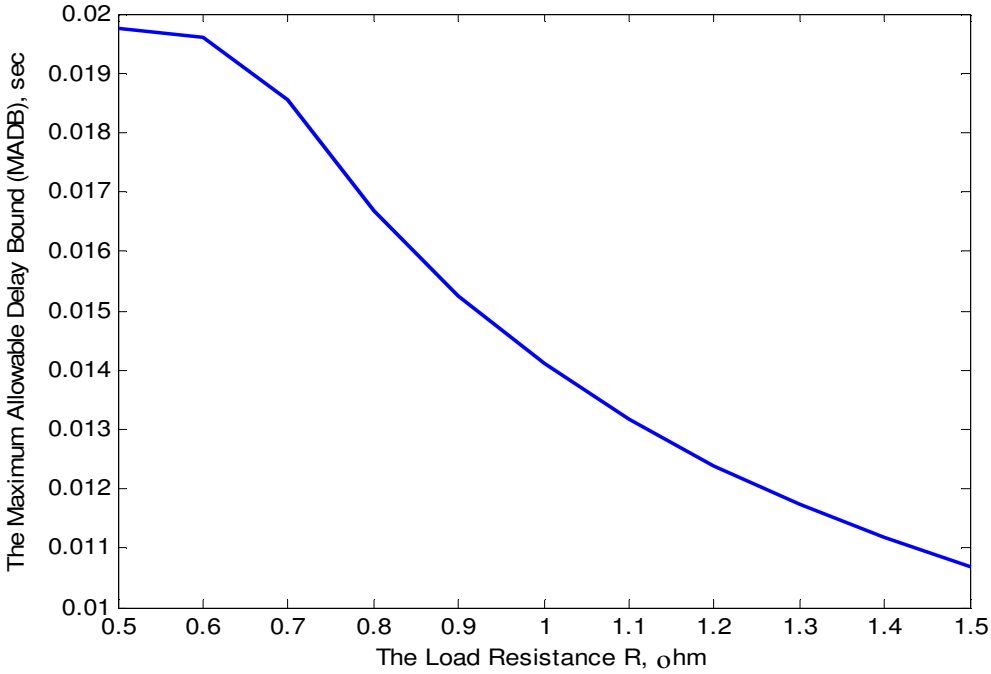

Figure 5.13 The MADB for different values of the load resistance

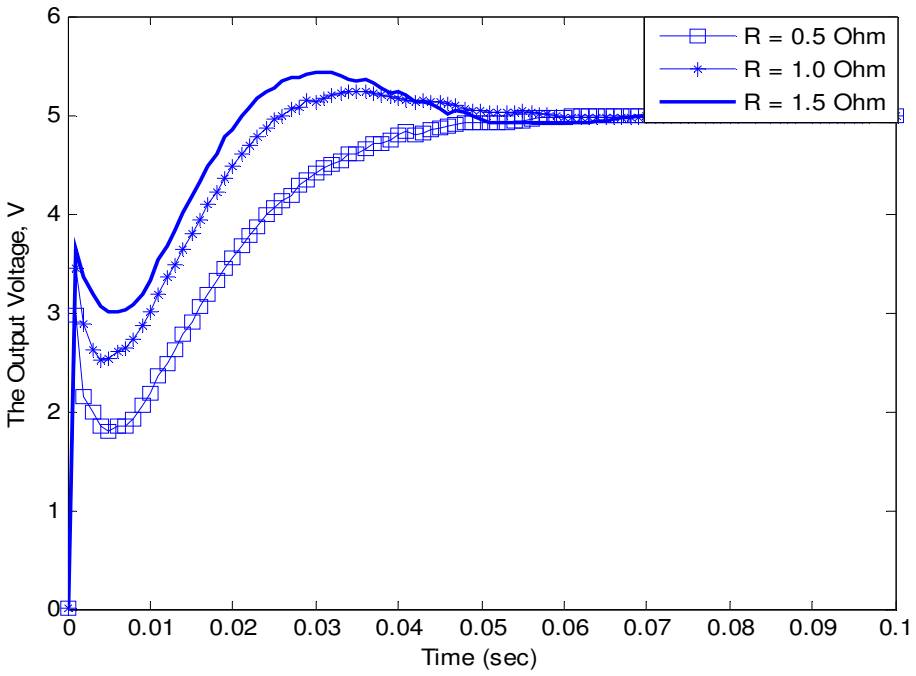

Figure 5.14 The Output Voltage Responses with different values of resistances

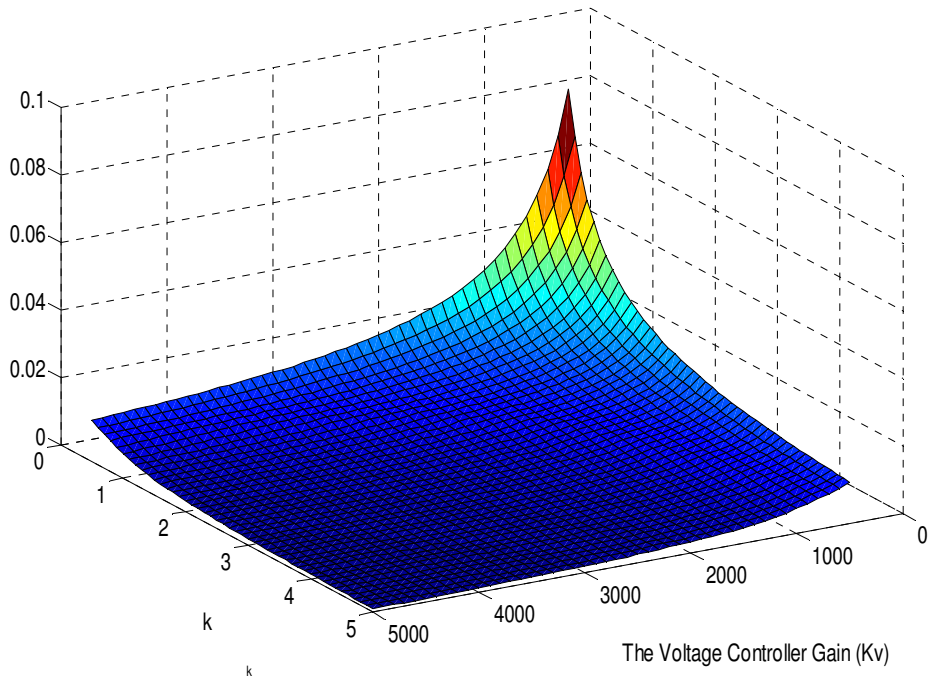

Figure 5.15 The MADB as function of the output voltage feedback gain, k, and the voltage controller K_v

It is also found that the MADB is less dependent on the other system parameters such as the current controllers' parameters. The voltage controller gain and the output voltage feedback gain are very important parameters in the controller design, and the MADB decreases with increasing the voltage controller gain or the output voltage feedback gain. Increasing the output voltage feedback gain makes the system response faster and hence the required MADB will be lower.

For a deterministic network such as the CAN, the method can give us a guideline tool for assigning the priority and control tasks on the network. On the other hand, when the activities on the network are random, the time delay will be random and the jump linear system approach can be adapted to design a stochastic stabilizing controller for the system. This analysis can help the engineers to determine the range of parameter choices when the network time delay is known.

5.5.2 Networked Control with Constant Time Delay

In many cases, the time delay can be constant, varied, or random but bounded as we have seen in Chapter 2. In these cases, the worst-case time delay (maximum network time delay) can be used as a designing guide. In the networks with low load, the time delay is either constant or varied but bounded. The first case study is the CAN with seven nodes where the system node, which is the master controller, has a middle priority in the network as shown in Figure 5.16. The time delay in the CAN with low load is shown in Figure 5.17. In this case only the system node occupies the CAN bus.

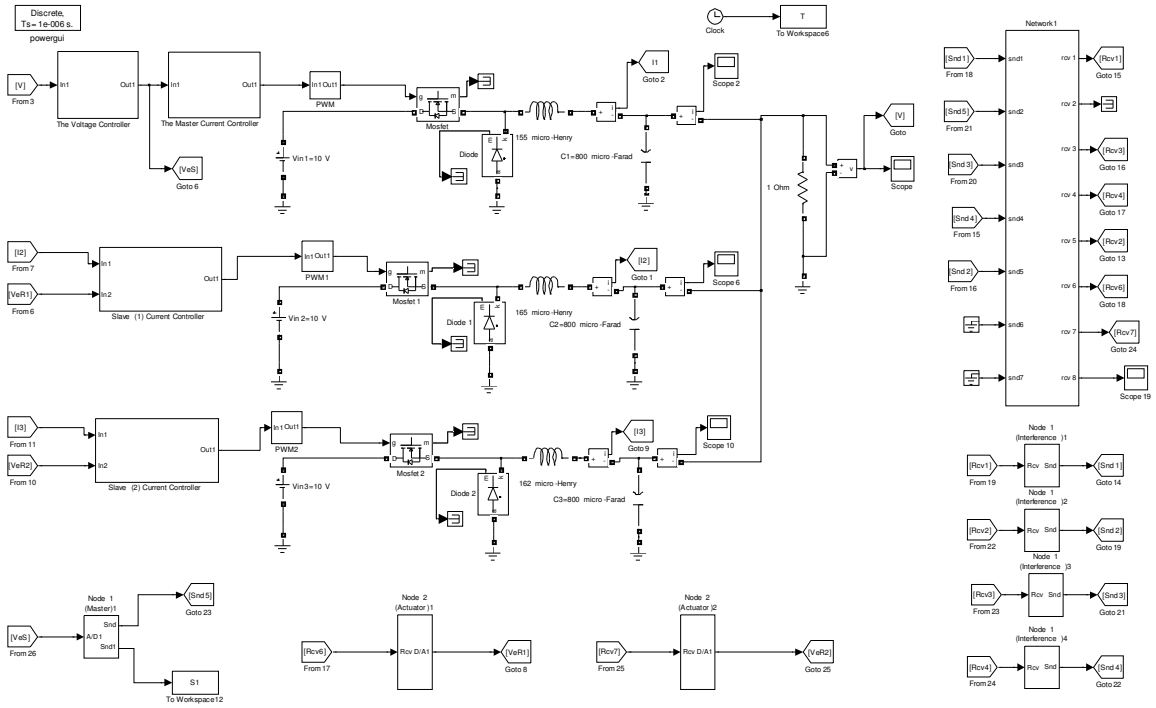

Figure 5.16 The parallel DC/DC converters controlled over CAN bus

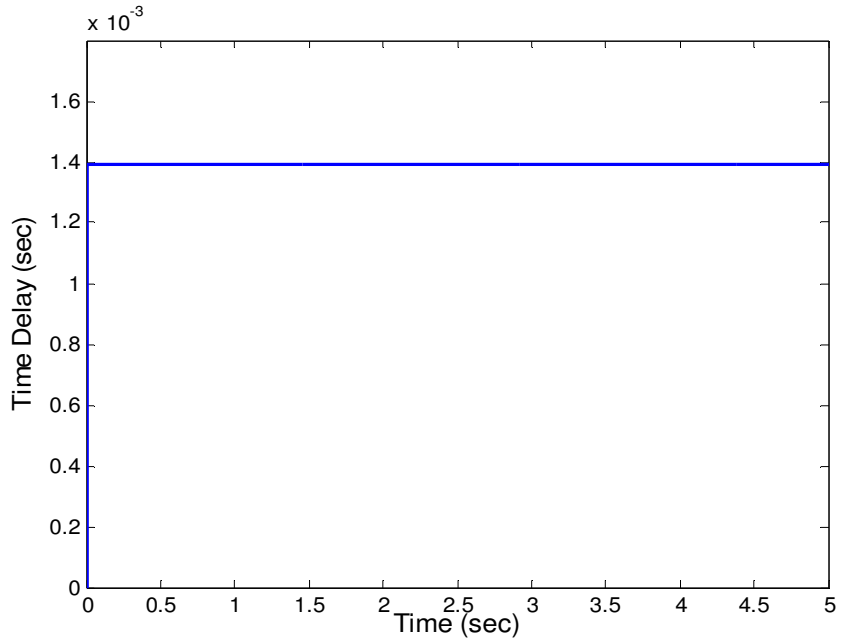

Figure 5.17 The time delay in CAN with low load

The bit rate in the network is 100 kbit/s and the message length is 128 bits. Under low load conditions, the waiting time delay is zero, and the time delay will have only a transmission time delay component, which is 1.28 ms in addition to 0.1 ms analogue to digital conversion time delay. Sampling the system with 0.01 s, the total delay becomes 11.28 ms. As it can be seen from Figure 5.17, the time delay is constant. For our system to be stable using Theorem 5.1 the voltage controller should be less than 70 because the MADB with $K_v = 70$ is estimated to be 11.5 ms. The output voltage of the system with $K_v = 70$ is shown in Figure 5.18. The master reference current generated at the master node and the reference current signal received at the slaves nodes are shown in Figure 5.19.

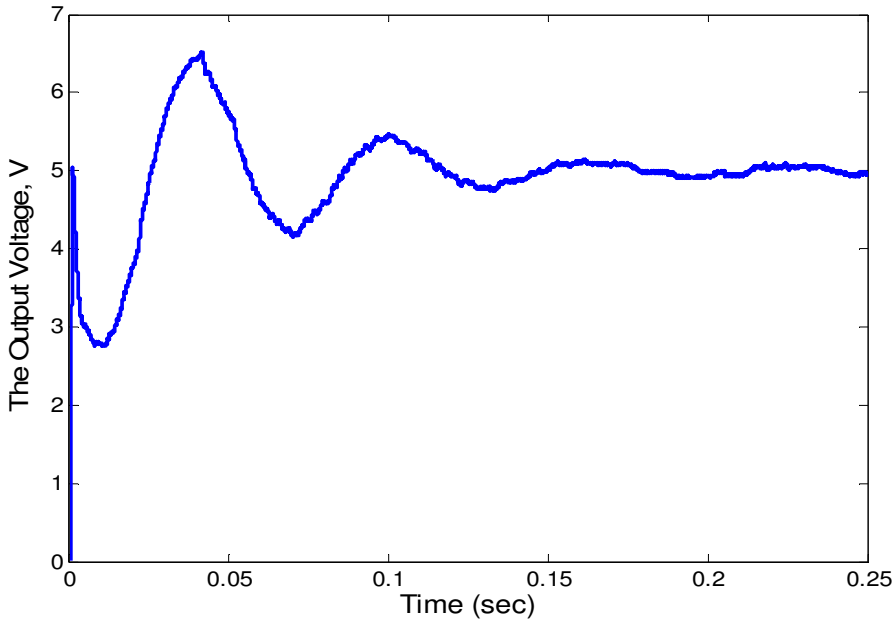

Figure 5.18 The output Voltage of the system under low load CAN

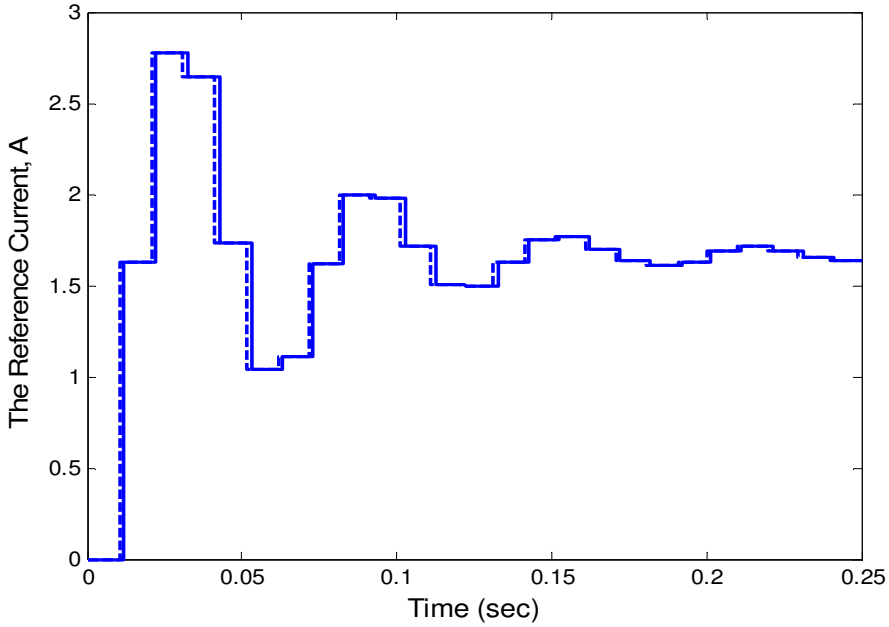

Figure 5.19 (dashed line): The master reference current at the sending node, (solid line): The reference current signal at the slave node.

5.5.3 Networked Control with Periodic Time Delay

When all the activities on the network are periodic over a deterministic control network, the time delay is expected to be periodic. In this case, all the nodes communicate over the CAN bus with periodic messages. The system node has middle priority among the other nodes as shown in Figure 5.16. The time delay is expected to be periodic as shown in Figure 5.20.

The CAN has seven nodes with 100 kbits/s bit rate. The length of the system node message is 128 bits, and the period of the load messages is 0.01 s, while the system node uses 5 ms sampling period. The network utilization is given by:

$$U_T = \frac{5 \cdot 128/100000}{0.01} + \frac{128/100000}{0.005} = 0.8960$$

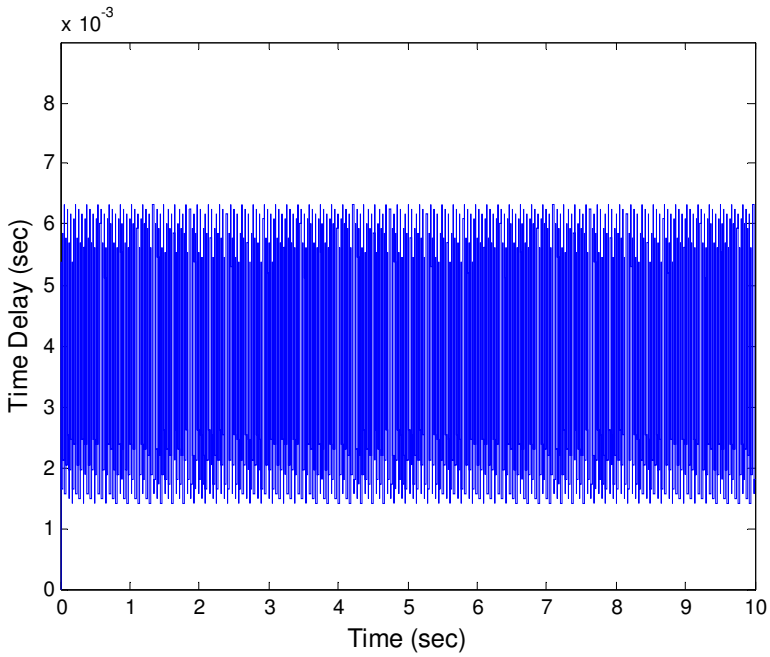

Figure 5.20 The time delay with periodic messages in the CAN

Although the network is approximately loaded the time delay is periodic and bounded. The time delay is periodic with minimum value equals 1.28 ms, and maximum value of 6.3 ms. The minimum time delay occurs when the network is idle, and it involves only the network transmission time delay. On the other hand, the worst-case time delay occurs when the system node just starts to send the data; the higher-priority node is already waiting for ongoing message to finish transmission. With $K_v = 125$ the MADB is 7.3 ms, and this controller will guarantee the system stability when it is controlled over this network because the MADB is larger than the worst-case time delay. The output voltage response with $K_v = 125$ and the reference currents at the master and the slave nodes are shown in Figure 5.21 and Figure 5.22.

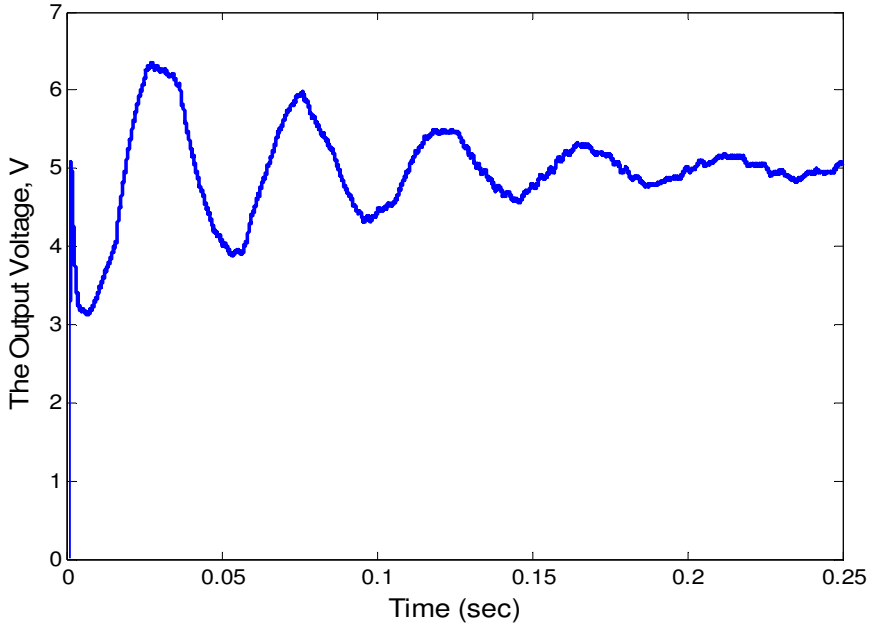

Figure 5.21 The output voltage of the system under low load CAN

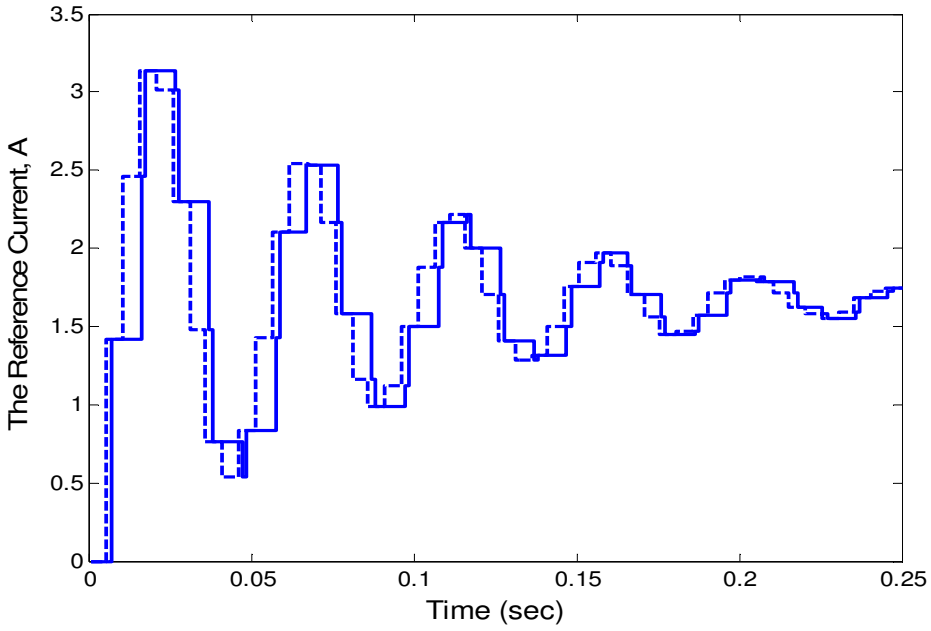

Figure 5.22 (dashed line): The master reference current at the sending node, (solid line): the reference current signal at the slave node.

As can be seen from Figure 5.22 the reference current signals are received with periodic time delay. The controller voltage is fixed in our case, and a switching controller can be used to improve the performance of the system when the messages are time stamped.

5.5.4 Networked Control with Independent Random Time Delay

In this case, the time delay is random but independent, which means there is no correlation between the previous, current and next time delay. In this case, we have the Ethernet with seventeen nodes and the speed of the network is the 10 Mbit/s standard speed. The Ethernet uses non deterministic protocol, and the time delay is expected to be random under medium load. The Simulink implementation of the parallel DC/DC buck converters controlled over Ethernet is shown in Figure 5.23 and Figure 5.24.

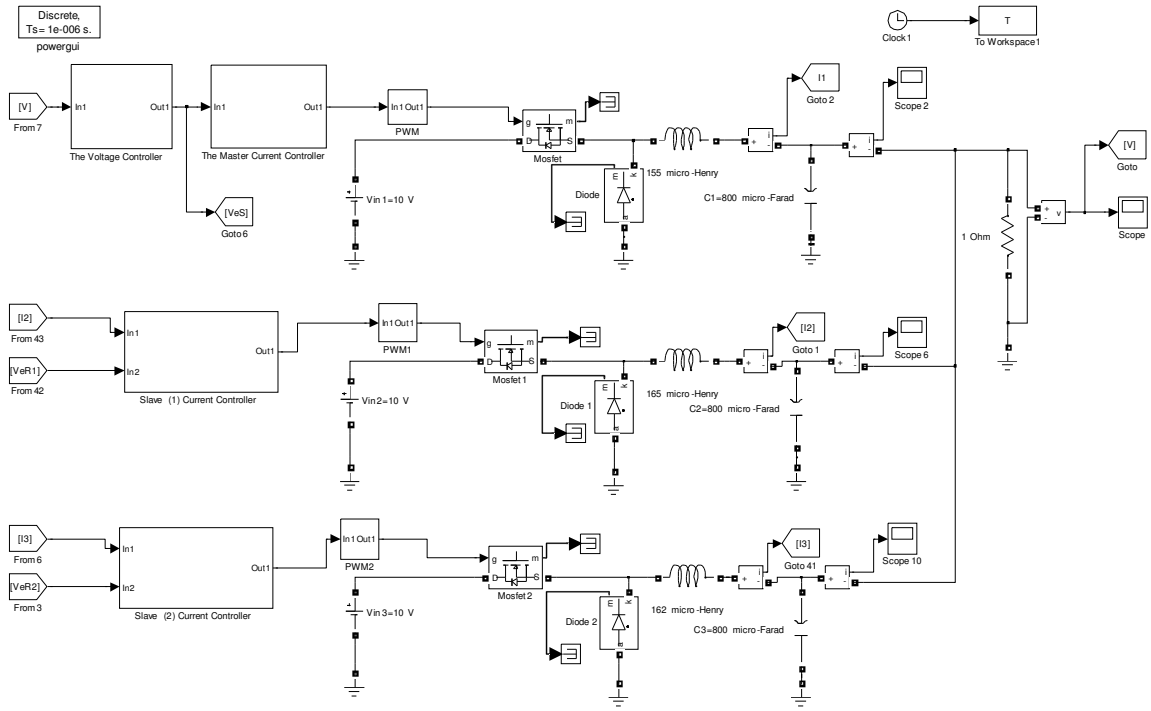

Figure 5.23 The Parallel DC/DC buck converter system controlled over Ethernet

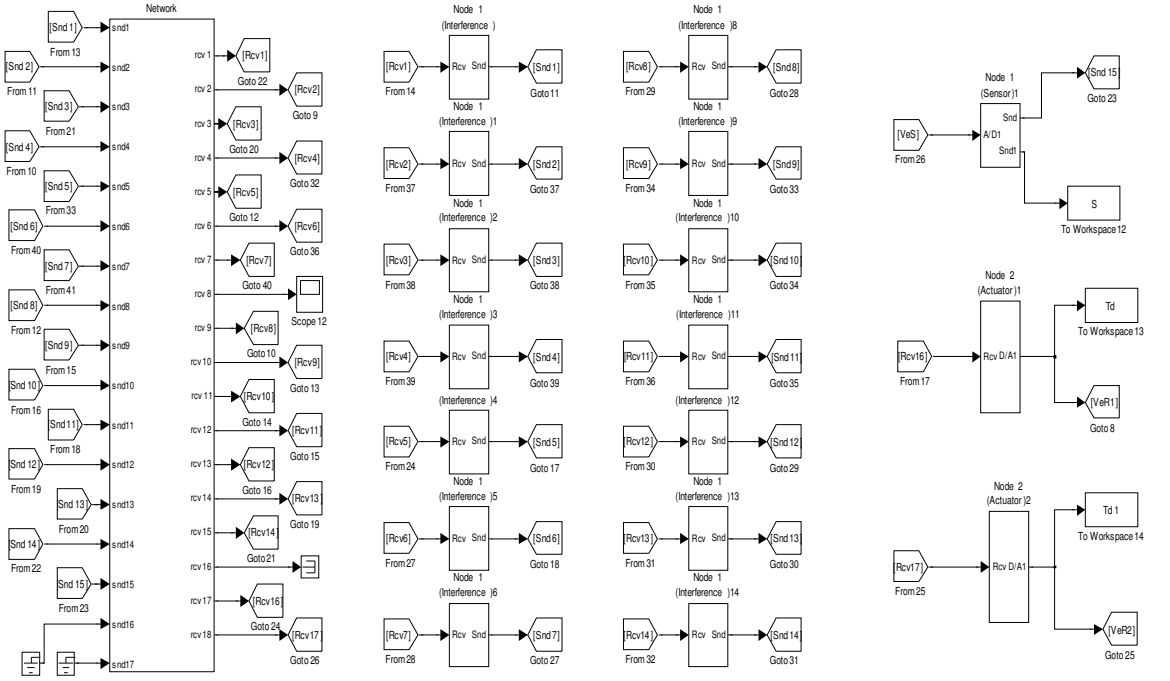

Figure 5.24 The Ethernet with seventeen nodes

The size of the load messages is 1526 bytes with 0.03 s period to simulate a data network. Even with the periodic messages the time delay is random as shown in Figure 5.25, and this because of the non deterministic protocol implemented by the Ethernet. The probability distribution function is shown in Figure 5.26, and it is observed that most of the time delays are less than 2 ms. The master controller sends the reference current with minimum Ethernet message size, which is 576 bits. The utilization is given by:

$$U_T = \frac{14 \cdot 1526 \cdot 8 / 10000000}{0.03} + \frac{72 \cdot 8 / 10000000}{0.005} = 0.5812$$

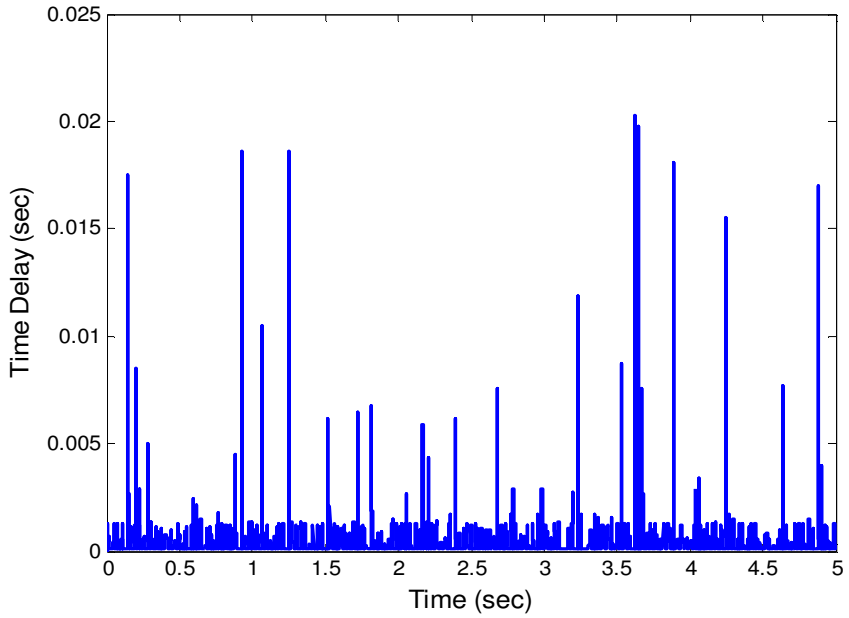

Figure 5.25 The time delay in the Ethernet with seventeen nodes

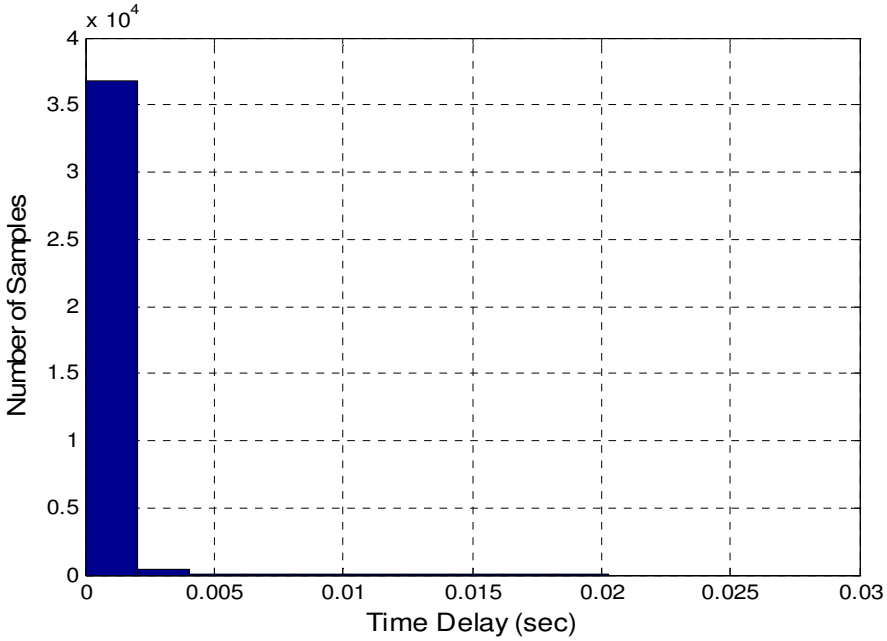

Figure 5.26 The probability distribution function of the time delay in Figure 5.25

The time delay is random and bounded by 20 ms as can be seen from Figure 5.26. Another interesting property in Figure 5.26 is that most of the time delays are under 2 ms with

bursts at higher time delays. The worst-case time delay is 20 ms using Theorem 5.1 and selecting $K_v = 25$ the MADB is 24.3 ms, which is larger than the worst-case time delay. The output voltage response of the system with $K_v = 25$ controlled over the Ethernet is shown in Figure 5.27. The received reference current signal and the master reference current signal are shown in Figure 5.28. When the Ethernet is loaded the time delay may be unbounded, and this is because of the increased number of collisions and the unfairness in the Ethernet protocol.

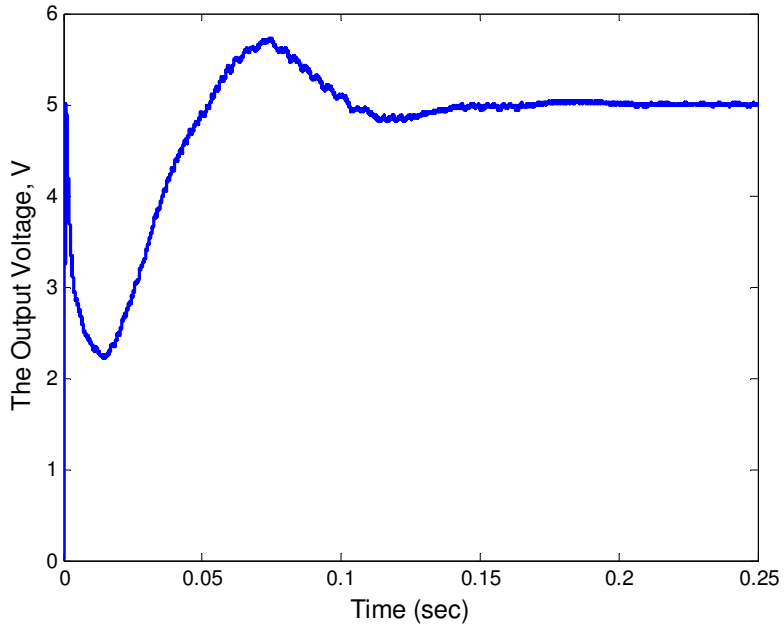

Figure 5.27 The output Voltage of the system controlled over the Ethernet

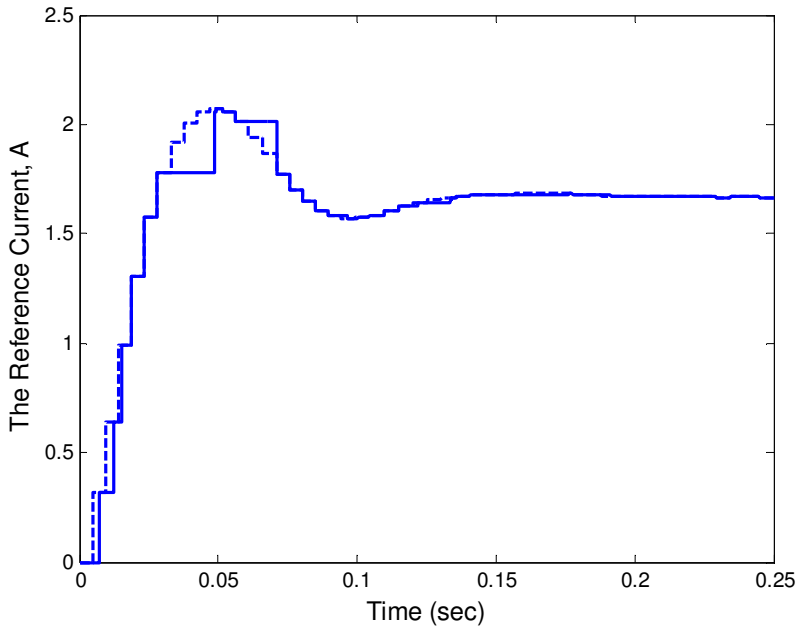

Figure 5.28 (dashed line): The master reference current at the sending node, (solid line): the reference current signal at the slave node

5.5.5 Networked Control with Random Time Delay Governed by Markov Chain:

From the analysis with the constant time delay, we found that the parameters that affect the time delay are the output voltage feedback gain, k, the voltage controller gain, K_v, and the load resistance, R. Practically, the parameter that we will use to design a stabilizing controller is the voltage controller gain. When the random time delay is governed by Markov Chain and there is only one way of transferring the data from the master controller to the slaves' controllers the system in (5.14) becomes one mode DTMJLS. Assuming that the time delay has the following transition probability:

$$P = \begin{bmatrix} 0.5 & 0.5 & 0 \\ 0.3 & 0.6 & 0.1 \\ 0.3 & 0.6 & 0.1 \end{bmatrix}$$

Since we have only one variable to be varied, we can use the method developed in Chapter 4 to find the range of K_v that guarantees the stochastic stability of the system for the given transition probability matrix. The random time delay specified by the transition probability is shown in Figure 5.29.

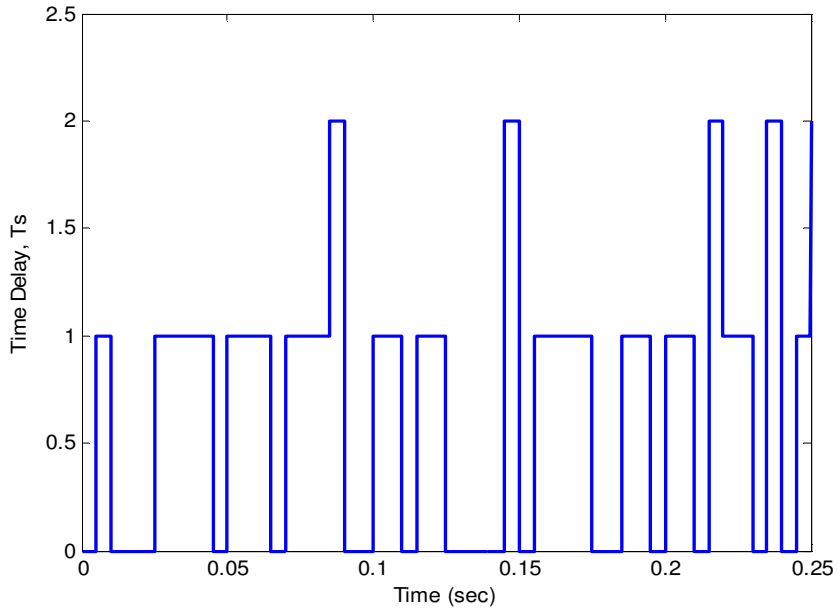

Figure 5.29 The random time delay between the master controller and the slaves controller

The sampling time is chosen to be $T_s = 0.005 \cdot s$. After solving the feasibility problem (Section 4.5.1), with the given transition probability the system is stochastically stable with $K_v = 125$. Under constant time delay with $K_v = 125$, using Theorem 5.1 the MADB is 7.3 ms. The random time delay jumps from 0 ms to 5 ms to 10 ms, which represents a network with different three states. As we can see from the results of Theorem 5.1, the system is unstable with 10 ms constant time delay, although the system is stochastically stable. From this we conclude that the stability of every mode is not necessary for the stochastic stability of the system. The output voltage of the system with the random time delay and $K_v = 125$

is shown in Figure 5.30. The reference current at the master controller and the received reference current signals are shown in Figure 5.31.

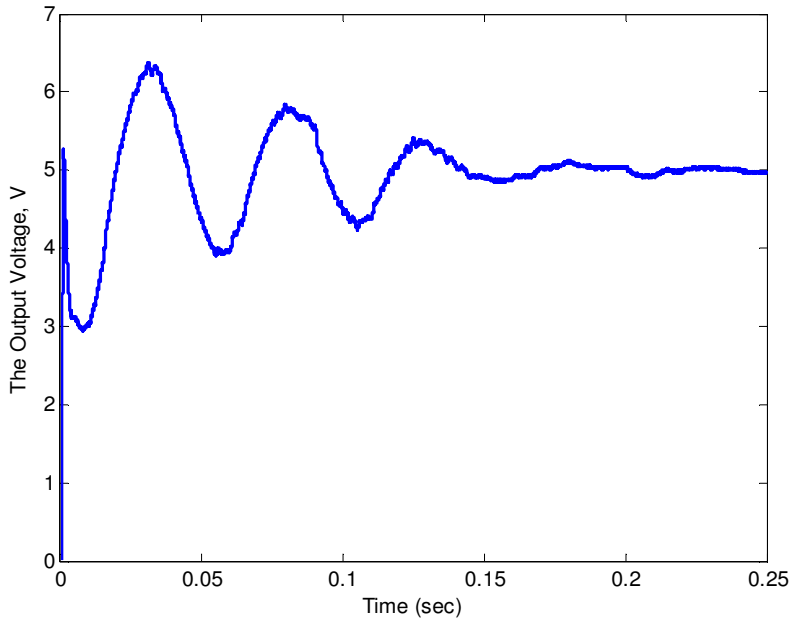

Figure 5.30 The output voltage with random time delay and $K_v = 125$.

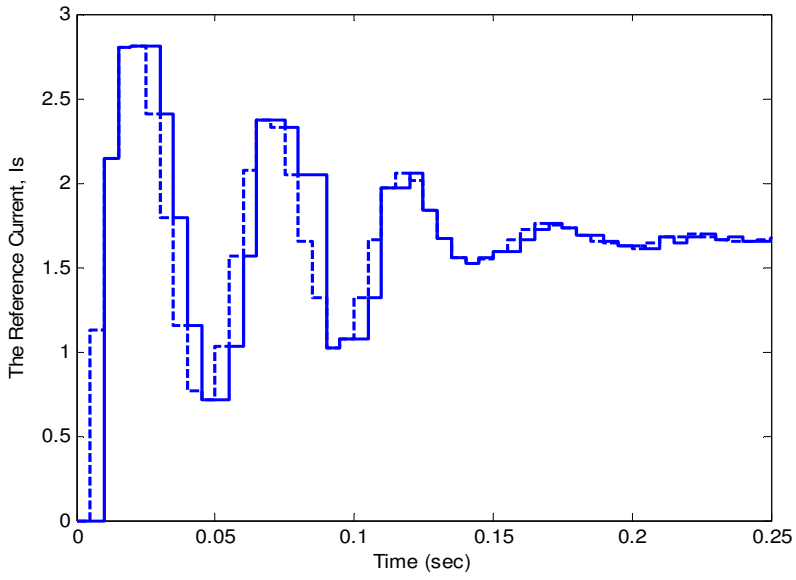

Figure 5.31 (dashed line): The master reference current at the sending node, (solid line): the reference current signal at the slave node.

With $K_v = 125$ and different transition probability with high probability of longer time delays given as:

$$P = \begin{bmatrix} 0.5 & 0.5 & 0 \\ 0.1 & 0.4 & 0.5 \\ 0.1 & 0.4 & 0.5 \end{bmatrix}$$

Solving the feasibility problem in Chapter 4 the system is stochastically unstable. The random time delay and the system output voltage with $K_v = 125$ are shown in Figure 5.32 and Figure 5.33.

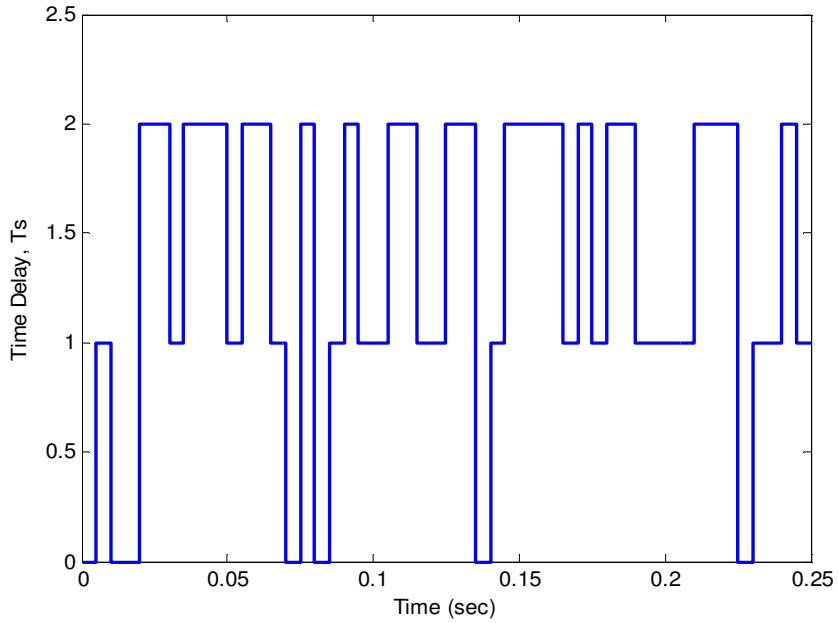

Figure 5.32 The random time delay between the master controller and the slaves controller

Using the TrueTime 1.5 simulator in this last example the master node has middle priority on the CAN bus as shown in Figure 5.16 and the load messages in the network are random with 0.01 s period. The time delay from the master to the slaves is shown in Figure 5.34.

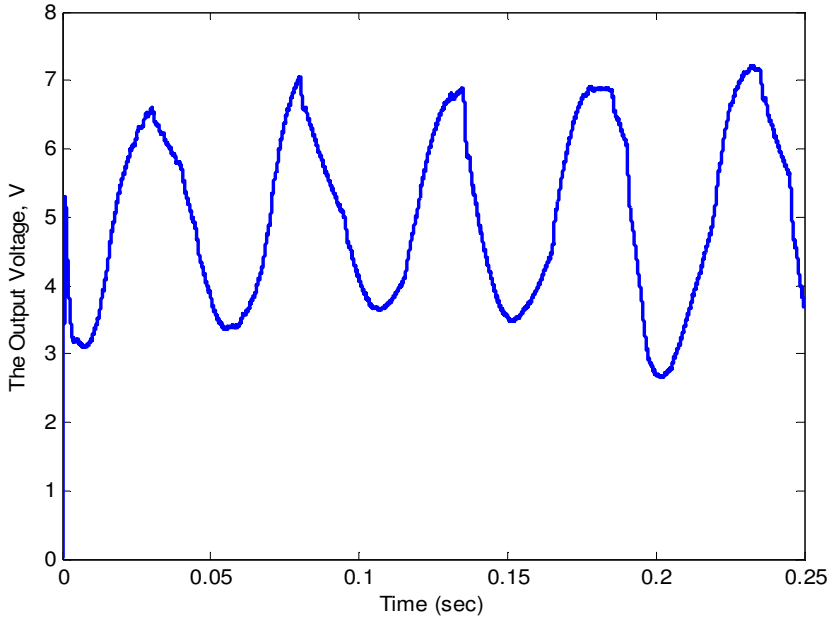

Figure 5.33 The output voltage with random time delay and $K_v = 125$.

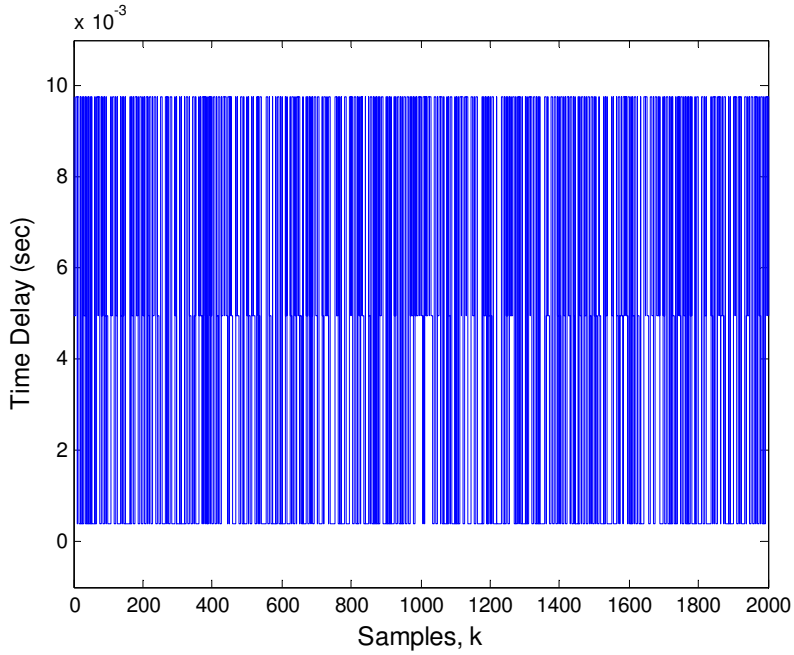

Figure 5.34 The time delay from the master controller to the slaves controllers

As can be seen from Figure 5.34 the time delay has three values 0.1 ms, 5 ms and 9.8 ms, which represents the three different states of the network. From the time delay analysis, it

can be noticed that there is a correlation between these different three states. The histogram of the time delay in Figure 5.34 is shown in Figure 5.35.

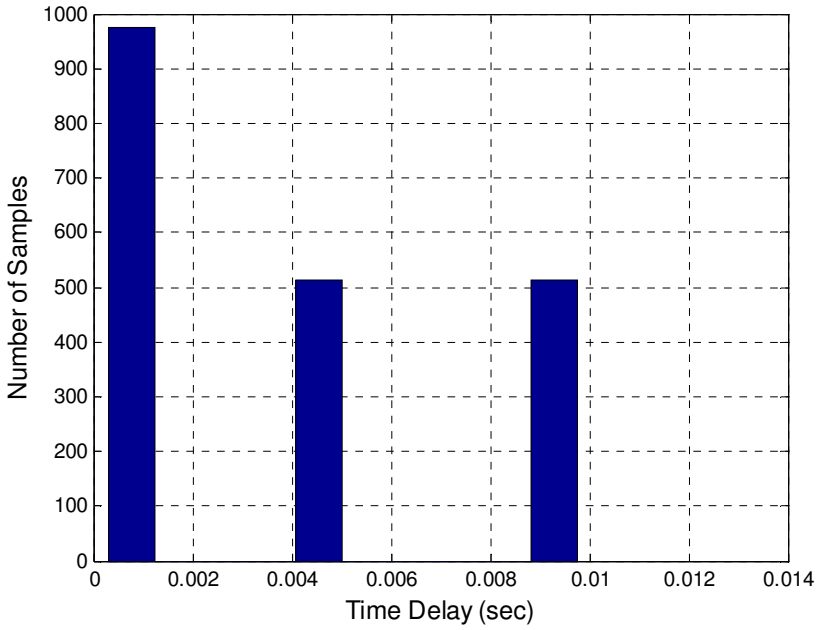

Figure 5.35 The histogram of the time delay in Figure 5.34

The histogram shows that the time delay has discrete jumps between these three different values in a random fashion governed by Markov Chain. Many simulations carried out to estimate the correlation between these three different values. The resulting probability transition matrix is given as:

$$P = \begin{bmatrix} 0.7505 & 0 & 0.2495 \\ 0.4746 & 0 & 0.5254 \\ 0 & 1 & 0 \end{bmatrix}$$

This probability transition matrix represents the model of the time delay in this network. Using the Matlab, we can generate the random time delay governed by Markov Chain with the given transition probability matrix. The modelled random time delay is shown in Fig-

ure 5.36. A comparison has been made between the time delay induced in the network by the TrueTime 1.5 simulator and the time delay generated by the model represented by the transition probability matrix. The histogram of the induced network time delay and the histogram of the time delay generated by the transition probability matrix are shown in Figure 5.37.

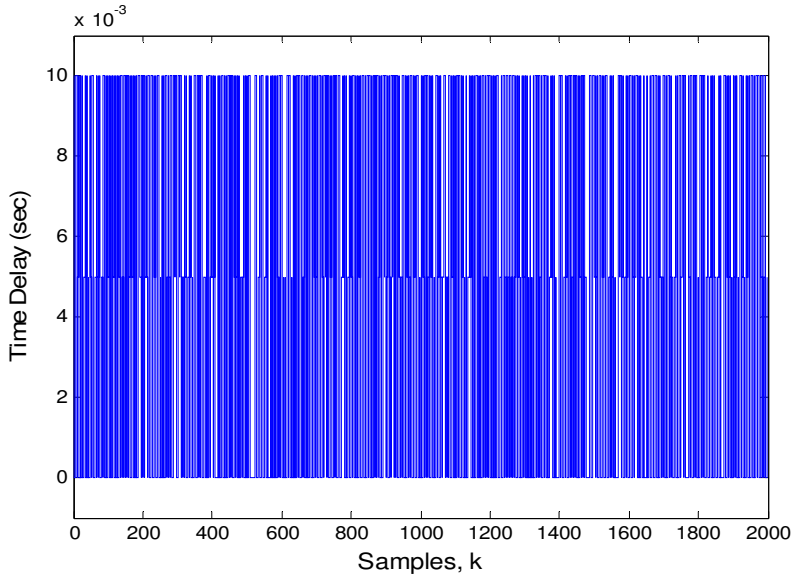

Figure 5.36 The random time delay generated by the transition probability, *P*

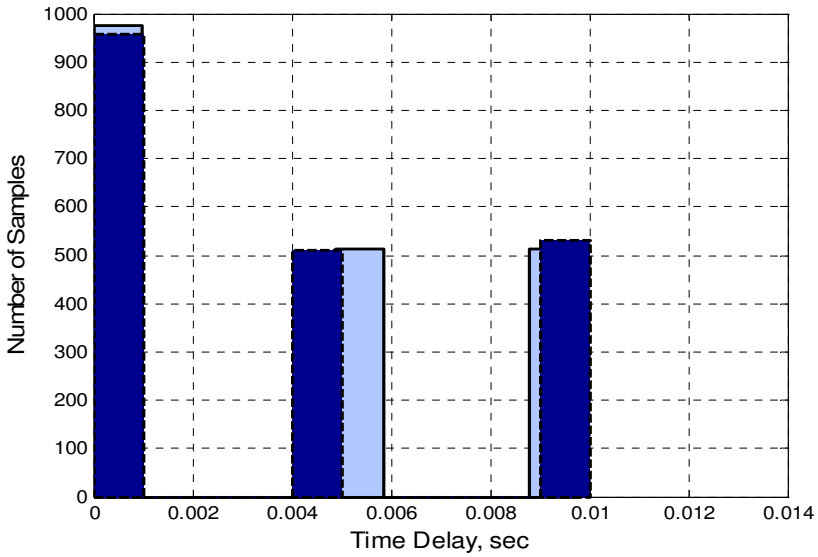

Figure 5.37 The histogram of the network time delay generated by the TrueTime 1.5 simulator and the modelled random time delay

The good agreement between the induced time delay in the network and the modelled time delay by Markov Chain is very clear in Figure 5.37. With the given transition probability and with $K_v = 250$ and $k = 5$, solving the feasibility problem in Chapter 4 we found that the system is stochastically unstable. The voltage response when the system is controlled over CAN with random load and with $K_v = 250$ and $k = 5$ is shown in Figure 5.38 which clearly proves that the system is stochastically unstable. Solving the feasibility problem with $K_v = 225$ and $k = 2$ the solution is feasible and the system is stochastically stable. The response of the output voltage of the system controlled over the CAN with $K_v = 225$ and $k = 2$ is shown in Figure 5.39.

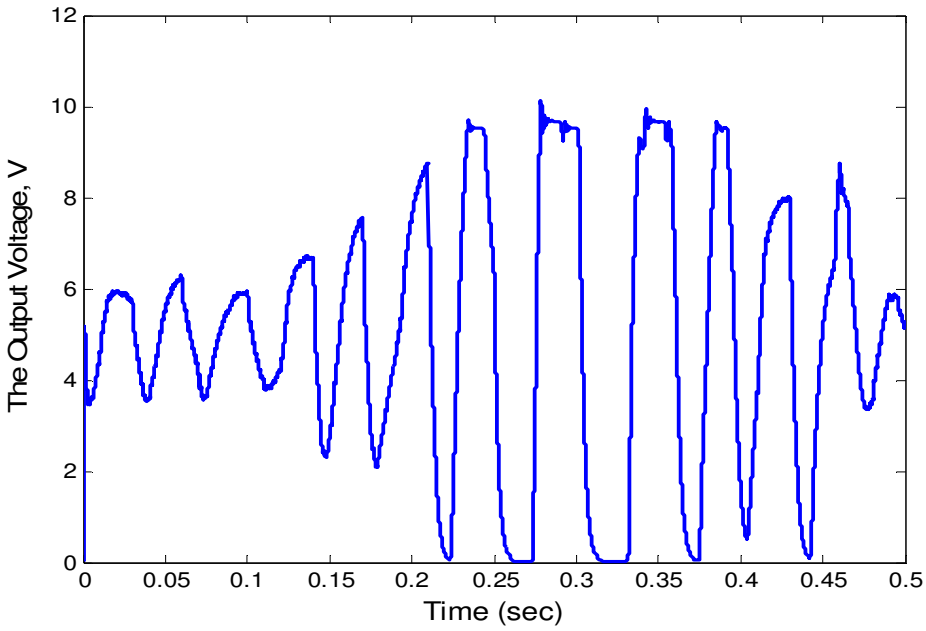

Figure 5.38 The output voltage of the system with $K_v = 250$ and $k = 5$

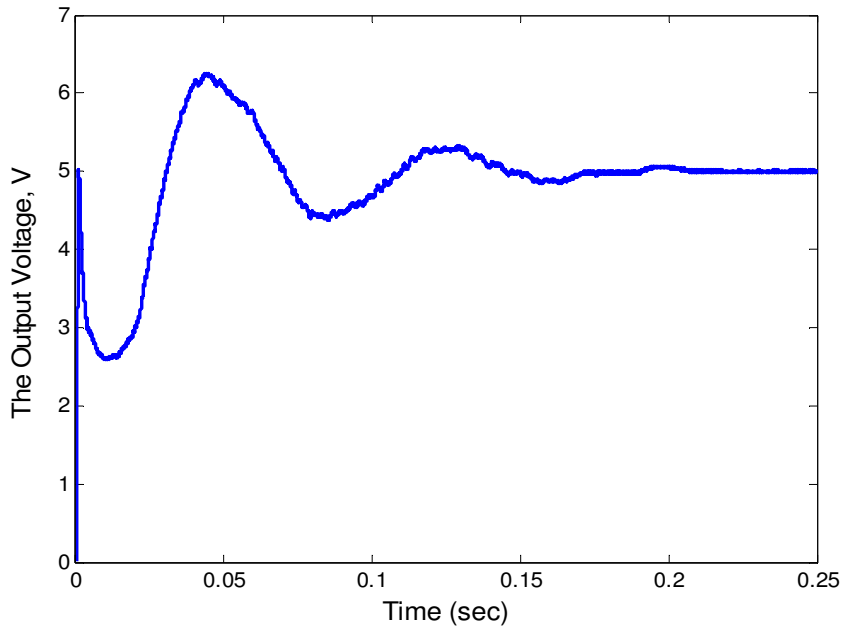

Figure 5.39 The output voltage of the system with $K_v = 225$ and $k = 2$

With $K_v = 225$ and $k = 2$, the MADB using Theorem 5.1 is 3.8 ms and the system is stochastically stable even with 5 ms and 10 ms random time delay. We can choose $K_v < 85$ and $k <= 1$ and the MADB will be 10.1 ms, which will guarantee the stability of the system. Using the proposed theorem, we can select the controller parameters to have MADB larger than the worst-case time delay which is simpler and takes less time than the Markovian jump system approach. For example, solving the feasibility problem for the parallel DC/DC converters system took more than half an hour on 2.13 GHz computer. Increasing the voltage controller gain and the output voltage feedback gain will improve the performance of the system as we have seen in Figure 5.10 and Figure 5.12, on the other hand, the robustness of the stability of the system against the time delay will decrease.

5.6 Summary

In this chapter, the problem of controlling a parallel DC/DC buck converter system through a shared network is discussed. The system implements the master-slave control strategy where the reference current signal is sent through a shared network. The shared network will introduce time delay, and some of the data will be lost. As the time delay has four different types, which are the constant, periodic, random but independent and random governed by Markov Chains. The new proposed method in Chapter 3 is compared with the method presented in Chapter 4. The proposed method relies on using the constant time delay model and was presented in Chapter 3, and the second method uses the Markovian jump system approach developed in Chapter 4. The method in Chapter 3 is simpler and requires less computation. The first method is used to estimate the MADB and to select the controller parameters to achieve the required MADB. The MADB is chosen to be larger than the worst-case time delay for the constant, periodic and random time delay.

CHAPTER SIX: TIME DELAY TOLERANCE ESTIMATION FOR A CLASS OF NONLINEAR AND UNCERTAIN NETWORKED CONTROL SYSTEMS

6.1 Introduction

Although the most widely used approaches for designing a controller are developed based on the linearized system model, the actual systems in practice are generally nonlinear, time varying and uncertain. In this chapter, the stability analysis and control of a class of nonlinear networked control system, and uncertain networked control system are studied. The nonlinear system model has the structure of the linearized model with added nonlinearities and perturbations, which are assumed to be bounded and satisfy a quadratic matrix restriction inequality. Two different approaches were studied, and they have led to two stability criteria for a class of nonlinear networked control systems. A number of application examples are chosen to demonstrate the merit of the method described in this chapter. The examples are also studied by other scholars from the previous literature report. The application demonstrated that the method developed is much simpler than those reported in the

literature and easier to use by the users. A class of uncertain NCS is studied in this chapter where the uncertainties are norm bounded. A stability theorem in the form of LMI is derived based on using the finite difference approximation for the delay term. The results of the theorem have been compared with the published results.

6.2 Recent Study on Nonlinear Networked Control Systems with Time Delays

As we know, there are many reported work for the stability analysis of network control systems with linear plant and linear controller, the networked control system with nonlinear plant seems to have not gathered much attention from research community. Lyapunov functional, Lyapunov-Krasovski functional and Lyapunov-Razumikhin functional based methods are most widely used to study the stability of networked control systems where the problem is usually formulated as Linear Matrix Inequalities. In (Yang et al. 2004) Razumikhin and Lyapunov Theorem are used to derive a sufficient stability condition for the stability of a class of nonlinear networked control systems. The system studied in (Yang et al. 2004) is a nonlinear system modelled by a linearized system description combined with a bounded nonlinear part. The discrete-time approach for stabilizing a class of nonlinear systems is presented in (Ma et al. 2006) where the quadratic Lyapunov functional is used to derive a discrete linear controller for the affine nonlinear plant. The time delay between the sensor and the controller is assumed to be lumped together and to be smaller than one sampling period. In (Walsh et al. 2001) a multi-input-multi-output continuous system is studied where the effect of the network induced time delay is modelled as an error state-vector which is regarded as a vanishing perturbation. The switching Lyapunov functional

is used in (Yu et al. 2009) to derive stability conditions for a networked control system with bounded nonlinear uncertainty, where packet-loss dependent controllers can be derived and the stability is formulated as LMI. In (Yu et al. 2005a) the sampled-data approach is used for a networked control system with nonlinearity and the stability criteria is formulated as LMIs. Their method can be used to calculate the maximum nonlinearity bound for a given time delay and controller, but their results are conservative. The maximum nonlinear bound is calculated by solving a constrained convex optimization problem. Additionally, in (Yu et al. 2005b) the same approach has been used to estimate the maximum nonlinear bound by solving a constrained convex optimization problem. The Lyapunov-Krasovski functional is used in (Sun et al. 2006) to derive an LMI to analyze the system stability and for designing a stabilizing controller for a networked control system with time-delay, drop-outs and bounded time-varying nonlinearity with control input. The fuzzy-logic approach has been addressed in many papers (Chang et al. 2005;Jiang et al. 2008b;Wang et al. 2009). The most widely used approach is the Takagi-Sugeno modelling. The Authors in (Wang et al. 2009) modelled a class of nonlinear networked control system using Takagi-Sugeno model. They use the approximate model of the discrete nonlinear system to represent the actual system model.

In (Siljak et al. 2000) the authors introduced new LMI method for stability analysis and stabilization of linear systems with norm bounded nonlinear perturbation. Although the results of the maximum nonlinearity bound are less conservative, the method is limited to free delay systems.

In the following section, the mathematical model of the nonlinear networked control system is given. The system is stabilized with a linear controller, and the stability problem is formulated as LMI using the approach in (Siljak et al. 2000). A simple and conservative

analytical formula relating the nonlinearity bound with the time delay is derived using Lyapunov theorem.

6.3 Stability of a class of nonlinear networked control systems:

6.3.1 Mathematical Model of Networked Control System with Nonlinearity

Suppose a nonlinear system can be described by a linear model with added nonlinear perturbations as:

$$\dot{\mathbf{x}}(t) = \mathbf{A}\mathbf{x}(t) + \mathbf{B}\mathbf{u}(t) + \mathbf{h}(t, \mathbf{x}(t)) \tag{6.1}$$

where $\mathbf{x}(t) \in \Re^n$ is the system state vector and $\mathbf{u}(t) \in \Re^m$ is the system control input. $\mathbf{A} \in \Re^{n \times n}$ and $\mathbf{B} \in \Re^{n \times m}$ are matrices with appropriate sizes.

The nonlinear functions as the elements in the vector field **h** are assumed to be piecewise-continuous function of both t and $\mathbf{x}$. $\mathbf{h}(t, \mathbf{x}(t))$ satisfies the quadratic inequality (Yu et al. 2005a;Yu et al. 2005b);

$$\mathbf{h}^T(t, \mathbf{x}(t))\mathbf{h}(t, \mathbf{x}(t)) \le \alpha^2 \mathbf{x}^T(t)\mathbf{H}^T\mathbf{H}\mathbf{x}(t) \tag{6.2}$$

where $\alpha > 0$ is the nonlinearity bounding parameter and **H** is a constant matrix. For any given **H**;

$$\mathbf{H}_\alpha = \{\mathbf{h} : \mathbf{R}^{n+1} \to \mathbf{R}^n \mid \mathbf{h}^T(t, \mathbf{x}(t))\mathbf{h}(t, \mathbf{x}(t)) \le \alpha^2 \mathbf{x}^T(t)\mathbf{H}^T\mathbf{H}\mathbf{x}(t) \ \ \forall (t, x) \in R_+ \times \mathbf{R}^n\}$$

The constraint (6.2) can be interpreted as (Siljak et al. 2000);

$$\left\|\mathbf{h}(t,\mathbf{x}(t))\right\| \le \alpha\left\|\mathbf{H}\mathbf{x}(t)\right\| \tag{6.3}$$

Definition 5.1: (Khalil 1992)

The equilibrium point $\boldsymbol{x} = 0$ of (6.1) is

- Stable, if for each $\in > 0$, there is $\varphi = \varphi(\in) > 0$ such that

$$\left\|\mathbf{x}(0)\right\| < \varphi \text{ implies that } \left\|\mathbf{x}(t)\right\| < \in, \qquad \forall t \ge 0$$

- Unstable, if not stable.

- Asymptotically stable, if it is stable and φ can be chosen such that

$$\left\|\mathbf{x}(0)\right\| < \varphi \text{ implies that } \lim_{t\to\infty}\mathbf{x}(t) = 0$$

Stabilizing the system with a linear controller, which is given by;

$$\mathbf{u}(t) = \mathbf{K}\mathbf{x}(t-\tau) \tag{6.4}$$

where τ is given by (3.4). Applying (6.4) into (6.1);

$$\dot{\mathbf{x}}(t) = \mathbf{A}x(t) + \mathbf{B}\mathbf{K}\mathbf{x}(t-\tau) + \mathbf{h}(t,\mathbf{x}(t))$$

$$\dot{\mathbf{x}}(t) = (\mathbf{A}+\mathbf{B}\mathbf{K})x(t) + \mathbf{B}\mathbf{K}(\mathbf{x}(t-\tau)-\mathbf{x}(t)) + \mathbf{h}(t,\mathbf{x}(t)) \tag{6.5}$$

If H 3.1 and H 3.2 hold then the time delay term can be approximated using the finite difference approximation by Tyler series expansion. The expression for $\mathbf{x}(t-\tau)$ can be obtained by Taylor expansion as:

$$\mathbf{x}(t-\tau) = \sum_{n=0}^{\infty}(-1)^n\frac{\tau^n}{n!}\mathbf{x}^{(\mathbf{n})}(t) \tag{6.6}$$

The second-order approximation of the delay term is given by;

$$\mathbf{x}(\mathbf{t}-\tau)=\mathbf{x}(t)-\tau\dot{\mathbf{x}}(t)+(\tau^2/2)\ddot{\mathbf{x}}(t)+\mathbf{R}_3(\mathbf{x},\tau)$$

$$\mathbf{x}(\mathbf{t}-\tau)\approx\mathbf{x}(t)-\tau\dot{\mathbf{x}}(t)+(\tau^2/2)\ddot{\mathbf{x}}(t) \tag{6.7}$$

From (6.7) it can be seen that $\mathbf{R}_3(x,\tau)$ depends on the time delay, τ, and the higher-order derivatives of $\mathbf{x}(t)$ which can be neglected if the time delay is small enough. For a small time delay and slowly time varying nonlinear perturbations the second derivative can be approximated as:

$$\ddot{\mathbf{x}}(t)\approx(\mathbf{A}+\mathbf{BK})\dot{\mathbf{x}}(t) \tag{6.8}$$

Substituting (6.7) and (6.8) into (6.5);

$$\begin{aligned}\dot{\mathbf{x}}(t)&\cong(\mathbf{A}+\mathbf{BK})x(t)\\&\quad+\mathbf{BK}(-\tau\dot{\mathbf{x}}(t)+(0.5\tau^2)(\mathbf{A}+\mathbf{BK})\dot{\mathbf{x}}(t))+\mathbf{h}(t,\mathbf{x}(t))\\\dot{\mathbf{x}}(t)&\cong\left[\mathbf{I}+\tau\mathbf{BK}(\mathbf{I}-0.5\tau(\mathbf{A}+\mathbf{BK}))\right]^{-1}\left[\mathbf{A}+\mathbf{BK}\right]\mathbf{x}(t)\\&\quad+\left[\mathbf{I}+\tau\mathbf{BK}(\mathbf{I}-0.5\tau(\mathbf{A}+\mathbf{BK}))\right]^{-1}\mathbf{h}(t,\mathbf{x}(t))\end{aligned} \tag{6.9}$$

Equation (6.9) can be written as:

$$\dot{\mathbf{x}}(t)\cong\mathbf{N}(\tau)\left[\mathbf{A}+\mathbf{BK}\right]\mathbf{x}(t)+\mathbf{g}(t,\mathbf{x}(t)) \tag{6.10}$$

where;

$$\begin{aligned}g(t,\mathbf{x}(t))&=\mathbf{N}(\tau)\mathbf{h}(t,\mathbf{x}(t))=\left[\mathbf{I}+\mathbf{M}(\tau)\right]^{-1}\mathbf{h}(t,\mathbf{x}(t))\\&=\left[\mathbf{I}+\tau\mathbf{BK}(\mathbf{I}-0.5\tau(\mathbf{A}+\mathbf{BK}))\right]^{-1}\mathbf{h}(t,\mathbf{x}(t))\end{aligned}$$

According to (6.2) with the time delay the quadratic inequality can be written as;

$$g^T(t,\mathbf{x}(t))g(t,\mathbf{x}(t))\le\alpha^2\mathbf{x}^T(t)\mathbf{H}^T\mathbf{N}(\tau)^T\mathbf{N}(\tau)\mathbf{H}\mathbf{x}(t) \tag{6.11}$$

which can be interpreted as;

$$\left\| g(t,\mathbf{x}(t)) \right\| \le \alpha \left\| \mathbf{N}(\tau)\mathbf{H}\mathbf{x}(t) \right\| \le \alpha \left\| \mathbf{N}(\tau) \right\| \left\| \mathbf{H} \right\| \left\| \mathbf{x}(t) \right\| \tag{6.12}$$

The constraint can be written as;

$$\mathbf{z}(t)^T \begin{bmatrix} -\alpha^2 \mathbf{H}^T \mathbf{N}(\tau)^T \mathbf{N}(\tau)\mathbf{H} & 0 \\ 0 & \mathbf{I} \end{bmatrix} \mathbf{z}(t) \le 0 \tag{6.13}$$

where; $\mathbf{z}(t) = \begin{bmatrix} \mathbf{x}(t) \\ g(t,x(t)) \end{bmatrix}$

Choosing the quadratic Lyapunov functional candidate and taking its derivative;

$$\begin{aligned} \dot{\mathbf{V}}(x) &= \mathbf{x}^{\mathbf{T}}(t)\mathbf{P}\dot{\mathbf{x}}(t) + \dot{\mathbf{x}}^{\mathbf{T}}(t)\mathbf{P}\mathbf{x}(t) \\ \dot{\mathbf{V}}(x) &\cong \mathbf{x}^{\mathbf{T}}\mathbf{P}\left(\mathbf{N}(\tau)(\mathbf{A}+\mathbf{B}\mathbf{K})\mathbf{x}(t) + g(t,\mathbf{x}(t))\right) \\ &\quad + \left(\mathbf{x}(t)^T(\mathbf{A}+\mathbf{B}\mathbf{K})^T\mathbf{N}(\tau)^T + g^T(t,\mathbf{x}(t))\right)\mathbf{P}\mathbf{x} \\ \dot{\mathbf{V}}(x) &\cong \mathbf{x}(t)^T\left(\mathbf{P}\mathbf{N}(\tau)(\mathbf{A}+\mathbf{B}\mathbf{K}) + (\mathbf{A}+\mathbf{B}\mathbf{K})^T\mathbf{N}(\tau)^T\mathbf{P}\right)\mathbf{x}(t) \\ &\quad + g^T(t,\mathbf{x}(t))\mathbf{P}\mathbf{x}(t) + \mathbf{x}(t)^T\mathbf{P}g(t,\mathbf{x}(t)) \end{aligned} \tag{6.14}$$

It is assumed that the linear time delay is stable; that is for $\mathbf{P} = \mathbf{P}^T$ and $\mathbf{Q} = \mathbf{Q}^T$ we have:

$$\mathbf{P}\mathbf{N}(\tau)(\mathbf{A}+\mathbf{B}\mathbf{K}) + (\mathbf{A}+\mathbf{B}\mathbf{K})^T\mathbf{N}(\tau)^T\mathbf{P} < \mathbf{0}$$

Then (6.14) can be written as;

$$\mathbf{z}(t)^T \begin{bmatrix} (\mathbf{A}+\mathbf{B}\mathbf{K})^T\mathbf{N}(\tau)^T\mathbf{P} + \mathbf{P}\mathbf{N}(\tau)(\mathbf{A}+\mathbf{B}\mathbf{K}) & \mathbf{P} \\ \mathbf{P} & \mathbf{0} \end{bmatrix} \mathbf{z}(t) < 0 \tag{6.15}$$

Following the approach in (Siljak et al. 2000) by combining (6.13) and (6.15) we get;

$$\begin{bmatrix} (\mathbf{A}+\mathbf{B}\mathbf{K})^T\mathbf{N}(\tau)^T\mathbf{P} + \mathbf{P}\mathbf{N}(\tau)(\mathbf{A}+\mathbf{B}\mathbf{K}) + \varepsilon\alpha^2\mathbf{H}^T\mathbf{N}(\tau)^T\mathbf{N}(\tau)\mathbf{H} & \mathbf{P} \\ \mathbf{P} & -\varepsilon\mathbf{I} \end{bmatrix} < 0$$

Lemma 6.1 (Schur Complement): (Mahmoud 2000)

For a given symmetric matrix

$$\mathbf{\Omega} = \begin{bmatrix} \mathbf{\Omega}_{11} & \mathbf{\Omega}_{12} \\ \mathbf{\Omega}_{12}{}^{T} & \mathbf{\Omega}_{22} \end{bmatrix}$$

where $\mathbf{\Omega}_{11}$, $\mathbf{\Omega}_{12}$ *and* $\mathbf{\Omega}_{22}$ *are block matrices, and* $\mathbf{\Omega}_{11}$ *is a square matrix. The following three conditions are equal in value:*

1) $\mathbf{\Omega} < 0$

2) $\mathbf{\Omega}_{22} < 0,\ \mathbf{\Omega}_{11} - \mathbf{\Omega}_{12}\mathbf{\Omega}_{22}{}^{-1}\mathbf{\Omega}_{12}{}^{T} < 0$

3) $\mathbf{\Omega}_{11} < 0,\ \mathbf{\Omega}_{22} - \mathbf{\Omega}_{12}{}^{T}\mathbf{\Omega}_{11}{}^{-1}\mathbf{\Omega}_{12} < 0$

Letting $\mathbf{Y} = \varepsilon \cdot \mathbf{P}^{-1},\ \varepsilon > 0$, and using Lemma 6.1 we finally get;

$$\begin{bmatrix} \mathbf{N}(\tau)(\mathbf{A}+\mathbf{BK})\mathbf{Y} + \mathbf{Y}(\mathbf{A}+\mathbf{BK})^{T}\mathbf{N}(\tau)^{T} & \mathbf{I} & \mathbf{Y}\mathbf{H}^{T}\mathbf{N}(\tau)^{T} \\ \mathbf{I} & -\mathbf{I} & \mathbf{0} \\ \mathbf{N}(\tau)\mathbf{H}\mathbf{Y} & \mathbf{0} & -\gamma\mathbf{I} \end{bmatrix} < 0 \qquad (6.16)$$

where $\gamma = 1/\alpha^{2}$

Theorem 6.1

System (6.1) with the linear controller (6.4) and a given time delay, τ, is robustly stable with degree α if the following is feasible

Minimize γ

Subject to $\mathbf{Y} > 0$ and (6.16)

The optimization problem in Theorem 6.1 is quasi-convex in γ which can be solved easily using the Matlab LMI Toolbox. For systems with slow dynamic and small time delays, where the first derivative approximation assumption can be held the matrix $\mathbf{M}(\tau)$ can be approximated as $\mathbf{M}(\tau) \approx \tau \mathbf{BK}$, which can lead to less conservative results.

Corollary 6.1

Let H 3.1 and H 3.2 hold, then the nonlinear system (6.1) with the controller (6.4) is robustly stable with degree α if

$$\alpha < \frac{\lambda_{\min}(\mathbf{Q})}{2\|\mathbf{P}\|_2 \cdot \|\mathbf{H}\|_2 \cdot \|\mathbf{N}(\tau)\|}$$

Proof

Choosing a Lyapunov functional candidate as:

$$\mathbf{V}(x) = \mathbf{x}^{\mathbf{T}}\mathbf{P}\mathbf{x} > 0 \qquad \forall \ \mathbf{x} \neq \mathbf{0} \tag{6.17}$$

The objective for the next step is to find the range of τ that will ensure $\dot{\mathrm{V}}(x) < 0$ for $\forall \ \mathbf{x} \neq \mathbf{0}$ (Goodall et al. 2001;Wang et al. 1998). Taking the derivative of (6.17) along with the system trajectory (6.10),

$$\begin{aligned}
&\dot{\mathbf{V}}(x) = \mathbf{x}^{\mathbf{T}}(t)\mathbf{P}\dot{\mathbf{x}}(t) + \dot{\mathbf{x}}^{\mathbf{T}}(t)\mathbf{P}\mathbf{x}(t) \\
&\cong \mathbf{x}^{\mathbf{T}}\mathbf{P}\big(\mathbf{N}(\tau)(\mathbf{A}+\mathbf{BK})\mathbf{x}(t) + \mathbf{N}(\tau)h(t,\mathbf{x}(t))\big) \\
&+ \big(\mathbf{x}(t)^T(\mathbf{A}+\mathbf{BK})^T\mathbf{N}(\tau)^T + h^T(t,\mathbf{x}(t))\mathbf{N}(\tau)^T\big)\mathbf{P}\mathbf{x} \\
&\cong \mathbf{x}^{\mathbf{T}}(t)\mathbf{P}\mathbf{N}(\tau)(\mathbf{A}+\mathbf{BK})\mathbf{x}(t) \\
&+ \mathbf{x}(t)^T(\mathbf{A}+\mathbf{BK})^T\mathbf{N}(\tau)^T\mathbf{P}\mathbf{x}(t) + 2\mathbf{x}^{\mathbf{T}}(t)\mathbf{P}\mathbf{N}(\tau)h(t,\mathbf{x}(t)) \\
&\cong \mathbf{x}^{\mathbf{T}}(t)\big(\mathbf{P}\mathbf{N}(\tau)(\mathbf{A}+\mathbf{BK}) + (\mathbf{A}+\mathbf{BK})^T\mathbf{N}(\tau)^T\mathbf{P}\big)\mathbf{x}(t) \\
&+ 2\mathbf{x}^{\mathbf{T}}(t)\mathbf{P}\mathbf{N}(\tau)h(t,\mathbf{x}(t))
\end{aligned} \tag{6.18}$$

If there exists $\mathbf{P} = \mathbf{P}^T > 0$ and $\mathbf{Q} = \mathbf{Q}^T > 0$, satisfying:

$$\mathbf{PN}(\tau)(\mathbf{A} + \mathbf{BK}) + (\mathbf{A} + \mathbf{BK})^T \mathbf{N}(\tau)^T \mathbf{P} = -\mathbf{Q} \tag{6.19}$$

Substituting (6.19) into (6.18) we get:

$$\dot{\mathbf{V}}(\mathbf{x}(t)) = -\mathbf{x}^{\mathbf{T}}(t)\mathbf{Q}\mathbf{x}(t) + 2\mathbf{x}^{\mathbf{T}}(t)\mathbf{PN}(\tau)h(t, \mathbf{x}(t)) \tag{6.20}$$

For any $\alpha > 0$, there exist $r > 0$ such that

$$\left\|h(t, \mathbf{x}(t)\right\|_2 < \alpha \left\|\mathbf{H}\right\| \cdot \left\|\mathbf{x}(t)\right\|_2, \qquad \forall \left\|\mathbf{x}(t)\right\|_2 < r$$

Then;

$$\left\|\mathbf{N}(\tau)h(t, \mathbf{x}(t)\right\| < \left\|\mathbf{N}(\tau)\right\| \cdot \left\|h(t, \mathbf{x}(t)\right\| < \alpha \left\|\mathbf{N}(\tau)\right\| \cdot \left\|\mathbf{H}\right\| \cdot \left\|\mathbf{x}(t)\right\|_2 \tag{6.21}$$

Also we have (Khalil 1992);

$$\mathbf{x}^T(t)\mathbf{Q}\mathbf{x}(t) \geq \lambda_{\min}(\mathbf{Q}) \left\|\mathbf{x}(t)\right\|_2^2 \tag{6.22}$$

Using (6.21) and (6.22) into (6.20) we finally have;

$$\dot{\mathbf{V}}(\mathbf{x}(t)) < -\left[\lambda_{\min}(\mathbf{Q}) - 2\alpha \left\|\mathbf{P}\right\|_2 \left\|\mathbf{H}\right\|_2 \left\|\mathbf{N}(\tau)\right\|\right] \left\|\mathbf{x}(t)\right\|_2^2 \tag{6.23}$$

From (6.23) it can be found that if

$$\alpha < \frac{\lambda_{\min}(\mathbf{Q})}{2\left\|\mathbf{P}\right\|_2 \left\|\mathbf{H}\right\|_2 \cdot \left\|\mathbf{N}(\tau)\right\|}$$

then $\dot{\mathrm{V}}(x) < 0$, the system will be robustly stable with degree of α. We can see from Corollary 6.1 that the MADB decreases with increasing α. Setting $\alpha \approx 0$ and supposing that

the second-order term can be neglected, then Corollary 6.1 reduces to Corollary 3.1 in Chapter 3 as follows;

$$\tau < \frac{1}{\|\mathbf{BK}\|}\left[1-\frac{2\alpha\|\mathbf{P}\|_2 \cdot \|\mathbf{H}\|_2}{\lambda_{\min}(\mathbf{Q})}\right]$$

$$\tau < \frac{1}{\|\mathbf{BK}\|}\left[1-0\frac{2\|\mathbf{P}\|_2 \cdot \|\mathbf{H}\|_2}{\lambda_{\min}(\mathbf{Q})}\right] \rightarrow \qquad \tau < \frac{1}{\|\mathbf{BK}\|}$$

Increasing α means moving away from the equilibrium point. We noticed as the system moves away from the equilibrium point the MADB decreases. The boundary of the domain of attraction is when $\alpha \approx \frac{\lambda_{\min}(\mathbf{Q})}{2\|\mathbf{P}\|_2 \cdot \|\mathbf{H}\|_2}$, substituting into Corollary 6.1 we have; $\tau < (1-1)/\|\mathbf{BK}\|$ that implies $0 < \tau < 0$, which means that the MADB on the boundary is approximately zero.

6.3.2 Estimation of Domain of Attraction

In nonlinear systems, we are not only interested in the asymptotic stability of the system but also in finding or estimating the domain of attraction. The domain of attraction is defined as the region where the limit of every trajectory of the nonlinear system originating in R_A is the equilibrium point. R_A is shown in Figure 6.1. It is assumed that the origin is asymptotically stable. In (Khalil 1992) the domain of attraction of the equilibrium point (the origin) is defined as:

$$R_A = \{x \in R^n \mid \phi(t;x) \rightarrow 0 \text{ as } t \rightarrow \infty\} \tag{6.24}$$

where $\phi(t;x)$ is the initial state at $t = 0$. It is difficult to find the domain of attraction but we can estimate a region Ω_c, that is $\Omega_c \subset R_A$, using Lyapunov's method. In this region $\mathbf{V}(x)$ will be positive definite and $\dot{\mathbf{V}}(x)$ is negative definite.

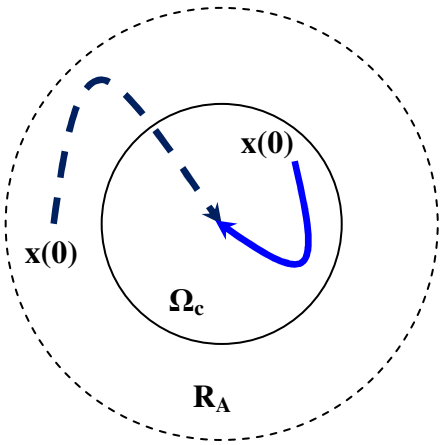

Figure 6.1 The region of attraction

The estimate of the domain of attraction Ω_c in (Khalil 1992) is defined as:

$$\Omega_c = \{x \in R^n \mid V(x) \le c\} \tag{6.25}$$

$$c < \min_{\|x\|_2 = r} \mathbf{V}(x) \tag{6.26}$$

where c is a positive constant. Since;

$$\mathbf{x}^T \mathbf{P}(\tau)\mathbf{x} \ge \lambda_{\min}(\mathbf{P}(\tau))\|x\|_2^2 \tag{6.27}$$

c can be chosen as

$$c \le \lambda_{\min}(\mathbf{P}(\tau))r^2 \tag{6.28}$$

From (6.28) we can draw some conclusions on the relation between the time delay and the domain of attraction because of the dependence of $\lambda_{\min}(\mathbf{P}(\tau))$ on the time delay through

(6.19). A few references (Yu et al. 2005a;Yu et al. 2005b) reported that increasing the time delay decreases the nonlinearity bound. In the following section, a number of examples picked from literature are studied for comparison and discussion.

6.3.3 Examples of applications

In general, two approaches are applied to controller design for NCSs. The first design approach is to estimate the maximum allowable delay bound for the system, and then the network is scheduled to limit the time delay to be less than the MADB. The second approach is to design the controller while taking the time delay and data dropouts into account. In this work, the first approach has been adopted. In this section, a number of examples are studied to demonstrate the approach proposed and compare it with the previously published cases. In particular, the results derived using the method proposed in this paper have been compared with the results using the LMI method given in (Yu et al. 2005a;Yu et al. 2005b).

Example 6.1:

The first example has been studied in (Yu et al. 2005a;Yu et al. 2005b) with the sampled-data approach, the system is given by

$$\dot{\mathbf{x}}(t) = \begin{bmatrix} 1 & 1 \\ 0 & 0.99 \end{bmatrix}\mathbf{x}(t) + \begin{bmatrix} 0 \\ 10 \end{bmatrix}\mathbf{u}(t) + \mathbf{h}(t, \mathbf{x}(t)) \quad \text{with } \mathbf{H} = \begin{bmatrix} 1 & 0 \\ 0 & 0 \end{bmatrix}$$

The controller is chosen in (Yu et al. 2005a;Yu et al. 2005b) to be $\mathbf{K} = \begin{bmatrix} -0.2999 & -0.2989 \end{bmatrix}$. With $\alpha \approx 0$ and using Theorem 6.1 the MADB is 0.291 s. For 0.2509 s time delay, the maximum nonlinearity can be estimated using Theorem 6.1, solving the optimization problem using the LMI Matlab Toolbox, we have:

$$\alpha_{\max} = 0.1533 \text{ with } \mathbf{Y} = \begin{bmatrix} 8.191 & -48.094 \\ -48.094 & 311.1583 \end{bmatrix}$$

Using Corollary 6.1:

$$\mathbf{P} = \begin{bmatrix} 0.7213 & -1.2213 \\ -1.2213 & 2.4487 \end{bmatrix} \qquad \mathbf{Q} = \mathbf{I} \quad \|\mathbf{P}\|_2 = 3.0809 \qquad \lambda_{\max}(\mathbf{P}) = 3.0809$$

$$\alpha_{\max} = \frac{\lambda_{\min}(\mathbf{Q})}{2\|\mathbf{P}\|_2 \|\mathbf{H}\|_2 \cdot \left\| [\mathbf{I} + \tau \mathbf{BK}(\mathbf{I} - 0.5\tau(\mathbf{A} + \mathbf{BK}))]^{-1} \right\|} = 0.0184$$

The maximum nonlinearity bound given in (Yu et al. 2005a;Yu et al. 2005b) is 0.0013, which shows that the results of the proposed method are less conservative. Moreover, the results of Theorem 6.1 are less conservative than the results of Corollary 6.1. The trajectory of the system is shown in Figure 6.2. For the comparison, the nonlinear function and the initial conditions for the simulation are given by;

$$h(t, \mathbf{x}(t)) = \begin{bmatrix} \alpha x_1 \sin(x_1) \\ 0 \end{bmatrix} \qquad \mathbf{x}(0) = \begin{bmatrix} -15 & 10 \end{bmatrix}^T$$

In (Yu et al. 2005a;Yu et al. 2005b) with 0.22 s time delay and $\mathbf{K} = \begin{bmatrix} -0.359 & -0.317 \end{bmatrix}$, the maximum nonlinearity bound is $\alpha_{\max} = 0.1365$, using Corollary 6.1 $\alpha_{\max} = 0.0252$ while using Theorem 6.1 $\alpha_{\max} = 0.2555$. In (Peng et al. 2008) $\alpha_{\max} = 0.1636$ with 0.2509 s time delay. Corollary 6.1 and Theorem 6.1 still give conservative results compared with some of the published ones; however, the method has its advantages over those published methods previously in (Peng et al. 2008;Yu et al. 2005a;Yu et al. 2005b), where the proposed method is very easy and simple in application and use. The MADB as a function of the nonlinearity is given in Figure 6.3. It can be easily seen that as the nonlinearity increases the MADB decreases.

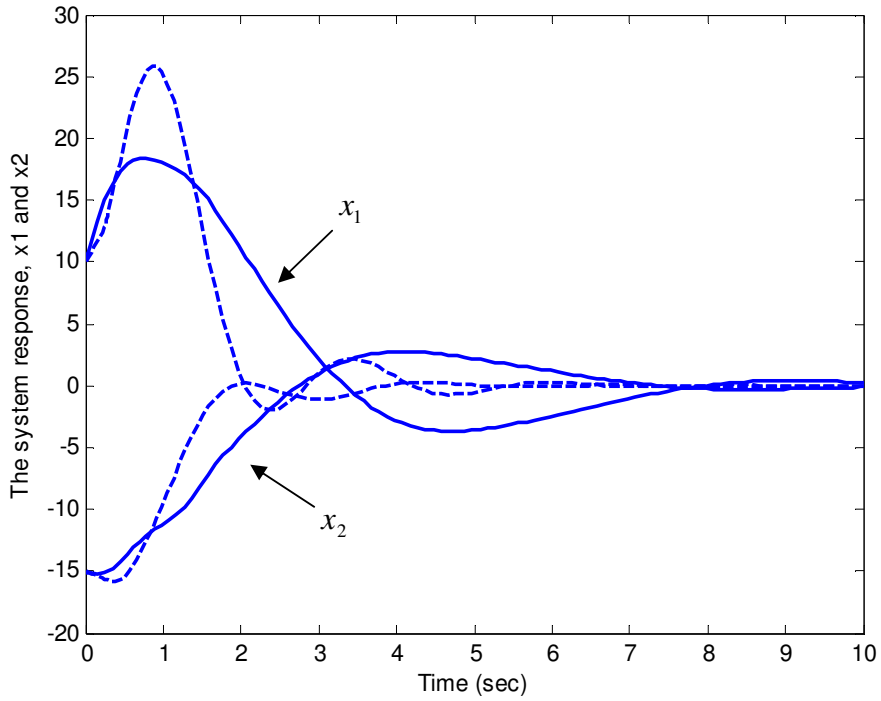

Figure 6.2 The system response with zero time delay (solid-line) and 0.2509 s time delay (dashed-line)

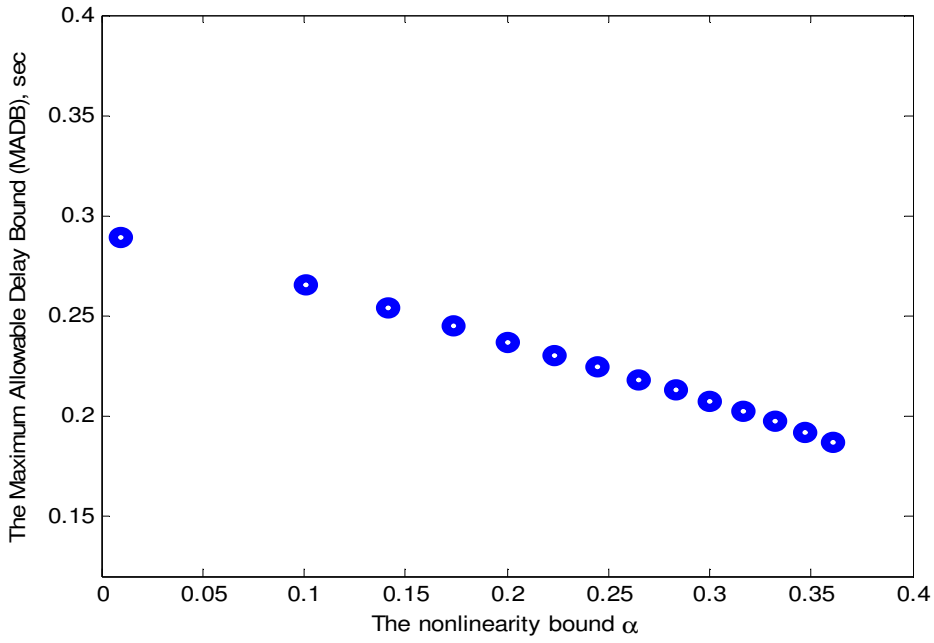

Figure 6.3 The MADB as a function of the nonlinearity bound using Theorem 6.1

Example 6.2:

This example has been studied in (Wang et al. 2009) with the sampled-data approach, the system is given by

$$\dot{\mathbf{x}}(t)=\begin{bmatrix}0 & 1 & 0\\ 0 & -0.5 & 1\\ 3 & 3 & -2.5\end{bmatrix}\mathbf{x}(t)+\begin{bmatrix}0\\ 1\\ 0.6\end{bmatrix}\mathbf{u}(t)+\begin{bmatrix}0\\ 0\\ x_1(t)\sin(x_1(t))\end{bmatrix}$$

The controller in (Wang et al. 2009) is designed to be $\mathbf{K}=\begin{bmatrix}9.0255 & 9.3741 & 5.1724\end{bmatrix}$. Setting $\alpha\approx 0$ and using theorem 6.1, the MADB is estimated as 0.0601 s. The maximum nonlinearity bound for the delay-free system is 4.3. The MADB as a function of the nonlinearity is shown in Figure 6.4. The system response with 0.03 s and $\alpha=3$ is shown in Figure 6.5.

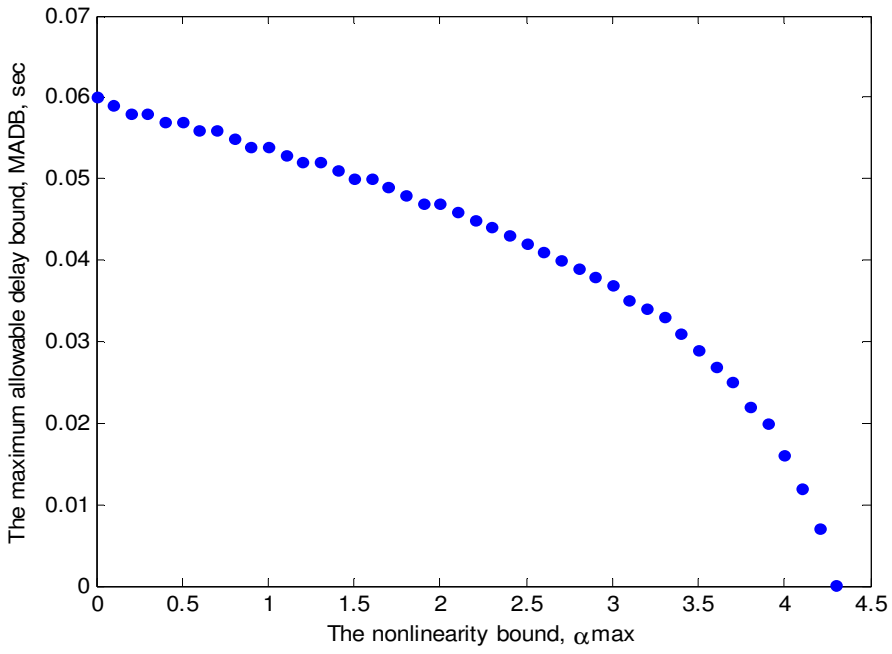

Figure 6.4 The MADB as a function of the maximum nonlinearity bound using Theorem 6.1

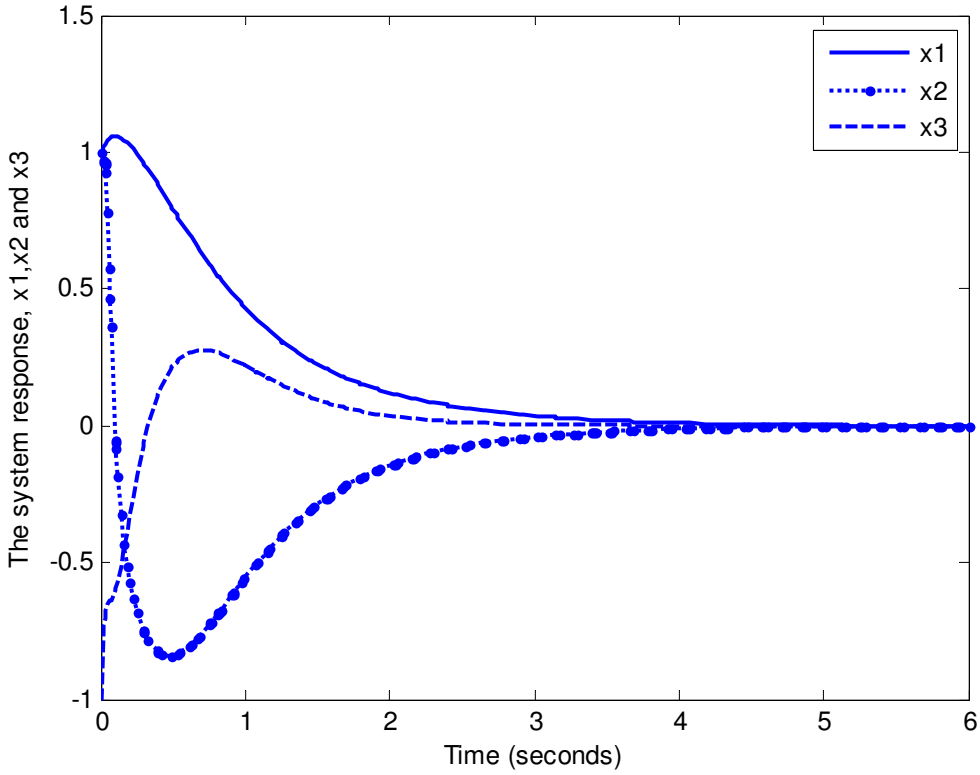

Figure 6.5 The system response with 0.03 s time delay and $\alpha = 3$

From Figure 6.3 and Figure 6.4 clearly with increasing the nonlinearity bound the MADB will be allowed to decrease. The same relation has been noticed in (Yu et al. 2005a;Yu et al. 2005b). Furthermore, in all our simulations, we found that increasing the nonlinearity reduces the MADB.

Using the finite difference approximation with first-order approximation, the MADB with zero nonlinearity is 0.0801 s. The response of the system with 0.0801 s is shown in Figure 6.6. The MADB as a function of the nonlinearity with both the first-order and the second-order approximation is shown in Figure 6.7.

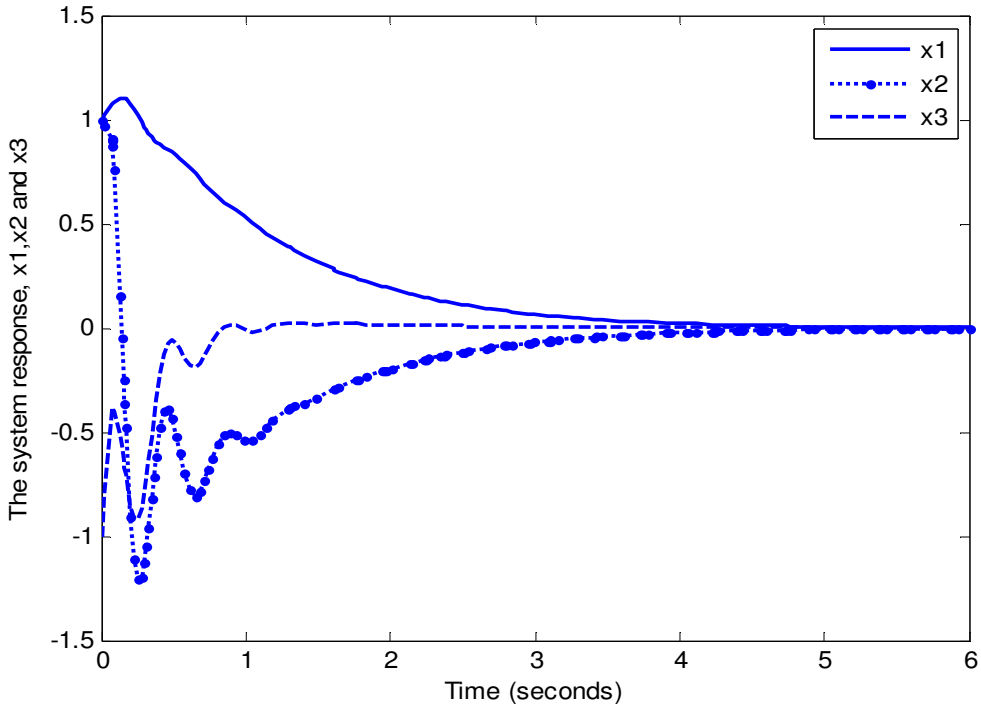

Figure 6.6 The system response with 0.0801 s time delay and $\alpha = 0$

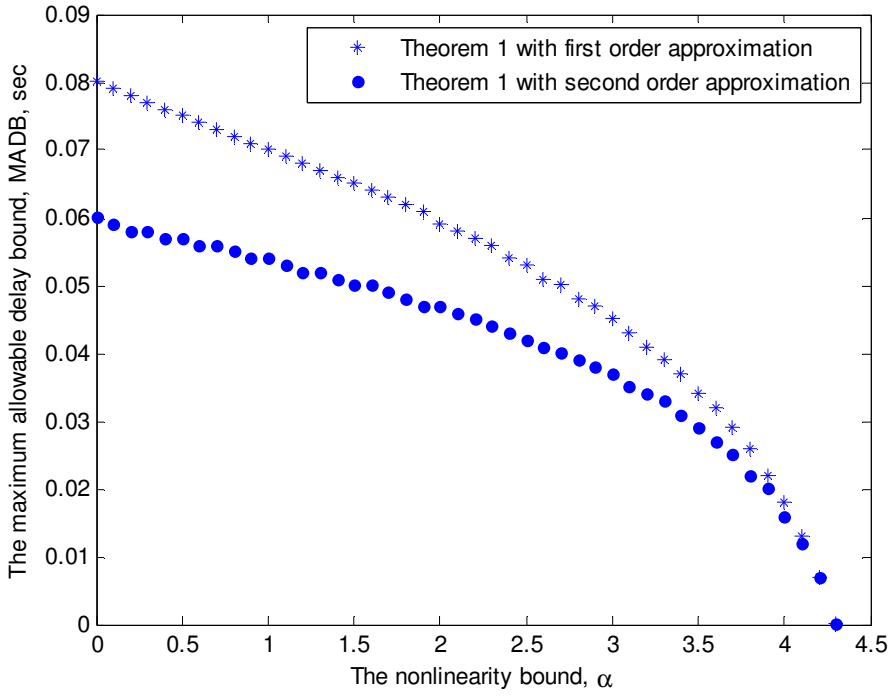

Figure 6.7 The MADB as a function of the maximum nonlinearity bound using Theorem 6.1

From Figure 6.7 we can choose a set of nonlinearity bound and time delay under which the system is stable, for example, the response of the system with 0.04 s time delay and $\alpha = 3$ is shown in Figure 6.8, which proves that the system is stable.

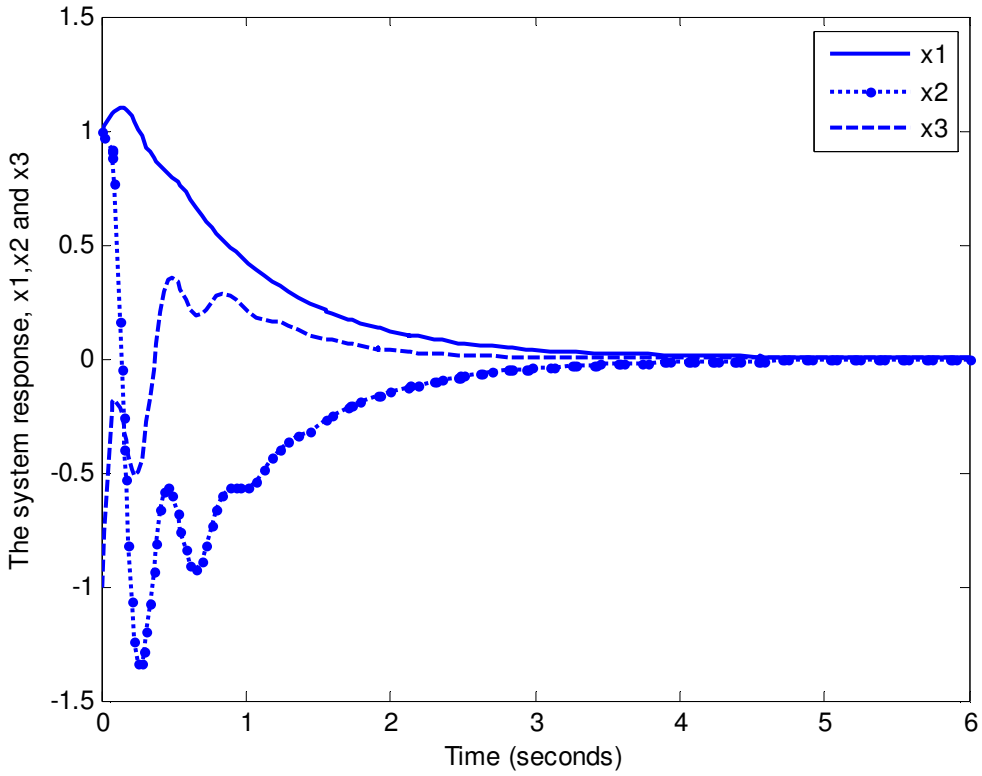

Figure 6.8 The system response with 0.04 s time delay and $\alpha = 3$

Example 6.3: (Estimation of Region of Attraction)

A nonlinear system is given by:

$$\dot{x}(t) = x^2(t) + u(t)$$

In (Yang et al. 2004) the system is stabilized with a linear controller as:

$$u(t) = -\frac{1}{2}x(t-\tau)$$

In (Yang et al. 2004) the authors use Razumikhin and Lyapunov theorem and the derived stability criterion is given by;

$$\tau = \frac{1-\varepsilon}{\frac{1}{2}q(1+\varepsilon)}$$

where $\alpha\|\mathbf{H}\| = \frac{\varepsilon}{2\|\mathbf{P}\|}$, it is clear that increasing ε or increasing α decreases the MADB. According to (Yang et al. 2004) the maximum time delay is attained when $\varepsilon \to 0^+$ and $q \to 1^+$, substituting into the above equation we get:

$$\tau = \frac{1-0}{\frac{1}{2}(1+0)} = 2$$

The MADB reported in (Yang et al. 2004) is 2 s. Using Theorem 6.1 with $\mathbf{H} = 1$ and $\mathbf{K} = -1/2$, the MADB is 2 s. Choosing $\mathbf{K} = -2$; from (6.19) with $\mathbf{M}(\tau) \approx \tau\mathbf{BK}$, we have

$$\mathbf{P}[\mathbf{I} + \tau\mathbf{BK}]^{-1}[\mathbf{A} + \mathbf{BK}] + [\mathbf{A} + \mathbf{BK}]^T[\mathbf{I} + \tau\mathbf{BK}]^{-T}\mathbf{P} = -\mathbf{Q}$$

Choosing $\mathbf{Q} = 1$;

$$\mathbf{P}[1 - 2\tau]^{-1}[0 - 2] + [0 - 2]^T[1 - 2\tau]^{-T}\mathbf{P} = -1$$

$$\frac{-2P}{1-2\tau} + \frac{-2P}{1-2\tau} = -1 \quad \rightarrow \quad \frac{-4P}{1-2\tau} = -1 \quad \rightarrow \quad P = \frac{1}{4}(1-2\tau)$$

For P to be positive $\tau < 0.5$, so the MADB is 0.5 s. Using Theorem 6.1 with $\mathbf{H} = 1$, the MADB is 0.5 s.

Using the first-order finite difference approximation for the delay term, the time delay nonlinear system is given by;

$$\dot{x}(t) = (1-2\tau)^{-1}\left(x^2(t) - 2x(t)\right)$$

The system is stable if $\tau < 0.5$. Choosing Lyapunov functional candidate as;

$$\mathbf{V}(x) = \mathbf{x}^{\mathbf{T}}\mathbf{P}\mathbf{x} > 0 \qquad \forall \ \mathbf{x} \neq \mathbf{0}$$

$$\dot{\mathbf{V}}(x) = \dot{\mathbf{x}}^{\mathbf{T}}\mathbf{P}\mathbf{x} + \mathbf{x}^{\mathbf{T}}\mathbf{P}\dot{\mathbf{x}}$$

$$\dot{V}(x) = 2(1-2\tau)^{-1}x(t)P(x(t)-2)x(t) = 2(1-2\tau)^{-1}x^2(t)P(x(t)-2)$$

$$x(\mathrm{t}) < 2 \qquad \rightarrow \qquad \dot{V}(x) < 0$$

The equilibrium points of the system are: $x = 0$ and $x = 2$, we will study the domain of the attraction at the origin; for the system to be stable we must have;

$$x(t) < 2 \qquad \text{that implies} \qquad x^2(t) < 4$$

The domain of attraction is estimated through (6.28);

$$c \leq \lambda_{\min}(\mathbf{P})r^2 \qquad \text{where} \quad r = 2 \ \text{ and } \ \mathbf{P} = \frac{1}{4}(1-2\tau),$$

$$c \leq \frac{1}{4}(1-2\tau)\cdot 2^2 \qquad c \leq (1-2\tau)$$

We can see that increasing the time delay decreases the domain of attraction and when the time delay approaches the MADB then the domain of attraction becomes very small.

The system response with different time delays is shown in Figure 6.9. From Figure 6.9 the system is still stable even with 0.75 s, which shows the results of Theorem 6.1 are still conservative.

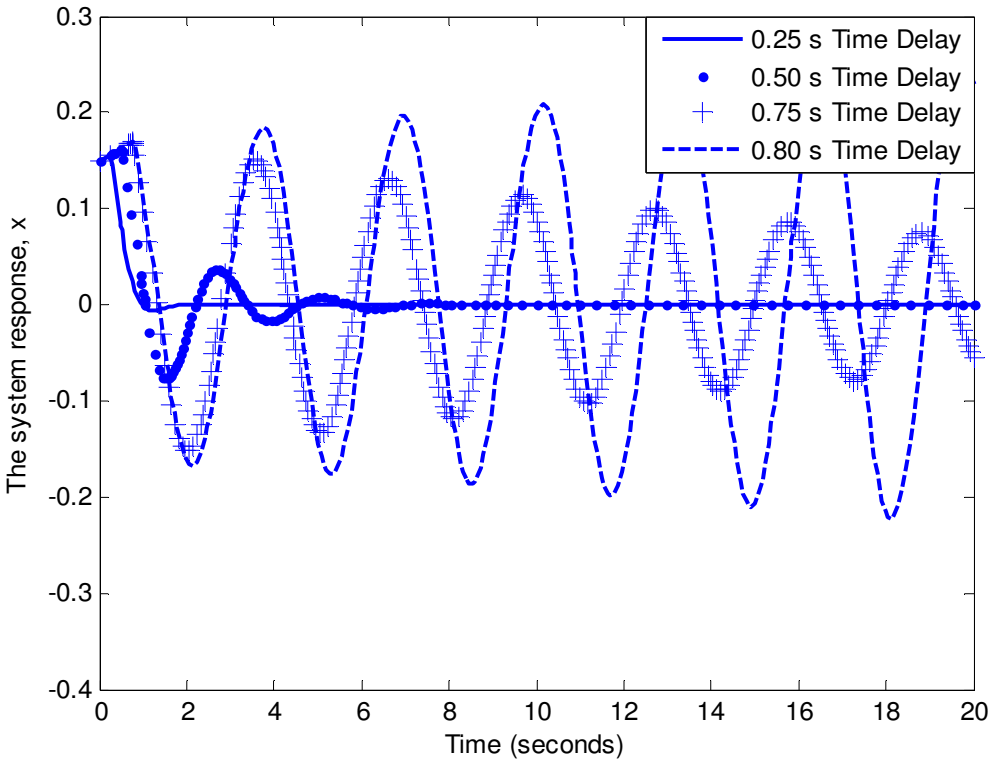

Figure 6.9 The response of the system in Example 6.3 with 0.15 initial condition

Figure 6.10 and Figure 6.11 show the system response with 0.76 s time delay. In Figure 6.10 the initial condition is 0.15, and we can see that the system is stable while in Figure 6.11 the initial condition is 0.5, and the system is unstable. Increasing the initial condition reduces the MADB, and this is the same conclusion obtained from Corollary 6.1. Additionally, increasing the time delay reduces the domain of attraction.

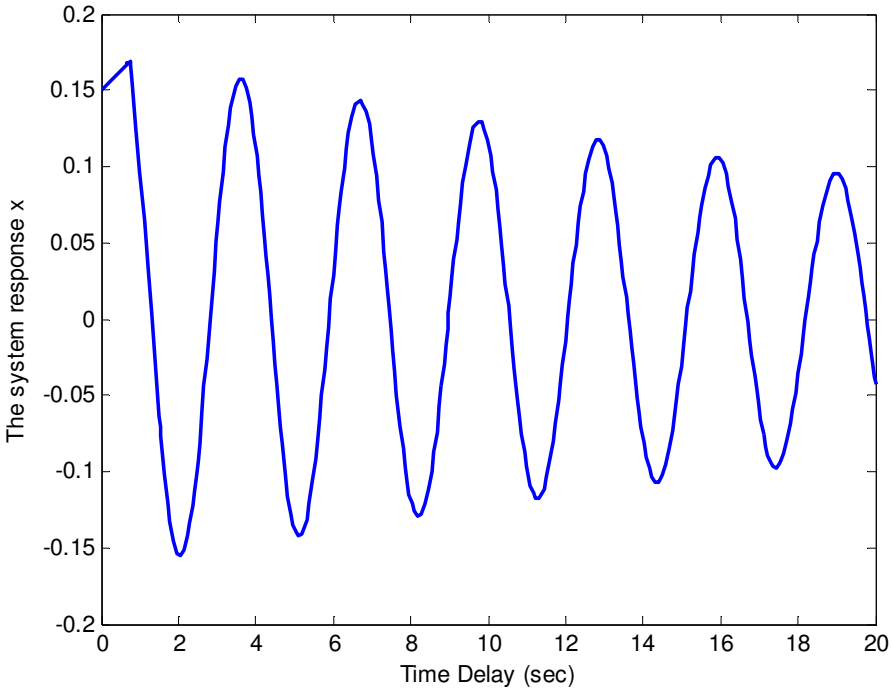

Figure 6.10 The system response with 0.76 s time delay and 0.15 initial condition

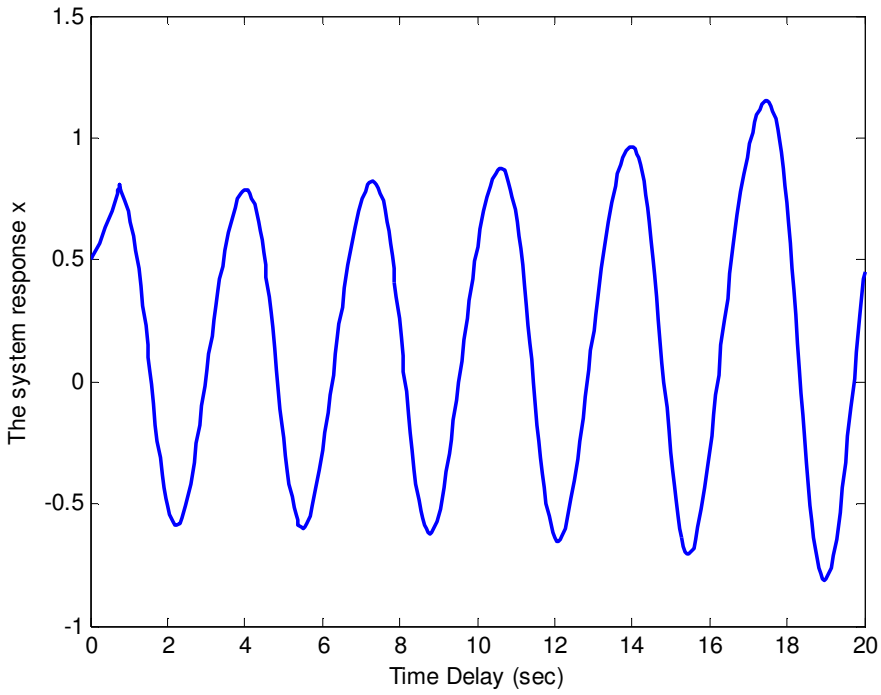

Figure 6.11 The system response with 0.76 s time delay and 0.5 initial condition.

6.4 Stability of Uncertain Networked Control System

Practically, it is impossible to have an accurate model of the system and this is because of the noise in the measurement, the slowly varying system parameters and component aging. Therefore, these imperfections are represented in the system model as uncertainty. There are many types of uncertainty, and we are studying the norm bounded uncertainty in the following analysis. The uncertain NCS has been studied by many researchers, see for example; (Peng et al. 2006;Lu et al. 2002;Yan et al. 2006;Yan et al. 2008;Huang et al. 2006;Su 1994;Xei et al. 2002;Mahmoud 2000;Mahmoud et al. 1994;Liu et al. 1998;Parlakci 2006;Su et al. 1992;Li et al. 1997;Cao et al. 1998;Yue et al. 2006).

In (Peng et al. 2006) the authors consider an uncertain NCS with parameter uncertainty where the delays are in the states and the control signals. A multiple Lyapunov function is constructed, and an LMI is derived from which the MADB can be determined. In (Lu et al. 2002) the Lyapunov-Krasovski theorem is used to derive improved delay-dependent stability criteria in LMI form. The authors in (Yan et al. 2006; Yan et al. 2008) studied the multi-input-multi-output uncertain NCS, and the Lyapunov theorem is used to derive stability theorem to estimate the MADB.

Some papers consider uncertain NCS with uncertainty only in the system matrix, see for example (Xei et al. 2002;Yue et al. 2006). A simple conservative analytical stability criterion based on Lyapunov function is proposed in (Su et al. 1992). From the published methods in the literature, we found that the analytical stability criteria are more conservative than the results of the LMI methods. In the next section, the model of the uncertain NCS is introduced and stability theorem in LMI form is derived.

6.4.1 Mathematical Model of Uncertain Networked Control System

Let us consider a class of uncertain NCS described by;

$$\dot{\mathbf{x}}(t) = \left[\mathbf{A} + \Delta\mathbf{A}(t, \mathbf{x}(t))\right]\mathbf{x}(t) + \left[\mathbf{A}_d + \Delta\mathbf{A}_d(t, \mathbf{x}(t))\right]\mathbf{x}(t-\tau) \tag{6.29}$$

where $\mathbf{x}(t) \in \Re^n$ is the system state vector, $\mathbf{A}$ and $\mathbf{A}_d$ are known matrices of appropriate dimensions that represent the system and the controller parameters. Equation (6.29) can be used to model networked control system with state feedback controller, dynamic controller or multi-units interconnected NCS. $\Delta\mathbf{A}(t, \mathbf{x}(t))$ and $\Delta\mathbf{A}_d(t, \mathbf{x}(t))$ characterize the uncertainties in the system model and they must satisfy the following assumption (Lu et al. 2002;Yan et al. 2006;Yan et al. 2008;Huang et al. 2006):

$$\left[\Delta\mathbf{A}(t, \mathbf{x}(t)) \quad \Delta\mathbf{A}_d(t, \mathbf{x}(t))\right] = \mathbf{H}\mathbf{F}(t, \mathbf{x}(t))\left[\mathbf{E}_1 \quad \mathbf{E}_2\right] \tag{6.30}$$

where $\mathbf{H}$, $\mathbf{E}_1$ and $\mathbf{E}_2$ are known real constant matrices of appropriate dimension, and $\mathbf{F}(t, \mathbf{x}(t))$ is an unknown matrix function with Lebesgue-measurable elements and satisfies the following constraint;

$$\mathbf{F}^T(t, \mathbf{x}(t)) \cdot \mathbf{F}(t, \mathbf{x}(t)) \le \mathbf{I} \tag{6.31}$$

Using the finite difference approximation, the delay term $\mathbf{x}(t-\tau)$ can be approximated as:

$$\mathbf{x}(t-\tau) \cong \mathbf{x}(t) - \tau\dot{\mathbf{x}}(t) \tag{6.32}$$

Substituting (6.32) into (6.29):

$$\dot{\mathbf{x}}(t) = \left[\mathbf{I} + \tau \cdot \mathbf{A}_d + \tau \cdot \Delta\mathbf{A}_d(t, \mathbf{x}(t))\right]^{-1}\left[\mathbf{A} + \mathbf{A}_d + \Delta\mathbf{A}(t, \mathbf{x}(t)) + \Delta\mathbf{A}_d(t, \mathbf{x}(t))\right]\mathbf{x}(t) \tag{6.33}$$

For simplicity, the following matrix variables are used: $\mathbf{D} = \mathbf{A} + \mathbf{A}_d$, $\mathbf{C} = \mathbf{I} + \tau \cdot \mathbf{A}_d$, $\Delta\mathbf{C} = \tau \cdot \Delta\mathbf{A}_d(t, \mathbf{x}(t))$, $\Delta\mathbf{D} = \Delta\mathbf{A}(t, \mathbf{x}(t)) + \Delta\mathbf{A}_d(t, \mathbf{x}(t))$. Substituting these new matrix variables into (6.33) we get:

$$\dot{\mathbf{x}}(t) = [\mathbf{C} + \Delta\mathbf{C}]^{-1}[\mathbf{D} + \Delta\mathbf{D}]\mathbf{x}(t) \tag{6.34}$$

Choosing Lyapunov functional candidate and taking its derivative;

$$\mathbf{V}(x) = \mathbf{x}^{\mathbf{T}}\mathbf{P}\mathbf{x}$$

$$\dot{\mathbf{V}}(x) = \dot{\mathbf{x}}^{\mathbf{T}}\mathbf{P}\mathbf{x} + \mathbf{x}^{\mathbf{T}}\mathbf{P}\dot{\mathbf{x}}$$

$$\dot{\mathbf{V}}(x) \cong \mathbf{x}^{\mathbf{T}}\left([\mathbf{D} + \Delta\mathbf{D}]^T [\mathbf{C} + \Delta\mathbf{C}]^{-T}\mathbf{P} + \mathbf{P}[\mathbf{C} + \Delta\mathbf{C}]^{-1}[\mathbf{D} + \Delta\mathbf{D}]\right)\mathbf{x}$$

For $\dot{\mathbf{V}}(x) < 0$, we must have;

$$[\mathbf{D} + \Delta\mathbf{D}]^T [\mathbf{C} + \Delta\mathbf{C}]^{-T}\mathbf{P} + \mathbf{P}[\mathbf{C} + \Delta\mathbf{C}]^{-1}[\mathbf{D} + \Delta\mathbf{D}] < 0$$

$$[\mathbf{C} + \Delta\mathbf{C}]\mathbf{P}^{-1}[\mathbf{D} + \Delta\mathbf{D}]^T + [\mathbf{D} + \Delta\mathbf{D}]\mathbf{P}^{-1}[\mathbf{C} + \Delta\mathbf{C}]^T < 0 \tag{6.35}$$

Letting $\mathbf{Q} = \mathbf{P}^{-1} > 0$, then we have;

$$[\mathbf{C} + \Delta\mathbf{C}]\mathbf{Q}[\mathbf{D} + \Delta\mathbf{D}]^T + [\mathbf{D} + \Delta\mathbf{D}]\mathbf{Q}[\mathbf{C} + \Delta\mathbf{C}]^T < 0$$

$$\begin{aligned}&\mathbf{C}\mathbf{Q}\mathbf{D}^T + \mathbf{D}\mathbf{Q}\mathbf{C}^T + \mathbf{C}\mathbf{Q}\Delta\mathbf{D}^T + \Delta\mathbf{D}\mathbf{Q}\mathbf{C}^T \\ &+ \Delta\mathbf{C}\mathbf{Q}\mathbf{D}^T + \mathbf{D}\mathbf{Q}\Delta\mathbf{C}^T + \Delta\mathbf{C}\mathbf{Q}\Delta\mathbf{D}^T + \Delta\mathbf{D}\mathbf{Q}\Delta\mathbf{C}^T < 0\end{aligned} \tag{6.36}$$

Before we proceed to the analysis we will use the following lemmas:

Lemma 6.2: (Mahmoud 2000)

Let $\mathbf{\Sigma}_1$, $\mathbf{\Sigma}_2$ *and* $\mathbf{\Sigma}_3$ *be real constant matrices of compatible dimensions and* $\mathbf{F}(t, \mathbf{x}(t))$ *be a real matrix function satisfying* $\mathbf{F}^T(t, \mathbf{x}(t)) \cdot \mathbf{F}(t, \mathbf{x}(t)) \le \mathbf{I}$. *Then the following holds;*

$$\boldsymbol{\Sigma}_3 + \boldsymbol{\Sigma}_1\mathbf{F}(t,\mathbf{x}(t))\boldsymbol{\Sigma}_2 + \boldsymbol{\Sigma}_2{}^T\mathbf{F}^T(t,\mathbf{x}(t))\boldsymbol{\Sigma}_1{}^T \le \boldsymbol{\Sigma}_3 + \varepsilon^{-1}\boldsymbol{\Sigma}_1\boldsymbol{\Sigma}_1{}^T + \varepsilon\boldsymbol{\Sigma}_2{}^T\boldsymbol{\Sigma}_2 \qquad \varepsilon > 0$$

Lemma 6.3: (Mahmoud 2000)

Let $\boldsymbol{\Sigma}_1$, $\boldsymbol{\Sigma}_2$, $\boldsymbol{\Sigma}_3$ *and* $\boldsymbol{\Sigma}_4$ *be real constant matrices of compatible dimensions and* $\mathbf{F}(t,\mathbf{x}(t))$ *be a real matrix function satisfying* $\mathbf{F}^T(t,\mathbf{x}(t))\cdot\mathbf{F}(t,\mathbf{x}(t)) \le \mathbf{I}$ *and a scalar* $\rho > 0$ *satisfying* $\mathbf{I} - \rho\boldsymbol{\Sigma}_2{}^T\boldsymbol{\Sigma}_2 > 0$*, then the following holds:*

$$\begin{aligned}\boldsymbol{\Sigma}_4 + (\boldsymbol{\Sigma}_3 + \boldsymbol{\Sigma}_1\mathbf{F}(t,\mathbf{x}(t))\boldsymbol{\Sigma}_2)(\boldsymbol{\Sigma}_3 + \boldsymbol{\Sigma}_1\mathbf{F}(t,\mathbf{x}(t))\boldsymbol{\Sigma}_2)^T \\ \le \boldsymbol{\Sigma}_4 + \rho^{-1}\boldsymbol{\Sigma}_1\boldsymbol{\Sigma}_1{}^T + \boldsymbol{\Sigma}_3(\mathbf{I} - \rho\boldsymbol{\Sigma}_2{}^T\boldsymbol{\Sigma}_2)^{-1}\boldsymbol{\Sigma}_3{}^T\end{aligned}$$

Equation (6.36) can be written as;

$$\begin{aligned}\mathbf{G}_1 + \mathbf{CQ}\Delta\mathbf{D}^T + \Delta\mathbf{DQC} = \mathbf{G}_1 + \mathbf{CQE}_1{}^T\mathbf{F}^T(t,\mathbf{x}(t))\mathbf{H}^T + \mathbf{HF}(t,\mathbf{x}(t))\mathbf{E}_1\mathbf{QC}^T \\ + \mathbf{CQE}_2{}^T\mathbf{F}^T(t,\mathbf{x}(t))\mathbf{H}^T + \mathbf{HF}(t,\mathbf{x}(t))\mathbf{E}_2\mathbf{QC}^T\end{aligned} \tag{6.37}$$

Using Lemma 6.2 into (6.37) we get:

$$\begin{aligned}&\mathbf{G}_1 + \mathbf{CQE}_1{}^T\mathbf{F}^T(t,\mathbf{x}(t))\mathbf{H}^T + \mathbf{HF}(t,\mathbf{x}(t))\mathbf{E}_1\mathbf{QC}^T \\ &+ \mathbf{CQE}_2{}^T\mathbf{F}^T(t,\mathbf{x}(t))\mathbf{H}^T + \mathbf{HF}(t,\mathbf{x}(t))\mathbf{E}_2\mathbf{QC}^T \\ &\le \mathbf{G}_1 + \rho^{-1}\mathbf{HH}^T + \rho\mathbf{CQE}_1{}^T\mathbf{E}_1\mathbf{QC}^T + \varepsilon^{-1}\mathbf{HH}^T + \varepsilon\mathbf{CQE}_2{}^T\mathbf{E}_2\mathbf{QC}^T\end{aligned} \tag{6.38}$$

Applying Lemma 6.2 into (6.38);

$$\begin{aligned}&\mathbf{G}_2 + \Delta\mathbf{CQD}^T + \mathbf{DQ}\Delta\mathbf{C}^T = \\ &\mathbf{G}_2 + \tau\cdot\mathbf{HF}(t,\mathbf{x}(t))\mathbf{E}_2\mathbf{QD}^T + \tau\cdot\mathbf{DQE}_2{}^T\mathbf{F}^T(t,\mathbf{x}(t))\mathbf{H}^T \\ &\le \mathbf{G}_2 + \tau\cdot\left[\xi^{-1}\mathbf{HH}^T + \xi\mathbf{DQE}_2{}^T\mathbf{E}_2\mathbf{QD}^T\right]\end{aligned} \tag{6.39}$$

Again using Lemma 6.2 into (6.39)

$$\mathbf{G}_3 + \Delta\mathbf{CQ}\Delta\mathbf{D}^T + \Delta\mathbf{DQ}\Delta\mathbf{C}^T = \mathbf{G}_3 + \tau\cdot\mathbf{HF}(t,\mathbf{x}(t))\mathbf{E}_2\mathbf{QE}_1{}^T\mathbf{F}^T(t,\mathbf{x}(t))\mathbf{H}^T$$

$$\tau \cdot \mathbf{HF}(t,\mathbf{x}(t))\mathbf{E}_2\mathbf{Q}\mathbf{E}_2{}^T\mathbf{F}^T(t,\mathbf{x}(t))\mathbf{H}^T$$

$$\tau \cdot \mathbf{HF}(t,\mathbf{x}(t))\mathbf{E}_1\mathbf{Q}\mathbf{E}_2{}^T\mathbf{F}^T(t,\mathbf{x}(t))\mathbf{H}^T$$

$$\tau \cdot \mathbf{HF}(t,\mathbf{x}(t))\mathbf{E}_2\mathbf{Q}\mathbf{E}_2{}^T\mathbf{F}^T(t,\mathbf{x}(t))\mathbf{H}^T$$

$$= \mathbf{G}_3 + \tau \cdot \mathbf{HF}(t,\mathbf{x}(t))\left(\mathbf{E}_2\mathbf{Q}\mathbf{E}_1{}^T + \mathbf{E}_1\mathbf{Q}\mathbf{E}_2{}^T\right)\mathbf{F}^T(t,\mathbf{x}(t))\mathbf{H}^T$$

$$+ 2\tau \cdot \mathbf{HF}(t,\mathbf{x}(t))\mathbf{E}_2\mathbf{Q}\mathbf{E}_2{}^T\mathbf{F}^T(t,\mathbf{x}(t))\mathbf{H}^T \tag{5.40}$$

Assuming that $\mathbf{E}_2\mathbf{Q}\mathbf{E}_1{}^T + \mathbf{E}_1\mathbf{Q}\mathbf{E}_2{}^T = \mathbf{\Sigma}_2\mathbf{\Sigma}_2{}^T$, using Lemma 6.3 with $\mathbf{\Sigma}_3 = \mathbf{0}$, we get;

$$\begin{aligned} &= \mathbf{G}_3 + \tau \cdot \mathbf{HF}(t,\mathbf{x}(t))\left(\mathbf{E}_2\mathbf{Q}\mathbf{E}_1{}^T + \mathbf{E}_1\mathbf{Q}\mathbf{E}_2{}^T\right)\mathbf{F}^T(t,\mathbf{x}(t))\mathbf{H}^T \\ &+ 2\tau \cdot \mathbf{HF}(t,\mathbf{x}(t))\mathbf{E}_2\mathbf{Q}\mathbf{E}_2{}^T\mathbf{F}^T(t,\mathbf{x}(t))\mathbf{H}^T \\ &\le \mathbf{G}_3 + \tau \cdot (\alpha^{-1} + 2\beta^{-1})\mathbf{H}\mathbf{H}^T = \mathbf{G}_3 + \tau \cdot \mu^{-1}\mathbf{H}\mathbf{H}^T \end{aligned} \tag{6.41}$$

Using the results of (6.37)-(6.41) finally we get;

$$\begin{aligned} &\mathbf{C}\mathbf{Q}\mathbf{D}^T + \mathbf{D}\mathbf{Q}\mathbf{C}^T + \rho^{-1}\mathbf{H}\mathbf{H}^T + \varepsilon^{-1}\mathbf{H}\mathbf{H}^T + \tau\xi^{-1}\mathbf{H}\mathbf{H}^T + \tau \cdot \mu^{-1}\mathbf{H}\mathbf{H}^T \\ &+ \rho\mathbf{C}\mathbf{Q}\mathbf{E}_1{}^T\mathbf{E}_1\mathbf{Q}\mathbf{C}^T + \varepsilon\mathbf{C}\mathbf{Q}\mathbf{E}_2{}^T\mathbf{E}_2\mathbf{Q}\mathbf{C}^T + \tau\xi\mathbf{D}\mathbf{Q}\mathbf{E}_2{}^T\mathbf{E}_2\mathbf{Q}\mathbf{D}^T < 0 \end{aligned} \tag{6.42}$$

Recall;

$$\begin{aligned} \mathbf{M} &= \mathbf{Q}\mathbf{A}^T + \mathbf{Q}\mathbf{A}_d^T + \tau \cdot \mathbf{A}_d\mathbf{Q}\mathbf{A}^T + \tau \cdot \mathbf{A}_d\mathbf{Q}\mathbf{A}_d^T \\ &+ \mathbf{A}\mathbf{Q} + \mathbf{A}_d\mathbf{Q} + \tau \cdot \mathbf{A}\mathbf{Q}\mathbf{A}_d^T + \tau \cdot \mathbf{A}_d\mathbf{Q}\mathbf{A}_d^T \\ &+ \rho^{-1}\mathbf{H}\mathbf{H}^T + \varepsilon^{-1}\mathbf{H}\mathbf{H}^T + \tau\xi^{-1}\mathbf{H}\mathbf{H}^T + \tau \cdot \mu^{-1}\mathbf{H}\mathbf{H} \end{aligned}$$

Then (6.42) becomes:

$$\mathbf{M} + \rho\mathbf{C}\mathbf{Q}\mathbf{E}_1{}^T\mathbf{E}_1\mathbf{Q}\mathbf{C}^T + \varepsilon\mathbf{C}\mathbf{Q}\mathbf{E}_2{}^T\mathbf{E}_2\mathbf{Q}\mathbf{C}^T + \tau\xi\mathbf{D}\mathbf{Q}\mathbf{E}_2{}^T\mathbf{E}_2\mathbf{Q}\mathbf{D}^T < 0 \tag{6.43}$$

Using Lemma 6.1 (Schur Complement) to (6.43) we have;

$$\begin{bmatrix} \mathbf{M} & \mathbf{CQE}_1^T & \mathbf{CQE}_2^T & \mathbf{DQE}_2^T \\ \mathbf{E}_1\mathbf{QC}^T & \rho^{-1}\mathbf{I} & \mathbf{0} & \mathbf{0} \\ \mathbf{E}_2\mathbf{QC}^T & \mathbf{0} & \varepsilon^{-1}\mathbf{I} & \mathbf{0} \\ \mathbf{E}_2\mathbf{QD}^T & \mathbf{0} & \mathbf{0} & \tau^{-1}\xi^{-1}\mathbf{I} \end{bmatrix} < 0$$

Theorem 6.2

The time delay uncertain NCS given by (6.29) is asymptotically stable if for a given $\mathbf{Q} = \mathbf{Q}^T > 0$, and scalars $\rho > 0$, $\varepsilon > 0$, $\xi > 0$ and $\mu > 0$, the following holds;

Minimize τ^{-1}

$$\begin{bmatrix} \mathbf{M} + \left(\rho^{-1} + \varepsilon^{-1} + \tau\xi^{-1} + \tau\mu^{-1}\right)\mathbf{HH}^T & (\mathbf{I} + \tau \cdot \mathbf{A}_d)\mathbf{QE}_1^T & (\mathbf{I} + \tau \cdot \mathbf{A}_d)\mathbf{QE}_2^T & (\mathbf{A} + \mathbf{A}_d)\mathbf{QE}_2^T \\ \mathbf{E}_1\mathbf{Q} + \tau \cdot \mathbf{E}_1\mathbf{QA}_d^T & \rho^{-1}\mathbf{I} & \mathbf{0} & \mathbf{0} \\ \mathbf{E}_2\mathbf{Q} + \tau \cdot \mathbf{E}_2\mathbf{QA}_d^T & \mathbf{0} & \varepsilon^{-1}\mathbf{I} & \mathbf{0} \\ \mathbf{E}_2\mathbf{Q}^T\mathbf{A} + \mathbf{E}_2\mathbf{QA}_d^T & \mathbf{0} & \mathbf{0} & \tau^{-1}\xi^{-1}\mathbf{I} \end{bmatrix} < 0$$

This optimization problem can be solved using the LMI toolbox. The theorem in its current form is used to study the stability of the uncertain networked control system and for the controller design, the change of variables and using Schur complement can be used to put it into controller design form. In the following some numerical examples picked from literature are used for comparison.

6.4.2 Examples of Applications

Example 6.4

Consider the uncertain NCS given by:

$$\dot{\mathbf{x}}(t) = \begin{bmatrix} -2 + 0.5\cos t & 0 \\ 0 & -2.5 + 0.6\sin t \end{bmatrix}\mathbf{x}(t) + \begin{bmatrix} -1 + 0.5\cos t & 0 \\ -1 & -1 + 0.6\sin t \end{bmatrix}\mathbf{x}(t - \tau)$$

$$\mathbf{H} = \mathbf{E}_1 = \mathbf{E}_2 = \begin{bmatrix} \sqrt{0.5} & 0 \\ 0 & \sqrt{0.6} \end{bmatrix} \qquad \mathbf{F}(t, \mathbf{x}(t)) = \begin{bmatrix} \cos t & 0 \\ 0 & \sin t \end{bmatrix}$$

Solving the optimization problem in Theorem 6.2 with the LMI Matlab toolbox, the MADB is 0.8356 s. In (Lu et al. 2002) the MADB is 10.6742 s and in (Su et al. 1992) it is 0.857 s and in (Cao et al. 1998) the MADB is 0.1381 s. Even Theorem 6.2 still gives more conservative results the method is simpler and involves less computation. The system response with 0.8356 s time delay is shown in Figure 6.12 and clearly the system is stable.

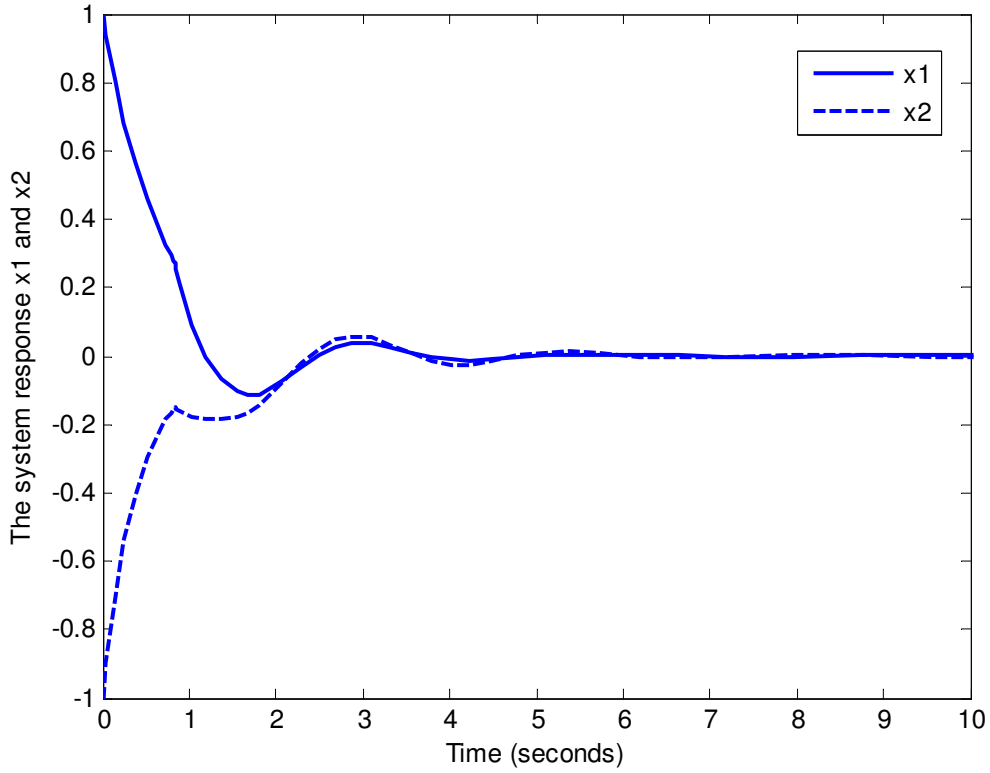

Figure 6.12 The uncertain NCS with 0.8356 s time delay.

Example 6.5:

Consider the uncertain NCS given by:

$$\dot{\mathbf{x}}(t)=\begin{bmatrix}-2+0.2\cos t & 0\\ 1 & -3+0.2\sin t\end{bmatrix}\mathbf{x}(t)+\begin{bmatrix}-1.4+0.2\cos t & 0\\ -0.8 & -1.5+0.2\sin t\end{bmatrix}\mathbf{x}(t-\tau)$$

$$\mathbf{H}=\begin{bmatrix}0.2 & 0\\ 0 & 0.2\end{bmatrix}\qquad \mathbf{E}_1=\mathbf{E}_2=\begin{bmatrix}1 & 0\\ 0 & 1\end{bmatrix}\qquad \mathbf{F}(t,\mathbf{x}(t))=\begin{bmatrix}\cos t & 0\\ 0 & \sin t\end{bmatrix}$$

Using Theorem 6.2 the MADB is 0.6666 s. For the deterministic system the MADB is 0.6666 s. In (Lu et al. 2002) the MADB is 1.3686 s. In (Li et al. 1997) the MADB is 0.3142 s. In (Su 1994) the MADB is 0.2117 s. In (Liu et al. 1998) the MADB is 0.3025 s. The system response is shown in Figure 6.13 with 0.6667 s time delay.

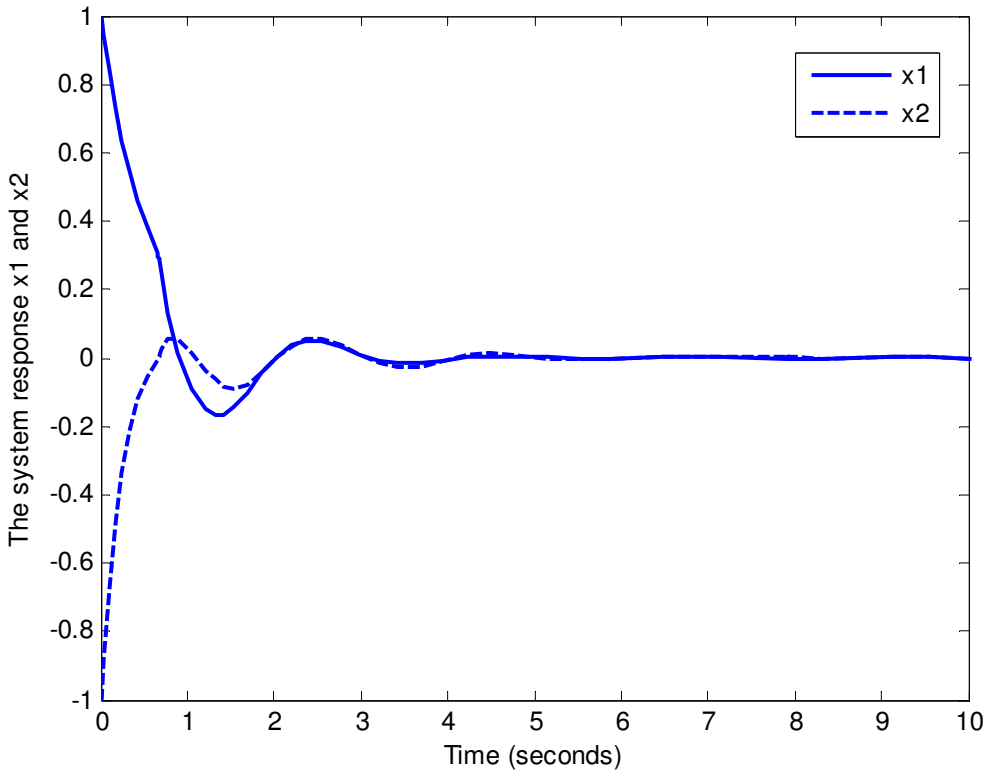

Figure 6.13 The uncertain NCS with 0.6667 s time delay.

Example 6.6:

Consider the uncertain following NCS:

$$\dot{\mathbf{x}}(t)=\begin{bmatrix}-2+0.3\cos t & 0\\ 0 & -1+0.2\sin t\end{bmatrix}\mathbf{x}(t)+\begin{bmatrix}-1+0.2\cos t & 0\\ -1 & -1+0.3\sin t\end{bmatrix}\mathbf{x}(t-\tau)$$

$$\mathbf{H}=\begin{bmatrix}1 & 0\\ 0 & 1\end{bmatrix}\quad \mathbf{E}_1=\begin{bmatrix}0.3 & 0\\ 0 & 0.2\end{bmatrix}\quad \mathbf{E}_2=\begin{bmatrix}0.2 & 0\\ 0 & 0.3\end{bmatrix}\quad \mathbf{F}(t,\mathbf{x}(t))=\begin{bmatrix}\cos t & 0\\ 0 & \sin t\end{bmatrix}$$

Using Theorem 6.2 the MADB is estimated to be 0.9071 s. In (Su et al. 1992) the MADB is 0.1614 s. In (Cao et al. 1998) the MADB is 0.2558 s. In (Yan et al. 2008) the MADB is 0.609 s. The system response with 0.9071 s is shown in Figure 6.14 and the system is stable.

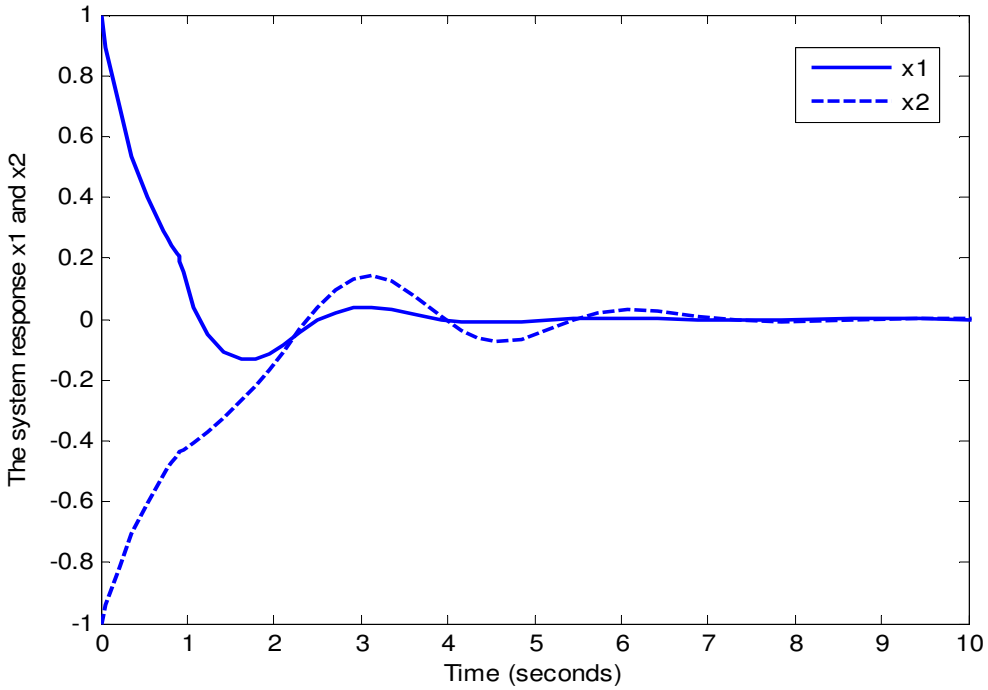

Figure 6.14 The uncertain system with 0.907 s time delay.

6.5 Summary

The method proposed for the networked control systems in Chapter 3 has been extended to study the stability of nonlinear networked control systems and uncertain networked control systems. The nonlinear networked control system under study has the structure of a linearized system model augmented with uncertainties and nonlinear perturbations. The nonlinearity is assumed to be bounded and satisfy a linear quadratic restriction inequality. A new theorem has been derived, which is based on using the finite difference approximation for the delay term. The theorem is in LMI form, which can be easily solved using the Matlab LMI Toolbox. Applying the theorem, the MADB can be estimated for the nonlinear system which provides the important information in scheduling the network. A number of examples have been studied, and the method showed comparable results with those published previously while the method is very easy to use. It is found that the MADB decreases with increasing the nonlinearity boundary values, and the time delay increase will result in shrinking the domain of attraction for the nonlinear networked control system. A simple analytical relation between the maximum permissible nonlinearity and the time delay bound has been derived. An NCS with norm bounded uncertainty has been studied in this chapter. The uncertain NCS can represent a distributed energy system with uncertainties caused either from the measurement or the slowly time-varying parameters. A stability theorem in LMI form is derived, and the results of the method are compared with the results of the methods available in the literature. In some examples, the proposed method is less conservative. We noticed that the MADB decreases with increasing the uncertainty bound.

CHAPTER SEVEN: CONCLUSIONS AND FUTURE WORK

The stabilization of networked distributed energy control systems is studied in this thesis. The two main issues in these systems are the time delay and data dropouts that can bring instability to the system. The data dropouts are considered as a special case of the time delay. A necessary part in the controller design is to take the time delay into account and to identify the time delay characteristics. The work described in the thesis has reported my progress and contributions in this area.

My major contributions and conclusions drawn from the study are summarized in this chapter and the direction of the possible future work is suggested.

7.1 Main Conclusions

It is necessary to understand the networks used in networked control systems, and the time delay characteristics induced in the NCSs; the first part of the thesis was dedicated to study the time delay characteristics in shared networks. From my study, it is found:

- The time delay in shared networks can be constant, periodic, random but bounded, random governed by Markov Chain and, in some cases, random but unbounded. In the cases with the first four types of delays, the controller can be designed, and the stability can be analyzed but in the last case where the time delay is unbounded, the main requirement for the NCS stability is not fulfilled, which is the guarantee of receiving the information within a bounded period of time.
- The types of time delays depend on the network characteristics. The parameters that affect the time delays are: the network protocol, the bit rate, the message priority, the message length and the network utilization.
- Two candidate control networks were chosen in my study, which are the Ethernet and the CAN. The transmission can be guaranteed in the CAN even with high network utilization while in the Ethernet it cannot be because the Ethernet is a non prioritized protocol.

For the case where the time delay is bounded, the worst-case time delay can be used as an extra factor for the controller design. The method for estimating the MADB is proposed, which can help in the network scheduling. The following merits have been proven in the research:

- The method for estimating the MADB presented in Chapter 3 is built on the assumption that the finite difference approximation for the delay term can be used without significant error, and this can be true for the following reasons: Firstly, the time delay in a computer network is very small in order of milli- or micro seconds and at the worst few tenth of the second. Secondly, in most of the real control sys-

tem applications the linearized model is used, which is based on neglecting the higher-order terms. Finally, the performance of the systems with a significant higher-order term is not accepted from control system engineering view point.

- The method has been used to estimate the MADB in NCSs. The results of the method demonstrated the advantages compared with most of the methods reported in the previous literature; in addition, the method has a simple structure and easy to use in practice.
- The method has been applied to different types of NCSs; these are NCS with state feedback controller, NCS with dynamic controller and to networked control of a distributed interconnected system. As a case study the method has been applied to a power system consists of three interconnected synchronous generators, and the simulation results show that the estimated MADB lies within the stability margin of the system and can be achieved with the current network technology.

It is found that the time delay of NCSs in some cases can be modelled using Markov Chain and in this situation, the system becomes a hybrid stochastic system, and the stochastic stability analysis approach has to be used to study the stability of the system. From the study, the following points are found:

- For the robust stability of a networked distributed energy system with random time delay the controller design problem has the form of BMI, which is difficult to be solved directly. Using the V-K iteration algorithm the BMI problem can be solved, and we found that the algorithm can achieve the local optimum controller. This means the algorithm improves the decay rate in every iteration.

- In order to achieve more robustness another V-loop and K-loop are nested in the algorithm, this can improve the decay rate.
- The initialization is a crucial part in solving the BMI. For the initialization, we can start with any aggressive initial controller and probability transition matrix as the problem is feasible.
- The proposed method for estimating the MADB has been used to estimate the MADB with the initial and the derived controller, and we found that increasing the robustness of the controller results in increasing the MADB. This means choosing the MADB to be larger than the worst-case network time delay can achieve the controller robustness against the time delay.
- When the time delay is modelled using Markov Chain, the system will have many modes. The stability of every node is not necessary for the mean square stability of the system.

The parallel DC/DC converter system controlled through a shared network has been studied in Chapter 5. The method for estimating the MADB is applied to estimate the MADB for three parallel DC/DC buck converters, and the simulation results show that the MADB lies within the estimated MADB range. The parameters that affect the MADB are studied, and we found that the output feedback gain, the voltage controller gain and the load resistance affect the MADB strongly. Three different network scenarios have been studied, where the time delay is constant, periodic and random but bounded. In all these cases when the MADB is selected to be larger than the worst-case time delay the stability of the system is guaranteed, which is simpler with less computation time compared with the other approaches.

The parameters that affect the MADB are used to study the stochastic stability of the parallel DC/DC buck converters. The stochastic controller can guarantee the stability of the system even if the MADB is less than the worst-case network time delay.

The proposed method has been extended for NCS with norm bounded nonlinearity and to uncertain NCS. For the NCS with norm bounded nonlinearity two stability criteria are derived. One of the stability theorems (Theorem 6.1) is in LMI form, and the other is in an analytical form (Corollary 6.1). We found:

- For the NCS with bounded nonlinearity increasing the maximum nonlinearity bound decreases the MADB.
- The analytical criterion, Corollary 6.1, showed that increasing the time delay decreases the domain of attraction.
- A stability theorem for a class of uncertain NCS has been derived. Compared with the published methods the proposed method is much simpler while giving comparable results.

7.2 Suggested Future Work

The research work can be continued from what the thesis has achieved and the work reported in the thesis led me to believe the following future work should be carried out with future funding support.

- Even with the advances in network technology we believe that the doors are open for newer applications to NCSs. The main obstacle is the current methods for studying the NCS, because they still use the same classical view to the large and complex systems. The plug and play functionality needs more intelligent techniques to deal with the control coordination between the distributed interconnected systems. Inventing new techniques can lead to more applications to NCSs. Improving the network protocol such as using the switching Ethernet can enhance the performance of the NCSs greatly.
- The proposed method in Chapter 3 needs more improvement to derive conditions for using the finite difference approximation and this of course will depend on studying the higher derivatives of the system. By this, the error in the method can be roughly estimated.
- In the V-K iteration algorithm, the solution time is considerable long and this is because the whole system interactions need to be considered in the model. We suggest using simpler models that represents the interaction between the distributed interconnected units.
- Studying the stability of the nonlinear NCS is very rich research area. For distributed energy system such as the power system, the stability over a wide range of operating points is necessary and hence the models will be nonlinear.

References

[1] Acharya, K., Tahir, M., & Mazumder, S. K., 2006. Communication fault-tolerant wireless network control of a load-sharing multiphase interactive power network, *In 37th IEEE Power Electronics Specialists Conference, June 18-22*, Jeju, Republic of Korea: IEEE, pp. 1-8.

[2] Ait-Rami, M. & El Ghaoui, L., 1995. H_∞ state-feedback control of jump linear systems, *In Proceedings of 1995 34th IEEE Conference on Decision and Control, 13-15 Dec*, New York, NY, USA: IEEE, pp. 951-952.

[3] Andersson, M., Henriksson, D., Cervin, A., & Arzen, K. E., 2005. Simulation of wireless networked control systems, *In 44th IEEE Conference on Decision and Control, and the European Control Conference, December 12-15,* Seville, Spain: IEEE, pp. 476-481.

[4] Antsaklis, P. J., 2006. Networked Control Systems Research: A Brief Discussion of Challenges and Opportunities, *Workshop on: Beyond SCADA: Networked Embedded Control for Cyber-Physical Systems , 8-9 November*, Pittsburgh, PA: pp. 1-3.

[5] Antunes, D., Hespanha, J. P., & Silvestre, C., 2009. Stability of impulsive systems driven by renewal processes, *In Proceedings of 2009 American Control Conference,* pp. 4032-4037.

[6] Baillieul, J. & Antsaklis, P.J., 2007. Control and communication challenges in networked real-time systems. *Proceedings of the IEEE*, 95, (1) 9-28

[7] Banjerdpongchai, D., 1997 *Parametric Robust Controller Synthesis Using Linear Matrix Inequalities*. University of Stanford.

[8] Beccuti, A. G. & Morari, M., 2006. A distributed solution approach to centralized emergency voltage control, *In the Proceedings of the 2006 American Control Conference, 14-16 June*, Piscataway, NJ, USA: IEEE, pp. 3445-3450.

[9] Bhowmik, S., Tomsovic, K., & Bose, A., 2004. Communication models for third party load frequency control. *IEEE Transactions on Power Systems*, 19, (1) 543-548

[10] Bosch, R. CAN Specifications. Stuttgart, Germany, 1991, Robert Bosch GmbH, Postfach.

[11] Bose, A., 2004. Designing the next generation real-time control, communications and communication system for the electricity infrastructure, *In 2004 IEEE Power Engineering Society General Meeting, 6-10 June*, Piscataway, NJ, USA: IEEE, p. 2.

[12] Bose, A., 2005. Improved communication/computation infrastructure for better monitoring and control, *In 2005 IEEE Power Engineering Society General Meeting, 12-16 June*, Piscataway, NJ, USA: IEEE, pp. 2715-2716.

[13] Boukas, E. K. & Shi, P., 1997. H_∞ control for discrete-time linear systems with Markovian jumping parameters, *In Proceedings of the 36th IEEE Conference on Decision and Control*, pp. 4134-4139.

[14] Boyd, S., El Ghaoui, L., Feron, E., & Balakrishan, V., 1995. Linear matrix inequalities in system and control theory. *SIAM Review*, 37, (3) 479

[15] Branicky, M. S., Phillips, S. M., & Wei, Z., 2000. Stability of networked control systems: explicit analysis of delay, *In Proceedings of 2000 American Control Conference, 28-30 June*, Danvers, MA, USA, pp. 2352-2357.

[16] Branicky, M. S., Phillips, S. M., & Wei, Z., 2002. Scheduling and feedback co-design for networked control systems, *In Proceedings of the 41st IEEE Conference on Decision and Control*, pp. 1211-1217.

[17] Cao, Y.-Y., Sun, Y.-X., & Cheng, C., 1998. Delay-dependent robust stabilization of uncertain systems with multiple state delays. *IEEE Transactions on Automatic Control*, 43, (11) 1608-1612

[18] Casavola, A. & Franze, G., 2008. Coordination strategies for networked control systems: A power system application, *In 10th International Conference on Control, Automation, Robotics and Vision*, pp. 503-508.

[19] Chan, W.-C. & Hsu, Y.-Y. 1983. An Optimal Variable Structure Stabilizer for Power System Stabilization. *IEEE Transactions on Power Apparatus and Systems*, (6) 1738-1746

[20] Chang, L.-F. & Li, H.-G., 2005. A class of nonlinear networked control system based on exact T-S model, *In Proceedings of 2005 International Conference on Machine Learning and Cybernetics, 18-21 Aug*, Piscataway, NJ, USA: IEEE, pp. 808-812.

[21] Chen, C.L. & Hsu, Y.Y. 1987. Coordinated Synthesis of Multimachine Power System Stabilizer Using an Efficient Decentralized Modal Control (DMC) Algorithm. *IEEE Transactions on Power Systems*, 2, (3) 543-550

[22] Cheng, L., Kong, L., Ma, C., & Zhu, X. 2007. Stability and Maximum Delay Bound of Networked Control Systems with Multi-Step. *Information Technology Journal*, 6, (5) 780-783

[23] Chenine, M., Nordstrom, L., & Johnson, P., 2007. Factors in assessing performance of wide area communication networks for distributed control of power systems, *In 2007 IEEE Lausanne POWERTECH, July 1-5*, Lausanne, Switzerland: IEEE, pp. 1682-1687.

[24] Chow, M.-Y. & Tipsuwan, Y., 2001. Network-based control systems: a tutorial, *In 27th Annual Conference of the IEEE Industrial Electronics Society, 29 Nov.-2 Dec*, Piscataway, NJ, USA: IEEE, pp. 1593-1602.

[25] Corrigan, S. 2008, *Controller Area Network Physical Layer Requirements*, Texas Instruments, SLLA270.

[26] Cory, B.J. & Gale, P.F. 1993. Satellites for power system applications. *Power Engineering Journal*, 7, (5) 201-207

[27] Costa, O.L.V. 1993. Stability Results for Discrete-Time Linear Systems with Markovian Jumping Parameters. *Journal of Mathematical Analysis and Applications*, 197, 154-178

[28] De Brabandere, K., Bolsens, B., Van den Keybus, J., Woyte, A., Driesen, J., Belmans, R., & Leuven, K. U., 2004. A voltage and frequency droop control method for parallel inverters, *In 2004 IEEE 35th Annual Power Electronics Specialists Conference, 20-25 June*, Piscataway, NJ, USA: IEEE, pp. 2501-2507.

[29] De Souza, C. E. & Li, X. 1995. Delay-dependent stability of linear time-delay systems: an LMI approach, *In IEEE Mediterranean Symposium on Control and Automation*, pp. 201-205.

[30] De Souza, C. E. & Fragoso, M. D., 1997. H_∞ filtering for discrete-time linear systems with Markovian jumping parameters, *In Proceedings of the 36th IEEE Conference on Decision and Control*, pp. 2181-2186.

[31] De Souza, C. E., 2003. A mode-independent H_∞ filter design for discrete-time Markovian jump linear systems, *In Proceedings of the 42nd IEEE Conference on Decision and Control*, pp. 2811-2816.

[32] El Ghaoui, L. & Rami, M.A. 1996. Robust state-feedback stabilization of jump linear systems via LMIs. *International Journal of Robust and Nonlinear Control*, 6, (9-10) 1015-1022

[33] Ericsson, G. 1998. Communication utilization in power system control. A state-of-the-practice description. *IEEE Transactions on Power Delivery*, 13, (4) 984-989

[34] Fardanesh, B. 2002. Future trends in power system control. *IEEE Computer Applications in Power*, 15, (3) 24-31

[35] Fleming, R.J., Mohan, M.A., & Parvatisam, K. 1981. Selection of Parameters of Stabilizers in Multimachine Power Systems. *Power Apparatus and Systems, IEEE Transactions on*, PAS-100, (5) 2329-2333

[36] Gahinet, P., Nemirovski, A., Laub, A. J., & Chilali, M., 1995. LMI Control Toolbox for Use with Matlab. version 1. The MathWorks, Inc.

[37] Ganjefar, S. & Rezaei, M. 2009. A new method to control dynamic stability of power system through wave variables and signal prediction via internet. *International Journal of Recent Trends in Engineering*, 1, (1) 62-66

[38] Golub, G.H. & C.F.Van Loan 1989. *Matrix Computations* Johns Hopkins University Press.

[39] Goodall, D.P. & Wang, J. 2001. Stabilization of a class of uncertain nonlinear affine systems subject to control constraints. *International Journal of Robust and Nonlinear Control*, 11, (9) 797-818

[40] Green, T.C. & Prodanovic, M. 2007. Control of inverter-based micro-grids. *Electric Power Systems Research*, 77, (9) 1204-1213

[41] Gu, K., Kharitonov, V.L., & Chen, J. 2003. *Stability of Time Delay Systems* Boston, Birkhauser.

[42] Guerrero, J.M., de Vicuna, L.G., Matas, J., Castilla, M., & Miret, J. 2004. A wireless controller to enhance dynamic performance of parallel inverters in distributed generation systems. *IEEE Transactions on Power Electronics*, 19, (5) 1205-1213

[43] Guerrero, J.M., Matas, J., de Vicuna, L.G., Castilla, M., & Miret, J. 2006. Wireless-control strategy for parallel operation of distributed-generation inverters. *IEEE Transactions on Industrial Electronics*, 53, (5) 1461-1470

[44] Hanmandlu, M. & Suryanarayana, N.V. 1993. High-gain stabilizer for a multimachine power system. *IEE Proceedings D: Control Theory and Applications*, 140, (5) 293-297

[45] Hardiansyah, Seizo, F., & Juichi, I. 2000. The Dynamic Stability Improvement of Multimachine Power Systems by Multilevel Optimal Control. *Technical report of the Technological University of Nagaoka*, 21, 15-20

[46] Hassibi, A., How, J., & Boyd, S., 1999. A path-following method for solving BMI problems in control, *In Proceedings of the 1999 American Control Conference, 2-4 June*, Piscataway, NJ, USA: IEEE, pp. 1385-1389.

[47] Hauser, C.H., Bakken, D.E., & Bose, A. 2005. A failure to communicate: next generation communication requirements, technologies, and architecture for the electric power grid. *IEEE Energy Magazine*, 3, (2) 47-55

[48] Henriksson, D. & Cervin, A., 2004. TRUETIME 1.2—Reference Manual. Sweden, Department of Automatic Control: Lund Institute of Technology.

[49] Henriksson, D., Cervin, A., Andersson, M., & Arzen, K. E., 2006. TrueTime: simulation of networked computer control systems, *In Proceedings of the 2nd IFAC Conference on Analysis and Design of Hybrid Systems, 7-9 June*, Italy, Italy: IFAC, pp. 272-273.

[50] Holbert, K.E., Heydt, G.I., & Hui, N. 2005. Use of satellite technologies for power system measurements, command, and control. *Proceedings of the IEEE*, 93, (5) 947-955

[51] Huang, D. & Nguang, S. K., 2006. State feedback guaranteed cost control of uncertain networked control, *In 1st International Symposium on Systems and Control in Aerospace and Astronautics, January 19-21*, Harbin, China: IEEE, pp. 858-863.

[52] Jian, S., Liu, G., & Jie, C., 2008. State feedback stabilization of networked control systems, *In Proceedings of 2008 Chinese Control Conference, 16-18 July*, Piscataway, NJ, USA: IEEE, pp. 457-461.

[53] Jiang, X., Han, Q.L., Liu, S., & Xue, A. 2008. A new H_∞ stabilization criterion for networked control systems. *IEEE Transactions on Automatic Control*, 53, (4) 1025-1032

[54] Jiang, X. & Han, Q.-L. 2008. On designing fuzzy controllers for a class of nonlinear networked control systems. *IEEE Transactions on Fuzzy Systems*, 16, (4) 1050-1060

[55] Jing, W., Liqian, Z., & Tongwen, C., 2007. An MPC Approach to Networked Control Design, *In Proceedings of 2007 Chinese Control Conference*, pp. 10-14.

[56] Ju, H., Ding, M., Su, J., Du, Y., & Chang, L., 2007. Communicationless parallel inverters based on inductor current feedback control, *In Proceedings of 22nd Annual IEEE Applied Power Electronics Conference and Exposition, Febrary 25, 2007 - March 1*, Anaheim, CA, United states: IEEE., pp. 1385-1389.

[57] Jun, M. & Safonov, M. G., 2000. Stability analysis of a system with time-delayed states, *In Proceedings of 2000 American Control Conference, 28-30 June*, Danvers, MA, USA, pp. 949-952.

[58] Katiraei, F., Iravani, R., Hatziargyriou, N., & Dimeas, A. 2008. Microgrids management. *IEEE Energy Magazine*, 6, (3) 54-65

[59] Khalil, A. F. & Wang, J., 2010. A new stability and time-delay tolerance analysis approach for Networked Control Systems, *In Proceedings of 49th IEEE Conference on Decision and Control*, pp. 4753-4758.

[60] Khalil, A. F. & Wang, J. 2010. A New Stability Analysis and Time-Delay Tolerance Estimation Approach for Output Feedback Networked Control Systems, *In United Kingdom International Control Conference*, pp. 4753-4758.

[61] Khalil, A. F. & Wang, J., 2011 A New Method for Estimating the Maximum Allowable Delay in Networked Control of bounded nonlinear systems, *In Proceedings of 17th International Conference on Automation and Computing*, pp. 80-85.

[62] Khalil, H.K. 1992. *Nonlinear Systems* Macmillan Publishing Company.

[63] Kim, D.S., Lee, Y.S., Kwon, W.H., & Park, H.S. 2003. Maximum allowable delay bounds of networked control systems. *Control Engineering Practice*, 11, (11) 1301-1313

[64] Kim, K. 2005. A Delay-Dependent Stability Criterion In Time Delay System. *The Korean Society for Industrial and Applied Mathematics,* 9, (2) 1-11

[65] Kok, K., Warmer, C., Kamphuis, R., Mellstrand, P., & Gustavsson, R., 2005. Distributed control in the electricity infrastructure, *In 2005 International Conference on Future Power Systems, 16-18 Nov*, Piscataway, NJ, USA: IEEE, pp. 1-7.

[66] Lachs, W.R., Sutanto, D., & Logothetis, D.N. 1996. Power system control in the next century. *IEEE Transactions on Power Systems*, 11, (1) 11-18

[67] Lai, Y.M., Tan, S.C., & Tsang, Y.M., 2009. Wireless control of load current sharing information for parallel-connected DC/DC power converters. *Power Electronics, IET*, 2, (1) 14-21

[68] Lasseter, B., 2001. Microgrids [distributed power generation], *In Proceedings of 2001 Winter Meeting of the IEEE Power Engineering Society, 28 Jan.-1 Feb*, Piscataway, NJ, USA: IEEE, pp. 146-149.

[69] Lasseter, R. H. & Paigi, P., 2004. Microgrid: a conceptual solution, *In 2004 IEEE 35th Annual Power Electronics Specialists Conference, 20-25 June*, Piscataway, NJ, USA: IEEE, pp. 4285-4290.

[70] Lee, S. & Park, J. 1998. Design of power system stabilizer using observer/sliding mode, observer/sliding mode-model following and H_∞/sliding mode controllers for small-signal stability study. *International Journal of Electrical Power & Energy Systems*, 20, (8) 543-553

[71] Li, X. & De Souza, C.E. 1997. Delay-dependent robust stability and stabilization of uncertain linear delay systems: a linear matrix inequality approach. *IEEE Transactions on Automatic Control*, 42, (8) 1144-1148

[72] Lian, F.-L., Moyne, J.R., & Tilbury, D.M. 2001. Performance evaluation of control networks: Ethernet, ControlNet, and DeviceNet. *IEEE Control Systems Magazine*, 21, (1) 66-83

[73] Ling, W., Ding, X., & E, D., 2007. Some basic issues in networked control systems, *In 2007 Second IEEE Conference on Industrial Electronics and Applications, 23-25 May*, Piscataway, NJ, USA: IEEE, pp. 2098-2102.

[74] Liu, L.-M., Tong, C.-N., & Zhang, H.-J., 2005. Analysis and design of networked control systems with long delays based on Markovian jump model, *In Proceedings of 2005 International Conference on Machine Learning and Cybernetics, 18-21 Aug*, Piscataway, NJ, USA: IEEE, pp. 953-959.

[75] Liu, L.-M. & Tong, C.-N., 2008. Stabilization design of networked control systems, *In 2008 International Conference on Machine Learning and Cybernetics, 12-15 July*, Piscataway, NJ, USA: IEEE, pp. 2137-2142.

[76] Liu, P.-L. & Su, T.-J. 1998. Robust stability of interval time-delay systems with delay-dependence. *Systems & Control Letters*, 33, (4) 231-239

[77] Liu, P.-L. 2003. Exponential stability for linear time-delay systems with delay dependence. *Journal of the Franklin Institute*, 340, (6-7) 481-488

[78] Lu, C.Y., Tsai, J.S.-H., & Su, T.J. 2002. On improved delay-dependent robust stability criteria for uncertain systems with multiple-state delays. *IEEE Transactions on Circuits and Systems I: Fundamental Theory and Applications*, 49, (2) 253-256

[79] Ma, D., Dimirovski, G. M., Stefanovski, J. D., & Zhao, J., 2006. Exponential stability synthesis of networked nonlinear control systems in FMS, *In 2006 IEEE International Conference on Mechatronics, ICM, July 3-5*, Budapest, Hungary, pp. 414-419.

[80] Mahmoud, M.S. & Al-Muthairi, N.F. 1994. Quadratic stabilization of continuous time systems with state-delay and norm-bounded time-varying uncertainties. *IEEE Transactions on Automatic Control*, 39, (10) 2135-2139

[81] Mahmoud, M. S. & Ismail, A., 2003. Role of delays in networked control systems, *In Proceedings of the 10th IEEE International Conference on Electronics, Circuits, and Systems, 14-17 Dec*, Piscataway, NJ, USA: IEEE, pp. 40-43.

[82] Mahmoud, M.S. 2000. *Robust Control and Filtering For Time Delay systems* New York, Marcel Dekker, Inc.

[83] Mak, K.-H. & Holland, B. 2002. Migrating electrical power network SCADA systems to TCP/IP and Ethernet networking. *Power Engineering Journal*, 16, (6) 305-311

[84] Markvart, T. 2006. Microgrids. Power systems for the 21st Century? *Refocus*, 7, (4) 44-48

[85] Marshall, J.E., Gorecki, H., Korytowski, A., & Walton, K. 1992. *Time-Delay Sysytems: Stability and Performance Criteria with Applications* Ellis Horwood.

[86] Marwali, M.N., Jin-Woo, J., & Keyhani, A. 2004. Control of distributed generation systems - Part II: Load sharing control. *IEEE Transactions on Power Electronics*, 19, (6) 1551-1561

[87] Mazumder, S.K., Tahir, M., & Kamisetty, S.L. 2005. Wireless PWM control of a parallel DC-DC buck converter. *IEEE Transactions on Power Electronics*, 20, (6) 1280-1286

[88] Mazumder, S.K., Tahir, M., & Acharya, K. 2008. Master-slave current-sharing control of a parallel dc-dc converter system over an RF communication interface. *IEEE Transactions on Industrial Electronics*, 55, (1) 59-66

[89] Mazumder, S.K. & Acharya, K. 2008. Multiple Lyapunov function based reaching condition for orbital existence of switching power converters. *IEEE Transactions on Power Electronics*, 23, (3) 1449-1471

[90] Mazumder, S.K., Tahir, M., & Acharya, K. 2010. An Integrated Modeling Framework for Exploring Network Reconfiguration of Distributed Controlled Homogenous Power Inverter Network using Composite Lyapunov Function Based Reachability Bound. *Simulation*, 86, (2) 75-92

[91] Meyer, C.D. 2000. *Matrix Analysis and Applied Linear Algebra* SIAM.

[92] Middlebrook, R. D. & Cuk, S. 1976, A generalized Unified Approach to Modelling Switching-Converter Power Stages, *IEEE Power Electronics Specialists Conference*, pp. 73-86.

[93] Millan, P., Jurado, I., Vivas, C., & Rubio, F. R., 2008. An algorithm to compensate for large data dropouts in Networked control systems, *In IEEE International Conference on Emerging Technologies and Factory Automation, 2008*, pp. 105-112.

[94] Mohd, A., Ortjohann, E., Morton, D., & Omari, O. 2010. Review of control techniques for inverters parallel operation. *Electric Power Systems Research*, 80, (12) 1477-1487

[95] Montestruque, L.A. & Antsaklis, P. 2004. Stability of Model-Based Networked Control Systems With Time-Varying Transmission Times . *IEEE Transactions on Automatic Control*, 49, (9) 1562-1572

[96] Moore, P. & Crossley, P. 1999. GPS applications in power systems. Part 1. Introduction to GPS. *Power Engineering Journal*, 13, (1) 33-39

[97] Mori, T. 1985. Criteria for asymptotic stability of linear time-delay systems. *IEEE Transactions on Automatic Control*, AC-30, (2) 158-161

[98] Mori, T. & Kokame, H. 1989. Stability of $x(t)=Ax(t)+Bx(t-\tau)$. *IEEE Transactions on Automatic Control,* , 34, (4) 460-462

[99] Naduvathuparambil, B., Valenti, M. C., & Feliachi, A., 2002. Communication delays in wide area measurement systems, *In Proceedings of the Thirty-Fourth Southeastern Symposium on System Theory, 18-19 March*, Piscataway, NJ, USA: IEEE, pp. 118-122.

[100] Naghshtabrizi, P. 2007. *Delay Impulsive Systems: A Framework For Modeling Networked Control Systems.* PhD University of California Santa Barbara.

[101] Nesic, D. & Teel, A.R. 2004. Input-output stability properties of networked control systems. *IEEE Transactions on Automatic Control*, 49, (10) 1650-1667

[102] Nilsson, J. 1998. *Real-time Control Systems with Delays.* PhD Lund Institute of Technology.

[103] Ogata, K. 1996. *Modern Control Engineering*, third ed. Prentice Hall.

[104] Park, H.S., Kim, Y.H., Kim, D.-S., & Kown, W.H. 2002. A scheduling method for network-based control systems. *IEEE Transactions on Control Systems Technology*, 10, (3) 318-330

[105] Parlakci, M.N.A. 2006. Robust stability of uncertain time-varying state-delayed systems. *IEE Proceedings-Control Theory and Applications*, 153, (4) 469-477

[106] Peng, C., Tian, Y.C., & Tade, M.O. 2008. State feedback controller design of networked control systems with interval time-varying delay and nonlinearity. *International Journal of Robust and Nonlinear Control*, 18, (12) 1285-1301

[107] Peng, C. & Yue, D. 2006. State feedback controller design of networked control systems with parameter uncertainty and state-delay. *Asian Journal of Control*, 8, (4) 385-392

[108] Pogaku, N., Prodanovic, M., & Green, T.C. 2007. Modeling, analysis and testing of autonomous operation of an inverter-based microgrid. *IEEE Transactions on Power Electronics*, 22, (2) 613-625

[109] Prodanovic, M., Green, T.C., & Mansir, H. 2000. Survey of control methods for three-phase inverters in parallel connection. *IEE Conference Publication* (475) 472-477

[110] Prodanovic, M. & Green, T.C. 2006. High-quality power generation through distributed control of a power park microgrid. *IEEE Transactions on Industrial Electronics*, 53, (5) 1471-1482

[111] Ren, J., Li, C.-W., & Zhao, D.-Z. 2009. CAN-based synchronized motion control for induction motors. *International Journal of Automation and Computing*, 6, (1) 55-61

[112] Sadeghzadeh, N., Afshar, A., & Menhaj, M. B., 2008. An MLP neural network for time delay prediction in networked control systems, *In Proceedings of 2008 Chinese Control and Decision Conference*, pp. 5314-5318.

[113] Shanxu, D., Yu, M., Jian, X., Yong, K., & Jian, C., 1999. Parallel operation control technique of voltage source inverters in UPS, *In Proceedings of Third IEEE International Conference on Power Electronics and Drive Systems, 27-29 July*, Piscataway, NJ, USA: IEEE, pp. 883-887.

[114] Shaobu, W., Xiangyu, M., & Tongwen, C. 2012. Wide-Area Control of Power Systems Through Delayed Network Communication. *IEEE Transactions on Control Systems Technology*, 20, (2) 495-503

[115] Shi, P. & Boukas, E. K., 1998. Control for Markovian jumping discrete-time systems with different forms of uncertainties, *In Proceedings of the 1998 American Control Conference*, pp. 728-732.

[116] Shi, Y. & Yu, B. 2009. Output Feedback Stabilization of Networked Control Systems With Random Delays Modeled by Markov Chains. *IEEE Transactions on Automatic Control,* , 54, (7) 1668-1674

[117] Shi, Y., Yu, B., & Huang, J., 2009. Mixed H_2/H_∞ control of networked control systems with random delays modeled by Markov chains, *In Proceedings of 2009 American Control Conference*, pp. 4038-4043.

[118] Sidhu, T. S., Demeter, E., & Faried, S. O., 2004. Power system protection and control integration over Ethernet-based communication channels, *In Canadian Conference on Electrical and Computer Engineering, 2-5 May*, Piscataway, NJ, USA: IEEE, pp. 225-228.

[119] Siljak, D.D. & Stipanovic, D.M. 2000. Robust Stabilization of Nonlinear Systems: The LMI Approach. *Mathematical Problems in Engineering*, 6, 461-493

[120] Siri, K. & Lee, C. Q., 1990. Current distribution control of converters connected in parallel, *In Conference Record of the 1990 IEEE Industry Applications Society Annual Meeting, 7-12 Oct*, New York, NY, USA: IEEE, pp. 1274-1280.

[121] St Iliescu, S. & Fagarasan, I., 2008. Modern approaches in power system control, *In 2008 IEEE International Conference on Automation, Quality and Testing, Robotics, 22-25 May*, Piscataway, NJ, USA: IEEE, pp. 41-44.

[122] Su, J.-H. 1994. Further results on the robust stability of linear systems with a single time delay. *Systems & Control Letters*, 23, (5) 375-379

[123] Su, T.J. & Huang, C.G. 1992. Robust stability of delay dependence for linear uncertain systems. *IEEE Transactions on Automatic Control*, 37, (10) 1656-1659

[124] Sui, S., Zhu, K., Zhai, W., & Zhuang, G. 2010. Simulation research of networked control systems based on TrueTime. *Microcomputer Information* (13) 38-39

[125] Sun, J. & Liu, G. P., 2006. Robust stabilization of a class of nonlinear networked control systems, *In 25th Chinese Control Conference, August 7-11*, Harbin, China: IEEE, pp. 2035-2040.

[126] Sun, Y. & El-Farra, N.H. 2008. Quasi-decentralized model-based networked control of process systems. *Chemical Engineering*, 32, (9) 2016-2029

[127] Tabbara, M., Nesic, D., & Teel, A.R. 2007. Stability of Wireless and Wireline Networked Control Systems. *Automatic Control*, 52, (9) 1615-1630

[128] Tabbara, M., Neic, D., & Teel, A. R., 2005. Input-output stability of wireless networked control systems, *In 44th IEEE Conference on Decision and Control, and the European Control Conference, December 12-15*, Seville, IEEE, pp. 209-214.

[129] Tang, B., Lui, G.-P., & Gui, W.-H. 2008. Improvement of state feedback controller design for networked control systems. *IEEE Transactions on Circuits and Systems-II: Analog and Digital Signal Processing*, 55, (5) 464-468

[130] Tomsovic, K., Bakken, D. E., Venkatasubramanian, V., & Bose, A., 2005. Designing the next generation of real-time control, communication, and computations for large power systems, *In Energy Infrastructure Defense Systems*, 5 edn, IEEE, pp. 965-979.

[131] Tuladhar, A., Jin, H., Unger, T., & Mauch, K., 1997. Parallel operation of single phase inverter modules with no control interconnections, *In Proceedings of 97 Applied Power Electronics Conference, 23-27 Feb*, New York, NY, USA: IEEE, pp. 94-100.

[132] Ukai, H., Nakamura, K., & Matsui, N. 2003. DSP- and GPS-based synchronized measurement system of harmonics in wide-area distribution system. *IEEE Transactions on Industrial Electronics*, 50, (6) 1159-1164

[133] Vesely, V. & Quang, T.N. 2011. Robust Power System Stabilizer Via Networked Control System. *Journal of Electrical Engineering*, 62, (5) 286-291

[134] Walsh, G. C., Hong, Y., & Bushnell, L., 1999. Stability analysis of networked control systems, *In Proceedings of the 1999 American Control Conference, 2-4 June*, Piscataway, NJ, USA: IEEE, pp. 2876-2880.

[135] Walsh, G.C., Beldiman, O., & Bushnell, L.G. 2001. Asymptotic behavior of nonlinear networked control systems. *Automatic Control, IEEE Transactions on*, 46, (7) 1093-1097

[136] Wang, F.Y., Liu, D., Yang, S.X., & Li, L. 2007. Guest Editorial: Networking, Sensing, and Control for Networked Control Systems: Architectures, Algorithms, and Applications. *Systems, Man, and Cybernetics, Part C: Applications and Reviews, IEEE Transactions on*, 37, (2) 157-159

[137] Wang, F.Y. & Liu, D. 2008. *Networked Control Systems: Theory and Applications*, 1 ed. Springer.

[138] Wang, J., J.Pu, P.R.Moore, & Z.Zhang 1998. Modelling study and robust control of air motor systems. *International Journal of Control*, 71, 459-476

[139] Wang, J., Kotta, U., & Jia, K. 2007. Tracking control of nonlinear pneumatic actuator systems using static state feedback linearization of the input-output map. *Proceedings of the Estonian Academy of Sciences.Physics, Mathematics*, 56, (1) 47-66

[140] Wang, Y., Jiang, B., & Mao, Z., 2009. Fault tolerant control design for a kind of nonlinear networked control system with communication constraints, *In 2009 Chinese Control and Decision Conference, 17-19 June*, Piscataway, NJ, USA: IEEE, pp. 896-901.

[141] Wang, Y.-L. & Yang, G.-H., 2008. Packet dropout compensation for networked control systems: A multiple communication channels method, *In Proceedings of 2008 American Control Conference*, pp. 1973-1978.

[142] Wei, Z., 1993. Computer network and data communications for power system real time control, *In Proceedings of IEEE Region 10 International Conference on Computers, Communications and Automation, 19-21 Oct*, New York, NY, USA: IEEE, pp. 477-480.

[143] Wu, F. F., Moslehi, K., & Bose, A., 2005. Power system control centers: Past, present, and future, 11 edn, IEEE., pp. 1890-1908.

[144] Wu, J., Zhang, L., & Chen, T. 2009. Model predictive control for networked control systems. *International Journal of Robust and Nonlinear Control*, 19, (9) 1016-1035

[145] Wu, M. & He, Y., 2007. Improved stabilization method for networked control systems, *In 26th Chinese Control Conference, 26-31 July*, Piscataway, NJ, USA: IEEE, pp. 544-548.

[146] Xiao, L., Hassibi, A., & How, J. P., 2000. Control with random communication delays via a discrete-time jump system approach, *In Proceedings of 2000 Ameri-*

can Control Conference, 28-30 June, Danvers, MA, USA: American Autom. Control Council, pp. 2199-2204.

[147] Xiaoyang, T., Guodong, L., Xiaoru, W., & Shan, Z., 2005. The analysis of communication architecture and control mode of wide area power systems control, *In Proceedings of 2005 International Symposium on Autonomous Decentralized Systems, 4-8 April*, Piscataway, NJ, USA: IEEE, pp. 59-65.

[148] Xie, L., Zhang, J.-M., & Wang, S.-Q., 2002. Stability analysis of networked control system, *In Proceedings of 2002 International Conference on Machine Learning and Cybernetics, 4-5 Nov*, Piscataway, NJ, USA: IEEE, pp. 757-759.

[149] Xue, Y. & Liu, K., 2008. Controller design for variable-sampling networked control systems with dynamic output feedback, *In Proceedings of 7th World Congress on Intelligent Control and Automation, 25-27 June*, Piscataway, NJ, USA: IEEE, pp. 6391-6396.

[150] Yan, H., Huang, X., Wang, M., & Zhang, H., 2006. Delay-dependent robust stability of networked control systems with uncertainties and multiple time-varying delays, *In 2006 IEEE International Conference on Mechatronics and Automation, 25-28 June*, Piscataway, NJ, USA: IEEE, pp. 373-378.

[151] Yan, H., Meng, M. Q. H., & Huang, X., 2008. Modeling and robust stability criterion of uncertain networked control systems with time-varying delays, *In Proceedings of 7th World Congress on Intelligent Control and Automation, 25-27 June*, Piscataway, NJ, USA: IEEE, pp. 188-192.

[152] Yang, F. & Fang, H., 2007. Control strategy design of networked control systems based on maximum allowable delay bounds, *In 2007 IEEE International Conference on Control and Automation, 30 May-1 June*, Piscataway, NJ, USA: IEEE, pp. 794-797.

[153] Yang, J. & Wang, X., 2004. Stability of a class of nonlinear networked control systems, *In Fifth World Congress on Intelligent Control and Automation, 15-19 June*, Piscataway, NJ, USA: IEEE, pp. 1401-1405.

[154] Yang, T. C., Ding, Z. T., & Yu, H., 2000. Research into Quasi-decentralised control, *In Proceedings of the 3th World Congress on Intelligent Control and Automation, June 28, July 2*, Hefei, China: IEEE, pp. 2893-2898.

[155] Yang, T.C. 2006. Networked control system: a brief survey. *IEE Proceedings-Control Theory and Applications*, 153, (4) 403-412

[156] Yang, T. C., Fei, M. R., Xue, D. Y., & Yu, H. N., 2006. Some issues in the study of networked control system, *In 45th IEEE Conference on Decision and Control, December 13-15*, San Diego, CA, USA: IEEE., pp. 5604-5608.

[157] Yongqing, W., Xiaofeng, Z., Mingzhong, Q., & Jun, K., 2008. Control of parallel inverters based on CAN bus in large-capacity motor drives, *In 2008 Third IEEE International Conference on Electric Unity Deregulation, 6-9 April 2008*, Piscataway, NJ, USA: IEEE, pp. 1375-1379.

[158] Yu, B. & Shi, Y., 2008. State Feedback Stabilization of Networked Control Systems With Random Time Delays and Packet Dropout, *In ASME 2008 Dynamic Systems and Control Conference*, Michigan, USA: pp. 639-645.

[159] Yu, J., Wang, L., Yu, M., Chen, J., & Jia, Y., 2009. Robust controller design for networked control systems with nonlinear uncertainties, *In 2009 American Control Conference, 10-12 June*, Piscataway, NJ, USA: IEEE, pp. 2803-2808.

[160] Yu, M., Wang, L., & Chu, T. 2005. Sampled-data stabilisation of networked control systems with nonlinearity. *IEE Proceedings-Control Theory and Applications*, 152, (6) 609-614

[161] Yu, M., Wang, L., Chu, T., & Xie, G. 2008. Modelling and control of networked systems via jump system approach. *IET Control Theory & Applications*, 2, (6) 535-541

[162] Yu, M., Wang, L., & Chu, T., 2005. Robust stabilization of nonlinear sampled-data systems, *In Proceedings of the 2005 American Control Conference, 8-10 June*, Piscataway, NJ, USA: IEEE, pp. 3421-3426.

[163] Yu, X. & Tomsovic, K. 2004. Application of linear matrix inequalities for load frequency control with communication delays. *IEEE Transactions on Power Systems*, 19, (3) 1508-1515

[164] Yue, D., Han, Q. L., & Peng, C., 2004. State feedback controller design of networked control systems, *In Proceedings of the 2004 IEEE International Conference on Control Applications, 2-4 Sept*, Piscataway, NJ, USA: IEEE, pp. 242-247.

[165] Yue, D., Han, Q.L., & Peng, C. 2004. State feedback controller design of networked control systems. *IEEE Transactions on Circuits and Systems II: Analog and Digital Signal Processing*, 51, (11) 640-644

[166] Yue, D., Peng, C., & Tang, G.Y. 2006. Guaranteed cost control of linear systems over networks with state and input quantisations. *IEE Proceedings-Control Theory and Applications*, 153, (6) 658-664

[167] Zhang, G., Chen, X., & Chen, T., 2007. A model predictive control approach to networked systems, *In 46th IEEE Conference on Decision and Control, 12-14 Dec*, Piscataway, NJ, USA: IEEE, pp. 3339-3344.

[168] Zhang, J. M., Xie, X. G., Wu, X. K., & Zhaoming, Q., 2004. Stability study for paralleled DC/DC converters, *In 35th Power Electronics Specialists Conference.* IEEE, pp. 1569-1575.

[169] Zhang, L., Shi, Y., Chen, T., & Huang, B. 2005. A New Method for Stabilization of Networked Control Systems With Random Delays. *Automatic Control, IEEE Transactions on*, 50, (8) 1177-1181

[170] Zhang, L., Shi, Y., Chen, T., & Huang, B., 2005. A new method for stabilization of networked control systems with random delays, *In Proceedings of the 2005 American Control Conference, 8-10 June*, Piscataway, NJ, USA: IEEE, pp. 633-637.

[171] Zhang, W., Branicky, M.S., & Phillips, S.M. 2001. Stability of networked control systems. *IEEE Control Systems Magazine*, 21, (1) 84-99

[172] Zhang, Y., Ma, H., & Xu, F., 2007. Study on networked control for power electronic systems, *In IEEE 38th Annual Power Electronics Specialists Conference, 17-21 June*, Piscataway, NJ, USA: IEEE, pp. 833-838.

[173] Zhang, Y., Zhong, Q., & Wei, L., 2008. Stability analysis of networked control systems with transmission delays, *In Chinese Control and Decision Conference, July 2-4*, Yantai, Shandong, China: IEEE, pp. 340-343.

[174] Zhang, Y., Zhong, Q., & Wei, L., 2008. Stability of networked control systems with communication constraints, *In Chinese Control and Decision Conference, July 2-4*, Yantai, Shandong, China: IEEE. pp. 335-339.

[175] Zhu, X. & Wang, Z., 2007. CAN based NCS for power plants, *In 2007 IEEE International Conference on Control and Automation, 30 May-1 June*, Piscataway, NJ, USA: IEEE, pp. 2345-2348.

[176] Zhu, X. L. & Yang, G. H., 2008. New results on stability analysis of networked control systems, *In 2008 American Control Conference, June 11-1*, Seattle, WA, USA: IEEE, pp. 3792-3797.

Appendix A: The Examples Used in Chapter 3 for Generating Table 3.1

Example 1:

$$\dot{x}(t)=\begin{bmatrix}0 & 1\\ 0 & -0.1\end{bmatrix}x(t)+\begin{bmatrix}0\\ 0.1\end{bmatrix}u(t) \qquad y(t)=\begin{bmatrix}1 & 0\end{bmatrix}x(t)+[0]u(t) \qquad u(t)=\begin{bmatrix}-3.75 & -11.5\end{bmatrix}x(t)$$

Example 2:

$$\dot{x}(t)=\begin{bmatrix}0 & 1\\ 0 & -0.1\end{bmatrix}x(t)+\begin{bmatrix}0\\ 0.1\end{bmatrix}u(t) \qquad y(t)=\begin{bmatrix}1 & 0\end{bmatrix}x(t)+[0]u(t) \qquad u(t)=\begin{bmatrix}-100 & -100\end{bmatrix}x(t)$$

Example 3:

$$\dot{x}(t)=\begin{bmatrix}0 & 1\\ 0 & -0.1\end{bmatrix}x(t)+\begin{bmatrix}0\\ 0.1\end{bmatrix}u(t) \qquad y(t)=\begin{bmatrix}1 & 0\end{bmatrix}x(t)+[0]u(t) \qquad u(t)=\begin{bmatrix}-1000 & -1000\end{bmatrix}x(t)$$

Example 4:

$$\dot{x}(t)=\begin{bmatrix}0 & 1\\ 1 & 0\end{bmatrix}x(t)+\begin{bmatrix}0\\ 1\end{bmatrix}u(t) \qquad y(t)=\begin{bmatrix}1 & 0\end{bmatrix}x(t)+[0]u(t) \qquad u(t)=\begin{bmatrix}-13 & -7\end{bmatrix}x(t)$$

Example 5:

$$\dot{x}(t)=\begin{bmatrix}1 & 0.5\\ -0.1 & -1\end{bmatrix}x(t)+\begin{bmatrix}0.7\\ -1\end{bmatrix}u(t) \qquad y(t)=\begin{bmatrix}1 & 0\end{bmatrix}x(t)+[0]u(t) \qquad u(t)=\begin{bmatrix}-2.6884 & -0.6649\end{bmatrix}x(t)$$

Example 6:

$$\dot{x}(t)=\begin{bmatrix}0 & 1\\ 0 & 0\end{bmatrix}x(t)+\begin{bmatrix}0\\ 1\end{bmatrix}u(t) \qquad y(t)=\begin{bmatrix}1 & 0\end{bmatrix}x(t)+[0]u(t) \qquad u(t)=\begin{bmatrix}-1 & -2\end{bmatrix}x(t)$$

Example 7:

$$\dot{x}(t)=\begin{bmatrix}0 & 1\\ 1 & 0\end{bmatrix}x(t)+\begin{bmatrix}0\\ 1\end{bmatrix}u(t) \qquad y(t)=\begin{bmatrix}1 & 0\end{bmatrix}x(t)+[0]u(t) \qquad u(t)=\begin{bmatrix}-1.006 & -1.006\end{bmatrix}x(t)$$

Example 8:

$$\dot{x}(t)=\begin{bmatrix}0 & 1 & 0\\ 0 & 0 & 1\\ 0 & -2 & -3\end{bmatrix}x(t)+\begin{bmatrix}0\\ 0\\ 1\end{bmatrix}u(t) \qquad Q=\begin{bmatrix}100 & 0 & 0\\ 0 & 1 & 0\\ 0 & 0 & 1\end{bmatrix} \text{ and } \quad R=[0.01] \quad \text{using LQR then}$$

$$u(t)=\begin{bmatrix}-100 & -53.12 & -11.6711\end{bmatrix}x(t)$$

Example 9:

$$\dot{x}(t)=\begin{bmatrix}0 & 1 & 0\\ 0 & 0 & 1\\ 0 & -2 & -3\end{bmatrix}x(t)+\begin{bmatrix}0\\ 0\\ 1\end{bmatrix}u(t) \qquad u(t)=\begin{bmatrix}-160 & -54 & -11\end{bmatrix}x(t)$$

Example 10:

$$\dot{x}(t)=\begin{bmatrix}0 & 1.000 & 0 & 0\\ 20.601 & 0 & 0 & 0\\ 0 & 0 & 0 & 1\\ -0.4905 & 0 & 0 & 0\end{bmatrix}x(t)+\begin{bmatrix}0\\ -1\\ 0\\ 0.5\end{bmatrix}u(t) \qquad u(t)=\begin{bmatrix}298.1504 & 60.6972 & 163.0989 & 73.3945\end{bmatrix}x(t)$$